

SCALE 5.1 Predictions of PWR Spent Nuclear Fuel Isotopic Compositions

March 2010

**Prepared by
G. Radulescu
I. C. Gauld
G. Ilas**

DOCUMENT AVAILABILITY

Reports produced after January 1, 1996, are generally available free via the U.S. Department of Energy (DOE) Information Bridge:

Web site: <http://www.osti.gov/bridge>

Reports produced before January 1, 1996, may be purchased by members of the public from the following source:

National Technical Information Service
5285 Port Royal Road
Springfield, VA 22161
Telephone: 703-605-6000 (1-800-553-6847)
TDD: 703-487-4639
Fax: 703-605-6900
E-mail: info@ntis.fedworld.gov
Web site: <http://www.ntis.gov/support/ordernowabout.htm>

Reports are available to DOE employees, DOE contractors, Energy Technology Data Exchange (ETDE) representatives, and International Nuclear Information System (INIS) representatives from the following source:

Office of Scientific and Technical Information
P.O. Box 62
Oak Ridge, TN 37831
Telephone: 865-576-8401
Fax: 865-576-5728
E-mail: reports@adonis.osti.gov
Web site: <http://www.osti.gov/contact.html>

This report was prepared as an account of work sponsored by an agency of the United States Government. Neither the United States government nor any agency thereof, nor any of their employees, makes any warranty, express or implied, or assumes any legal liability or responsibility for the accuracy, completeness, or usefulness of any information, apparatus, product, or process disclosed, or represents that its use would not infringe privately owned rights. Reference herein to any specific commercial product, process, or service by trade name, trademark, manufacturer, or otherwise, does not necessarily constitute or imply its endorsement, recommendation, or favoring by the United States Government or any agency thereof. The views and opinions of authors expressed herein do not necessarily state or reflect those of the United States Government or any agency thereof.

Nuclear Science and Technology Division

**SCALE 5.1 Predictions of PWR Spent Nuclear Fuel
Isotopic Compositions**

G. Radulescu
I. C. Gauld
G. Ilas

Date Published: March 2010

Prepared by
OAK RIDGE NATIONAL LABORATORY
P.O. Box 2008
Oak Ridge, Tennessee 37831-6283
managed by
UT-BATTELLE, LLC
for the
U.S. DEPARTMENT OF ENERGY
under contract DE-AC05-00OR22725

CONTENTS

	<u>Page</u>
LIST OF FIGURES	v
LIST OF TABLES	ix
ACRONYMS	xiii
1 PURPOSE	1
2 QUALITY ASSURANCE REQUIREMENTS	3
3 USE OF SOFTWARE	5
3.1 STANDARDIZED COMPUTER ANALYSIS FOR LICENSING EVALUATION (SCALE) CODE SYSTEM.....	5
3.2 EXCEL.....	5
4 INPUT DATA.....	7
5 ASSUMPTIONS.....	9
5.1 INITIAL URANIUM ISOTOPIC CONTENTS	9
5.2 MODERATOR TEMPERATURE AND DENSITY	9
5.3 EFFECTIVE FUEL TEMPERATURE.....	10
5.4 BORON LETDOWN CURVE	10
6 EXPERIMENTAL PROGRAMS AND DATA	11
6.1 SELECTION OF SPENT FUEL ISOTOPIC COMPOSITION DATA	11
6.2 SUMMARY OF DATA USED IN PREVIOUS YMP ANALYSES	11
6.3 REVIEW OF RADIOCHEMICAL ANALYSIS DATA.....	13
6.4 DATA QUALIFICATION	16
6.5 EXPERIMENTAL DATA ANALYSIS	17
6.6 NUCLEAR DATA.....	19
6.7 ANALYTICAL MEASUREMENT UNCERTAINTIES	21
7 EXPERIMENTAL DATA	23
7.1 TRINO VERCELLESE	23
7.2 OBRIGHEIM (KWO).....	31
7.2.1 Karlsruhe Reprocessing Plant (WAK).....	31
7.2.2 JRC Research Program	33
7.3 TURKEY POINT UNIT 3	40
7.4 H. B. ROBINSON UNIT 2	42
7.5 CALVERT CLIFFS UNIT 1.....	45
7.5.1 PNL Measurements.....	46
7.5.2 KRI Measurements	47
7.5.3 103-MLA098	49
7.5.4 104-MKP109.....	50
7.5.5 106-NBD107.....	51
7.6 TAKAHAMA UNIT 3.....	55
7.7 TMI UNIT I	61
7.7.1 ANL Measurements	62
7.7.2 GE-VNC Measurements	66
7.8 GÖSGEN REACTOR: ARIANE PROGRAM.....	69
7.9 GKN UNIT II.....	74
7.10 GÖSGEN REACTOR: MALIBU PROGRAM	75

CONTENTS (continued)

	<u>Page</u>
8 ASSEMBLY DESIGN AND IRRADIATION HISTORY DATA.....	79
8.1 TRINO VERCELLESE	79
8.2 OBRIGHEIM.....	88
8.3 TURKEY POINT UNIT 3	95
8.4 H. B. ROBINSON UNIT 2	99
8.5 CALVERT CLIFFS UNIT 1.....	105
8.6 TAKAHAMA UNIT 3.....	116
8.7 TMI UNIT 1.....	121
8.8 GÖSGEN: ARIANE PROGRAM	131
8.9 GKN II.....	136
8.10 GÖSGEN: MALIBU PROGRAM.....	140
9 SCALE TWO-DIMENSIONAL DEPLETION CALCULATION METHOD.....	141
9.1 METHOD DESCRIPTION.....	141
9.2 MODELING APPROACH.....	141
9.2.1 Input File Format for Depletion Calculations	141
9.2.2 Fuel Mixture Modeling Simplifications.....	144
9.2.3 Modeling Approach for H. B. Robinson Assembly BO-5, Calvert Cliffs Assembly BT03, and TMI Assembly NJ05YU	144
9.3 TRITON/NEWT MODELING	144
9.3.1 Trino Vercellese.....	144
9.3.2 Obrigheim	146
9.3.3 Turkey Point Unit 3	147
9.3.4 H. B. Robinson Unit 2.....	148
9.3.5 Calvert Cliffs.....	149
9.3.6 Takahama Unit 3.....	151
9.3.7 TMI Unit 1	153
9.3.8 Gösgen: ARIANE Program	156
9.3.9 GKN II.....	158
10 CALCULATION RESULTS	161
10.1 RESULTS OF THE T-DEPL CALCULATIONS	161
10.2 SENSITIVITY CALCULATIONS.....	185
10.2.1 Assembly Model Simplifications.....	185
10.2.2 Trino Vercellese Fuel Density Sensitivity Calculations	186
10.2.3 Trino Vercellese Fuel Temperature Sensitivity Calculations	187
10.3 GRAPHICAL REPRESENTATIONS OF E/C VALUES FOR THE BURNUP CREDIT ISOTOPES.....	188
11 SUMMARY	189
12 REFERENCES.....	191
APPENDIX A: GRAPHICAL REPRESENTATIONS OF E/C VALUES FOR THE BURNUP CREDIT ISOTOPES	A-1
APPENDIX B: ELECTRONIC DATA SPECIFICATIONS	B-1

LIST OF FIGURES

		<u>Page</u>
Fig. 1.	Enrichment and burnup values of spent fuel samples used for validation compared to the actual and projected spent fuel assembly inventory and typical loading curve for PWR SNF assuming actinide and fission product burnup credit	15
Fig. 2.	Schematic core map for the Trino Vercellese reactor showing the locations of the measured assemblies during cycle 1 and cycle 2.....	81
Fig. 3.	(a) S-E quarter showing locations of cruciform assemblies containing control rods, fuel rods, and stainless steel fillers during cycle 1; (b) control group locations during cycle 2	82
Fig. 4.	Horizontal cross section of the Trino Vercellese square fuel assembly	83
Fig. 5.	Location of Trino Vercellese measured fuel rods	83
Fig. 6.	Layout of the KWO fuel assemblies showing the location of the guide tubes	90
Fig. 7.	Core maps of the Obrigheim reactor during different irradiation cycles, showing the locations of control rods	91
Fig. 8.	Location of measured fuel rods in Obrigheim assemblies BE124 and BE210.....	92
Fig. 9.	Position of 21 guide tubes (×) and locations of measured fuel rods G9, G10, and H9 from Turkey Point assemblies D01 and D04.....	98
Fig. 10.	Core arrangement for H. B. Robinson Unit 2 reactor core	102
Fig. 11.	Locations of fuel rod N-9, instrument tube, and guide tubes in assembly BO-5.....	103
Fig. 12.	Axial burnup profiles for assembly exposures during cycles 1 and 2	104
Fig. 13.	Assembly layout for Calvert Cliffs samples from assemblies D047 and D101.....	107
Fig. 14.	Assembly layout for Calvert Cliffs samples from assembly BT03	108
Fig. 15.	Assembly layout for Takahama-3 spent fuel samples.	116
Fig. 16.	Assembly layout for TMI-1 samples—NJ05YU.....	122
Fig. 17.	Assembly layout for TMI-1 samples—NJ070G.....	122
Fig. 18.	Assemblies surrounding assembly NJ070G	130
Fig. 19.	Assembly layout for Gösgen (ARIANE) samples	132
Fig. 20.	Assembly layout for GKN II (REBUS) sample.....	137
Fig. 21.	TRITON/NEWT model for Trino Vercellese assembly 509-069, rod E11.....	145
Fig. 22.	TRITON/NEWT model for Trino Vercellese assembly 509-104, rod M11.....	146
Fig. 23.	TRITON/NEWT model for KWO assembly BE124, fuel rod G7.....	147
Fig. 24.	TRITON/NEWT model for Turkey Point Unit 3 assembly D01, rod G9.....	148
Fig. 25.	TRITON/NEWT model for H. B. Robinson Unit 2 assembly BO-5: (a) for cycle 1 of irradiation; (b) for cycle 2 of irradiation.....	149
Fig. 26.	TRITON/NEWT model for Calvert Cliffs samples from assembly D047.	149
Fig. 27.	TRITON/NEWT model for Calvert Cliffs samples from assembly D101.	150

LIST OF FIGURES (continued)

	<u>Page</u>
Fig. 28. TRITON/NEWT model for Calvert Cliffs samples from assembly BT03, cycle 1.....	150
Fig. 29. TRITON/NEWT model for Calvert Cliffs samples from assembly BT03, cycles 2-4.....	151
Fig. 30. TRITON/NEWT model for Takahama-3 SF95 spent fuel samples.....	152
Fig. 31. TRITON/NEWT model for Takahama-3 SF96 spent fuel samples.....	152
Fig. 32. TRITON/NEWT model for Takahama-3 SF97 spent fuel samples.....	153
Fig. 33. TRITON/NEWT model for TMI-1 samples in assembly NJ05YU.....	154
Fig. 34. TRITON/NEWT model for TMI-1 samples in rod O12 of assembly NJ070G.	155
Fig. 35. TRITON/NEWT model for TMI-1 samples in rod O1 of assembly NJ070G	155
Fig. 36. TRITON/NEWT assembly model for Gösgen (ARIANE) – sample GU1	157
Fig. 37. TRITON/NEWT assembly model for Gösgen (ARIANE) – sample GU3/4, cycles 16 –17 .	157
Fig. 38. TRITON/NEWT assembly model for Gösgen (ARIANE) – sample GU3/4, cycle 18.....	158
Fig. 39. TRITON/NEWT assembly model for GKN II (REBUS) spent fuel sample.....	159
Fig. A.1. Ratio of experimental-to-calculated (E/C) ²³⁴ U concentration versus sample burnup.....	A-3
Fig. A.2. Ratio of experimental-to-calculated (E/C) ²³⁵ U concentration versus sample burnup.....	A-3
Fig. A.3. Ratio of experimental-to-calculated (E/C) ²³⁶ U concentration versus sample burnup.....	A-4
Fig. A.4. Ratio of experimental-to-calculated (E/C) ²³⁸ U concentration versus sample burnup.....	A-4
Fig. A.5. Ratio of experimental-to-calculated (E/C) ²³⁸ Pu concentration versus sample burnup	A-5
Fig. A.6. Ratio of experimental-to-calculated (E/C) ²³⁹ Pu concentration versus sample burnup	A-5
Fig. A.7. Ratio of experimental-to-calculated (E/C) ²⁴⁰ Pu concentration versus sample burnup	A-6
Fig. A.8. Ratio of experimental-to-calculated (E/C) ²⁴¹ Pu concentration versus sample burnup	A-6
Fig. A.9. Ratio of experimental-to-calculated (E/C) ²⁴² Pu concentration versus sample burnup	A-7
Fig. A.10. Ratio of experimental-to-calculated (E/C) ²³⁷ Np concentration versus sample burnup.....	A-7
Fig. A.11. Ratio of experimental-to-calculated (E/C) ²⁴¹ Am concentration versus sample burnup	A-8
Fig. A.12. Ratio of experimental-to-calculated (E/C) ^{242m} Am concentration versus sample burnup	A-8
Fig. A.13. Ratio of experimental-to-calculated (E/C) ²⁴³ Am concentration versus sample burnup	A-9
Fig. A.14. Ratio of experimental-to-calculated (E/C) ⁹⁵ Mo concentration versus sample burnup	A-9
Fig. A.15. Ratio of experimental-to-calculated (E/C) ⁹⁹ Tc concentration versus sample burnup.....	A-10
Fig. A.16. Ratio of experimental-to-calculated (E/C) ¹⁰¹ Ru concentration versus sample burnup.....	A-10
Fig. A.17. Ratio of experimental-to-calculated (E/C) ¹⁰³ Rh concentration versus sample burnup.....	A-11
Fig. A.18. Ratio of experimental-to-calculated (E/C) ¹⁰⁹ Ag concentration versus sample burnup.....	A-11
Fig. A.19. Ratio of experimental-to-calculated (E/C) ¹⁴³ Nd concentration versus sample burnup.....	A-12

LIST OF FIGURES (continued)

	<u>Page</u>
Fig. A.20. Ratio of experimental-to-calculated (E/C) ^{145}Nd concentration versus sample burnup.....	A-12
Fig. A.21. Ratio of experimental-to-calculated (E/C) ^{147}Sm concentration versus sample burnup	A-13
Fig. A.22. Ratio of experimental-to-calculated (E/C) ^{149}Sm concentration versus sample burnup	A-13
Fig. A.23. Ratio of experimental-to-calculated (E/C) ^{150}Sm concentration versus sample burnup	A-14
Fig. A.24. Ratio of experimental-to-calculated (E/C) ^{151}Sm concentration versus sample burnup	A-14
Fig. A.25. Ratio of experimental-to-calculated (E/C) ^{152}Sm concentration versus sample burnup	A-15
Fig. A.26. Ratio of experimental-to-calculated (E/C) ^{151}Eu concentration versus sample burnup	A-15
Fig. A.27. Ratio of experimental-to-calculated (E/C) ^{153}Eu concentration versus sample burnup	A-16
Fig. A.28. Ratio of experimental-to-calculated (E/C) ^{155}Gd concentration versus sample burnup.....	A-16

LIST OF TABLES

	<u>Page</u>
Table 1. Summary of direct inputs for spent fuel sample modeling	7
Table 2. Uranium isotope dependence on X wt % ^{235}U enrichment	9
Table 3. Principal isotopes for burnup credit applications	11
Table 4. Summary of experiments used for validation of spent fuel compositions.....	14
Table 5. Nuclear data used for experiment data evaluation.....	20
Table 6. Summary of the Trino Vercellese measured spent fuel.....	24
Table 7. Experimental techniques and uncertainties for Trino Vercellese spent fuel samples.....	25
Table 8. Burnup values derived from experimental measurements.....	26
Table 9. Experimental results for Trino Vercellese fuel samples (mg/g U_{initial})	28
Table 10. Experimental techniques and uncertainties for Obrigheim measurements at WAK	31
Table 11. Summary of measured Obrigheim assemblies reprocessed at WAK	32
Table 12. Measurement data for Obrigheim assemblies reprocessed at WAK (mg/g U_{initial}).....	33
Table 13. Summary of Obrigheim KWO fuel samples from assemblies BE124 and BE210.....	34
Table 14. Measurement methods and uncertainties in Obrigheim measurements at JRC	35
Table 15. Obrigheim sample burnup values from JRC measurements.....	36
Table 16. Experimental results for Obrigheim JRC samples ^a (mg/g U_{initial}).....	38
Table 17. Summary of the Turkey Point Unit 3 spent fuel samples	40
Table 18. Experimental results (mg/g U_{initial}) for Turkey Point fuel samples	41
Table 19. Experimental techniques and uncertainties for Turkey Point measurements	42
Table 20. Summary of H. B. Robinson fuel samples.....	42
Table 21. Experimental results (mg/g U_{initial}) for H. B. Robinson fuel samples	44
Table 22. Experimental techniques and uncertainties for H. B. Robinson measurements	44
Table 23. Summary of Calvert Cliffs fuel samples.....	45
Table 24. Experimental techniques and uncertainties for Calvert Cliffs measurements at PNL.....	47
Table 25. Experimental techniques and uncertainties for Calvert Cliffs measurements at KRI.....	49
Table 26. Measurement results for Calvert Cliffs 103-MLA098 samples (mg/g U_{initial})	50
Table 27. KRI experimental lanthanide results for Calvert Cliffs samples (g/g ^{145}Nd).....	52
Table 28. Measurement results for Calvert Cliffs 104-MKP109 samples (mg/g U_{initial})	53
Table 29. Measurement results for Calvert Cliffs 106-NBD107 samples (mg/g U_{initial})	54
Table 30. Summary of Takahama Unit 3 fuel samples from assemblies NT3G23 and NT3G24.....	55
Table 31. Experimental techniques and uncertainties for Takahama-3 samples	57

LIST OF TABLES (continued)

	<u>Page</u>
Table 32. Experimental results (g/g $U_{initial}$) for Takahama-3 samples from rod SF95	58
Table 33. Experimental results (g/g $U_{initial}$) for Takahama-3 samples from rod SF96	59
Table 34. Experimental results (g/g $U_{initial}$) for Takahama-3 samples from rod SF97	60
Table 35. Summary of TMI Unit 1 fuel samples from assemblies NJ05YU and NJ070G	61
Table 36. Experimental techniques and uncertainties for TMI-1 samples measurements at ANL	63
Table 37. Experimental results (g/g $U_{initial}$) for TMI-1 samples measured at ANL	64
Table 38. Experimental techniques and uncertainties for TMI-1 samples measurements at GE-VNC	67
Table 39. Experimental results (g/g $U_{initial}$) for TMI-1 samples measured at GE-VNC	68
Table 40. Summary of Gösgen (ARIANE) fuel samples	69
Table 41. Experimental techniques and uncertainties for ARIANE Program Gösgen samples	71
Table 42. Experimental results for ARIANE Program Gösgen samples	72
Table 43. Decay time at the time of measurement for ARIANE Program Gösgen samples	73
Table 44. Experimental techniques and uncertainties for REBUS Program GKN II sample	76
Table 45. Experimental results for GKN II (REBUS) sample	77
Table 46. Decay time data for GKN II (REBUS) sample	78
Table 47. Assembly design and operating data for Trino Vercellese	84
Table 48. Summary of general operation data for cycles 1 and 2	86
Table 49. Initial isotopic composition of Trino Vercellese fuel	86
Table 50. Moderator temperature and density at sample locations for Trino Vercellese samples	87
Table 51. Fuel burnup, operating power histories, and temperature for Trino Vercellese pellet samples	87
Table 52. Assembly design and operating data for Obrigheim measured spent fuel	89
Table 53. Initial isotopic composition of KWO fuel	93
Table 54. Irradiation history of Obrigheim assemblies BE124 and BE210	93
Table 55. Specific power and final burnup data for KWO assemblies BE168, BE170, BE171, BE172, and BE176	93
Table 56. Operating parameter values for KWO samples	94
Table 57. Assembly design and operating data for Turkey Point Unit 3	96
Table 58. Initial composition of Turkey Point fuel assemblies	97
Table 59. Turkey Point Unit 3 operating data	97
Table 60. Turkey Point sample specific powers and temperatures	97
Table 61. Assembly design and operating data for H. B. Robinson	100

LIST OF TABLES (continued)

	<u>Page</u>
Table 62. Atom densities for borosilicate glass	103
Table 63. Operating and fuel temperature data for H. B. Robinson spent fuel samples.....	105
Table 64. Moderator conditions for H. B. Robinson spent fuel samples.....	105
Table 65. Assembly design and operating data for Calvert Cliffs measured spent fuel	109
Table 66. Sample location data for Calvert Cliffs samples	110
Table 67. Moderator temperature and density data for Calvert Cliffs samples	110
Table 68. Concentration of soluble boron in moderator for Calvert Cliffs samples.....	111
Table 69. Effective fuel temperature data for Calvert Cliffs samples	111
Table 70. Burnup values for Calvert Cliffs spent fuel samples	112
Table 71. Linear heat generation data for fuel rod MKP109.....	113
Table 72. Linear heat generation data for fuel rod MLA098.....	114
Table 73. Linear heat generation data for fuel rod NBD107	114
Table 74. Sample burnup at the end of each cycle for Calvert Cliffs samples	115
Table 75. Decay time data for Calvert Cliffs samples.....	115
Table 76. Assembly design data for Takahama-3 spent fuel samples	118
Table 77. Burnup, power, sample location, and moderator data for Takahama-3 samples	119
Table 78. Operation history data for Takahama-3 spent fuel samples.....	120
Table 79. Soluble boron concentration in moderator for Takahama-3 spent fuel samples.....	120
Table 80. Sample burnup for Takahama-3 spent fuel samples.....	121
Table 81. Assembly design data for TMI-1 samples.....	123
Table 82. Burnup and starting moderator density data for TMI-1 samples.....	125
Table 83. Burnup as a function of time for TMI-1 samples from assembly NJ05YU.....	126
Table 84. Fuel temperature and concentration of soluble boron in moderator for TMI-1 samples from assembly NJ05YU	127
Table 85. Moderator density multiplication factors for TMI-1 samples from assembly NJ05YU.....	128
Table 86. Burnup as a function of time for TMI-1 samples from assembly NJ070G	129
Table 87. Fuel temperature and concentration of soluble boron in moderator for TMI-1 samples from assembly NJ070G	129
Table 88. Moderator density multiplication factors for TMI-1 samples from assembly NJ070G.....	129
Table 89. Modeling data for the assemblies adjoining the SW corner of assembly NJ070G.....	130
Table 90. Assembly design data for Gösgen (ARIANE) samples.....	133
Table 91. Operating history data for Gösgen (ARIANE) sample GU1	134

LIST OF TABLES (continued)

	<u>Page</u>
Table 92. Operating history data for Gösgen (ARIANE) samples GU3 and GU4	135
Table 93. Assembly design data for GKN II (REBUS) sample	138
Table 94. Operating history data for GKN II (REBUS) sample	139
Table 95. Cycle average power data for GKN II (REBUS) sample	140
Table 96. Cycle average moderator and fuel data for GKN II (REBUS) sample	140
Table 97. SCALE calculation results for Trino Vercellese spent fuel samples	162
Table 98. SCALE calculation results for Obrigheim spent fuel samples	166
Table 99. SCALE calculation results for Turkey Point Unit 3 spent fuel samples.....	170
Table 100. SCALE calculation results for H. B. Robinson Unit 2 spent fuel samples.....	170
Table 101. SCALE calculation results for Calvert Cliffs Unit 1 spent fuel samples.....	171
Table 102. SCALE calculation results for the Takahama Unit 3 spent fuel samples	173
Table 103. SCALE calculation results for the TMI Unit 1 spent fuel samples	177
Table 104. SCALE calculation results for Gösgen (ARIANE) spent fuel samples.....	181
Table 105. SCALE calculation results for GKN II (REBUS) spent fuel sample	183
Table 106. SCALE calculation results for Gösgen (MALIBU) spent fuel samples	184
Table 107. Comparison between isotopic compositions obtained with detailed and simplified lattice pin model	186
Table 108. Fuel density sensitivity calculation results for Trino Vercellese spent fuel samples.....	187
Table 109. Fuel temperature sensitivity calculation results for Trino Vercellese spent fuel samples	188

ACRONYMS

ANL	Argonne National Laboratory
ARIANE	<u>A</u> ctinide <u>R</u> esearch in a <u>N</u> uclear <u>E</u> lement
ASTM	American Society for Testing and Materials
ATM	Approved Testing Material
B&W	Babcock & Wilcox
BPR	burnable poison rod
BU	burnup
C/E	ratio of calculated-to-measured isotopic concentration
CE	Combustion Engineering
CEA	Commissariat à l'Énergie Atomique (France)
CFR	<i>Code of Federal Regulations</i>
CRG	control rod group
CSNF	commercial spent nuclear fuel
DOE	(U.S.) Department of Energy
DTN	data tracking number
DVD	digital video disc
E/C	experimental to calculated
EFPD	effective full power days
ENDF	Evaluated Nuclear Data File
EOC	end of cycle
EPRI	Electric Power Research Institute
FIMA	fission per initial metal atom
FPD	full power days
GE-VNC	General Electric Vallecitos Nuclear Center
GKN II	Gemeinschaftskernkraftwerk Unit II in Neckarwestheim/Neckar
GRS	Gesellschaft für Reaktorsicherheit mbH
HEDL	Hanford Engineering and Development Laboratory
IAEA	International Atomic Energy Agency
ICP-MS	inductively coupled plasma mass spectrometry
ID	identifier
IDA	isotope dilution analysis
IDMS	isotope dilution mass spectrometry
IRCh	Institute of Radiochemistry
ITU	European Institute for Transuranium Elements
JAERI	Japan Atomic Energy Research Institute
JRC	Joint Research Center, European Commission
KRI	Khlopin Radium Institute
KWO	Kernkraftwerk Obrigheim
LA	license application; luminescent analysis
LANL	Los Alamos National Laboratory
LHGR	linear heat generation rate
MALIBU	Radiochemical analysis of <u>MOX</u> <u>A</u> nd <u>UOX</u> <u>L</u> WR fuels <u>I</u> rradiated to high <u>B</u> urnup
MCC	Materials Characterization Center (PNL)
NEA	Nuclear Energy Agency
NRC	(U.S.) Nuclear Regulatory Commission
NSTD	Nuclear Science and Technology Division
OECD	Organization for Economic Cooperation and Development
OCRWM	Office of Civilian Radioactive Waste (Management)

ORNL	Oak Ridge National Laboratory
PNL	Pacific Northwest National Laboratory
PSI	Paul Scherrer Institute (Switzerland)
PWR	pressurized water reactor
RCA	radiochemical assay (data)
REBUS	Reactivity Tests for a Direct Evaluation of the <u>B</u> urnup Credit on <u>S</u> electe <i>d</i> Irradiated LWR Fuel Bundles
RSD	relative standard deviation
SCALE	Standardized Computer Analysis for Licensing Evaluation
SCK·CEN	Studiecentrum voor Kernenergie – Centre d'étude de l'Energie Nucléaire (Belgium)
SIMS	secondary ion mass spectrometry
TIMS	thermal ionization mass spectrometry
TMI	Three Mile Island
WAK	Karlsruhe Reprocessing Plant
XRFA	X-ray fluorescent analysis
YMP	Yucca Mountain Project

1 PURPOSE

The purpose of this calculation report is to document the comparison to measurement of the isotopic concentrations for pressurized water reactor (PWR) spent nuclear fuel determined with the Standardized Computer Analysis for Licensing Evaluation (SCALE) 5.1 (Ref. 1) depletion calculation method. Specifically, the depletion computer code and the cross-section library being evaluated are the two-dimensional (2-D) transport and depletion module, TRITON/NEWT,^{2, 3} and the 44GROUPNDF5 (Ref. 4) cross-section library, respectively, in the SCALE 5.1 code system.

This calculation report was developed in support of licensing activities for the proposed repository at Yucca Mountain, Nevada, and the development of the report is consistent with *Test Plan for: Isotopic Validation for Postclosure Criticality of Commercial Spent Nuclear Fuel*.⁵ The calculation report describes a comprehensive evaluation of radiochemical measurement, assembly design, and irradiation history data for 118 PWR spent fuel samples obtained from low-, moderate-, and high-burnup spent fuel assemblies from nine PWRs: Trino Vercellese, Kernkraftwerk Obrigheim (KWO), Turkey Point Unit 3, H. B. Robinson Unit 2, Calvert Cliffs Unit 1, Three Mile Island (TMI) Unit 1, Takahama Unit 3, Gösgen, and GKN II. The initial fuel enrichments and burnup values for the samples considered vary from 2.453 to 4.657 wt % ²³⁵U and from 7.2 to 70.4 GWd/MTU, respectively. The majority of the spent fuel samples were obtained from UO₂ rods in assemblies with no exposure to either burnable poison rods or control rods. However, the evaluated spent fuel samples also include samples from UO₂ assemblies containing burnable poison rods and samples from gadolinia rods. The report also describes the TRITON/NEWT models developed and provides the values obtained for the ratio of experimental-to-calculated (E/C) isotopic concentrations.

2 QUALITY ASSURANCE REQUIREMENTS

Development of this report has been determined to be subject to the Yucca Mountain Project quality assurance requirements as described in *Test Plan for: Isotopic Validation for Postclosure Criticality of Commercial Spent Nuclear Fuel*.⁵ The Test Plan identifies Oak Ridge National Laboratory (ORNL)–Office of Civilian Radioactive Waste (OCRW) quality assurance procedures applicable to the development, documentation, and electronic management of the data for this report.

The development of the calculation and analysis documentation was performed in accordance with ORNL-OCRW-19.1, *Calculation Packages*.⁶ The Test Plan for the development of the report was prepared in accordance with ORNL-OCRW-21.0, *Scientific Investigations*.⁷ The control of electronic data was performed in accordance with ORNL-OCRW-23.0, *Control of the Electronic Management of Data*.⁸ The computer codes used in this calculation have been qualified per ORNL-OCRW-19.0, *Software Control*.⁹

3 USE OF SOFTWARE

3.1 STANDARDIZED COMPUTER ANALYSIS FOR LICENSING EVALUATION (SCALE) CODE SYSTEM

The SCALE (Ref. 1) code system was used to perform transport and depletion calculations.^{2,3} The SCALE 5.1 code system used herein has been qualified per ORNL-OCRW-19.0, *Software Control*.⁹

- Software Title: SCALE
- Version/Revision Number: Version 5.1
- Status/Operating System: Qualified/Linux 2.6.9-42.0.2 ELsmp #1, x86_64 GNU/Linux (Ref. 10)
- Computer Type: CPILE2 Linux cluster of the Nuclear Systems Analysis, Design, and Safety organization, Nuclear Science and Technology Division, ORNL

Rationale for Selection: SCALE is accepted by the U.S. Nuclear Regulatory Commission (NRC) for criticality safety applications.¹¹ This computer code system has multiple unique capabilities relevant to this work including automated sequences to produce problem-dependent multigroup cross-section data and analysis sequences for transport and depletion calculations.

The input and output files for the SCALE depletion calculations are located on a DVD that accompanies this report (refer to Appendix B for the contents of the DVD), so that an independent repetition of the calculations may be performed.

3.2 EXCEL

The commercial off-the-shelf software Microsoft Office Excel (copyright Microsoft Corporation) was used in calculations to manipulate the inputs and to tabulate and chart results using standard mathematical expressions and operations. Microsoft Excel was used only as a worksheet and not as a software routine. Therefore, Excel is exempt from the requirements of ORNL-OCRW-19.0, *Software Control*.⁹ All necessary information for reproducing the operations performed is provided on the DVD that accompanies this report, so that an independent repetition of the operations may be performed.

4 INPUT DATA

Direct inputs to the isotopic composition validation include measured isotopic concentrations and burnup of spent nuclear fuel samples, design and irradiation parameters for the analyzed spent fuel assemblies, material compositions and densities, nuclear data, etc., as detailed in the following sections.

Table 1 provides a summary of the direct inputs documented in the report, the sources of input data, and a justification for use as direct inputs. The direct inputs were obtained from primary reports published by radiochemical assay measurement programs, from industry handbooks, and from NRC- and industry-approved documents.

Table 1. Summary of direct inputs for spent fuel sample modeling

Parameter	Value	Source	Justification
Trino Vercellese data ^a	See Sects. 7.1 and 8.1	Refs. 12, 13, and 14	Primary experimental reports
KWO data ^a	See Sects. 7.2 and 8.2	Refs. 15, 16, 17, 18, 19, and 20	Primary experimental reports
Turkey Point Unit 3 data ^a	See Sects. 7.3 and 8.3	Refs. 21, 22, 23, 24, and 25	Primary experimental reports
H. B. Robinson Unit 2 data ^a	See Sects. 7.4 and 8.4	Refs. 26, 27, 28, and 29	Primary experimental reports
Calvert Cliffs Unit 1 data ^a	See Sects. 7.5 and 8.5	Refs. 30, 31, 32, 33, 34, 35, 36, 37, 38, 39, and 40	Primary experimental reports
Takahama Unit 3 data ^a	See Sects. 7.6 and 8.6	Refs. 41, 42, and 43	Primary experimental reports
TMI Unit 1 data ^a	See Sects. 7.7 and 8.7	Refs. 44, 45, 46, and 47	Primary experimental reports
Gösgen: ARIANE Program data ^a	See Sects. 7.8 and 8.8	Ref. 48	Primary experimental reports
GKN II data ^a	See Sects. 7.9 and 8.9	Refs. 49, 50, 51, 52, and 53	Primary experimental reports
Gösgen: MALIBU Program data ^a	See Sects. 7.10 and 8.10	Refs. 54 and 55	Primary experimental reports
General power plant data		Refs. 56 and 57	Industry-approved documents
Steam tables		Ref. 58	NRC-approved document
Nuclear data and fundamental general physics constants		Refs. 59, 60, 61, 62, 63	Industry handbooks

^aData consists of measured spent fuel isotopic compositions, sample burnup, measurement uncertainties, and assembly design and irradiation parameters.

5 ASSUMPTIONS

Values for certain physical and operational parameters (e.g., moderator density and temperature at the sample location along the fuel rod length, or the concentrations of ^{234}U and ^{236}U in initial fuel compositions) required as input data for depletion calculations are not always available in the original documents that describe spent fuel isotopic composition data. The following assumptions were used in all the calculations documented in this report to determine unavailable data.

5.1 INITIAL URANIUM ISOTOPIC CONTENTS

The uranium minor isotopes ^{234}U and ^{236}U are usually measured in irradiated fuel, but their concentration in fresh fuel is not always available. Uranium-234 depletes through neutron capture to form additional ^{235}U and is a long-lived isotope unaffected by reactor downtime and discharge from the reactor. Over long periods, minute quantities of ^{234}U are produced through alpha emissions in ^{238}Pu ($T_{1/2} = 87.7$ years). Uranium-236 is a long-lived isotope that depletes through neutron capture to form additional ^{237}U . However, the ^{236}U thermal capture cross section is small compared to that of ^{235}U . As a result, more ^{236}U is produced than is lost during reactor operation.

The fresh fuel uranium isotopic concentrations are assumed to have the dependence on X wt % ^{235}U enrichment as shown in Table 2 (Ref. 64). The isotopic ratio factors shown in the table were derived from mass spectrometric analyses of initial fuel for the Yankee Reactor Core V. Therefore, these isotopic ratio factors are mostly applicable to all fresh UO_2 fuel produced in the United States. However, the relationships shown in Table 2 were also used to determine the initial compositions of the evaluated spent fuel samples from the European reactors Trino Vercellese and Obrigheim because the applicable primary references do not provide the fuel ^{234}U and ^{236}U initial concentrations. As a result, the variability of the ^{234}U and ^{236}U validation results for the evaluated Trino Vercellese and Obrigheim samples may be large as compared to the variability obtained for the other spent fuel samples.

Table 2. Uranium isotope dependence on X wt % ^{235}U enrichment

Isotope	Assay, wt %
^{234}U	$0.0089 X$
^{235}U	$1.0000 X$
^{236}U	$0.0046 X$
^{238}U	$100-1.0135 X$

5.2 MODERATOR TEMPERATURE AND DENSITY

The moderator temperature as a function of the distance from the bottom of the active fuel region of the fuel rod is calculated using the following equation that was derived in Ref. 65. The equation is based on the assumption that the power density in the fuel rod varies approximately according to an idealized sinusoidal function that has the maximum value in the center of the fuel rod.

$$T(z) = T_{in} + \frac{T_{out} - T_{in}}{2} \left(1 - \cos \frac{\pi \cdot z}{H} \right) , \quad (1)$$

where

$T(z)$ = temperature (K) at height z (cm) with respect to the bottom of the fuel region,

T_{in} = inlet temperature (K),

T_{out} = outlet temperature (K),

H = total active fuel height (cm).

The moderator density depends on the coolant pressure and moderator temperature, which is determined as described by Eq. (1). The moderator density is taken directly from, or obtained by interpolating tabulated, compressed water density data available in Ref. 58 as a function of water pressure and temperature.

5.3 EFFECTIVE FUEL TEMPERATURE

Effective fuel temperature is an input parameter that is used to calculate resonance absorption in the fuel. For spent fuel samples with unavailable effective fuel temperature data, such as those from fuel assemblies irradiated in the Trino Vercellese and H. B. Robinson reactors, the temperature data for fuel assemblies with a similar design were used in the calculations. Thus, the effective fuel temperatures for the Trino Vercellese spent fuel samples were determined using data in Ref. 85, Table C-1, providing effective fuel temperature values versus specific power values for Yankee Rowe PWR fuel assemblies (see Sect. 8.1), whereas the effective fuel temperatures for the H. B. Robinson spent fuel samples were determined from the curve provided in Ref. 16, Fig. 2, showing effective fuel temperature versus rod linear power for Obrigheim fuel assemblies (see Sect. 8.4).

For spent fuel isotopic composition data sets for which fuel centerline and surface temperatures were available, the effective fuel temperature was assumed to be described by Eq. (2) (Ref. 66). This equation has been derived for an effective fuel temperature to be used for calculating resonance absorption in a $^{238}\text{UO}_2$ lump with a nonuniform temperature profile.

$$T_{eff} = T_s + \frac{4}{9}(T_c - T_s) . \quad (2)$$

In Eq. (2), T_{eff} is the effective fuel temperature, and T_c and T_s are the temperatures at the center and surface of the fuel rod, respectively.

5.4 BORON LETDOWN CURVE

Cycle-averaged soluble boron concentrations were available for many of the spent fuel samples considered. For those samples, it is assumed that soluble boron concentration during an irradiation cycle decreases linearly. Adjustment factors for computing soluble boron concentrations at various time steps within a cycle were taken from the boron letdown curve available in Ref. 67.

6 EXPERIMENTAL PROGRAMS AND DATA

6.1 SELECTION OF SPENT FUEL ISOTOPIC COMPOSITION DATA

Validation of the TRITON depletion analysis sequence is based on benchmarking code predictions against measured spent fuel isotopic concentrations. A total of 118 spent fuel samples selected from commercial PWR fuel assemblies were evaluated in this report. Most samples were obtained by sectioning individual fuel rods. Several samples were obtained from dissolved assemblies at a fuel reprocessing plant. Consistent with the *Disposal Criticality Analysis Methodology Topical Report* (Ref. 68), the evaluated spent fuel isotopic composition data sets provide measured isotopic concentrations for a set of 29 actinides and fission products, referred to as “principal isotopes” that are used in burnup-credit criticality calculations. The principal isotopes are listed in Table 3.

Table 3. Principal isotopes for burnup credit applications

Actinide isotopes		Fission product isotopes	
²³³ U	²³⁹ Pu	⁹⁵ Mo	¹⁴⁹ Sm
²³⁴ U	²⁴⁰ Pu	⁹⁹ Tc	¹⁵⁰ Sm
²³⁵ U	²⁴¹ Pu	¹⁰¹ Ru	¹⁵¹ Sm
²³⁶ U	²⁴² Pu	¹⁰³ Rh	¹⁵² Sm
²³⁸ U	²⁴¹ Am	¹⁰⁹ Ag	¹⁵¹ Eu
²³⁷ Np	^{242m} Am ^a	¹⁴³ Nd	¹⁵³ Eu
²³⁸ Pu	²⁴³ Am	¹⁴⁵ Nd	¹⁵⁵ Gd
		¹⁴⁷ Sm	

^aThe *m* refers to a long-lived metastable state of ²⁴²Am.

Radiochemical analysis measurements are reported for all of the principal isotopes with the exception of ²³³U for which the concentrations in spent fuel are lower than the detection limit at the time of measurement. At longer decay times, a significant amount of ²³³U is generated by the alpha decay of ²³⁷Np ($T_{1/2} > 10^6$ years). The concentration of ²³³U at long decay times can therefore be indirectly validated from ²³⁷Np measurements.

6.2 SUMMARY OF DATA USED IN PREVIOUS YMP ANALYSES

Isotopic analysis used to support the Yucca Mountain Project License Application (LA) submitted on June 3, 2008, included radiochemical assay for 74 samples for PWR fuel. The samples were obtained for the following reactors, as documented in the report titled *Calculation of Isotopic Bias and Uncertainty for PWR Spent Nuclear Fuel*.⁶⁹

Trino Vercellese	14 samples
Yankee Rowe	8 samples
Turkey Point	5 samples
Mihama	9 samples
H. B. Robinson	4 samples
Obrigheim	6 samples
Calvert Cliffs	9 samples
Three Mile Island	19 samples

Not all of the experimental data sets used in previous analyses to determine isotopic bias and uncertainty⁶⁹ were included in the current report.

The data for Mihama were omitted due to incomplete documentation of design and reactor operating information and due to unusually large variations observed in measured results for samples with similar burnup.⁷⁰ Future use of this set of data was not recommended because of the unexplained variation in the results, which may indicate problems related to the radiochemical analysis of samples or the incomplete documentation of operating data.

The Yankee Rowe (Yankee) reactor data were also omitted. The analyses performed for the Yankee data exhibit deviations of the measured data as compared with corresponding calculated data that were much larger than the deviations observed for other similar data sets considered. These deviations are thought to be due to samples located near the edge of the assembly that were exposed to control blades used in this reactor. The control blades perturb the neutronic environment of the fuel rods located at the periphery of the assembly. There was insufficient documented information on the blade insertion levels to enable the blades to be modeled. Evaluation of the Yankee data has also been hindered by the inability to access primary reference reports on the reactor operation for the irradiation cycles, referenced in earlier analyses as Safety Analysis Reports for the reactor. As it has not been possible to access the reports at this time, the reactor operating data could not be confirmed. For these reasons the Yankee data are not included in the current report.

The current report includes a total of 118 fuel samples and provides an analysis of additional data from several recent experimental programs (some proprietary) and from samples measured in previous experiments that have not been evaluated before (see Table 4).

The most significant differences compared to previously reported analyses are summarized below.

Trino Vercellese

All previously analyzed samples (14) are included in this report, and 17 previously unevaluated samples from the same experiment were added.

Obrigheim

Previous analyses of Obrigheim reactor fuel included data for six batch samples from five dissolved assemblies (each batch = half assembly) obtained from the Karlsruhe reprocessing plant. In this report, all ten batches were evaluated, and the two batch results for each assembly were combined, providing full assembly average data for five assemblies. In addition, 22 Obrigheim fuel rods samples measured under a different European benchmark program were included in this study. The fuel rod samples were not previously evaluated in the LA.

Calvert Cliffs

All Calvert Cliffs samples previously evaluated in the LA (nine samples) are included in this report. Additional measurements of lanthanide fission product isotopes for four of these samples made at the Khlopin Radium Institute (KRI) in Russia, measurements not previously used, are included in this report. The KRI data also include one measurement of ¹⁰³Rh.

Gösgen

New measurement data for UO₂ spent fuel from the Gösgen reactor, in Switzerland, are included in this report. The Gösgen data are obtained from the ARIANE and MALIBU international experimental programs⁷¹ coordinated by Belgonucleaire in Belgium. Measurements are reported for three samples in the ARIANE program and three samples in the MALIBU program. These data include extensive isotopic measurements that involve multiple laboratories for cross-check verification. Therefore, these data are

considered to be of high quality and reliability. The isotopic measurement data include all nuclides of importance to burnup credit. The Belgonucleaire programs are commercial proprietary, although only the MALIBU data are considered restricted from public access at this time.⁷¹

GKN II

New measurement data for one UO₂ fuel sample are available for the GKN II reactor in Neckarwestheim, Germany. The measurements are reported as part of the REBUS International Program,⁷² also coordinated by Belgonucleaire. These data include full isotopic measurements for nuclides of importance to burnup credit isotopic validation.

6.3 REVIEW OF RADIOCHEMICAL ANALYSIS DATA

The total number of measured spent fuel samples used in the isotopic composition validation is 118. Their initial enrichment and burnup vary between 2.453 and 4.657 wt % ²³⁵U and between 7.2 and 70.4 GWd/MTU, respectively. A summary of the experiments used to validate calculated spent fuel compositions is provided in Table 4. A comparison between sample burnup and enrichment values and the loading curve for the PWR SNF obtained from Ref. 73 is illustrated in Fig. 1. Physical parameters and irradiation conditions of the spent fuel samples are representative of the range of initial enrichment and burnup values for the inventory of commercial spent fuel assemblies in the United States.

Table 4. Summary of experiments used for validation of spent fuel compositions

Reactor	Measurement laboratory ^a	Experimental program name	Assembly design	Enrichment (wt % ²³⁵ U)	No. of samples/fuel rods	Burnup (GWd/MTU)
Trino Vercellese	JRC Ispra, Karlsruhe	EUR	15 × 15	2.719, 3.13, 3.897	15/5	7.2–17.5
	JRC Ispra, Karlsruhe	EUR	15 × 15	3.13	16/5	12.8–25.3
Obrigheim	JRC Ispra, Karlsruhe	EUR	14 × 14	2.83, 3.00	22/6	15.6–37.5
	ITU, IRCh, WAK, IAEA	ICE	14 × 14	3.13	5/5	27.0–29.4
Turkey Point-3	Battelle-Columbus	NWTS (CLIMAX)	15 × 15	2.556	5/2	30.5–31.6
H. B. Robinson-2	PNL	ATM-101 ^b	15 × 15	2.561	4/1	16.0–31.7
Calvert Cliffs-1	PNL, KRI	ATM-104	14 × 14	3.038	3/1	27.4–44.3
	PNL	ATM-103	14 × 14	2.72	3/1	18.7–33.2
	PNL, KRI	ATM-106	14 × 14	2.453	3/1	31.4–46.5
Takahama-3	JAERI	JAERI	17 × 17	2.63, 4.11	16/3	7.8–47.3
TMI-1	ANL	DOE YMP ^c	15 × 15	4.013	11/1	44.8–55.7
	GE-VNC	DOE YMP	15 × 15	4.657	8/3	22.8–29.9
Gösgen	SCK·CEN, ITU	ARIANE ^d	15 × 15	3.5, 4.1	3/2	29.1–59.7
	SCK·CEN, PSI, CEA	MALIBU ^d	15 × 15	4.3	3/1	47.2–70.4
GKN II	SCK·CEN	REBUS ^d	18 × 18	3.8	1/1	54.1

^aANL = Argonne National Laboratory; GE-VNC = General Electric Vallecitos Nuclear Center; PNL = Pacific Northwest National Laboratory; KRI = Khlopin Radium Institute; JAERI = Japan Atomic Energy Research Institute (now Japan Atomic Energy Agency); JRC = Joint Research Center, European Commission; ITU = European Institute for Transuranium Elements; IRCh = Institute for Radiochemistry at Karlsruhe; WAK = Karlsruhe Reprocessing Plant; IAEA = International Atomic Energy Agency; SCK·CEN = Studiecentrum voor Kernenergie – Centre d'étude de l'Energie Nucléaire; PSI = Paul Scherrer Institute; CEA = Commissariat à l'Energie Atomique.

^bATM = Approved Testing Material.

^cDOE YMP = U.S. Department of Energy Yucca Mountain Project.

^dInternational Experimental Programs coordinated by Belgonucleaire, Belgium – currently managed by SCK·CEN Laboratory (Ref. 71).

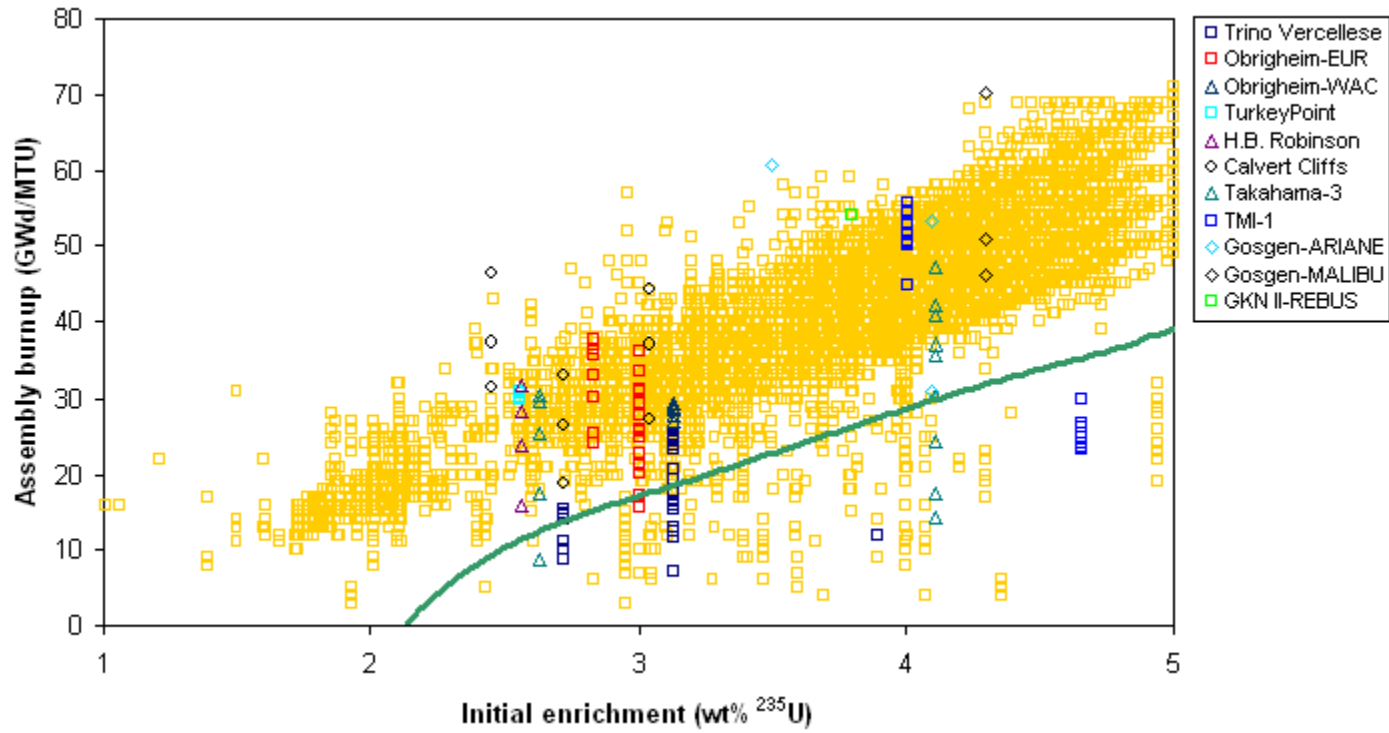


Fig. 1. Enrichment and burnup values of spent fuel samples used for validation compared to the actual and projected spent fuel assembly inventory and typical loading curve for PWR SNF assuming actinide and fission product burnup credit. (Note: Each point for the existing inventory represents multiple assemblies.)

In this report, measured values for all isotopes were evaluated. Reported values of isotopic ratios, which could not be directly converted to absolute contents, were not included. The number of measured nuclides is substantially greater than the list of principal isotopes considered in burnup credit. The additional isotopes include many that are of radiological importance (neutron and gamma ray emitters, e.g., ²⁴⁴Cm and ¹³⁷Cs), are important to decay heat (e.g. ¹³⁴Cs), and others that are important to longer term waste management safety analyses (e.g., ⁷⁹Se, ¹³⁵Cs). It is the intent that this report will serve not only as a radiochemical analysis database for burnup credit isotopic validation, but also validation for many other safety- and design-related applications important to post-closure and pre-closure analyses.

The complete list of nuclides evaluated in this report is listed below. Nuclides identified as the principal isotopes for burnup credit are shown in italics.

Actinides

- *²³⁴U, ²³⁵U, ²³⁶U, ²³⁸U*
- *²³⁸Pu, ²³⁹Pu, ²⁴⁰Pu, ²⁴¹Pu, ²⁴²Pu*
- *²³⁷Np, ²⁴¹Am, ^{242m}Am, ²⁴³Am*
- *²⁴²Cm, ²⁴³Cm, ²⁴⁴Cm, ²⁴⁵Cm, ²⁴⁶Cm, ²⁴⁷Cm*

Lanthanides

- *¹⁴³Nd, ¹⁴⁴Nd, ¹⁴⁵Nd, ¹⁴⁶Nd, ¹⁴⁸Nd, ¹⁵⁰Nd*
- *¹⁴⁴Ce, ¹⁴⁷Pm*
- *¹⁴⁷Sm, ¹⁴⁸Sm, ¹⁴⁹Sm, ¹⁵⁰Sm, ¹⁵¹Sm, ¹⁵²Sm, ¹⁵⁴Sm*
- *¹⁵¹Eu, ¹⁵²Eu, ¹⁵³Eu, ¹⁵⁴Eu, ¹⁵⁵Eu*
- *¹⁵⁴Gd, ¹⁵⁵Gd, ¹⁵⁶Gd, ¹⁵⁷Gd, ¹⁵⁸Gd, ¹⁶⁰Gd*

Volatile fission products

- *¹³³Cs, ¹³⁴Cs, ¹³⁵Cs, ¹³⁷Cs*

Metallic and other fission products

- *⁹⁰Sr, ⁹⁵Mo, ⁹⁹Tc, ¹⁰¹Ru, ¹⁰⁶Ru, ¹⁰³Rh, ¹⁰⁹Ag*
- *⁷⁹Se, ¹⁰⁵Pd, ¹⁰⁸Pd, ¹²⁶Sn, ¹²⁹Sb*

As noted previously, no measurements of ²³³U are included because of the very low concentrations in commercial spent fuel at the time of the laboratory analyses.

6.4 DATA QUALIFICATION

Qualification of the experimental data is not addressed in this report. However, as part of this work, the original data were obtained from primary experimental reports, reviewed, and evaluated for consistency. In several cases, measured isotopes were removed from consideration due to measurement results that were grossly out of trend when compared to other measurements made at the same laboratory or other measurements on similar fuel measured at independent laboratories. In some cases it is likely that the observed discrepancies are due to typographical errors in the experimental reports, or random or systematic measurement problems related to one or more samples or isotopes. Removal of measured data is discussed in the sections describing each experimental data set.

Many experimental programs described in this report used independent laboratory cross-check analyses. In some cases, samples from the same fuel assembly were measured at different laboratories. In other cases, laboratories performed independent radiochemical analysis on effectively the same sample, providing verification of measurements. The cross-check measurements provide a high degree of confidence to the radiochemical analysis results since in many cases the laboratories used different radiochemical techniques. Comparison of laboratory results also provides a reliable measure of experimental accuracy.

6.5 EXPERIMENTAL DATA ANALYSIS

Isotopic composition data were reported by laboratories in a number of different units. Isotopic data were converted in this report to a consistent basis of milligrams per gram of initial (unirradiated) uranium (mg/g U). This facilitates comparison of measurement data from different experiments and provides a consistent basis for comparison of measured with calculated results. In all cases, the unit conversion was performed independently of the code calculations.

The conversion of data reported measurement in units of $g/g \text{ fuel}$ to $mg/g \text{ U (initial)}$ is done using Eq. (3).

$$m(mg/gU) = m(g/g_{fuel}) (g \text{ fuel} / gU) \cdot 10^3 \text{ mg} / g . \quad (3)$$

The fraction of uranium mass with respect to the unirradiated fuel mass can be determined, if not provided, using Eq. (4), where \overline{M}_U is the average uranium atomic weight corresponding to the initial fuel enrichment.

$$gU / g \text{ fuel} = \frac{U}{UO_2} = \frac{\overline{M}_U}{(\overline{M}_U + 2M_O)} , \quad (4)$$

and

$$\overline{M}_U = 1 / \sum_i \frac{w_{U_i}}{M_{U_i}} .$$

In Eq. (4), M_O is the relative atomic mass for oxygen, M_{U_i} is the relative atomic mass for uranium isotope i , and w_{U_i} is the weight fraction of each uranium isotope. The weight fraction of uranium in fuel is about 0.8815 for the samples evaluated in this report.

In some cases, data reported as activity in disintegrations per second (dps), or curies (Ci), were converted to a mass basis. As an example, mass values m , in units of $mg/g \text{ U}$, were calculated from reported activities in $dps/(g \text{ fuel})$ using Eq. (5):

$$m(mg/gU) = \frac{\Lambda}{\lambda} \frac{M}{N_A} \frac{10^3}{0.8815} , \quad (5)$$

where

- Λ = reported activity in units of dps/(g fuel),
- λ = decay constant (s^{-1}),
- M = relative atomic mass,
- N_A = Avogadro's constant (mol^{-1}),
- 0.8815 = weight fraction of uranium in fuel [Eq. (4)].

The radiochemical analysis results were in some cases reported with respect to the measured total uranium or ^{238}U content in the fuel after irradiation. In order to compare measured data obtained from the different experimental programs, the data were converted to units of mg/g $U_{initial}$. The initial uranium in the measured sample was derived directly from the radiochemical analysis measurement data using the following procedures.

The initial concentration of heavy metal (uranium) atoms present in the fuel after irradiation is determined from the isotopic contents in the fuel sample according to:

$$\sum N_0 = \sum N_E + \sum \Delta N \quad , \quad (6)$$

where

- $\sum N_0$ = number of initial uranium atoms initially present,
- $\sum N_E$ = number of heavy metal atoms after irradiation,
- $\sum \Delta N$ = number of heavy metal atoms fissioned.

The sum is performed over all heavy metal nuclides (U, Np, Pu, Am, Cm). The integral number of fissions occurring in the fuel during irradiation can be determined by measurement of fission products with properties that make them reliable monitors of fission, i.e., their concentrations are proportional to the number of heavy element atoms fissioned. The isotope ^{148}Nd is a widely-used fission monitor that is used as a standard test method for atom fission⁷⁴ in ASTM E 321. Cesium-137 can also be used, provided that the decay of ^{137}Cs during the irradiation period is taken into account. Other isotopes like ^{150}Nd , $^{143}Nd+^{144}Nd$, and $^{145}Nd+^{146}Nd$ have also been used as reliable burnup monitors.⁷⁵ The method used in the current report relies primarily on measurements of ^{148}Nd that are reported for most fuel samples.

The number of atoms fissioned is calculated from the measured ^{148}Nd atom concentration and the effective fission yield of ^{148}Nd according to the relationship:

$$\sum \Delta N = \frac{N_{^{148}Nd}}{\bar{Y}_{^{148}Nd}} \quad , \quad (7)$$

where

- $N_{^{148}Nd}$ = total number of atoms of ^{148}Nd isotope measured,
- $\bar{Y}_{^{148}Nd}$ = effective fission product yield for ^{148}Nd .

Values for the ^{148}Nd fission yield exhibit only a small dependence of burnup, because the ^{148}Nd cumulative fission yields for ^{235}U and ^{239}Pu are similar. The effective ^{148}Nd yield values applied in this report were 0.0176 for the GKN II UO_2 fuel (Ref. 50) and 0.0170 for the other cases (e.g., TMI-1 UO_2

fuel) (Ref. 76). The estimate of the initial heavy metal mass is not very sensitive to this parameter because the amount of heavy metal fissioned represents typically less than 5% of the initial fuel mass.

Expressing the data in terms of mass m , Eq. (6) can be written:

$$\frac{m_{U_0}}{\overline{M}_U} = \sum \frac{m_E}{M_E} + \frac{1}{\overline{Y}_n} \frac{m_n}{M_n}, \quad (8)$$

where m_E is the measured mass and M_E is the relative atomic mass for each of the major heavy elements, and m_n and M_n are the measured mass and relative atomic mass of the of fission product burnup indicator (in this case ^{148}Nd). To a good approximation,

$$\overline{M}_U = M_E \approx 238$$

and therefore, the initial uranium mass in the unirradiated fuel, m_{U_0} , is calculated as

$$m_{U_0} \approx \sum_k m_{U_k} + m_{^{237}\text{Np}} + \sum_l m_{\text{Pu}_l} + \sum_m m_{\text{Am}_m} + \sum_n m_{\text{Cm}_n} + \frac{(238)}{(148)} \frac{m_{^{148}\text{Nd}}}{\overline{Y}_{^{148}\text{Nd}}}. \quad (9)$$

The majority of the heavy element mass in the irradiated fuel is associated with the uranium and plutonium isotopes. For samples that did not measure americium, and/or curium, their omission resulted in less than a 0.1% error in the estimated initial uranium content.

As an example of the procedure, measurement data m_i in units of mg/g ^{238}U in the sample, were adjusted to a basis of mg/g U initial uranium as follows:

$$m_i(\text{mg} / \text{g}U_{\text{initial}}) = \frac{m_i(\text{mg} / \text{g}^{238}\text{U})}{\sum_k m_{U_k} + m_{^{237}\text{Np}} + \sum_l m_{\text{Pu}_l} + \sum_m m_{\text{Am}_m} + \sum_n m_{\text{Cm}_n} + \frac{(238)}{(148)} \frac{m_{^{148}\text{Nd}}}{\overline{Y}_{^{148}\text{Nd}}}}, \quad (10)$$

where the measured mass for each of the isotopes in the denominator has units of mg/g ^{238}U .

6.6 NUCLEAR DATA

The nuclear data used to convert experimental measurements from reported units to mass units in this report was obtained from recent evaluations maintained by the National Nuclear Data Center (NNDC) at Brookhaven National Laboratory. These data included relative atomic mass values and radionuclide half-lives. The data are taken mostly from the adopted properties of the various nuclides as given in the Evaluated Nuclear Structure Data File (ENSDF).⁵⁹ ENSDF data are based on experiments and are published in Nuclear Data Sheets⁶⁰ for $A > 20$ and in Nuclear Physics⁶¹ for $A \leq 20$. Atomic mass data, used to derive nuclide mass values from atomic ratio measurements reported for some experiments, is obtained from the 2003 Atomic Mass Evaluation.⁶² The nuclear data used in this report are listed in Table 5.

The decay half-lives differ to some extent from the values used by the computer code calculations. The values used in this report were based on the latest evaluations available and were more recent than values used in the computer models, which are based on ENDF/B-VI Rel. 1. In general the half-life values

agreed to better than 3%. One exception is the half-life of ^{126}Sn , which increased from 10^5 in ENDF/B-VI to 2.30×10^5 years in ENSDF.

Other physical constants and unit conversion factors are:⁶³

$$N_A = \text{Avogadro's constant} = 6.02241 \times 10^{23} \text{ atoms} \cdot \text{mol}^{-1}$$

$$1 \text{ Ci} = 3.7 \times 10^{10} \text{ Bq}$$

$$1 \text{ Bq} = 1 \text{ disintegration} \cdot \text{s}^{-1}$$

Table 5. Nuclear data used for experiment data evaluation

Nuclide	Mass number	Relative atomic mass (u) ^a	Half-life ^b		Decay constant (s^{-1})
U	234	234.041	2.455E+05	Y ^c	8.9468E-14
	235	235.044	7.04E+08	Y	3.1200E-17
	236	236.046	2.342E+07	Y	9.3785E-16
	238	238.051	4.468E+09	Y	4.9160E-18
Pu	236	236.046	2.858	Y	7.6853E-09
	238	238.050	87.7	Y	2.5045E-10
	239	239.052	24110	Y	9.1101E-13
	240	240.054	6561	Y	3.3477E-12
	241	241.057	14.29	Y	1.5371E-09
	242	242.059	3.75E+05	Y	5.8572E-14
Am	241	241.057	432.2	Y	5.0820E-11
	242m	242.060	141	Y	1.5578E-10
	243	243.061	7370	Y	2.9803E-12
Cm	242	242.059	162.8	D ^c	4.9278E-08
	244	244.063	18.1	Y	1.2135E-09
Np	237	237.048	2.144E+06	Y	1.0245E-14
Se	79	78.918	2.95E+05	Y	7.4456E-14
Sr	90	89.908	28.9	Y	7.6002E-10
Tc	99	98.906	2.111E+05	Y	1.0405E-13
Ru	106	105.907	373.59	D	2.1474E-08
Sn	126	125.908	2.30E+05	Y	9.5498E-14
Cs	134	133.907	2.0652	Y	1.0636E-08
	135	134.906	2.30E+06	Y	9.5498E-15
	137	136.907	30.08	Y	7.3020E-10
Nd	143	142.910	Stable		
	144	143.910	Stable		
	145	144.913	Stable		
	146	145.913	Stable		
	148	147.917	Stable		
	150	149.921	Stable		
Ce	144	143.914	284.91	D	2.8158E-08
Eu	154	153.923	8.590	Y	2.5570E-09

^aRef. 62.

^bRef. 77.

^cY = years; D = days.

6.7 ANALYTICAL MEASUREMENT UNCERTAINTIES

Measurement uncertainties as reported by the laboratories have been included in this report. For experiments where uncertainty values are not given, it has been possible in some cases to derive approximate values by comparing reported measurement results for different fuel samples with similar properties. In general, it is difficult to apply the experimental uncertainties in the analysis in a quantitative fashion because the significance and method of evaluation of these uncertainties vary from one laboratory to another. Some laboratories report uncertainty associated only with the reproducibility of mass spectrometry results. In other cases the reported uncertainty includes additional sources of error due to sample preparation, isotopic dilution techniques, or standards. Sometimes reported uncertainties were based on past experience of the laboratory, whereas in other cases they were based on direct comparison of multiple measurement results for the same sample obtained independently by different laboratories using different radiochemical techniques. The inconsistent basis of the reported uncertainties makes it unreliable to use the uncertainty to weight data from different laboratories.

Nevertheless, the measurement uncertainties are listed in this report as they provide some indication of estimated measurement accuracy. However, it is not recommended that they be used quantitatively without further analysis to confirm the reported values. Comparisons of calculations and measurements in the current report include the estimated error from the experiment only in the experiment-to-calculation (E/C) isotopic concentration ratio. Additional errors in E/C values arise from calculational uncertainty related to the model input, nuclear cross section data, and reactor operating conditions. Uncertainty in the sample burnup, a value determined from the measurement data, can also have a significant effect on the level of agreement between calculations and measurements. Although error in the sample burnup manifests itself in the calculations, the error arises mainly from uncertainties and bias in the measurement.

7 EXPERIMENTAL DATA

This section describes the postirradiation analysis programs, the measurement techniques, and the reported isotopic concentrations and uncertainties for the evaluated spent fuel samples, as provided by the primary references (see Sect.4). Summary tables containing sample characteristics and isotopic concentrations relative to the initial uranium mass, which were derived from the reported experimental data, are provided in this section.

7.1 TRINO VERCELLESE

Trino Vercellese was a PWR in Italy with a net generating capacity of 270 MWe, which was designed by Westinghouse Electric Corp. (West). First power was achieved in October 1964 with an initial core consisting of West 15×15 assemblies.⁵⁷

As part of a joint European research program, the isotopic composition of fuel samples from eight rods selected from three assemblies identified as 509-104 (core location L-7), 509-032 (H-10), and 509-049 (G-7), which were irradiated in the reactor for one cycle, were measured using nondestructive and destructive methods.¹² Sixteen fuel samples from six rods from assembly 509-069, which was irradiated for two reactor cycles, were also measured.¹³ A summary of the 31 evaluated fuel samples from this program are listed in Table 6. The assembly configuration and the position of the measured fuel rods in each assembly are illustrated in Fig. 4 and Fig. 5, respectively (see Sect. 8.1). The samples are identified by the rod location followed by the axial sampling position, numbered 1 to 9 from the top of the rod. Additional samples from fuel rod locations identified in the experimental reports as residing in perturbed assembly periphery locations were not analyzed due to potential exposure to control rods used in the reactor for which documentation was not available.

Measurements were performed at laboratories of the European Ispra and Karlsruhe establishments of the Joint Research Centre. A total of 31 fuel samples with reported measurement data are evaluated in this report. Of these samples, eight samples were measured at both laboratories, providing an independent cross-check of the measurement accuracy. The measurements are described briefly.

Mass spectrometry with isotopic dilution was used to determine the isotopic compositions and concentrations of uranium, plutonium and neodymium isotopes, using calibrated spikes of ^{233}U , ^{242}Pu , and ^{150}Nd . Mass spectrometry without isotopic dilution was applied to measure americium. Alpha spectrometry was used for determination of some plutonium isotopes, ^{241}Am , ^{242}Cm , and ^{244}Cm , using measured activity ratios and mass spectrometry data. Atom and mass ratios were reported by the laboratories, as was the absolute isotopic mass with respect to initial mass of uranium in the sample.

Gamma-ray spectroscopy was used to measure the activities of radioactive fission products ^{106}Ru , ^{134}Cs , ^{137}Cs , ^{144}Ce , and ^{154}Eu for samples measured at Ispra. The fission product activities were reported with respect to the mass of final uranium in the samples. Activity results were converted to mass units in this report using Eq. (5), and normalized to a basis of initial uranium in the sample using the ratio of final-to-initial uranium determined from the measurements (see spreadsheet *DVD/xls/Experimental_data.xls*).

Measurements performed by the European Institute for Transuranium Elements (ITU) at Karlsruhe did not include fission products, except for ^{148}Nd and ^{137}Cs values used for burnup verification, but did include fission gas collection during dissolution and measurement of Xe and Kr isotopic ratios by mass spectrometry. The xenon and krypton measurements are not analyzed in this report.

Table 6. Summary of the Trino Vercellese measured spent fuel

Assembly	Sample No.	Measurement laboratory	Sample	Initial enrichment (wt % ²³⁵ U)	Axial location ^a (cm)	Burnup ^b (GWd/MTU)
509-032	1	Ispra	E11-1	3.13	246.7	7.243
	2	Ispra	E11-4	3.13	165.6	15.377
	3	Ispra	E11-7	3.13	81.4	15.898
	4	Ispra	E11-9	3.13	28.8	11.529
	5	Karlsruhe	H9-4	3.13	165.6	16.556
	6	Ispra	H9-7	3.13	81.4	17.450
	7	Ispra	H9-9	3.13	28.8	12.366
509-049	8	Ispra	L5-1	2.719	246.7	7.822 ^c
	9	Ispra-Karlsruhe	L5-4	2.719	165.6	14.323
	10	Ispra-Karlsruhe	L5-9	2.719	28.8	10.187
	11	Ispra	J8-1	2.719	246.7	8.713
	12	Ispra	J8-4	2.719	165.6	14.770
	13	Karlsruhe	J8-7	2.719	81.4	15.193
	14	Karlsruhe	J8-9	2.719	28.8	11.127
509-104	15	Ispra-Karlsruhe	M11-7	3.897	81.4	12.042
509-069	16	Ispra	E11-1	3.13	246.7	12.859 ^c
	17	Karlsruhe	E11-2	3.13	221.1	20.602
	18	Karlsruhe	E11-4	3.13	165.6	23.718
	19	Ispra	E11-5	3.13	137.1	24.518
	20	Karlsruhe	E11-7	3.13	81.4	24.304
	21	Karlsruhe	E11-8	3.13	55.4	23.406
	22	Karlsruhe	E11-9	3.13	28.8	19.250
	23	Ispra	E5-4	3.13	165.6	23.867
	24	Karlsruhe	E5-7	3.13	81.4	24.548
	25	Ispra	E5-9	3.13	28.8	19.208
	26	Ispra	J9-4	3.13	165.6	24.849 ^c
	27	Karlsruhe	J9-7	3.13	81.4	25.258
	28	Ispra	L5-4	3.13	165.6	24.330
	29	Ispra	L5-7	3.13	81.4	24.313 ^c
	30	Karlsruhe	L11-4	3.13	165.6	23.928
	31	Ispra-Karlsruhe	L11-7	3.13	81.4	24.362

^aDistance between sample axial location and the bottom of the active fuel (Ref. 14).

^bBurnup based on measured ¹⁴⁸Nd concentration except as noted.

^cBurnup based on measured ¹³⁷Cs concentration using destructive methods because no analysis of ¹⁴⁸Nd was reported.

Measurement data was adjusted by the laboratories to the time corresponding to discharge for all isotopes except ²⁴¹Am, which was reported near the actual time of measurement (about 3 years after discharge) to avoid introducing potentially large errors associated with the correction.^{12,13} Isotopic data for plutonium was corrected for ²³⁸Pu formation from ²⁴²Cm decay, and correction of ²³⁶Pu and ²⁴¹Pu for decay. Note that ²³⁹Pu includes the contribution from short-lived ²³⁹Np decay.

The reported measurement uncertainties are summarized in Table 7. Experimental uncertainties for uranium and plutonium were determined by comparison between the results for the nine replicate samples analyzed at both Ispra and Karlsruhe. The relative standard deviations were derived from the differences of the replicate samples. Note that the reported error of 4.3% for ²³⁸U depletion reduces to about 0.1% in the final ²³⁸U content due to the small amount of ²³⁸U depleted during irradiation. Measurement uncertainties for americium and curium isotopes were similarly obtained from Ispra-Karlsruhe interlaboratory comparisons. Uncertainties for ²⁴¹Am, measured only by Ispra, and ¹⁴⁸Nd were obtained

from other reported intercomparison studies in Ref. 14. The relative error for the γ -spectroscopy measurements were reported by Ispra (^{134}Cs , ^{137}Cs , ^{106}Ru , ^{144}Ce , and ^{154}Eu) and include statistical errors of the gamma measurements, errors due to calibration standards, and errors due to the determination of the amount of uranium in the measured solutions. Comparison of ^{137}Cs measurements made at Ispra and Karlsruhe confirmed the estimated measurement error.

Table 7. Experimental techniques and uncertainties for Trino Vercellese spent fuel samples

Nuclide	Technique ^a	RSD (%) ^b
U-235 depleted ^c	IDMS	1.6%
U-235	IDMS	<2.5%
U-236	IDMS	2.4%
U-238 depleted ^c	IDMS	4.3%
U-238	IDMS	<0.1%
Pu-238	IDMS	2.7%
Pu-239	IDMS	2.0%
Pu-240	IDMS	2.2%
Pu-241	IDMS	2.3%
Pu-242	IDMS	2.8%
Cm-242	α spec	2%
Cm-244	α spec	7%
Am-241	α spec	20%
Am-242	α spec	11%
Am-243	α spec	8%
Nd-148	IDMS	<1%
Ru-106 ^d	γ spec	3%
Cs-134 ^d	γ spec	2.5%
Cs-137 ^d	γ spec	1.5%
Ce-144 ^d	γ spec	1.7%
Eu-154 ^e	γ spec	5%

^aMain technique is listed; some nuclides require multiple techniques to eliminate interferences.

^bRelative standard deviation (RSD) (see *DVD/xls/Experimental_data.xls*, worksheet *trinoll*).

^c ^{235}U and ^{238}U contents and uncertainties reported as depleted content.

^dRef. 12, pp. 28 and 30.

^eRef. 13, p. 23.

Americium results were only reported for samples of assembly 509-069, and Ispra was the only laboratory to measure ^{241}Am . The error in the Am isotopes (20%) is relatively large due to the measurement method by α -spectrometry and data regression analysis that required using activity ratios of Am and mass spectrometry data. Error in the determination of ^{236}Pu by α -spectrometry, reported for some samples measured at Ispra, is about 10% due to the very small concentration in the fuel and consequently low counting rates.

The total error in the determination of ^{148}Nd , including the uncertainties due to the isotopic dilution procedures and standards, is reported to be about 1%. The reported burnup values for each sample based on destructive ^{148}Nd and ^{137}Cs (corrected for decay during irradiation) and nondestructive ^{137}Cs data (measured only at Ispra) are listed in Table 8. These values are derived by the laboratories from the

experimental data. The error in the estimated burnup from destructive ^{137}Cs gamma measurements is 4%, and the error using the ^{148}Nd method is 2% (Refs. 12 and 13). The ^{148}Nd and ^{137}Cs burnup values are seen to be in good agreement with an average difference of 1.6% and maximum difference of 4%. The average difference in the burnup estimated by ^{137}Cs between the Ispra and Karlsruhe laboratories is about 2%. The ^{148}Nd burnup has the smallest uncertainty and was used in this study when available. In cases where ^{148}Nd values were measured at both the Ispra and Karlsruhe, an average of the two burnup values was used. For samples without measured ^{148}Nd values (e.g., 509-069 E11-1, J9-4), burnup was based on the destructive ^{137}Cs values.

Table 8. Burnup values derived from experimental measurements

Assembly	Sample	Laboratory	Burnup based on ^{148}Nd ^a (MWd/MTU)	Burnup based on ^{137}Cs ^a (MWd/MTU)	Burnup based on ^{137}Cs ^b (MWd/MTU)	Recommended burnup (MWd/MTU)
509-032	E11-1	Ispra	7,243	7,415	7,340	7,243
	E11-4	Ispra	15,377	15,156	14,697	15,377
	E11-7	Ispra	15,898	15,477	15,251	15,898
	E11-9	Ispra	11,529	11,226	12,119	11,529
	H9-4	Karlsruhe	16,556	16,400	16,719	16,556
	H9-7	Ispra	17,450	17,064	16,885	17,450
	H9-9	Ispra	12,366	12,219	12,415	12,366
509-049	L5-1	Ispra		7,822	7,987	7,822
	L5-4	Ispra	14,155	14,099	14,645	
	L5-4	Karlsruhe	14,490	13,883		14,323
	L5-9	Ispra		10,478	11,252	
	L5-9	Karlsruhe	10,187	10,444		10,187
	J8-1	Ispra	8,713	8,307	8,584	8,713
	J8-4	Ispra	14,770	14,644	15,024	14,770
	J8-7	Karlsruhe	15,193	15,007	15,442	15,193
J8-9	Karlsruhe	11,127	11,142	10,706	11,127	
509-104	M11-7	Ispra	11,912	12,035	12,606	
	M11-7	Karlsruhe	12,172	12,242		12,042
509-069	E11-1	Ispra		12,859	15,030	12,859
	E11-2	Ispra		20,628	21,200	
	E11-2	Karlsruhe	20,602	21,296		20,602
	E11-4	Ispra		23,557	23,990	
	E11-4	Karlsruhe	23,718	23,969		23,718
	E11-5	Ispra	24,518	24,250		24,518
	E11-7	Ispra		23,953	22,822	
	E11-7	Karlsruhe	24,304	25,095		24,304
	E11-8	Karlsruhe	23,406	23,818		23,406
	E11-9	Karlsruhe	19,250	20,060	19,150	19,250
	E5-4	Ispra	23,867	23,715	22,640	23,867
	E5-7	Ispra		24,693	23,380	
	E5-7	Karlsruhe	24,548	24,683		24,548
	E5-9	Ispra	19,208	19,254	19,260	19,208
	J9-4	Ispra		24,849	25,030	
	J9-7	Karlsruhe	25,258	25,386	25,340	25,258
	L5-4	Ispra	24,330	23,988	24,070	24,330
L5-7	Ispra		24,313	24,230		
L11-4	Karlsruhe	23,928	24,050	25,770	23,928	
L11-7	Ispra	24,023	24,471	25,290		
L11-7	Karlsruhe	24,700	24,532		24,362	

^aBased on destructive measurements.^{12,13}

^bBased on nondestructive measurements performed only at Ispra.^{12,13}

The isotopic contents of the fuel samples are listed in Table 9. Results for samples measured at both Ispra and Karlsruhe were averaged. The data for americium and curium isotopes, reported as atom ratios to initial uranium atoms, were adjusted to mass ratios using the atomic weight for each isotope. The mass of depleted ^{238}U was only reported for samples from assembly 506-069. The ^{238}U content for other samples was calculated in this report using the measured $^{235}\text{U}/^{238}\text{U}$ atom ratio for each sample and the absolute ^{235}U content.

The measurements were evaluated by comparing the trends in the measured isotope concentrations as a function of burnup for samples with the same initial enrichment. In most cases the observed variance was consistent with the reported uncertainty. Analysis of the experimental data for ^{242}Pu indicates that the data for assembly 509-032 sample H9-9 is significantly out of trend with other data and this measurement point was rejected. It appears that the value is about an order of magnitude too large, and is most likely attributed to a reporting error.

Table 9. Experimental results for Trino Vercellese fuel samples (mg/g U_{initial})

Assembly	509-049 ^a	509-049 ^a	509-049 ^a	509-049 ^a	509-049 ^a	509-049 ^a	509-049 ^a	509-032 ^a	509-032 ^a	509-032 ^a
Sample ID	L5-1	L5-4	L5-9	J8-1	J8-4	J8-7	J8-9	E11-1	E11-4	E11-7
Burnup (MWd/MTU)	7,822	14,323	10,187	8,713	14,770	15,193	11,127	7,243	15,377	15,898
U-234	1.291E-01	1.435E-01	1.545E-01	1.367E-01	1.312E-01			2.110E-01	2.312E-01	1.410E-01
U-235	1.972E+01	1.503E+01	1.745E+01	1.854E+01	1.390E+01	1.386E+01	1.663E+01	2.329E+01	1.728E+01	1.661E+01
U-236										
U-238	9.658E+02	9.601E+02	9.639E+02	9.654E+02	9.603E+02	9.595E+02	9.635E+02	9.624E+02	9.558E+02	9.558E+02
Pu-236										
Pu-238										
Pu-239	3.608E+00	5.016E+00	4.116E+00	3.606E+00	4.769E+00	4.926E+00	4.134E+00	3.483E+00	5.266E+00	5.234E+00
Pu-240	5.150E-01	1.121E+00	7.325E-01	5.600E-01	1.160E+00	1.196E+00	8.020E-01	4.420E-01	1.118E+00	1.137E+00
Pu-241	2.040E-01	6.025E-01	3.375E-01	2.280E-01	6.150E-01	6.370E-01	3.710E-01	1.710E-01	6.140E-01	6.180E-01
Pu-242	1.532E-02	8.493E-02	3.373E-02	1.887E-02	9.938E-02	1.026E-01	4.205E-02	1.170E-02	8.425E-02	9.252E-02
Cm-242										
Cm-244										
Am-241										
Am-242m										
Am-243										
Ru-106	3.110E-02	6.575E-02	4.440E-02	3.345E-02	7.013E-02			2.522E-02	6.417E-02	6.855E-02
Nd-148		1.601E-01	1.141E-01	9.778E-02	1.649E-01	1.695E-01	1.245E-01	8.135E-02	1.718E-01	1.776E-01
Cs-134	1.046E-02	3.229E-02	1.757E-02	1.205E-02	3.467E-02			9.394E-03	3.601E-02	3.809E-02
Cs-137	2.911E-01	5.269E-01	3.908E-01	3.100E-01	5.467E-01			2.764E-01	5.700E-01	5.773E-01
Ce-144	1.330E-01	2.053E-01	1.640E-01	1.411E-01	2.113E-01			1.358E-01	2.249E-01	2.201E-01
Eu-154										

Table 9. Experimental results for Trino Vercellese fuel samples (mg/g U_{initial}) (continued)

Assembly	509-032 ^a	509-032 ^a	509-032 ^a	509-032 ^a	509-104 ^a	509-069 ^b	509-069 ^b	509-069 ^b	509-069 ^b	509-069 ^b
Sample ID	E11-9	H9-4	H9-7	H9-9	M11-7	E5-4	E5-7	E5-9	L5-4	L5-7
Burnup (MWd/MTU)	11,529	16,556	17,450	12,366	12,042	23,867	24,548	19,208	24,330	24,313
U-234			1.502E-01	1.676E-01						
U-235	2.017E+01	1.672E+01	1.631E+01	1.889E+01	2.663E+01	1.291E+01	1.221E+01	1.514E+01	1.297E+01	1.231E+01
U-236						3.530E+00	3.545E+00	3.270E+00	3.480E+00	3.570E+00
U-238	9.595E+02	9.551E+02	9.548E+02	9.471E+02	9.513E+02	9.496E+02	9.487E+02	9.536E+02	9.491E+02	9.476E+02
Pu-236						6.560E-07		3.130E-07	7.420E-07	7.640E-07
Pu-238						1.170E-01	1.155E-01	6.300E-02	1.100E-01	1.140E-01
Pu-239	4.418E+00	5.172E+00	5.234E+00	4.446E+00	4.586E+00	5.950E+00	5.980E+00	5.270E+00	6.060E+00	5.970E+00
Pu-240	7.750E-01	1.211E+00	1.247E+00	8.340E-01	7.165E-01	1.760E+00	1.785E+00	1.330E+00	1.770E+00	1.790E+00
Pu-241	3.690E-01	6.760E-01	6.940E-01	4.090E-01	3.475E-01	1.050E+00	1.055E+00	7.300E-01	1.060E+00	1.060E+00
Pu-242	3.709E-02	1.047E-01	1.080E-01		3.057E-02	2.400E-01	2.540E-01	1.350E-01	2.440E-01	2.500E-01
Cm-242						2.319E-02	2.513E-02	1.394E-02	2.523E-02	2.482E-02
Cm-244						8.964E-03	9.426E-03	2.544E-03	9.528E-03	8.790E-03
Am-241						2.223E-01	2.444E-01	1.526E-01	2.432E-01	2.989E-01
Am-242m							2.441E-03			
Am-243							4.617E-02			
Ru-106	4.701E-02		7.261E-02	5.047E-02	4.248E-02					
Nd-148	1.291E-01	1.848E-01	1.946E-01	1.366E-01	1.349E-01	2.669E-01	2.743E-01	2.164E-01	2.709E-01	
Cs-134	2.096E-02		4.287E-02	2.285E-02	2.108E-02	5.914E-02	6.135E-02	3.980E-02	5.911E-02	6.030E-02
Cs-137	4.185E-01		6.373E-01	4.495E-01	4.484E-01	8.354E-01	8.703E-01	6.780E-01	8.449E-01	8.553E-01
Ce-144	1.748E-01		2.407E-01	1.952E-01	1.813E-01					
Eu-154						1.698E-02	1.843E-02	1.113E-02	1.700E-02	1.774E-02

Table 9. Experimental results for Trino Vercellese fuel samples (mg/g U_{initial}) (continued)

Assembly	509-069 ^b	509-069 ^b	509-069 ^b	509-069 ^b	509-069 ^b	509-069 ^b	509-069 ^b	509-069 ^b	509-069 ^b	509-069 ^b	509-069 ^b	509-069 ^b
Sample ID	E11-1	E11-2	E11-4	E11-5	E11-7	E11-8	E11-9	L11-4	L11-7	J9-4	J9-7	
Burnup (MWd/MTU)	12,859	20,602	23,718	24,518	24,304	23,406	19,250	23,928	24,362	24,849	25,258	
U-234												
U-235	1.946E+01	1.436E+01	1.248E+01	1.227E+01	1.235E+01	1.262E+01	1.497E+01	1.282E+01	1.225E+01	1.201E+01	1.175E+01	
U-236	2.450E+00	3.315E+00	3.615E+00	3.620E+00	3.640E+00	3.590E+00	3.240E+00	3.760E+00	3.465E+00	3.640E+00	3.690E+00	
U-238	9.591E+02	9.522E+02	9.498E+02	9.491E+02	9.496E+02	9.502E+02	9.542E+02	9.489E+02	9.486E+02	9.483E+02	9.489E+02	
Pu-236		3.740E-07	7.190E-07	6.560E-07					6.860E-07			
Pu-238	2.500E-02	8.050E-02	1.090E-01	1.170E-01	1.170E-01	1.190E-01	6.800E-02	1.060E-01	1.160E-01	1.200E-01	1.340E-01	
Pu-239	4.580E+00	5.755E+00	5.895E+00	6.010E+00	6.070E+00	5.910E+00	5.630E+00	6.060E+00	5.995E+00	5.820E+00	5.830E+00	
Pu-240	8.400E-01	1.520E+00	1.755E+00	1.790E+00	1.825E+00	1.720E+00	1.410E+00	1.790E+00	1.810E+00	1.810E+00	1.840E+00	
Pu-241	4.000E-01	8.850E-01	1.030E+00	1.040E+00	1.060E+00	1.030E+00	7.800E-01	1.050E+00	1.055E+00	1.070E+00	1.080E+00	
Pu-242	4.600E-02	1.720E-01	2.435E-01	2.400E-01	2.575E-01	2.320E-01	1.470E-01	2.470E-01	2.590E-01	2.700E-01	2.820E-01	
Cm-242	5.188E-03	1.770E-02	2.436E-02	2.574E-02	2.665E-02	2.452E-02	1.739E-02	2.797E-02	2.467E-02	2.553E-02	2.848E-02	
Cm-244		4.677E-03	9.021E-03	9.918E-03	9.908E-03	7.590E-03	3.641E-03	9.159E-03	9.739E-03	1.070E-02	9.672E-03	
Am-241	8.439E-02	1.748E-01	2.089E-01	3.089E-01	3.011E-01				2.033E-01	2.120E-01		
Am-242m		1.389E-03	2.126E-03	2.777E-03	2.258E-03	2.177E-03	2.096E-03	1.963E-03	2.192E-03		2.085E-03	
Am-243		2.395E-02	4.535E-02	5.495E-02	4.586E-02	4.372E-02	3.013E-02	4.454E-02	4.249E-02		5.015E-02	
Ru-106												
Nd-148		2.309E-01	2.657E-01	2.803E-01	2.722E-01	2.623E-01	2.159E-01	2.679E-01	2.725E-01		2.826E-01	
Cs-134	1.925E-02	4.672E-02	5.862E-02	6.090E-02	6.007E-02				6.123E-02	6.288E-02		
Cs-137	4.527E-01	7.276E-01	8.313E-01	8.572E-01	8.439E-01				8.618E-01	8.751E-01		
Ce-144												
Eu-154	5.057E-03	1.351E-02	1.711E-02	1.507E-02	1.586E-02				1.650E-02	1.618E-02		

^aMeasurements for 509-049, 509-032, and 509-104 reported at discharge date of 4/28/1967 (Ref. 12).

^bMeasurements for 509-069 reported at discharge date of 7/9/1971, except for ²⁴¹Am, reported at 7/9/1974 (Ref. 13).

7.2 OBRIGHEIM (KWO)

Obrigheim KWO was a PWR in Germany with a net generating capacity of 357 MWe, which was designed by Siemens AG. First power was achieved in October 1968 with an initial core consisting of Reaktor-Brennelement Union (RBU) 14×14 assemblies.⁵⁷

Fuel assemblies from the Obrigheim Kernkraftwerk Obrigheim GmbH (KWO) reactor were the subject of post-irradiation examination and isotopic measurements. Isotopic measurements were performed under two separate experimental programs of the

- European institutes in the framework of the Isotopic Correlation Experiment (ICE) that performed measurements on fuel assemblies reprocessed at the Karlsruhe reprocessing plant and
- European JRC Ispra and Karlsruhe Establishments in the framework of a European benchmark-experiment activity.

7.2.1 Karlsruhe Reprocessing Plant (WAK)

Radiochemical analysis data for five KWO fuel assemblies, BE168, BE171, BE176, BE172, and BE170, reprocessed at the Karlsruhe Reprocessing Plant, were reported by Gesellschaft für Reaktorsicherheit mbH (GRS) in Germany.¹⁶ Independent measurements were performed at laboratories of the European Institute for Transuranium Elements (ITU), Institute for Radiochemistry at Karlsruhe (IRCh), Karlsruhe Reprocessing Plant (WAK), and International Atomic Energy Agency (IAEA). The experiments are unique in that full-length fuel assemblies were analyzed, instead of samples from individual fuel rods used in many experiments. The configuration of the Obrigheim KWO assembly is shown in Fig. 6 (see Sect. 8.2).

During reprocessing, each assembly was divided lengthwise and analyzed individually in two batches, each batch corresponding to a half assembly. In this report, the measurement data for the two batches were combined to obtain assembly-average isotopic concentrations. The main measurement techniques and experimental uncertainties are summarized in Table 10. The assemblies and batch numbers are summarized in Table 11. The burnup values for each batch, determined experimentally from ¹⁴⁸Nd measured at ITU had an estimated accuracy of about 4%.

Table 10. Experimental techniques and uncertainties for Obrigheim measurements at WAK

Assembly	Method	RSD ^a (%)
U-238 ^b		< 0.2
U-235	IDMS	0.7
U-236	IDMS	0.9
Pu-238	IDMS	6.3
Pu-239	IDMS	2.4
Pu-240	IDMS	2.7
Pu-241	IDMS	2.5
Pu-242	IDMS	3.6
Am-241	α -spec	<100
Am-243	α -spec	<100
Cm-242	α -spec	<100
Cm-244	α -spec	20

^aRelative standard deviation.

^bValues for ²³⁸U derived from other measurements.

Table 11. Summary of measured Obrigheim assemblies reprocessed at WAK

Assembly	Initial enrichment (wt % ²³⁵ U)	Batch	Batch burnup ^a (MWd/MTU)	Assembly burnup ^b (MWd/MTU)
BE 168	3.13	86	28,400	29,350
		87	30,300	
BE 171	3.13	88	28,270	28,655
		89	29,040	
BE 176	3.13	90	29,520	28,755
		91	27,990	
BE 172	3.13	92	26,540	27,890
		93	29,240	
BE 170	3.13	94	25,930	27,005
		95	28,080	

^aExperimental value based on ¹⁴⁸Nd provided in Ref. 16, Table 4.

^bAverage of the two reprocessing batches for each assembly.

All four laboratories measured the uranium and plutonium isotopes. Tabulated data representing average batch results from all laboratories, in units of grams per ton initial uranium, were obtained from GRS report GRS-A-962 (Ref. 16). Isotopic ratios of fission products Kr, Xe, Nd, and Cs (not evaluated in this report) and concentrations of americium and curium were measured only at ITU. The GRS data were independently verified by digitizing graphical measurement data available for each laboratory using figures published in Kernforschungszentrum Karlsruhe report KfK 3014 (Ref. 17). Measurements were performed three years after the fuel was discharged from the reactor and the data were adjusted to the time of discharge by each institute.

Measured isotope contents are listed in Table 12. The data for uranium and plutonium represent an average of the measurements from each of the four laboratories. In the case of ²³⁸Pu, the concentrations must be corrected for the contribution from ²⁴²Cm decay. Since curium isotopes were only measured by ITU, only the ITU values for ²³⁸Pu account for ²⁴²Cm decay and therefore were the only data used for ²³⁸Pu. The ITU data were obtained from digitized plots of the results from each laboratory.¹⁷ The uncertainty in the measurements was estimated in the current report as the standard deviation of the difference in measured values from each of the four laboratories. Data for ²³⁸U content was not reported by any laboratory but were derived in the current study using measurement data for the other heavy metal isotopes. Correction for the heavy metal mass loss from fission was estimated using the value of the fissions per initial metal atom (% FIMA). The sample % FIMA was determined from the sample burnup using a value of 9.6 ± 0.3 GWd/MTU per % FIMA.⁷⁴ The mass of all heavy metal isotopes (including ²³⁸U) plus the heavy metal loss based on the % FIMA value is the initial heavy metal content (known). Therefore, the residual obtained when ²³⁸U is excluded effectively represents the ²³⁸U content in the sample. The estimated uncertainty in the ²³⁸U content includes the uncertainty in the measured heavy metal content, burnup, and uncertainty in the % FIMA value.

Americium and curium data, reported only by ITU, were measured using α -spectrometry and mass spectrometry. Large measurement uncertainties were associated with interferences in α -spectrometry. In the case of ²⁴¹Am, adjustment of the data to the time of discharge resulted in significant experimental uncertainties of sometimes up to 100% and erratic behavior of the results when trended as a function of burnup. The concentration of ²⁴⁴Cm was measured with an estimated accuracy of 20%. Due to the large uncertainty and variability in most of the curium and americium data, only the results for ²⁴⁴Cm are considered acceptable for code validation in this report. For completeness, all measurement data are listed in Table 12.

Table 12. Measurement data for Obrigheim assemblies reprocessed at WAK (mg/g U_{initial})

Assembly	BE168	BE171	BE176	BE172	BE170
Burnup (MWd/MTU)	29,350	28,655	28,755	27,890	27,005
U-238 ^a	9.474E+02	9.481E+02	9.481E+02	9.491E+02	9.494E+02
U-235	9.346E+00	9.657E+00	9.504E+00	9.830E+00	1.043E+01
U-236	3.785E+00	3.738E+00	3.751E+00	3.680E+00	3.651E+00
Pu-238 ^b	1.192E-01	1.028E-01	1.069E-01	9.392E-02	8.875E-02
Pu-239	5.008E+00	4.923E+00	4.928E+00	4.793E+00	4.876E+00
Pu-240	2.046E+00	1.961E+00	1.982E+00	1.895E+00	1.881E+00
Pu-241	1.123E+00	1.076E+00	1.093E+00	1.031E+00	1.026E+00
Pu-242	4.290E-01	3.880E-01	4.035E-01	3.720E-01	3.445E-01
Am-241	6.550E-02	1.095E-01	1.140E-01	1.100E-01	1.125E-01
Am-243	2.585E-02	4.120E-02	4.415E-02	3.805E-02	2.710E-02
Cm-242	2.135E-02	2.010E-02	2.020E-02	2.180E-02	1.880E-02
Cm-244	1.755E-02	1.590E-02	1.675E-02	1.420E-02	1.245E-02

^aValues for ²³⁸U are derived from other measurement data.

^bValues for ²³⁸Pu are from ITU measurements only that were corrected for ²⁴²Cm decay.

7.2.2 JRC Research Program

Measurements of spent fuel samples from the Obrigheim KWO reactor were also performed under a European JRC experimental program at laboratories of the Ispra and Karlsruhe establishments.¹⁵ These Obrigheim measurements have not been evaluated previously by the Yucca Mountain Project.

Fuel samples were obtained from six rods of two assemblies, BE124 and BE210. Positions of measured fuel rods in the assemblies are illustrated in Fig. 8 (see Sect. 8.2). Four of the six rods from which samples were selected were located at the outer edge of the assembly. A total of 23 samples were measured; 17 were measured at Ispra and 6 were measured at Karlsruhe (4 samples were measured at both laboratories for the purposes of cross-checking). One sample, D1-P1, did not report absolute heavy metal contents and was thus not used in the current study. A summary of the fuel samples evaluated in the current report is given in Table 13. The samples are identified by the rod location in the assembly and axial position identified in one of five uniform axial segments, P1 (lower) to P5 (upper).

Isotopic measurement techniques used at Ispra and Karlsruhe were similar to those used in other JRC experimental programs (e.g., Trino Vercellese).¹³ Measurements included the isotopes of uranium, plutonium, americium and curium, and fission products ¹⁴⁸Nd, ¹³⁴Cs, ¹³⁷Cs, and ¹⁵⁴Eu. Isotopic ratios of krypton and xenon noble gases were measured at Karlsruhe, but are not used in this report.

The main radiochemical analysis techniques included:

- IDMS for isotopes of U, Pu, Am, and Nd
- γ -spectrometry for ¹³⁴Cs, ¹³⁷Cs, and ¹⁵⁴Eu
- α -spectrometry for ²³⁸Pu, ²⁴¹Am, ²⁴²Cm, and ²⁴⁴Cm

Results for ¹³⁴Cs, ¹³⁷Cs, and ¹⁵⁴Eu were only reported for samples measured at Ispra. The gamma measurements applied in this work were those obtained for the dissolved fuel solutions and not from nondestructive analysis. Karlsruhe used α -spectrometry only to measure ²⁴¹Am. Ispra used α -spectrometry for some samples, and higher-precision mass spectrometry with isotopic dilution for other samples. Mass

spectrometry also provided data for ^{242m}Am and ^{243}Am that were not available for the samples measured by α -spectrometry.

Table 13. Summary of Obrigheim KWO fuel samples from assemblies BE124 and BE210

Assembly	Sample No.	Measurement laboratory	Fuel sample	Enrichment (wt % ^{235}U)	Axial location (cm) ^a	Burnup (GWd/MTU) ^b
BE124	1	Karlsruhe	D1-P1	3.00	15.0	21.17 ^c
	2	Ispra	D1-P3	3.00	143.5	33.75
	3	Ispra	E3-P1	3.00	15.0	20.18
	4	Karlsruhe	E3-P2	3.00	31.5	29.35 ^c
	5	Ispra	E3-P3	3.00	143.5	36.26
	6	Ispra / Karlsruhe	E3-P4	3.00	231.5	30.92
	7	Ispra	E3-P5	3.00	258.5	22.86
	8	Ispra / Karlsruhe ^d	G7-P1	3.00	15.0	17.13
	9	Ispra	G7-P2	3.00	31.5	25.83
	10	Ispra / Karlsruhe	G7-P3	3.00	143.5	31.32
	11	Ispra	G7-P4	3.00	231.5	27.71
	12	Karlsruhe	G7-P5	3.00	258.5	25.81
	13	Karlsruhe	M14-P1	3.00	15.0	15.60
	14	Ispra	M14-P3	3.00	143.5	29.36
	15	Karlsruhe	M14-P4	3.00	231.5	24.90
BE210	16	Ispra / Karlsruhe	G14-P3-1	2.83	132.8	37.49
	17	Ispra	G14-P4-1	2.83	220.6	35.64
	18	Ispra	G14-P5-1	2.83	242.6	30.16
	19	Ispra	G14-P5-2	2.83	254.7	24.22
	20	Ispra	K14-P1	2.83	15.0	22.90 ^c
	21	Ispra	K14-P3-1	2.83	132.8	36.67
	22	Karlsruhe	K14-P4-1	2.83	220.6	32.90

^aDistance between sample axial location and the bottom of the active fuel.

^bBurnup values determined by laboratories from measured ^{148}Nd , except as noted.

^cBurnup value determined by ^{137}Cs destructive gamma measurements.

^dOnly Ispra measurements used for sample G7-P1.

Source: Ref. 15, Fig. 2.

Experimental uncertainties were reported based on a comparison of different laboratory measurements for the cross-check samples. Results for one of these samples, G7-P1, exhibited consistent isotopic differences between the two cross-check samples. This discrepancy is likely due to an actual difference in the burnup of the cross-check samples due to the large burnup gradient near the bottom of the fuel rod (section P1) from where the samples were obtained. Therefore, the G7-P1 sample was not included as the cross-check evaluation, and only the Ispra measurement results were used for this sample. Measurement data for the other cross-check samples were combined in the current report. The measurement methods and relative standard deviation uncertainty based on three cross-check samples, E3-P4, G7-P3, and G14-P3, are summarized in Table 14. Uncertainties listed for ^{134}Cs , ^{137}Cs , and ^{154}Eu isotopes, without reported laboratory cross-check data, are values reported by Ispra. Uncertainties for Am and Cm isotopes were not available but were obtained from other studies reported in Ref. 14.

Table 14. Measurement methods and uncertainties in Obrigheim measurements at JRC

Nuclide ID	Method	RSD (%)
U-235	IDMS	3.8
U-236	IDMS	0.1
U-238	IDMS	<0.1
Pu-238	α -spec	14.3
Pu-239	IDMS	0.32
Pu-240	IDMS	0.24
Pu-241	IDMS	1.27
Pu-242	IDMS	5.3
Am-241 ^a	α -spec / IDMS	20
Am-242m ^a	IDMS	N/A
Am-243 ^a	IDMS	N/A
Cm-242 ^b	α -spec	72
Cm-244 ^b	α -spec	28
Cs-134	γ -spec	1.5
Cs-137	γ -spec	1.5
Nd-148	IDMS	1.4
Eu-154	γ -spec	5.0

^aRef. 14, Table II.24.

^bRef. 14, Tables II.25 and II.26.

Source: Ref. 15, p. 166, unless otherwise noted.

Sample burnup values were determined by the laboratories using three independent methods: destructive analysis of ¹⁴⁸Nd, destructive analysis of ¹³⁷Cs, and nondestructive analysis of ¹³⁷Cs. Destructive analysis of ¹³⁷Cs was reported only for samples measured at Ispra. Nondestructive ¹³⁷Cs measurements were made at both laboratories and were reported for most samples. The reported burnup values are listed in Table 15. The estimated accuracy of the burnup determined by destructive ¹⁴⁸Nd, ¹³⁷Cs, and nondestructive ¹³⁷Cs measurements as reported by the laboratories¹³ is 1.5%, 2.5%, and 5.0% (relative standard deviation), respectively. The average agreement between the two destructive analysis methods is within 1.2%, with a relative standard deviation of 1.4%, excluding sample K14-P1 for which an 11% difference was observed. Agreement between destructive and nondestructive ¹³⁷Cs values is also good, with an average difference of 0.7% and relative standard deviation of 4.3%.

In the current study, the ¹⁴⁸Nd burnup values were used for all samples, except for E3-P2 and K14-P1, which exhibited large differences in the burnup based on the different burnup indicators, by about 16% and 11%, respectively. The discrepancy was further evaluated by plotting the trends in the ²³⁵U content as a function of the different burnup values for all five samples from rod E3 (see *DVD/xls/Experimental_data.xls*). The results indicate significant out-of-trend behavior using the ¹⁴⁸Nd burnup value consistent with an overestimation of the burnup. The ¹³⁷Cs burnup value for E3-P2, available from nondestructive measurement only, was 16% lower than the ¹⁴⁸Nd burnup value, and resulted in consistent agreement with data for other rod E3 samples based on trending analysis. The analysis indicates a likely problem with the Karlsruhe ¹⁴⁸Nd measurement for this sample. A similar analysis of sample K14-P1 suggested a likely problem in the ¹⁴⁸Nd burnup measured at Ispra. In this case,

the ^{137}Cs burnup value is also confirmed by both destructive and nondestructive measurements. The burnup values for all other samples were based on the ^{148}Nd method.

Table 15. Obrigheim sample burnup values from JRC measurements

Assembly	Fuel sample	Measurement laboratory	^{148}Nd burnup (MWd/MTU)	Destructive ^{137}Cs burnup (MWd/MTU)	Non-destructive ^{137}Cs burnup (MWd/MTU)	Recommended burnup (MWd/MTU)
BE124	D1-P1	Karlsruhe	21,170		19,520	21,170
	D1-P3	Ispra	33,750	33,160	33,760	33,750
	E3-P1	Ispra	20,180	19,540	19,420	20,180
	E3-P2	Karlsruhe	35,100		29,350	29,350
	E3-P3	Ispra	36,260	35,220	35,510	36,260
	E3-P4	Ispra	30,890	30,640	28,140	30,920
	E3-P4	Karlsruhe	30,940			
	E3-P5	Ispra	22,860	22,570	22,920	22,860
	G7-P1	Ispra	17,130	16,970	17,490	17,130
	G7-P1 ^a	Karlsruhe	22,700			
	G7-P2	Ispra	25,830	24,880	26,240	25,830
	G7-P3	Ispra	31,500	31,400	31,920	31,320
	G7-P3	Karlsruhe	31,140			
	G7-P4	Ispra	27,710	27,420	29,460	27,710
	G7-P5	Karlsruhe	25,810		28,830	25,810
	M14-P1	Karlsruhe	15,600		15,790	15,600
	M14-P3	Ispra	29,360	28,800	27,200	29,360
	M14-P4	Karlsruhe	24,900		27,460	24,900
BE210	G14-P3-1	Ispra	38,100	37,720	36,290	37,490
	G14-P3-1	Karlsruhe	36,880			
	G14-P4-1	Ispra	35,640	35,480	36,070	35,640
	G14-P5-1	Ispra	30,160	30,660	31,870	30,160
	G14-P5-2	Ispra	24,220	24,400	26,060	24,220
	K14-P1	Ispra	25,450	22,900	22,460	22,900
	K14-P3-1	Ispra	36,670	35,990	35,120	36,670
	K14-P4-1	Karlsruhe	32,900		34,630	32,900

^aKarlsruhe cross-check sample G7-P1 was determined to have a significantly different burnup than the corresponding Ispra sample and was not analyzed.

All measurement data were adjusted by the laboratories to the time of discharge. The concentration of ^{239}Pu includes the contribution from ^{239}Np . The measurement data are listed in Table 16. Fission product measurements were reported using final uranium in the sample as a basis and were adjusted in this report to initial uranium using ratio of initial to final uranium in the sample as determined from the measured uranium isotopes ^{235}U , ^{236}U , and ^{238}U . Data unit conversion was performed according to procedures and data described in Sect. 6.5.

The procedure of back-calculating isotopic concentrations to the time of discharge resulted in large experimental uncertainties for measured ^{241}Am . Because most of the ^{241}Am in the sample at the time of

measurement is produced by ^{241}Pu decay, the correction involves subtracting the large ^{241}Pu contribution from the measured ^{241}Am content, resulting in small ^{241}Am concentrations and a large increase in the relative error. The Ispra ^{241}Am results obtained by α -spectrometry exhibit erratic behavior with burnup and are inconsistent with results measured using mass spectrometry at Ispra and α -spectrometry at Karlsruhe.¹⁵ Consequently, the Ispra α -spectrometry data for ^{241}Am are not recommended for use. Experimental uncertainties were not reported and cross-check data were not available. Analysis of ^{241}Am data from similar JRC programs indicates the error is approximately 20% (Ref. 13, p. 58). Analysis of $^{242\text{m}}\text{Am}$ and ^{243}Am data show erratic trends with burnup and errors that likely exceed 20%. Therefore, these data are not considered acceptable for validation.

An analysis of the ^{244}Cm in the experimental report¹⁵ indicates that the Karlsruhe and Ispra results are generally compatible. The Karlsruhe measurement of sample E3-P2 was found to be out of trend with other data and is rejected. Evaluation of the ^{242}Cm measurement data in Ref. 13 found that the results reported by Karlsruhe are much higher than the results from Ispra, and that the Karlsruhe data do not agree with isotopic predictions or experience with other similar fuel measurements. Therefore, the ^{242}Cm results from Karlsruhe are not considered reliable for use as benchmark data and are similarly rejected.

Table 16. Experimental results for Obrigheim JRC samples ^a (mg/g U_{initial})

Assembly	BE124	BE124	BE124	BE124	BE124	BE124	BE124	BE124	BE124	BE124	BE124
Sample ID	D1-P1	D1-P3	E3-P1	E3-P2	E3-P3	E3-P4	E3-P5	G7-P1	G7-P2	G7-P3	G7-P4
Burnup (MWd/MTU)	21,170	33,750	20,180	29,350	36,260	30,915	22,860	17,130	25,830	31,320	27,710
U-235	1.369E+01	6.930E+00	1.275E+01	8.440E+00	6.090E+00	7.660E+00	1.185E+01	1.521E+01	1.076E+01	7.555E+00	1.009E+01
U-236	2.990E+00	4.060E+00	2.820E+00	3.770E+00	4.120E+00	3.870E+00	3.620E+00	2.920E+00	3.850E+00	3.960E+00	4.050E+00
U-238	9.541E+02	9.447E+02	9.571E+02	9.422E+02	9.430E+02	9.470E+02	9.534E+02	9.580E+02	9.508E+02	9.464E+02	9.484E+02
Pu-238	3.600E-02	1.560E-01	4.100E-02	1.040E-01	1.650E-01	1.140E-01	6.200E-02	3.100E-02	7.900E-02	1.415E-01	1.060E-01
Pu-239	4.350E+00	5.020E+00	4.280E+00	4.620E+00	4.770E+00	4.925E+00	4.650E+00	4.260E+00	4.700E+00	5.015E+00	5.080E+00
Pu-240	1.320E+00	2.360E+00	1.360E+00	1.990E+00	2.410E+00	2.230E+00	1.620E+00	1.160E+00	1.810E+00	2.280E+00	2.040E+00
Pu-241	6.200E-01	1.280E+00	6.200E-01	1.020E+00	1.260E+00	1.185E+00	8.400E-01	5.500E-01	9.400E-01	1.205E+00	1.110E+00
Pu-242	1.280E-01	5.640E-01	1.390E-01	3.800E-01	6.290E-01	4.760E-01	2.110E-01	9.900E-02	2.790E-01	4.890E-01	3.660E-01
Am-241	2.190E-02							1.400E-02	2.480E-02		
Am-242m								2.880E-04	4.940E-04		
Am-243								8.600E-03	3.900E-02		
Cm-242		1.565E-02	4.500E-03		1.479E-02	1.501E-02	7.100E-03	2.940E-03	8.580E-03	1.479E-02	1.188E-02
Cm-244	2.220E-03	3.397E-02	2.040E-03		4.162E-02	2.349E-02	5.130E-03	1.040E-03	9.490E-03	2.823E-02	1.652E-02
Cs-134		1.301E-01	4.301E-02		1.380E-01	1.116E-01	6.247E-02	3.498E-02	7.567E-02	1.190E-01	9.562E-02
Cs-137		1.219E+00	7.183E-01		1.294E+00	1.127E+00	8.298E-01	6.239E-01	9.140E-01	1.155E+00	1.006E+00
Nd-148	2.377E-01	3.792E-01	2.266E-01		4.078E-01	3.472E-01	2.571E-01	1.923E-01	2.901E-01	3.519E-01	3.117E-01
Eu-154		2.533E-02	7.574E-03		2.434E-02	2.058E-02	1.149E-02	5.337E-03	1.595E-02	2.376E-02	1.923E-02

^aMeasurements reported for reference date of 8/16/1974 corresponding to time of discharge.

Table 16. Experimental results for Obrigheim JRC samples^a (mg/g U_{initial}) (continued)

Assembly	BE124	BE124	BE124	BE124	BE210	BE210	BE210	BE210	BE210	BE210	BE210
Sample ID	G7-P5	M14-P1	M14-P3	M14-P4	G14-P3-1	G14-P4-1	G14-P5-1	G14-P5-2	K14-P1	K14-P3-1	K14-P4-1
Burnup (MWd/MTU)	25,810	15,600	29,360	24,900	37,490	35,640	30,160	24,220	22,900	36,670	32,900
U-235	1.009E+01	1.569E+01	8.780E+00	1.033E+01	4.730E+00	4.950E+00	6.270E+00	8.940E+00	1.003E+01	4.860E+00	5.040E+00
U-236	3.600E+00	2.730E+00	3.810E+00	3.600E+00	3.880E+00	3.950E+00	3.660E+00	3.330E+00	3.220E+00	3.860E+00	3.820E+00
U-238	9.502E+02	9.591E+02	9.483E+02	9.512E+02	9.426E+02	9.453E+02	9.507E+02	9.555E+02	9.528E+02	9.439E+02	9.472E+02
Pu-238	7.900E-02	2.500E-02	1.070E-01	7.600E-02	1.645E-01	1.590E-01	1.140E-01	6.500E-02	6.500E-02	1.690E-01	1.260E-01
Pu-239	5.080E+00	3.980E+00	5.020E+00	4.960E+00	4.560E+00	4.410E+00	4.360E+00	4.270E+00	4.600E+00	4.690E+00	4.510E+00
Pu-240	1.950E+00	1.040E+00	2.080E+00	1.860E+00	2.495E+00	2.380E+00	2.110E+00	1.720E+00	1.740E+00	2.470E+00	2.370E+00
Pu-241	1.050E+00	4.600E-01	1.120E+00	1.000E+00	1.310E+00	1.210E+00	1.090E+00	8.600E-01	9.000E-01	1.300E+00	1.210E+00
Pu-242	3.200E-01	7.500E-02	3.840E-01	2.990E-01	7.800E-01	6.800E-01	4.940E-01	2.850E-01	2.640E-01	7.350E-01	6.580E-01
Am-241		6.700E-03			4.100E-02	4.030E-02		2.770E-02	2.520E-02		
Am-242m					7.290E-04	1.930E-03	1.207E-03	7.100E-04		7.570E-04	
Am-243					1.540E-01	1.380E-01	4.200E-02	3.600E-02		1.400E-01	
Cm-242			1.130E-02		1.454E-02	1.436E-02	1.170E-02	7.560E-03	8.130E-03	1.775E-02	
Cm-244	1.068E-02	1.040E-03	1.799E-02	8.910E-03	5.288E-02	4.715E-02	2.207E-02	6.950E-03	6.530E-03	5.259E-02	3.168E-02
Cs-134			1.018E-01		1.511E-01	1.365E-01	1.022E-01	6.563E-02	6.536E-02	1.464E-01	
Cs-137			1.059E+00		1.382E+00	1.300E+00	1.124E+00	8.942E-01	8.367E-01	1.316E+00	
Nd-148	2.899E-01	1.752E-01	3.300E-01	2.795E-01	4.217E-01	4.006E-01	3.391E-01	2.725E-01	2.860E-01	4.123E-01	3.696E-01
Eu-154			2.019E-02		2.608E-02	2.488E-02	1.996E-02	1.294E-02	1.317E-02	2.770E-02	

^aMeasurements reported for reference date of 8/16/1974 corresponding to time of discharge.

7.3 TURKEY POINT UNIT 3

Turkey Point Unit 1 is a PWR in the United States with a net generating capacity of 699 MWe, which was designed by Westinghouse Electric Corp. (West). First power was achieved in November 1972 with an initial core consisting of West OFA/LOPAR 15 × 15 assemblies.⁵⁷

Radiochemical analysis of five fuel samples from two assemblies from the Turkey Point Unit 3 reactor was performed at the Battelle Columbus Laboratories.²¹ The samples were taken from five different fuel rods from sections located near the axial center of the assemblies, approximately 167 cm (66 in.) from the bottom of the fuel rod. Consequently, the samples had a very similar burnup and isotopic composition. Fuel rods G10, G9, and H9 were obtained from assembly D01. Fuel rods G10 and G9 were from assembly D04. The configuration of the Westinghouse 15 × 15 assembly showing the location of the measured fuel rods is illustrated in Fig. 9 (see Sect. 8.3). The characteristics of the measured samples are summarized in Table 17.

Table 17. Summary of the Turkey Point Unit 3 spent fuel samples

Sample No.	Assembly	Rod ID	Sample ID	Initial enrichment (wt % ²³⁵ U)	Axial location ^a (cm)	Burnup (GWd/MTU)	Cooling time (days)
1	D01	G9	D01-G9-15 ^c	2.556	167.6	30.72	927 ^b
2	D01	G10	D01-G10-4	2.556	167.0	30.51	927
3	D01	H9	D01-H9-7	2.556	167.0	31.56	927
4	D04	G9	D04-G9-9	2.556	167.6	31.26	927
5	D04	G10	D04-G10-7	2.556	167.0	31.31	927

^aHeight of sample location above bottom of fuel rod end plug.

^bValue not reported. Obtained from Refs. 23 and 24.

^cLast value designates the axial rod segment.

Source: Ref. 21, unless otherwise noted.

Isotopic measurements were reported for the uranium and plutonium isotopes and for ¹⁴⁸Nd. Measured ¹⁴⁸Nd content was used to determine the sample burnup using the procedures of ASTM E 321 (Ref. 74) and E 267 (Ref. 78) standards. The ASTM procedures use isotopic dilution mass spectrometry to determine the concentrations of uranium, plutonium, and neodymium, with ²³³U, ²⁴²Pu, and ¹⁵⁰Nd spikes. Measurement data were reported for isotopic abundances and atom ¹⁴⁸Nd/²³⁸U and ²³⁹Pu/²³⁸U ratios in the samples. The relative isotopic distribution of the xenon and krypton in the fission gas was also measured by mass spectrometry but was not analyzed in the current report.

The isotopic concentrations with respect to initial uranium in the fuel were determined from the measured atom ratios using the following procedures. Isotopic mass ratios were first calculated from reported atom ratios and all isotopes were then calculated relative to final ²³⁸U mass basis using the ²³⁹Pu/²³⁸U mass ratio. As an example of the procedure, the mass concentration of ²⁴⁰Pu is calculated with respect to measured ²³⁸U in the sample as

$$m_{240\text{Pu}} \left(\text{mg} / \text{g}^{238}\text{U} \right) = \frac{m_{240\text{Pu}} \left(\text{g}^{240}\text{Pu} / \text{g Pu} \right)}{m_{239\text{Pu}} \left(\text{g}^{239}\text{Pu} / \text{g Pu} \right)} m_{239\text{Pu}} \left(\text{g}^{239}\text{Pu} / \text{g}^{238}\text{U} \right) \frac{10^3 \text{ mg}}{\text{g}} . \quad (11)$$

The initial heavy metal mass of the sample was calculated as the sum of the measured uranium and plutonium isotopes after irradiation plus the heavy metal mass reduction due to fission as derived from the ¹⁴⁸Nd concentration using procedures defined in Sect. 6.5. The isotopes not measured in these samples

(Am, Cm) account for less than 0.1% of the heavy metal mass for these samples and negligible error in the procedure. The date of the measurements was not cited in the experimental report. An earlier evaluation²³ of the experimental data gives the time after discharge as 927 days, corresponding to a measurement date of June 3, 1980. This date was assumed in the current report. The long half-lives of most measured isotopes makes the results relatively insensitive to uncertainty in the measurement date. Only the value of ²⁴¹Pu ($T_{1/2} = 14.4$ years) is influenced by the decay time.

Uncertainties in the measurements were not reported. The uncertainties were estimated in this report by evaluating the variance of the measurements with respect to a linear regression fit of the data as a function of sample burnup. The samples are sufficiently similar in burnup that the expected changes in the composition will be nearly linear with burnup over the range of data. The root mean square error was used to estimate the standard deviation of the random error from the residual of the data and linear regression fit. The relative error was calculated by dividing the root mean square error by the mean of all data points. The reported measurement data and the estimated uncertainties are given in Table 18 and Table 19, respectively. The error for ¹⁴⁸Nd was taken from ASTM E 321 (Ref. 74) based on typical laboratory experience.

Table 18. Experimental results (mg/g $U_{initial}$) for Turkey Point fuel samples

Assembly	D01	D01	D01	D04	D04
Sample	G9-15	G10-4	H9-7	G9-9	G10-7
Burnup (MWd/MTU)	30,720	30,510	31,560	31,260	31,310
U-234	1.299E-01	1.299E-01	1.205E-01	1.113E-01	1.298E-01
U-235	5.793E+00	5.607E+00	5.515E+00	5.442E+00	5.593E+00
U-236	3.228E+00	3.229E+00	3.149E+00	3.131E+00	3.226E+00
U-238	9.506E+02	9.510E+02	9.499E+02	9.503E+02	9.502E+02
Pu-238	1.365E-01	1.370E-01	1.436E-01	1.392E-01	1.382E-01
Pu-239	4.860E+00	4.875E+00	4.966E+00	4.977E+00	4.823E+00
Pu-240	2.286E+00	2.311E+00	2.312E+00	2.337E+00	2.294E+00
Pu-241	1.075E+00	1.076E+00	1.113E+00	1.132E+00	1.080E+00
Pu-242	5.107E-01	5.286E-01	5.517E-01	5.467E-01	5.273E-01
Nd-148	3.342E-01	3.319E-01	3.434E-01	3.400E-01	3.405E-01

Table 19. Experimental techniques and uncertainties for Turkey Point measurements

Nuclide	Method	RSD ^a (%)
U-234	IDMS	5.2
U-235	IDMS	2.1
U-236	IDMS	0.9
U-238	IDMS	0.01
Pu-238	IDMS	1.0
Pu-239	IDMS	0.9
Pu-240	IDMS	0.8
Pu-241	IDMS	1.6
Pu-242	IDMS	2.1

^aThe relative standard deviation (RSD) values associated with the measurement techniques for the isotopes were determined in *DVD/xls/Experimental_data.xls*, worksheet *turk*.

7.4 H. B. ROBINSON UNIT 2

H. B. Robinson Unit 2 is a PWR in the United States with a net generating capacity of 769 MWe, which was designed by Westinghouse Electric Corp. (West). First power was achieved in September 1970 with an initial core consisting of West ANF Standard 15 × 15 assemblies.⁵⁷

Radiochemical analyses of four fuel samples from H. B. Robinson Unit 2 were performed at the Materials Characterization Center (MCC) at Pacific Northwest Laboratory (PNL) as part of the Approved Testing Materials (ATM) program.²⁶ The fuel sample material, designated ATM-101, was obtained from assembly BO-5 that was irradiated for the first two reactor operating cycles. The fuel rods were cut into segments at the Idaho Nuclear Engineering Laboratory and transported to the PNL hotcells at Hanford Engineering and Development Laboratory (HEDL) for destructive radiochemical analyses of the samples.

The burnup analyses were performed on four fuel samples obtained from rod N-9. The location of rod N-9 and the configuration of assembly BO-5 are shown in Fig. 11 (see Sect 8.4). The axial locations of the samples were selected to obtain a wide range of burnup values within the rod. The characteristics of the samples are listed in Table 20. The sample burnup was determined by the ¹⁴⁸Nd standard test method of the ASTM E 321 (Ref. 74). Note that the enrichment is given as 2.55 wt % ²³⁵U in the ATM-101 experimental report.²⁶ However, the Department of Energy Information Administration database of spent fuel, RW-859 (Ref. 79), correspondence from the Electric Power Research Institute (EPRI),²⁷ and Robinson 2 Plant Description²⁹ indicate the actual enrichment was 2.561 wt % ²³⁵U.

Table 20. Summary of H. B. Robinson fuel samples

Sample No.	Assembly	Initial enrichment (wt % ²³⁵ U)	Sample ID	Axial location ^a (cm)	Burnup (GWd/MTU)	Cooling time ^c (days)
1	BO-5	2.561	N-9B-S	11	16.02 ^b	3936
2	BO-5	2.561	N-9B-N	26	23.81 ^b	3936
3	BO-5	2.561	N-9C-J	199	28.47	3631
4	BO-5	2.561	N-9C-D	226	31.66	3631

^aRef. 26, Fig. B.6, for samples N-9B-S and N-9B-N, and Fig. B.2 and Fig. B.7 for samples N-9C-D and N-9C-J. Note that the legend and figure titles were reversed between Fig. B.7 and Fig. B.2.

^bRef. 26, Table 4.9. The burnup analyses were performed by HEDL according to ASTM Standard E 321.

^cRef. 26, Table F.1. Measurement times reports as April 1984 and February 1985.

The radiochemical analysis of samples N-9C-D and N-9C-J were made in April 1984. Samples N-9B-N and N-9B-S were measured later in February 1985. The analysis dates were taken to be the middle of each month. Another fuel rod, P8, was also measured by Battelle Columbus laboratories,^{80,36} but the P8 rod data have not been evaluated in this work at this time.

The measurements include isotopes of uranium, plutonium, neodymium, ²³⁷Np, ⁹⁹Tc, and ¹³⁷Cs. The uranium and plutonium isotopes were determined as part of the burnup analyses using ASTM Standard Procedure E 321. The ASTM procedure uses isotopic dilution mass spectrometry with the spikes ¹⁵⁰Nd, ²³³U, and ²⁴²Pu. Analyses for ²³⁷Np were made using a developmental procedure involving heavily spiking the samples with ²³⁹Np as a tracer and multiple neptunium separations. The ⁹⁹Tc was determined using a combination ion-exchange and solvent-extraction separation procedure and beta counting. The ¹³⁷Cs analyses were made by gamma spectral analysis using ASTM Standard Procedure E 692 (Ref. 81). Measurements of elemental uranium and plutonium were reported as g/g fuel, and neodymium was reported as atoms/g fuel. Data for ⁹⁹Tc and ¹³⁷Cs were reported as activities and converted to mass contents in the current report using procedures described in Sect. 6.5.

Measurement uncertainties were not given in the experimental report. It was assumed that the procedures and uncertainties are similar to those reported in later ATM-series measurements, also performed at the PNL MCC laboratory.³⁰ Neodymium uncertainty was reported separately³⁴ as <1% based on comparisons of the PNL data with independent measurements made at Los Alamos National Laboratory (LANL) and KRI for ¹⁴³Nd and ¹⁴⁵Nd. Repeat analyses of ¹⁴⁸Nd for samples N-9C-D and N-9C-J resulted in relative differences of about 2% and 0.7%, respectively. The estimated Nd isotope uncertainties were assumed to be about 1% based on these studies.

An independent verification of the burnup values in the current study using the reported ¹⁴⁸Nd measurements did not reproduce the burnup values cited by the laboratory. First, the exponent for the neodymium atom concentrations, listed as 10¹⁵ atoms per gram of fuel, is low by several orders of magnitude due to a reporting error. Furthermore, when atom % fission (% FIMA) is derived from the ¹⁴⁸Nd analysis results, the values are up to 14% larger than % FIMA values cited in the experimental report (Ref. 26, Table 4.9). However, if the reported values of Nd atoms/g fuel are assumed to be actually ¹⁴⁸Nd atoms, the calculated % FIMA values agree with values reported by the laboratory to within 1%, with the exception of sample N-9C-D, for which it was 4% less than the reported value. Based on this observation, the reported Nd atom concentrations ($\times 10^{15}$) were listed in this current report as ¹⁴⁸Nd atom concentrations ($\times 10^{18}$). A second discrepancy in the plutonium isotopic vector for sample N-9B-N was identified in Table F.1 of Ref. 26. Using data from Table 4.1 of the same report, the error was traced to a reporting error for ²³⁸Pu as the value is corrected in the current report. The measured isotopic compositions are listed in Table 21, and measurement methods and uncertainties are summarized in Table 22.

Table 21. Experimental results (mg/g U_{initial}) for H. B. Robinson fuel samples

Assembly	BO-5	BO-5	BO-5	BO-5
Sample	N-9C-D	N-9C-J	N-9B-N	N-9B-S
Burnup (MWd/MTU)	31,660	28,470	23,810	16,020
U-234	1.253E-01	1.339E-01	1.556E-01	1.755E-01
U-235	5.514E+00	7.010E+00	8.181E+00	1.209E+01
U-236	3.403E+00	3.204E+00	3.103E+00	2.487E+00
U-238	9.549E+02	9.460E+02	9.613E+02	9.605E+02
Pu-238	1.479E-01	1.293E-01	7.894E-02	3.208E-02
Pu-239	4.765E+00	5.162E+00	4.557E+00	4.132E+00
Pu-240	2.404E+00	2.236E+00	1.890E+00	1.241E+00
Pu-241	7.847E-01	7.733E-01	5.722E-01	3.447E-01
Pu-242	6.001E-01	4.682E-01	3.208E-01	1.155E-01
Np-237	3.778E-01	3.445E-01	2.953E-01	1.753E-01
Nd-143	6.550E-01	6.592E-01	5.711E-01	4.429E-01
Nd-144	1.162E+00	1.051E+00	8.794E-01	5.756E-01
Nd-145	5.853E-01	5.573E-01	4.819E-01	3.445E-01
Nd-146	5.998E-01	5.575E-01	4.631E-01	3.071E-01
Nd-148	3.299E-01	3.090E-01	2.611E-01	1.744E-01
Nd-150	1.628E-01	1.519E-01	1.249E-01	8.044E-02
Tc-99	6.691E-01	5.930E-01	5.360E-01	3.604E-01
Cs-137	9.317E-01	8.193E-01	7.043E-01	4.691E-01

Source: Ref. 26, Table F.1, except for ²³⁸Pu in sample N-9B-N which is from Table 4.12.

Table 22. Experimental techniques and uncertainties for H. B. Robinson measurements

Nuclide	Method	RSD ^a (%)
U-234	IDMS	1.6
U-235	IDMS	1.6
U-236	IDMS	1.6
U-238	IDMS	1.6
Pu-238	IDMS	1.6
Pu-239	IDMS	1.6
Pu-240	IDMS	1.6
Pu-241	IDMS	1.6
Pu-242	IDMS	1.6
Np-237	IDMS	1.9
Nd-143	IDMS	1.0
Nd-144	IDMS	1.0
Nd-145	IDMS	1.0
Nd-146	IDMS	1.0
Nd-148	IDMS	1.0
Nd-150	IDMS	1.0
Tc-99	β-counting	3.5
Cs-137	γ-spec	3.5

^aRelative standard deviation values from ATM-104 experiments, Ref. 31, Table 7.1. Neodymium uncertainties are based on reported data from Ref. 34.

7.5 CALVERT CLIFFS UNIT 1

Calvert Cliffs Unit 1 is a PWR in the United States with a generating capacity of 900 MWe, which was designed by Combustion Engineering Co. (CE). First power was achieved in December 1975 with an initial core consisting of CE 14 × 14 assemblies.⁵⁷

Isotopic measurements for spent fuel samples from Calvert Cliffs Unit 1 reactor were performed at the PNL MCC for the ATM Program designed to characterize spent fuel in support of geological repository studies for the Office of Civilian Radioactive Waste Management (OCRWM). Three assemblies from the Calvert Cliffs reactor were analyzed as part of the ATM-103, ATM-104, and ATM-106 experiments. One fuel rod from each assembly was destructively analyzed to provide detailed isotopic characterization. Three fuel samples were analyzed from each fuel rod, providing data for nine samples.

The assembly design is a Combustion Engineering (CE) 14 × 14 lattice with 176 fuel rods and 5 large guide tubes for the assembly control cluster. The assembly configuration and location of ATM-103 fuel rod MLA098 and ATM-104 fuel rod MKP109 are illustrated in Fig. 13, whereas the assembly configuration and location of ATM-106 fuel rod NBD107 are illustrated in Fig. 14 (see Sect. 8.5). The fuel rods are representative of the different regions of the assembly that include the central asymptotic flux region, and perturbed regions next to the water guide tube, and at the edge of the assembly. The fuel samples were cut from different axial positions, providing data for a wide burnup range.

Radiochemical assay of the fuel samples performed initially at PNL included measurements of the major actinides, neodymium, and several radiological fission products. Measurements were later performed at PNL to provide additional data for fission products with large neutron cross sections important to nuclear criticality safety, including isotopes of cesium, and the lanthanides samarium, europium, and gadolinium. To obtain data for estimating the error associated with the lanthanide measurements, several ATM fuel samples were analyzed independently at LANL and the Khlopin Radium Institute (KRI) in St. Petersburg, Russia. Measurement data from PNL and KRI were combined in the current report. The Calvert Cliffs samples evaluated in this report are summarized in Table 23.

Table 23. Summary of Calvert Cliffs fuel samples

Sample No.	Assembly	PNL sample ID	KRI sample ID	Initial enrichment ^c (wt % ²³⁵ U)	Axial location ^a (cm)	Burnup ^{b, c} (GWd/MTU)
1	D101	103-MLA098-JJ		2.72	361.7	18.68 ^c
2	D101	103-MLA098-BB		2.72	346.3	26.62
3	D101	103-MLA098-P		2.72	208.9	33.17
4	D047	104-MKP109-LL	87-81	3.038	360.7	27.35
5	D047	104-MKP109-CC	87-72	3.038	346.0	37.12
6	D047	104-MKP109-P	87-63	3.038	209.3	44.34
7	BT03	106-NBD107-MM		2.453	359.3	31.40
8	BT03	106-NBD107-GG	87-108	2.453	350.7	37.27
9	BT03	106-NBD107-Q		2.453	209.4	46.46

^aRef. 30, Table D.1; Ref. 31, Table C.1; Ref. 32, Table D.1. Distance measured from the top of fuel rod.

^bBurnup determinations were made by PNL using ¹⁴⁸Nd according to ASTM E 321.

^cBurnup values are reported in Ref. 30, Table 4.13 with enrichment from Table 4.1; Ref. 31, Table 7.2 with enrichment from Table 3.1; and Ref. 32, Table 4.16 with enrichment from Table 4.1.

7.5.1 PNL Measurements

The measurements at PNL were performed using the following main spectrometric methods:³¹

- isotope dilution mass spectrometry (IDMS) for Nd, U, and Pu nuclides, using a calibrated triple spike of ^{150}Nd , ^{233}U , and ^{242}Pu
- ICPMS measurements relative to ^{143}Nd and ^{145}Nd for the lanthanides Sm, Eu, and Gd
- mass spectrometry (MS) for ^{133}Cs (Ref. 35) and ^{135}Cs after elemental separation of cesium
- γ -spectrometry for ^{137}Cs and ^{126}Sn
- α -spectrometry for ^{241}Am and ^{237}Np
- β -spectrometry for ^{99}Tc and ^{90}Sr
- liquid scintillation counting for ^{79}Se

Isotopic measurements were reported in mass units of g/g fuel or activity in units of Ci/g gram fuel.

The lanthanide measurements were carried out using mass spectrometry without prior chemical separation into individual elements. This resulted in mass interference for nuclides with the same mass numbers 147 (Pm, Sm), 150 (Nd, Sm), 151 (Sm, Eu), and 155 (Eu, Gd), and measured data therefore included significant quantities of nuclides of more than one element. The measured data for these four mass numbers were adjusted by PNL using calculated isotopic ratios in order to infer information for individual isotopes.³⁴ Consequently, the PNL lanthanide data for these isotopes were not considered in this report for validation studies to avoid introducing potential errors related to the calculated adjustments.

A summary of the measured nuclides, methods, and experimental uncertainties reported by the laboratory are provided in Table 24. Measurement uncertainties for most isotopes were reported by the laboratory. No uncertainties were reported for the ^{133}Cs results. Note that PNL reported curium data that combined ^{242}Cm and ^{244}Cm . These values were not used in this study and results are not listed here. Experimental uncertainties for the lanthanides were evaluated by PNL using results of laboratory cross-check analyses performed for sample 87-81 measured at LANL and PNL using ICPMS, and at KRI using LA and IDMS measurement techniques. The burnup values used in the current study were the laboratory reported values based on measured ^{148}Nd using procedures of ASTM E 321 (Ref. 74). The relative standard error in the burnup is given as 2.5%.

The PNL measurement data for the Calvert Cliffs samples are publicly available on the spent fuel isotopic composition database SFCOMPO,³⁶ currently maintained and operated by the Organization for Economic Cooperation and Development (OECD)/ Nuclear Energy Agency (NEA) databank. The measurement data for ATM-104 served as the basis of an irradiated fuel benchmark for criticality calculations³⁵ and was used for the OECD/NEA burnup credit criticality safety calculation benchmark Phase I-B.⁸² The SFCOMPO database currently does not include the lanthanide measurements made at PNL or KRI used in the current report.

Table 24. Experimental techniques and uncertainties for Calvert Cliffs measurements at PNL

Nuclide ID	Method^a	RSD^{b, c} (%)
U-234	IDMS	1.6
U-235	IDMS	1.6
U-236	IDMS	1.6
U-238	IDMS	1.6
Pu-238	IDMS	1.6
Pu-239	IDMS	1.6
Pu-240	IDMS	1.6
Pu-241	IDMS	1.6
Pu-242	IDMS	1.6
Np-237	α -spec	1.9
Am-241	α -spec	4.9
Cs-133	IDMS	N/A
Cs-135	IDMS	14.0
Cs-137	γ -spec	3.5
Sr-90	β -spec	5.7
Tc-99	β -spec	3.5
Nd-143	IDMS	< 1.0
Nd-144	IDMS	N/A
Nd-145	IDMS	< 1.0
Nd-146	IDMS	N/A
Nd-148	IDMS	N/A
Nd-150	IDMS	N/A
Sm-147	ICPMS ^d	4.0
Sm-149	ICPMS	18.0
Sm-150	ICPMS	2.0
Sm-151	ICPMS	7.0
Sm-152	ICPMS	3.0
Eu-151	ICPMS	N/A
Eu-153	ICPMS	2.0
Eu-155	ICPMS	29.0
Gd-155	ICPMS	29.0

^aMain technique is listed; some nuclides require multiple techniques to eliminate interferences.

^bRelative standard deviation reported in Ref. 31 and Ref. 33 Appendix B (lanthanides).

^cN/A means that uncertainties were not reported for these isotopes.

^dLanthanide (Sm, Eu, and Gd) ICPMS measurements were performed without chemical separation and were not used in this work.

7.5.2 KRI Measurements

Additional lanthanide analyses were performed by KRI for Calvert Cliffs fuel samples from rod MKP109 and NBD107 at the request of PNL.³⁷ KRI lanthanide measurements were reported for fuel samples identified as 87-81, 87-72, and 87-63, obtained from rod segments corresponding to PNL sections

104-MKP109-LL, 104-MKP109-CC, and 104-MKP109-P, respectively. Lanthanide and rhodium (^{103}Rh) measurements are reported for sample 87-108 corresponding to the 106-NBD107-GG rod segment (see Table 23). The KRI measurements were reported in a series of technical reports³⁷ and were reproduced in PNL-13677 (Ref. 33).

The KRI measurements involved the following radiochemical analysis techniques:

- Chemical separation of rare earth elements and transuranics followed by chemical separation of lanthanides into individual elements;
- IDMS for neodymium and gadolinium isotopes using spikes of ^{142}Nd and ^{160}Gd ;
- Luminescent analysis (LA)—laser-induced fluorometry for absolute measurement of europium and samarium content in the sample; the content was determined by comparison of the sample luminescence intensity with that of standard solutions containing known quantities of europium and samarium;
- MS for europium and samarium nuclides to determine relative isotope ratios;
- HPGe γ -spectrometry for ^{154}Eu and ^{155}Eu ;
- Quadrapole ICPMS for ^{103}Rh using an internal standard and a combined internal standard plus standard addition techniques.

Chemical separation of lanthanides performed at KRI prior to mass spectrometry measurements eliminated the element interferences present in the PNL lanthanide data. Absolute contents however were not reported by KRI. Isotopic compositions were generally reported as the ratio of nuclide mass to the ^{145}Nd mass. Isotopic abundance (wt %) and relative element concentrations were also reported. For those nuclides not reported directly in $\text{g/g } ^{145}\text{Nd}$ units, values were derived in this report using the relative isotopic mass abundance values and the total mass concentration of each element in the sample. For example, concentrations of ^{156}Gd relative to ^{145}Nd were calculated as

$$m_{^{156}\text{Gd}} \left(\text{g} / \text{g } ^{145}\text{Nd} \right) = \frac{m_{\text{Gd}} \left(\text{mg} / \text{sample} \right)}{m_{\text{Nd}} \left(\text{mg} / \text{sample} \right)} \frac{m_{^{156}\text{Gd}} \left(\text{g} / \text{g Gd} \right)}{m_{^{145}\text{Nd}} \left(\text{g} / \text{g Nd} \right)}, \quad (12)$$

where m_{Gd} and m_{Nd} are the mass of elemental gadolinium and neodymium, respectively, in the sample. Uncertainties for the derived values were estimated using the same relative standard error as the values reported by KRI for sample 87-81 that included absolute error estimates for all measured isotopes.

The absolute lanthanide content for the KRI data was calculated in this report by normalizing the relative isotopic concentrations measured by KRI ($\text{g/g } ^{145}\text{Nd}$) using the absolute ^{145}Nd contents measured by PNL. The measured nuclides and experimental errors reported by KRI are listed in Table 25. Uncertainties in the KRI measurements were provided by the laboratory for most data used in this report. For data reported by KRI that did not explicitly provide uncertainty values, uncertainties were estimated using the relative error for other KRI samples. The measurements were obtained from Ref. 34, also data were reported in Ref. 37. However, reported values for ^{152}Sm , ^{154}Gd , ^{155}Gd , ^{156}Gd , and ^{158}Gd for sample 87-81 are incorrect due to a transcription error in Table 2.5.2 of Ref. 37.

Table 25. Experimental techniques and uncertainties for Calvert Cliffs measurements at KRI

Nuclide ID	Method ^a	RSD ^b (%)
Nd-143	IDMS	0.7–1.9
Nd-145	IDMS	N/A
Sm-147	MS, LA	2.5–3.3
Sm-149	MS, LA	7.4–20.0
Sm-150	MS, LA	2.3–4.2
Sm-151	MS, LA	3.2–4.7
Sm-152	MS, LA	2.7–3.8
Sm-154	MS, LA	5.7
Eu-151	MS, LA	9.7
Eu-154	MS, LA, γ -spec	8.6
Eu-155	MS, LA, γ -spec	2.7–16.7
Gd-155	IDMS	3.0–3.7
Rh-103	ICPMS	4.0

^aMain technique is listed; some nuclides require multiple techniques to eliminate interferences.

^bRelative standard deviation derived from Refs. 37 and 33 in *DVD/xls/Experimental_data.xls*.

^cKRI measurements were performed relative to the ¹⁴⁵Nd mass.

The ¹⁰³Rh measurement was made using two techniques: x-ray fluorescent analysis (xRFA) and ICPMS using several internal standard calibration techniques. In the current work only the ICPMS results were used because of large variability in the xRFA results. KRI also investigated use of several techniques including secondary ion mass spectrometry (SIMS) for some isotopes in sample 87-81. However, KRI reported that the samarium data measured by SIMS may not be reliable, and therefore, only the ICPMS results were used in the current work.

7.5.3 103-MLA098

Three fuel samples were analyzed from rod MLA098 located at the edge of assembly D101, designated ATM-103 test material.³⁰ The samples were identified as 103-MLA098-P, 103-MLA098-BB, and 103-MLA098-JJ. Radiochemical analyses for these samples were performed only at PNL. The fuel is representative of average burnup fuel at that time.

The measured isotope concentrations are listed in Table 26. Burnup values were determined by the laboratory based on the ¹⁴⁸Nd content; however, neodymium isotopic data were not reported in the ATM-103 experimental report. The ATM-103 analysis date is reported as April 1987, with a cooling time of 6.5 years after discharge. A reference measurement date of April 15, 1987, was used for this study. This date gives a cooling time of 2374 days. Measurement uncertainties were not given in the ATM-103 experimental report.³⁰ However, the measurement methods are consistent with subsequent ATM program measurements and the uncertainties are assumed to be the same as those cited in the ATM-104 report, listed in Table 24.

Table 26. Measurement results for Calvert Cliffs 103-MLA098 samples (mg/g $U_{initial}$)

Nuclide	Measurement laboratory	Measurement date ^a	103-MLA098-JJ	103-MLA098-BB	103-MLA098-P
U-234	PNL	4/15/1987	1.588E-01	1.373E-01	1.361E-01
U-235	PNL	4/15/1987	1.163E+01	7.873E+00	5.423E+00
U-236	PNL	4/15/1987	2.836E+00	3.392E+00	3.698E+00
U-238	PNL	4/15/1987	9.700E+02	9.686E+02	9.554E+02
Pu-238	PNL	4/15/1987	5.502E-02	1.099E-01	1.682E-01
Pu-239	PNL	4/15/1987	4.486E+00	4.824E+00	4.750E+00
Pu-240	PNL	4/15/1987	1.410E+00	2.003E+00	2.395E+00
Pu-241	PNL	4/15/1987	5.154E-01	7.739E-01	9.217E-01
Pu-242	PNL	4/15/1987	1.581E-01	3.745E-01	6.210E-01
Np-237	PNL	4/15/1987	1.984E-01	3.403E-01	3.887E-01
Am-241	PNL	4/15/1987	2.205E-01	3.276E-01	3.967E-01
Se-79	PNL	4/15/1987	2.534E-03	3.391E-03	4.093E-03
Sr-90	PNL	4/15/1987	2.770E-01	3.636E-01	4.312E-01
Tc-99	PNL	4/15/1987	4.684E-01	6.208E-01	7.486E-01
Sn-126	PNL	4/15/1987	7.903E-03	1.250E-02	1.553E-02
Cs-133	PNL	4/15/1987			
Cs-135	PNL	4/15/1987	2.747E-01	3.072E-01	3.269E-01
Cs-137	PNL	4/15/1987	5.998E-01	8.533E-01	1.053E+00

^aRef. 30. PNL measurements performed in April 1987 (6.5 years cooling time). A cooling time of 2374 days was used in this study.

7.5.4 104-MKP109

Three Calvert Cliffs fuel samples were measured from fuel rod MKP109 of assembly D047, designated as ATM-104 material. The rod is centrally located in the assembly, in an asymptotic flux region, and away from the guide tubes and periphery of the assembly. The three samples, identified as 104-MKP109-LL, 104-MKP109-CC, and 104-MKP109-P, were obtained from different axial locations of the rod.

The radiochemical analysis measurements were first performed at PNL in May 1987.³¹ Additional fission product measurements (¹³³Cs, isotopes of Nd, Sm, Eu, and Gd) were performed at PNL in October 1992, and the measured data were corrected for decay time to June 1987 (Ref. 34). These latter lanthanide measurements were performed without chemical separations and therefore included mass interference as discussed previously. In the current report the reference date for the PNL measurements was taken as May 31, 1987, corresponding to a cooling time of 1870 days, a value consistent with previous validation studies.³⁸ The dates of the KRI measurements were inferred from information in the primary experimental reports³⁷ corresponding to cooling times of approximately 4171 and 4656 days. Sample 104-MKP109-LL (87-81) was measured September 17, 1993, and samples 104-MKP109-CC (87-72) and 104-MKP109-P (87-63) were measured in January 1995 (date of spike solution calibration).

The KRI lanthanide results, normalized to g/g ¹⁴⁵Nd, are listed in Table 27. A comparison of the KRI and PNL neodymium isotopic results (with KRI values normalized to the ¹⁴⁵Nd concentration measurement by PNL) found that all isotopes agreed to within the estimated measurement uncertainty; better than 2%. In the current report, the neodymium data measured by PNL were used for validation. Data for Sm, Eu, and Gd were based entirely on the KRI measurements because of the larger number of isotopes measured and the use of chemical separations. Cross-check evaluation of the KRI and PNL data for Sm, Eu, and Gd found that the results for most nuclides agreed to within about 10% after adjusting data for the difference in measurement dates. However, nuclides with very low concentrations, less than about 0.01 g/g ¹⁴⁵Nd, were generally found to exhibit erratic behavior. Poor agreement was seen between the laboratories, and

the measurement data did not trend reliably as a function of sample burnup. The results for ^{149}Sm showed large differences between laboratory measurements. The relative measurement accuracy for ^{149}Sm estimated by KRI and PNL was 20% and 18%, respectively. The large error is likely associated with the low concentrations in the fuel, where the isotopic mass of ^{149}Sm is less than 0.5% of the elemental samarium mass. Large deviations were also observed for ^{151}Eu and ^{152}Eu , which were present in the samples at concentrations close to the detection threshold. Therefore, the lanthanide data for the isotopes ^{149}Sm , ^{151}Eu , and ^{152}Eu (^{152}Eu only reported by KRI) were rejected for use in validation in the current report.

Isotopic concentrations for the three 104-MKP109 samples are listed in Table 28. The data are compiled from three sources: the ATM-104 experimental report,³¹ subsequent fission product measurement performed at PNL,³⁴ and independent measurements made at KRI.³³ The KRI lanthanide data were measured in September 1993 and reported at the time of measurements. The KRI results were not adjusted to the time of the PNL measurements because some precursors were not measured. The KRI measurements method for ^{154}Eu included both mass and γ -spectrometry. The results obtained using the two methods are in good agreement and the recommended values are determined as a weighted average of the two results.

7.5.5 106-NBD107

Three fuel samples were analyzed from rod NBD107 of Calvert Cliffs Unit 1 assembly BT03 as part of the ATM-106 program.³² The fuel rod was located in a perturbed region at the edge of the center guide tube of the assembly. Rod NBD107 had a relatively high burnup for the enrichment. The samples were identified as 106-NBD107-MM, 106-NBD107-GG, and 106-NBD107-Q.

The measured isotopes are similar to those in the other ATM programs. One of the samples, section 106-NBD107-GG, had supplemental lanthanide measurements performed at KRI,³⁷ thus providing more complete fission product data. In addition, KRI measured the concentration of ^{103}Rh , an important fission product in spent fuel criticality safety analyses using burnup credit.

Lanthanide measurements for the NBD107 rod samples were not reported by PNL. Lanthanide data was measured at KRI on fuel material from sample 106-NBD107-GG, designated in the KRI measurements as sample 87-108. In addition, KRI performed ^{103}Rh measurements for this sample. The experimental data reported by PNL and KRI are listed as absolute contents in Table 29. The PNL measurements were reported for a reference measurement date given as June 1987, and a cooling time of 6.7 years after discharge. The effective date used in this work was July 1, 1987. The KRI rare earth measurements (Nd, Eu, Sm, Gd) of sample 87-108 were performed in April 1996 and the rhodium measurement was performed in March 1996.

The PNL experimental report states that the ^{234}U measurements may be suspect due to instrument drift. Although the results were corrected for drift, measurement error is likely larger than reported and these results are not recommended for use.

The ^{103}Rh concentration in the fuel was derived from separate analyzes of the rhodium and uranium content in the fuel sample. The mean value of the ICPMS rhodium measurement was $0.00676 \text{ mg} \pm 5\%$ and the uranium content was $9.96 \text{ mg} \pm 6\%$ in the sample (uncertainties represent the $p = 95\%$ confidence level). The ^{103}Rh mass content is calculated to be 0.068% with respect to the final uranium mass in the sample, with a 4% relative one standard deviation uncertainty. This value was adjusted to initial uranium in the sample using procedures described in Sect. 6.5 of this report.

Table 27. KRI experimental lanthanide results for Calvert Cliffs samples (g/g ¹⁴⁵Nd)

KRI Sample ID	87-81			87-72			87-63			87-108		
PNL Sample ID	104-MKP109-LL			104-MKP109-CC			104-MKP109-P			106-NBD107-GG		
Burnup ^b (GWd/MTU)	27.35			37.12			44.34			37.27		
Nuclide	g/g element ^c (%)	g/g ¹⁴⁵ Nd	σ (%)	g/g element (%)	g/g ¹⁴⁵ Nd	σ ^d (%)	g/g element (%)	g/g ¹⁴⁵ Nd	σ ^d (%)	g/g element (%)	g/g ¹⁴⁵ Nd	σ ^d (%)
ID-MS data												
Nd-142	<i>0.65^a</i>	0.039	2.6	1.25	<i>0.077</i>	2.6	0.76	<i>0.048</i>	2.6	0.71	<i>0.044</i>	2.6
Nd-143	<i>20.71</i>	1.218	0.7	18.15	1.120	0.9	16.37	1.040	1.9	15.96	0.99	2.0
Nd-144	<i>31.99</i>	1.882	0.6	33.93	<i>2.084</i>	0.6	35.34	<i>2.235</i>	0.6	35.64	<i>2.216</i>	0.6
Nd-145	<i>17.00</i>	1.000		16.28	1.000		15.81	1.000		16.08	1.000	
Nd-146	<i>16.54</i>	0.973	0.6	17.12	<i>1.052</i>	0.6	17.87	<i>1.130</i>	0.6	17.64	<i>1.097</i>	0.6
Nd-148	<i>8.90</i>	0.523	0.8	8.96	<i>0.550</i>	0.8	9.24	<i>0.584</i>	0.8	9.32	<i>0.580</i>	0.8
Nd-150	<i>4.21</i>	0.248	8.1	4.32	<i>0.265</i>	8.1	4.59	<i>0.290</i>	8.1	4.65	<i>0.289</i>	8.1
Sm-147	<i>34.40</i>	0.398	3.3	30.57	0.365	2.5	28	0.365	3.3	29.14	0.367	2.5
Sm-148	<i>14.92</i>	0.173	1.7	18.3	<i>0.218</i>	1.7	20.39	<i>0.226</i>	1.7	18.78	<i>0.236</i>	1.7
Sm-149	<i>0.40</i>	0.005	20.0	0.22	0.0025	12.0	0.41	0.0054	7.4	0.22	0.0030	13.3
Sm-150	<i>31.17</i>	0.361	4.2	32.89	0.391	2.3	33.06	0.431	3.2	32.84	0.414	1.5
Sm-151	<i>1.11</i>	0.013	38.5	1.08	0.0127	3.1	0.97	0.0127	4.7	0.86	0.0110	4.6
Sm-152	<i>13.41</i>	0.155	3.2	12.56	0.148	2.7	12.05	0.157	3.8	13.26	0.167	2.4
Sm-154	<i>4.54</i>	0.053	5.7	4.32	<i>0.051</i>	5.7	5.12	<i>0.067</i>	5.7	4.9	<i>0.062</i>	5.7
Eu-151	<i>1.88</i>	0.0031	9.7	0.74	<i>0.00140</i>	9.7	1.91	<i>0.00404</i>	9.7	0.84	<i>0.00183</i>	9.7
Eu-152	<i>0.90</i>	0.0002	100.0	0.04	<i>0.00008</i>	100.0	0.25	<i>0.00053</i>	100.0	0.08	<i>0.00017</i>	100.0
Eu-153	<i>89.72</i>	0.1472	1.8	91.98	<i>0.17416</i>	1.8	90.25	<i>0.19201</i>	1.8	93.9	<i>0.2046</i>	1.8
Eu-154	<i>6.44</i>	0.0105	8.6	6.26	<i>0.01185</i>	8.6	6.58	<i>0.01393</i>	8.6	4.48	<i>0.00976</i>	8.6
Eu-155	<i>1.06</i>	0.0018	16.7	0.98	0.00187	2.7	1.01	0.00215	2.8	0.71	0.00157	3.2
Gd-154	<i>13.67</i>	0.0236	2.1	13.28	<i>0.0202</i>	2.1	13.27	<i>0.0237</i>	2.1	11.46	<i>0.0173</i>	2.1
Gd-155	<i>6.29</i>	0.0108	3.7	6.58	0.0100	3.0	6.62	0.0118	3.4	6.35	0.0097	4.1
Gd-156	<i>64.09</i>	0.1100	1.8	65.10	<i>0.0989</i>	1.8	63.20	<i>0.1129</i>	1.8	66.26	<i>0.1000</i>	1.8
Gd-157	<i>0.47</i>	<0.00007		1.84	<i>0.0028</i>		3.24	<i>0.0058</i>		1.92	<i>0.00290</i>	
Gd-158	<i>13.98</i>	0.0241	2.1	13.20	<i>0.0201</i>	3.0	13.70	<i>0.0245</i>	2.1	13.56	<i>0.0205</i>	2.1
Gd-160	<i>1.48</i>	0.0025	12.0							0.46	<i>0.00069</i>	12.0
γ-spec data												
Eu-154					<i>0.0117</i>	5.1		0.0119	5.9			
Eu-155					<i>0.00182</i>	4.9		0.00209	5.7			

^aValues shown in italics are derived based on experimental data (see DVD/xls/Khlopin.xls). All other values are given in Ref. 33.

^bAs reported in Refs. 30 and 31.

^cMass abundances for sample 87-81 are derived from measured isotopic mass data reported as nanograms per sample (see DVD/xls/Khlopin.xls).

^dRelative uncertainties for derived concentrations assumed to be the same as sample 87-81.

Table 28. Measurement results for Calvert Cliffs 104-MKP109 samples (mg/g U_{initial})

Nuclide	Measurement laboratory ^a	104-MKP109-LL (87-81)	104-MKP109-CC (87-72)	104-MKP109-P (87-63)
U-234	PNL	1.815E-01	1.588E-01	1.361E-01
U-235	PNL	9.609E+00	5.865E+00	4.016E+00
U-236	PNL	3.562E+00	4.005E+00	4.186E+00
U-238	PNL	9.558E+02	9.446E+02	9.358E+02
Pu-238	PNL	1.146E-01	2.147E-01	3.049E-01
Pu-239	PNL	4.837E+00	4.943E+00	4.943E+00
Pu-240	PNL	1.950E+00	2.540E+00	2.885E+00
Pu-241	PNL	7.725E-01	1.024E+00	1.157E+00
Pu-242	PNL	3.279E-01	6.535E-01	9.530E-01
Np-237	PNL	3.048E-01	4.048E-01	5.338E-01
Am-241	PNL	2.830E-01	3.901E-01	4.331E-01
Se-79	PNL	3.361E-03	4.459E-03	4.794E-03
Sr-90	PNL	3.784E-01	4.864E-01	5.425E-01
Tc-99	PNL	6.354E-01	8.149E-01	8.944E-01
Sn-126	PNL	1.149E-02	1.672E-02	2.022E-02
Cs-133	PNL	9.643E-01	1.237E+00	1.407E+00
Cs-135	PNL	4.096E-01	4.519E-01	4.874E-01
Cs-137	PNL	8.768E-01	1.177E+00	1.424E+00
Nd-143	PNL	6.954E-01	8.123E-01	8.656E-01
Nd-144	PNL	1.070E+00	1.518E+00	1.864E+00
Nd-145	PNL	5.786E-01	7.408E-01	8.440E-01
Nd-146	PNL	5.559E-01	7.737E-01	9.416E-01
Nd-148	PNL	3.006E-01	4.073E-01	4.855E-01
Nd-150	PNL	1.407E-01	1.951E-01	2.360E-01
Sm-147	KRI	2.303E-01	2.704E-01	3.081E-01
Sm-148	KRI	1.001E-01	1.612E-01	2.246E-01
<i>Sm-149</i>	<i>KRI</i>	<i>2.893E-03^b</i>	<i>1.852E-03</i>	<i>4.558E-03</i>
Sm-150	KRI	2.089E-01	2.896E-01	3.638E-01
Sm-151	KRI	7.521E-03	9.408E-03	1.072E-02
Sm-152	KRI	8.968E-02	1.096E-01	1.325E-01
Sm-154	KRI	3.066E-02	3.805E-02	5.640E-02
<i>Eu-151</i>	<i>KRI</i>	<i>1.794E-03</i>	<i>1.045E-03</i>	<i>3.435E-03</i>
<i>Eu-152</i>	<i>KRI</i>	<i>1.157E-04</i>	<i>5.926E-05</i>	<i>4.473E-04</i>
Eu-153	KRI	8.516E-02	1.290E-01	1.612E-01
Eu-154	KRI	6.075E-03	8.780E-03	1.175E-02
Eu-155	KRI	1.041E-03	1.385E-03	1.815E-03
Gd-154	KRI	1.365E-02	1.495E-02	2.002E-02
Gd-155	KRI	6.248E-03	7.408E-03	9.959E-03
Gd-156	KRI	6.364E-02	7.329E-02	9.533E-02
Gd-157	KRI		2.072E-03	4.887E-03
Gd-158	KRI	1.394E-02	1.486E-02	2.066E-02
Gd-160	KRI	1.446E-03		

^aRef. 31, Table 7.2. PNL burnup measurements performed in May 1987. Ref. 34, Table 3.2. PNL radiochemical analyses performed during June 1987, or corrected to this date. A reference date of 05/31/1987 was used in this work, yielding a cooling time of 1870 days. KRI lanthanide measurements for sample 87-81 performed 9/17/1993, and samples 87-63 and 87-72 performed 01/ 15/1995, corresponding to decay times of 4171 and 4656 days, respectively.

^bValues shown in italics are not recommended for use due to likely experimental errors.

Table 29. Measurement results for Calvert Cliffs 106-NBD107 samples (mg/g U_{initial})

Nuclide	Measurement laboratory ^b	106-NBD107-MM ^a	106-NBD107-GG (87-108)	106-NBD107-Q ^a
U-234	PNL	1.736E-01	1.441E-01	8.497E-02
U-235	PNL	4.379E+00	3.074E+00	1.595E+00
U-236	PNL	3.244E+00	3.437E+00	3.449E+00
U-238	PNL	9.581E+02	9.572E+02	9.384E+02
Pu-238	PNL	1.618E-01	2.209E-01	3.224E-01
Pu-239	PNL	4.327E+00	4.351E+00	4.272E+00
Pu-240	PNL	2.345E+00	2.633E+00	2.948E+00
Pu-241	PNL	8.236E-01	9.223E-01	1.005E+00
Pu-242	PNL	6.197E-01	8.795E-01	1.326E+00
Np-237	PNL	2.967E-01	3.645E-01	4.290E-01
Am-241	PNL	3.901E-01	4.827E-01	7.207E-01
Se-79	PNL	3.088E-03	4.159E-03	4.425E-03
Sr-90	PNL	3.826E-01	4.271E-01	4.980E-01
Tc-99	PNL	5.101E-01	5.936E-01	7.221E-01
Rh-103	KRI		6.542E-01	
Sn-126	PNL	1.296E-02	1.470E-02	1.930E-02
Cs-133	PNL			
Cs-135	PNL	3.978E-01	4.086E-01	4.716E-01
Cs-137	PNL	9.761E-01	1.119E+00	1.464E+00
Nd-143	PNL		7.189E-01	
Nd-144	PNL		1.603E+00	
Nd-145	PNL		7.246E-01	
Nd-146	PNL		7.805E-01	
Nd-148	PNL		4.124E-01	
Nd-150	PNL		N/A	
Sm-147	KRI		2.659E-01	
Sm-148	KRI		1.713E-01	
<i>Sm-149</i>	<i>KRI^c</i>		<i>2.174E-03</i>	
Sm-150	KRI		3.000E-01	
Sm-151	KRI		7.970E-03	
Sm-152	KRI		1.210E-01	
Sm-154	KRI		4.470E-02	
<i>Eu-151</i>	<i>KRI</i>		<i>1.326E-03</i>	
<i>Eu-152</i>	<i>KRI</i>		<i>1.263E-04</i>	
Eu-153	KRI		1.483E-01	
Eu-154	KRI		7.074E-03	
Eu-155	KRI		1.138E-03	
Gd-154	KRI		1.254E-02	
Gd-155	KRI		7.028E-03	
Gd-156	KRI		7.248E-02	
Gd-157	KRI		2.100E-03	
Gd-158	KRI		1.483E-02	
Gd-160	KRI		5.032E-04	

^aSamples without reported lanthanide measurements by either PNL or KRI.

^bRef. 32. PNL Measurements performed in July 1987. KRI lanthanide measurements performed in April 1996, and rhodium measurements performed in March 1996 (Ref. 37). These dates yielded cooling times of 2447 for the PNNL measurements and 5658 and 5627 days for the KRI measurements (note that KRI measurements date of April can be used for all isotopes because rhodium is stable).

^cValues shown in italics are not recommended for use due to likely experimental errors.

7.6 TAKAHAMA UNIT 3

Takahama Unit 3 is a PWR in Japan with a net generating capacity of 870 MWe, which was designed by Mitsubishi Heavy Industries, Ltd. First power was achieved in May 1984 with an initial core consisting of Mitsubishi Nuclear Fuel (MNF)/Nuclear Fuel Industries (NFI) 15 × 15 assemblies.⁵⁷

From 1990 to 1999, Japan Atomic Energy Research Institute (JAERI) carried out a series of projects focused on obtaining high-quality experimental isotopic assay and criticality data to support the development of burnup credit for storage and transportation of spent fuel. The measurements included destructive radiochemical analyses of spent fuel samples, axial gamma scanning of spent fuel rods, and exponential experiments on spent fuel assemblies. The measured data were used by JAERI for evaluating the accuracy of depletion or criticality computer codes.

Sixteen samples selected from three fuel rods irradiated in assemblies NT3G23 and NT3G24 of the Takahama-3 reactor, which is operated in Japan, were included for destructive isotopic analyses. Five of these samples were from a UO₂-Gd₂O₃ fuel rod (SF96), and 11 samples were from two UO₂ fuel rods (SF96 and SF97). The reported burnup of these samples was between 8 and 47 GWd/MTU. The Takahama Unit 3 samples evaluated in this report are summarized in Table 30.

Table 30. Summary of Takahama Unit 3 fuel samples from assemblies NT3G23 and NT3G24

Assembly	Rod ID.	Sample No.	Sample ID	Enrichment (wt % ²³⁵ U)	Axial location (cm) ^a	Burnup (GWd/MTU)
NT3G23	SF95	1	SF95-1	4.11	20.1	14.30
		2	SF95-2	4.11	36.1	24.35
		3	SF95-3	4.11	88.1	35.42
		4	SF95-4	4.11	216.1	36.69
		5	SF95-5	4.11	356.1	30.40
	SF96	6	SF96-1	2.63	17.6	7.79
		7	SF96-2	2.63	33.6	16.44
		8	SF96-3	2.63	85.6	28.20
		9	SF96-4	2.63	213.6	28.91
		10	SF96-5	2.63	353.6	24.19
NT3G24G	SF97	11	SF97-1	4.11	16.3	17.69
		12	SF97-2	4.11	35.0	30.73
		13	SF97-3	4.11	62.7	42.16
		14	SF97-4	4.11	183.9	47.03
		15	SF97-5	4.11	292.6	47.25
		16	SF97-6	4.11	355.6	40.79

^aDistance measured from top of fuel.

Source: Ref. 41.

The elements in each sample were separated by using exchange separation methods. The following experimental techniques were used to determine the nuclide concentrations:⁴¹

- ID-MS
- major actinides: U, Pu
- lanthanides: Nd, Sm
- α-spectrometry plus MS
 - Am, Cm
- γ-spectrometry

- ^{106}Ru , ^{134}Cs , ^{137}Cs , ^{144}Ce , ^{154}Eu , ^{125}Sb
- α -spectrometry
 - ^{237}Np

A summary of the nuclides measured, methods used, and corresponding experimental uncertainties are presented in Table 31. The reported experimental uncertainties were not specific for each sample measurement but were typical values based on previous measurement experience at JAERI. Not all nuclides shown in the table were measured in each of the samples. The reported experimental relative standard deviation is less than 0.5% for all measured Pu, Sm, and Nd isotopes, as well as for ^{235}U and ^{238}U . For minor actinides measured by MS and α -spectrometry the experimental errors are larger, in the 2 to 10% range. The nuclides determined through γ -spectrometry have measurement errors between 3 and 10%.

The experimental results of the radiochemical analyses for the 16 samples from fuel rods SF95, SF96, and SF97 were reported as g/MTU initial. These data were reported at discharge time, except for samarium nuclides in samples from rod SF97 that were reported at 3.96 years after discharge. The measured data are presented in Table 32 through Table 34 in g/g U_{initial} .

Table 31. Experimental techniques and uncertainties for Takahama-3 samples

Nuclide ID	Method^a	RSD^b (%)
U-234	ID-MS	< 1.0
U-235	ID-MS	< 0.1
U-236	ID-MS	< 2.0
U-238	ID-MS	< 0.1
Pu-238	ID-MS	< 0.5
Pu-239	ID-MS	< 0.3
Pu-240	ID-MS	< 0.3
Pu-241	ID-MS	< 0.3
Pu-242	ID-MS	< 0.3
Np-237	α -spec	< 10.0
Am-241	MS, α -spec	< 2.0
Am-242m	MS, α -spec	< 10.0
Am-243	MS, α -spec	< 5.0
Cm-242	MS, α -spec	< 10.0
Cm-243	MS, α -spec	< 2.0
Cm-244	MS, α -spec	< 2.0
Cm-245	MS, α -spec	< 2.0
Cm-246	MS, α -spec	< 5.0
Cs-134	γ -spec	< 3.0
Cs-137	γ -spec	< 3.0
Ce-144	γ -spec	< 10.0
Nd-142	ID-MS	< 0.1
Nd-143	ID-MS	< 0.1
Nd-144	ID-MS	< 0.1
Nd-145	ID-MS	< 0.1
Nd-146	ID-MS	< 0.1
Nd-148	ID-MS	< 0.1
Nd-150	ID-MS	< 0.1
Sm-147	ID-MS	< 0.1
Sm-148	ID-MS	< 0.1
Sm-149	ID-MS	< 0.1
Sm-150	ID-MS	< 0.1
Sm-151	ID-MS	< 0.1
Sm-152	ID-MS	< 0.1
Sm-154	ID-MS	< 0.1
Eu-154	γ -spec	< 3.0
Ru-106	γ -spec	< 5.0
Sb-125	γ -spec	< 10.0

^aMain technique is listed; some nuclides require multiple techniques to eliminate interferences.

^bRelative standard deviation.

Source: Ref. 41.

Table 32. Experimental results (g/g $U_{initial}$) for Takahama-3 samples from rod SF95

Assembly	NT3G23	NT3G23	NT3G23	NT3G23	NT3G23
Sample ID	SF95-1	SF95-2	SF95-3	SF95-4	SF95-5
Burnup^a (GWd/MTU)	14.30	24.35	35.42	36.69	30.40
U-234	2.987E-04	2.850E-04	1.873E-04	1.870E-04	2.829E-04
U-235	2.674E-02	1.927E-02	1.326E-02	1.230E-02	1.544E-02
U-236	2.672E-03	4.024E-03	4.911E-03	4.999E-03	4.566E-03
U-238	9.499E-01	9.424E-01	9.338E-01	9.335E-01	9.388E-01
Pu-238	1.718E-05	7.102E-05	1.539E-04	1.588E-04	1.020E-04
Pu-239 ^b	4.227E-03	5.655E-03	6.194E-03	6.005E-03	5.635E-03
Pu-240	7.802E-04	1.539E-03	2.186E-03	2.207E-03	1.821E-03
Pu-241	3.690E-04	9.578E-04	1.486E-03	1.466E-03	1.153E-03
Pu-242	3.790E-05	1.844E-04	4.516E-04	4.803E-04	2.976E-04
Am-241	1.378E-05	2.344E-05	3.310E-05	2.351E-05	2.840E-05
Am-242m	1.840E-07	5.201E-07	7.877E-07	7.282E-07	5.687E-07
Am-243	2.682E-06	2.289E-05	8.047E-05	8.472E-05	4.400E-05
Cm-242	1.510E-06	7.672E-06	1.964E-05	2.328E-05	1.006E-05
Cm-243	1.415E-08	1.240E-07	3.720E-07	3.976E-07	2.293E-07
Cm-244	2.712E-07	5.042E-06	2.562E-05	2.837E-05	1.064E-05
Cm-245	5.519E-09	1.962E-07	1.396E-06	1.587E-06	4.839E-07
Cm-246	2.560E-10	1.190E-08	1.049E-07	1.251E-07	1.952E-08
Nd-142	3.429E-06	8.887E-06	2.116E-05	2.222E-05	1.371E-05
Nd-143	4.631E-04	7.149E-04	9.299E-04	9.373E-04	8.303E-04
Nd-144	3.276E-04	6.046E-04	9.347E-04	1.024E-03	7.928E-04
Nd-145	3.328E-04	5.384E-04	7.392E-04	7.598E-04	6.518E-04
Nd-146	2.809E-04	4.925E-04	7.340E-04	7.624E-04	6.185E-04
Nd-148	1.592E-04	2.736E-04	3.979E-04	4.126E-04	3.401E-04
Nd-150	7.200E-05	1.258E-04	1.895E-04	1.959E-04	1.572E-04
Cs-134	2.343E-05	7.012E-05	1.404E-04	1.471E-04	1.014E-04
Cs-137	5.405E-04	9.336E-04	1.347E-03	1.400E-03	1.148E-03
Ce-144	1.937E-04	3.160E-04	4.560E-04	4.301E-04	3.868E-04
Eu-154	4.093E-06	1.306E-05	2.525E-05	2.657E-05	1.817E-05
Ru-106	4.447E-05	8.340E-05	1.360E-04	1.401E-04	1.208E-04
Sb-125	1.471E-06	2.900E-06	3.733E-06	3.169E-06	3.262E-06

^aAs reported in Ref. 41. Values correspond to discharge date of 6/19/1992.

^bPu-239 includes the amount of Np-239.

Table 33. Experimental results (g/g U_{initial}) for Takahama-3 samples from rod SF96

Assembly	NT3G23	NT3G23	NT3G23	NT3G23	NT3G23
Sample ID	SF96-1	SF96-2	SF96-3	SF96-4	SF96-5
Burnup^a (GWd/MTU)	7.79	16.44	28.20	28.91	24.19
U-234	1.805E-04	1.522E-04	1.251E-04	1.250E-04	1.354E-04
U-235	1.944E-02	1.408E-02	8.638E-03	8.064E-03	9.937E-03
U-236	1.421E-03	2.411E-03	3.244E-03	3.302E-03	3.013E-03
U-238	9.660E-01	9.580E-01	9.476E-01	9.475E-01	9.522E-01
Pu-238	8.536E-06	4.172E-05	1.206E-04	1.248E-04	7.978E-05
Pu-239 ^b	3.781E-03	5.459E-03	6.001E-03	5.819E-03	5.519E-03
Pu-240	6.764E-04	1.494E-03	2.303E-03	2.327E-03	1.964E-03
Pu-241	2.622E-04	8.684E-04	1.498E-03	1.480E-03	1.203E-03
Pu-242	2.440E-05	1.615E-04	5.103E-04	5.411E-04	3.551E-04
Np-237	6.125E-05	1.323E-04	2.168E-04	2.252E-04	1.875E-04
Am-241	5.985E-06	1.735E-05	2.845E-05	3.094E-05	2.149E-05
Am-242m	1.218E-07	4.579E-07	6.413E-07	6.793E-07	5.647E-07
Am-243	1.147E-06	1.728E-05	8.872E-05	9.598E-05	5.078E-05
Cm-242	8.502E-07	5.781E-06	1.628E-05	1.679E-05	1.115E-05
Cm-244	9.560E-08	3.092E-06	2.862E-05	3.128E-05	1.280E-05
Nd-143	2.521E-04	4.778E-04	7.158E-04	7.184E-04	6.433E-04
Nd-144	1.536E-04	3.588E-04	7.292E-04	7.513E-04	5.927E-04
Nd-145	1.800E-04	3.575E-04	5.766E-04	5.880E-04	5.095E-04
Nd-146	1.536E-04	3.266E-04	5.795E-04	5.948E-04	4.910E-04
Nd-148	8.770E-05	1.851E-04	3.201E-04	3.280E-04	2.733E-04
Nd-150	4.130E-05	8.972E-05	1.591E-04	1.628E-04	1.331E-04
Cs-134	8.609E-06	3.759E-05	1.002E-04	1.047E-04	7.146E-05
Cs-137	2.813E-04	5.983E-04	1.018E-03	1.053E-03	8.572E-04
Ce-144	1.179E-04	2.250E-04	3.362E-04	3.453E-04	3.145E-04
Eu-154	2.309E-06	8.538E-06	1.973E-05	1.992E-05	1.423E-05
Ru-106	2.830E-05	6.053E-05	1.402E-04	1.291E-04	1.344E-04
Sb-125	1.433E-06	2.829E-06	3.658E-06	4.645E-06	3.690E-06

^aAs reported in Ref. 41. Values correspond to discharge date of 6/19/1992.

^bPu-239 includes the amount of Np-239.

Table 34. Experimental results (g/g U_{initial}) for Takahama-3 samples from rod SF97

Assembly	NT3G24	NT3G24	NT3G24	NT3G24	NT3G24	NT3G24
Sample ID	SF97-1	SF97-2	SF97-3	SF97-4	SF97-5	SF97-6
Burnup ^a (GWd/MTU)	17.69	30.73	42.16	47.03	47.25	40.79
U-234	2.939E-04	2.348E-04	2.010E-04	1.872E-04	1.865E-04	2.057E-04
U-235	2.347E-02	1.571E-02	1.030E-02	8.179E-03	7.932E-03	1.016E-02
U-236	3.115E-03	4.560E-03	5.312E-03	5.528E-03	5.532E-03	5.272E-03
U-238	9.493E-01	9.377E-01	9.282E-01	9.246E-01	9.247E-01	9.310E-01
Pu-238	2.370E-05	1.250E-04	2.581E-04	3.199E-04	3.188E-04	2.175E-04
Pu-239 ^b	3.844E-03	5.928E-03	6.217E-03	6.037E-03	5.976E-03	5.677E-03
Pu-240	9.347E-04	1.871E-03	2.471E-03	2.668E-03	2.648E-03	2.326E-03
Pu-241	4.237E-04	1.235E-03	1.689E-03	1.770E-03	1.754E-03	1.494E-03
Pu-242	6.185E-05	3.152E-04	6.517E-04	8.246E-04	8.341E-04	5.977E-04
Np-237	1.521E-04	4.034E-04	5.845E-04	6.604E-04	6.701E-04	5.570E-04
Am-241	1.492E-05	4.017E-05	4.909E-05	5.311E-05	5.327E-05	4.297E-05
Am-242m	2.270E-07	8.838E-07	1.179E-06	1.233E-06	1.200E-06	9.756E-07
Am-243	4.448E-06	5.132E-05	1.410E-04	1.924E-04	1.935E-04	1.170E-04
Cm-242	2.134E-06	1.049E-05	1.839E-05	2.044E-05	1.903E-05	1.616E-05
Cm-243	2.483E-08	2.773E-07	6.921E-07	8.721E-07	8.670E-07	5.600E-07
Cm-244	4.981E-07	1.384E-05	5.696E-05	8.810E-05	8.823E-05	4.221E-05
Cm-245	1.087E-08	6.848E-07	3.735E-06	6.042E-06	5.915E-06	2.363E-06
Cm-246	3.866E-10	4.222E-08	3.648E-07	7.440E-07	7.549E-07	2.481E-07
Cm-247		4.043E-10	4.974E-09	1.098E-08	1.075E-08	3.139E-09
Nd-143	5.450E-04	8.307E-04	1.008E-03	1.048E-03	1.049E-03	9.736E-04
Nd-144	4.661E-04	8.843E-04	1.331E-03	1.567E-03	1.599E-03	1.311E-03
Nd-145	4.045E-04	6.480E-04	8.387E-04	9.118E-04	9.179E-04	8.247E-04
Nd-146	3.502E-04	6.304E-04	8.929E-04	1.008E-03	1.014E-03	8.586E-04
Nd-148	1.945E-04	3.389E-04	4.662E-04	5.204E-04	5.226E-04	4.504E-04
Nd-150	8.570E-05	1.582E-04	2.234E-04	2.516E-04	2.518E-04	2.130E-04
Cs-134	2.983E-05	1.030E-04	1.829E-04	2.139E-04	2.144E-04	1.632E-04
Cs-137	6.617E-04	1.151E-03	1.582E-03	1.749E-03	1.761E-03	1.531E-03
Ce-144	2.026E-04	3.061E-04	3.720E-04	3.756E-04	3.750E-04	3.714E-04
Eu-154	5.253E-06	1.973E-05	3.293E-05	3.739E-05	3.707E-05	2.859E-05
Ru-106	5.163E-05	1.162E-04	1.829E-04	1.936E-04	1.162E-04	1.959E-04
Sb-125	2.462E-06	5.118E-06	4.966E-06	6.090E-06	7.507E-06	4.546E-06
Sm-147 ^c	1.529E-04	2.050E-04	2.355E-04	2.468E-04	2.479E-04	2.371E-04
Sm-148	4.092E-05	1.194E-04	1.978E-04	2.338E-04	2.357E-04	1.809E-04
Sm-149	2.935E-06	3.976E-06	4.259E-06	3.943E-06	3.799E-06	3.843E-06
Sm-150	1.323E-04	2.499E-04	3.599E-04	4.074E-04	4.113E-04	3.409E-04
Sm-151	9.324E-06	1.351E-05	1.503E-05	1.491E-05	1.465E-05	1.294E-05
Sm-152	6.526E-05	9.546E-05	1.191E-04	1.298E-04	1.319E-04	1.207E-04
Sm-154	1.425E-05	2.977E-05	4.536E-05	5.252E-05	5.298E-05	4.231E-05

^aAs reported in Ref. 41. ^bPu-239 includes the amount of Np-239.

^cMeasured data for Sm isotopes were reported at 3.96 years after discharge; at discharge time for all other isotopes (9/30/1993).

7.7 TMI UNIT 1

TMI Unit 1 is a PWR in the United States with a net generating capacity of 871 MWe, which was designed by Babcock & Wilcox Company (B&W). First power was achieved in June 1974 with an initial core consisting of B&W Mark B8 15 × 15 assemblies.⁵⁷

Measurements on 19 spent fuel samples from the TMI Unit 1 reactor were performed under the auspices of the DOE YMP. Fuel rods were obtained from two separate assemblies, identified as NJ05YU and NJ070G. Radiochemical analyses were performed at two independent experimental facilities: Argonne National Laboratory (ANL) and General Electric Vallecitos Nuclear Center (GE-VNC). Measurements on 11 of the samples from rod H6 of assembly NJ05YU were performed in 1998 and 2000 at ANL.⁴⁴ The other eight samples, from rods O1, O12, and O13 of assembly NJ070G, were analyzed in 1999 at GE-VNC.⁴⁵ The TMI Unit 1 samples evaluated in this report are summarized in Table 35.

Table 35. Summary of TMI Unit 1 fuel samples from assemblies NJ05YU and NJ070G

Assembly	Sample No.	Measurement laboratory	Sample ID	Enrichment (wt % ²³⁵ U)	Axial location (cm) ^a	Burnup (GWd/MTU) ^b
NJ05YU	1	ANL	A1B	4.013	38.735	44.8
	2	ANL	D2	4.013	322.072	44.8
	3	ANL	B2	4.013	115.062	50.1
	4	ANL	C1	4.013	235.458	50.2
	5	ANL	D1A4	4.013	292.379	50.5
	6	ANL	A2	4.013	74.676	50.6
	7	ANL	C3	4.013	156.21	51.3
	8	ANL	C2B	4.013	194.615	52.6
	9	ANL	B3J	4.013	77.013	53.0
	10	ANL	B1B	4.013	155.956	54.5
	11	ANL	D1A2	4.013	261.899	55.7
NJ070G	12	GE-VNC	O13S7	4.657	39.37	22.8
	13	GE-VNC	O12S4	4.657	39.37	23.7
	14	GE-VNC	O12S6	4.657	278.13	24.0
	15	GE-VNC	O1S1	4.657	39.37	25.8
	16	GE-VNC	O13S8	4.657	197.104	26.3
	17	GE-VNC	O12S5	4.657	197.104	26.5
	18	GE-VNC	O1S3	4.657	278.13	26.7
	19	GE-VNC	O1S2	4.657	197.104	29.9

^aDistance between sample axial location and the tip of bottom end plug.

^bBurnup values determined by laboratories from measured ¹⁴⁸Nd.

Source: Refs. 44 and 45.

Both fuel assemblies were irradiated during cycle 10. Following indications of fuel leakage during cycle 10, EPRI examined the root causes of fuel rod failure. A detailed description of the investigations performed and the conclusions of the investigations have been made publicly available in the EPRI report TR-108784-V1.⁸³ It was determined that the cause of fuel rod failure was localized cladding corrosion induced by crud that affected some of the fresh fuel assemblies during cycle 10. Crud accumulation appeared predominantly at the interface between neighboring fresh fuel assemblies and corner locations in fresh fuel assemblies, resulting in cladding and fuel temperatures well above normal operating temperatures. Assembly NJ070G was a fresh fuel assembly during cycle 10 with failed fuel. Rods O1, O12, and O13 of this assembly were intact but significantly affected by localized corrosion, as hot cell examination determined. Rod O1 was a corner rod with a higher average power than the other assembly

rods, whereas rods O12 and O13 were in close proximity to a failed rod (O11). The fuel in assembly NJ05YU was adjacent to the failed fuel rods and was identified as having elevated levels of crud deposits on the fuel rods. Localized phenomena may have introduced additional uncertainties related to the actual irradiation conditions of the fuel that may affect the accuracy of code predictions. The type of uncertainties and their importance to the fuel simulations was not addressed in this validation.

7.7.1 ANL Measurements

The radiochemical analysis at ANL considered 11 samples from fuel rod H6 of assembly NJ05YU, cut from rod segments provided by GE-VNC. The samples for analysis were prepared by dissolution of an approximately 0.1–0.2 g aliquot of homogenized fuel sample powder. Analyses were carried out by using inductively coupled plasma mass spectrometry (ICPMS), γ -spectrometry, and α -spectrometry to determine the isotopic mass of 31 nuclides. The use of isotopic dilution was limited to the uranium and plutonium isotopes, resulting in larger uncertainties for the other ICPMS results. The results were reported relative to the measured ^{238}U content in the sample, as g/g ^{238}U . Two measures of the experimental uncertainty, a within-sample precision and a bias uncertainty, were provided by ANL. The within-sample precision was estimated by ANL as one standard deviation through repeated measurements of samples, whereas the bias uncertainty was estimated from deviations of quality control standard solutions measured in two separate phases of measurement performed at different times; the bias uncertainty included the propagation of error for normalization to ^{238}U (Ref. 44).

The main experimental techniques used for each nuclide and the reported corresponding experimental uncertainties⁴⁴ are presented in Table 36. In addition to the bias values shown in the table, a bias uncertainty of 3.8% was reported for ^{238}U , but no explanation was provided on the significance of this value; it is assumed here that it refers to the absolute ^{238}U concentration measured directly. The within-sample precision shown in the table was calculated so that it accounted for error propagation due to normalization of the concentration to the ^{238}U content as

$$\sigma_{i,\text{within-sample}} = \sqrt{\left(\sigma_{i,\text{within-sample}}^{\text{reported}}\right)^2 + \left(\sigma_{^{238}\text{U},\text{within-sample}}^{\text{reported}}\right)^2}, \quad (13)$$

where i identifies the nuclide. The total uncertainty for the measured concentration of a nuclide i expressed relative to the ^{238}U content is shown in the sixth column of Table 36 and was obtained by combining the within-sample uncertainty, calculated as in Eq. (13), and the reported bias, as

$$\sigma_{i,\text{total}} = \sqrt{\left(\sigma_{i,\text{within-sample}}\right)^2 + \left(\sigma_{i,\text{bias}}^{\text{reported}}\right)^2}. \quad (14)$$

The total uncertainty is 3.7% for ^{235}U , in the range 5–8% for plutonium nuclides, and about 5–7% for neodymium isotopes.

The measurement results for the samples analyzed at ANL (Ref. 44) are shown in Table 37. The data are obtained from the reported units of g/g ^{238}U using the procedures described in Sect. 6.5.

Table 36. Experimental techniques and uncertainties for TMI-1 samples measurements at ANL

Nuclide ID	Method ^a	Reported within-sample precision (%)	Reported bias uncertainty (%)	Within-sample precision ^b accounting for normalization to ²³⁸U (%)	Total ^c uncertainty (%)
U-234	ICP-MS	3.0	2.7	3.4	4.4
U-235	ICP-MS	1.5	2.9	2.3	3.7
U-236	ICP-MS	4.6	3.1	4.9	5.8
U-238	ICP-MS	1.7	3.8	2.4	4.5
Np-237	ICP-MS	4.1	3.4	4.4	5.6
Pu-238	α -spec	6.8	3.6	7.0	7.9
Pu-239	ICP-MS	4.3	3.3	4.6	5.7
Pu-240	ICP-MS	5.1	3.1	5.4	6.2
Pu-241	ICP-MS	3.2	2.9	3.6	4.6
Pu-242	ICP-MS	5.9	2.8	6.1	6.7
Am-241	γ -spec	6.1	3.1	6.3	7.1
Am-242m	ICP-MS	NA	3.1		3.1
Am-243	ICP-MS	4.2	3.8	4.5	5.9
Mo-95	ICP-MS	1.7	3.4	2.4	4.2
Tc-99	ICP-MS	2.7	7.3	3.2	8.0
Ru-101	ICP-MS	1.6	5.3	2.3	5.8
Rh-103	ICP-MS	1.5	3.1	2.3	3.8
Ag-109	ICP-MS	4.7	3.1	5.0	5.9
Cs-137	γ -spec	3.6	2.7	4.0	4.8
Nd-143	ICP-MS	3.5	3.9	3.9	5.5
Nd-145	ICP-MS	4.8	3.5	5.1	6.2
Nd-148	ICP-MS	4.2	5.5	4.5	7.1
Sm-147	ICP-MS	3.3	9.4	3.7	10.1
Sm-149	ICP-MS	7.1	3.5	7.3	8.1
Sm-150	ICP-MS	3.5	3.2	3.9	5.0
Sm-151	ICP-MS	6.1	3.2	6.3	7.1
Sm-152	ICP-MS	2.7	3.2	3.2	4.5
Eu-151	ICP-MS	12.0	2.9	12.1	12.5
Eu-153	ICP-MS	3.9	3.0	4.3	5.2
Eu-155	γ -spec	6.4	2.7	6.6	7.2
Gd-155	ICP-MS	6.8	3.8	7.0	8.0

^aMain technique is listed; some nuclides require multiple techniques to eliminate interferences.

^bCalculated as shown in Eq. (13).

^cCalculated as shown in Eq. (14).

Table 37. Experimental results (g/g U_{initial}) for TMI-1 samples measured at ANL

Assembly	NJ05YU	NJ05YU	NJ05YU	NJ05YU	NJ05YU	NJ05YU	NJ05YU	NJ05YU	NJ05YU	NJ05YU	NJ05YU
Sample ID	A1B ^a	D2 ^b	B2 ^b	C1 ^b	D1A4 ^a	A2 ^b	C3 ^b	C2B ^a	B3J ^a	B1B ^a	D1A2 ^a
Burnup (GWd/MTU)	44.8	44.8	50.1	50.2	50.5	50.6	51.3	52.6	53.0	54.5	55.7
U-234	2.054E-04	1.923E-04	1.868E-04	1.977E-04	1.975E-04	1.912E-04	1.847E-04	1.808E-04	1.834E-04	1.877E-04	1.927E-04
U-235	8.605E-03	7.378E-03	6.205E-03	6.588E-03	7.485E-03	6.319E-03	6.251E-03	6.228E-03	6.111E-03	6.386E-03	6.966E-03
U-236	5.111E-03	5.334E-03	5.400E-03	5.470E-03	5.362E-03	5.497E-03	5.327E-03	5.185E-03	5.456E-03	5.402E-03	5.452E-03
Pu-238	4.033E-04	3.252E-04	3.144E-04	3.299E-04	3.747E-04	3.538E-04	2.511E-04	4.585E-04	3.982E-04	4.316E-04	3.809E-04
Pu-239	5.064E-03	5.427E-03	5.289E-03	5.405E-03	5.399E-03	5.340E-03	5.512E-03	4.991E-03	5.088E-03	5.107E-03	5.452E-03
Pu-240	2.342E-03	2.667E-03	2.728E-03	2.754E-03	2.621E-03	2.781E-03	2.844E-03	2.546E-03	2.654E-03	2.632E-03	2.708E-03
Pu-241	1.208E-03	1.366E-03	1.387E-03	1.423E-03	1.430E-03	1.358E-03	1.403E-03	1.329E-03	1.364E-03	1.362E-03	1.469E-03
Pu-242	6.793E-04	7.945E-04	9.146E-04	9.000E-04	9.414E-04	9.229E-04	9.233E-04	9.318E-04	1.106E-03	9.570E-04	9.637E-04
Np-237	6.040E-04	6.755E-04	6.917E-04	7.041E-04	6.848E-04	6.938E-04	6.823E-04	6.864E-04	7.060E-04	7.012E-04	7.058E-04
Am-241	3.466E-04	3.457E-04	3.412E-04	3.770E-04	5.261E-04	3.021E-04	3.028E-04	5.074E-04	5.060E-04	2.880E-04	3.350E-04
Am-242m	--	--	--	--	8.389E-07	--	--	1.679E-06	1.244E-06	1.031E-06	6.085E-07
Am-243	1.245E-04	1.923E-04	2.552E-04	2.458E-04	1.846E-04	2.541E-04	2.465E-04	1.956E-04	2.111E-04	2.043E-04	2.056E-04
Nd-143	9.850E-04	9.134E-04	9.987E-04	9.794E-04	1.080E-03	9.516E-04	9.510E-04	1.033E-03	1.060E-03	1.086E-03	1.111E-03
Nd-145	8.521E-04	8.289E-04	9.062E-04	8.972E-04	9.598E-04	8.777E-04	8.965E-04	9.411E-04	9.770E-04	9.847E-04	1.000E-03
Nd-148	4.869E-04	4.869E-04	5.447E-04	5.452E-04	5.482E-04	5.506E-04	5.577E-04	5.720E-04	5.761E-04	5.926E-04	6.058E-04
Cs-137	1.682E-03	1.617E-03	1.748E-03	1.811E-03	1.652E-03	1.765E-03	1.699E-03	1.762E-03	1.733E-03	1.758E-03	1.533E-03
Sm-147	2.258E-04	1.821E-04	1.859E-04	1.866E-04	2.353E-04	1.968E-04	1.819E-04	2.288E-04	2.479E-04	2.549E-04	2.515E-04
Sm-149	3.113E-06	3.094E-06	3.264E-06	3.188E-06	3.599E-06	3.816E-06	2.899E-06	3.358E-06	3.189E-06	3.423E-06	3.855E-06
Sm-150	3.577E-04	3.485E-04	3.754E-04	3.835E-04	4.125E-04	3.742E-04	3.619E-04	4.189E-04	4.525E-04	4.675E-04	4.525E-04
Sm-151	1.292E-05	1.264E-05	1.341E-05	1.247E-05	1.412E-05	1.256E-05	1.256E-05	1.329E-05	1.475E-05	1.500E-05	1.551E-05
Sm-152	1.217E-04	1.208E-04	1.295E-04	1.266E-04	1.338E-04	1.321E-04	1.256E-04	1.301E-04	1.419E-04	1.436E-04	1.423E-04
Eu-151	6.579E-07	7.034E-07	7.934E-07	6.856E-07	6.673E-07	8.832E-07	8.476E-07	7.030E-07	7.475E-07	5.696E-07	6.618E-07
Eu-153	1.468E-04	1.561E-04	1.674E-04	1.672E-04	1.744E-04	1.709E-04	1.607E-04	1.725E-04	1.834E-04	1.859E-04	1.891E-04
Eu-155	1.004E-05	1.227E-05	1.313E-05	1.432E-05	1.264E-05	1.284E-05	1.274E-05	9.964E-06	1.032E-05	1.546E-05	9.821E-06

Table 37. Experimental results (g/g U_{initial}) for TMI-1 samples measured at ANL (continued)

Assembly	NJ05YU	NJ05YU	NJ05YU	NJ05YU	NJ05YU	NJ05YU	NJ05YU	NJ05YU	NJ05YU	NJ05YU	NJ05YU
Sample ID	A1B ^a	D2 ^b	B2 ^b	C1 ^b	D1A4 ^a	A2 ^b	C3 ^b	C2B ^a	B3J ^a	B1B ^a	D1A2 ^a
Burnup (GWd/MTU)	44.8	44.8	50.1	50.2	50.5	50.6	51.3	52.6	53.0	54.5	55.7
Gd-155	8.224E-06	5.594E-06	6.547E-06	6.357E-06	1.394E-05	5.220E-06	6.666E-06	9.411E-06	1.041E-05	1.003E-05	1.019E-05
Mo-95	1.041E-03	9.199E-04	1.128E-03	1.100E-03	1.089E-03	1.118E-03	1.006E-03	1.098E-03	1.124E-03	1.150E-03	1.111E-03
Tc-99	1.422E-03	9.757E-04	1.091E-03	1.081E-03	1.191E-03	1.081E-03	1.034E-03	1.356E-03	1.244E-03	1.316E-03	1.138E-03
Ru-101	1.115E-03	9.478E-04	1.202E-03	1.164E-03	1.098E-03	1.155E-03	1.025E-03	1.172E-03	1.171E-03	1.187E-03	1.129E-03
Rh-103	5.956E-04	5.157E-04	6.288E-04	6.182E-04	6.027E-04	6.190E-04	5.475E-04	6.145E-04	6.203E-04	6.267E-04	6.168E-04
Ag-109	5.111E-05	4.655E-05	5.280E-05	5.359E-05	8.463E-05	5.968E-05	9.233E-05	6.532E-05	7.788E-05	4.399E-05	4.607E-05

^aCooling time for TMI-1 samples A1B, B1B, B3J, C2B, D1A2, and D1A4 is 1711 days (Ref. 46, p.12).

^bCooling time for TMI-1 samples A2, B2, C1, C3, and D2 is 1103 days (Ref. 46, p.12).

7.7.2 GE-VNC Measurements

The measurements performed at GE-VNC⁴⁵ considered eight samples selected from three fuel rods from assembly NJ070G. Most of the 32 nuclides for which isotopic concentrations were measured at GE-VNC were determined by using thermal ionization mass spectrometry (TIMS) and some through γ - or α -spectrometry. The nuclide concentrations in the samples measured by TIMS were determined from measurements of spiked and unspiked samples. The nuclide content was reported as g/g ²³⁸U. The main experimental techniques used for each nuclide and the corresponding experimental uncertainty as reported are presented in Table 38. The experimental errors, reported by GE-VNC as relative uncertainty at a 95% confidence level, are shown in the table. The relative standard deviation (RSD) shown in the fourth column of the table was obtained as half of the reported uncertainty at a 95% confidence level. The RSD for the GE-VNC measurements is 0.6% for all plutonium nuclides except for ²³⁸Pu, 0.5% for ²³⁵U, and 0.8% for neodymium isotopes.

The reported results of the radiochemical analyses for samples measured at GE-VNC⁴⁵ are shown in Table 39.

Table 38. Experimental techniques and uncertainties for TMI-1 samples measurements at GE-VNC

Nuclide ID	Method ^a	Reported uncertainty at 95% confidence (%)	RSD ^b (%)
U-234	TIMS	1.0	0.5
U-235	TIMS	1.0	0.5
U-236	TIMS	1.0	0.5
U-238	TIMS	1.0	0.5
Np-237	α -spec	5.8	2.9
Pu-238	α -spec	5.0	2.5
Pu-239	TIMS	1.2	0.6
Pu-240	TIMS	1.2	0.6
Pu-241	TIMS	1.2	0.6
Pu-242	TIMS	1.2	0.6
Am-241	TIMS, α -spec	7.0	3.5
Am-242m	TIMS, α -spec	7.0	3.5
Am-243	TIMS, α -spec	7.0	3.5
Cm-242	TIMS, α -spec	20.0	10.0
Cm-243	TIMS, α -spec	5.5	2.75
Cm-244	TIMS, α -spec	5.5	2.75
Cm-245	TIMS, α -spec	5.5	2.75
Cs-134	γ -spec	3.5	1.75
Cs-137	γ -spec	3.5	1.75
Nd-143	TIMS	1.5	0.75
Nd-145	TIMS	1.5	0.75
Nd-146	TIMS	1.5	0.75
Nd-148	TIMS	1.5	0.75
Nd-150	TIMS	1.5	0.75
Sm-147	TIMS	1.7	0.85
Sm-149	TIMS	1.8	0.9
Sm-150	TIMS	1.7	0.85
Sm-151	TIMS	1.7	0.85
Sm-152	TIMS	1.7	0.85
Eu-151	TIMS	1.7	0.85
Eu-153	TIMS	1.8	0.9
Gd-155	TIMS	2.7	1.35

^aMain technique is listed; some nuclides require multiple techniques to eliminate interferences.

^bRelative standard deviation; calculated here as half of the uncertainty reported at a 95% confidence level.

Source: Ref. 45.

Table 39. Experimental results (g/g U_{initial}) for TMI-1 samples measured at GE-VNC

Assembly	NJ070G	NJ070G	NJ070G	NJ070G	NJ070G	NJ070G	NJ070G	NJ070G
Sample ID	O13S7 ^b	O12S4 ^a	O12S6 ^a	O1S1 ^a	O13S8 ^b	O12S5 ^b	O1S3 ^a	O1S2 ^b
Burnup (GWd/MTU)	22.8	23.7	24.0	25.8	26.3	26.5	26.7	29.9
U-234	3.427E-04	3.332E-04	3.260E-04	3.263E-04	3.184E-04	3.126E-04	3.134E-04	3.037E-04
U-235	2.376E-02	2.356E-02	2.388E-02	2.203E-02	2.191E-02	2.181E-02	2.170E-02	1.916E-02
U-236	4.216E-03	4.299E-03	4.384E-03	4.529E-03	4.579E-03	4.615E-03	4.668E-03	4.990E-03
Pu-238	6.019E-05	6.270E-05	7.765E-05	7.192E-05	8.699E-05	8.799E-05	9.354E-05	1.084E-04
Pu-239	5.418E-03	5.435E-03	6.182E-03	5.448E-03	5.880E-03	6.000E-03	6.024E-03	5.588E-03
Pu-240	1.371E-03	1.389E-03	1.508E-03	1.519E-03	1.620E-03	1.647E-03	1.712E-03	1.850E-03
Pu-241	6.610E-04	6.890E-04	7.999E-04	7.539E-04	8.230E-04	8.397E-04	8.942E-04	9.149E-04
Pu-242	1.446E-04	1.483E-04	1.649E-04	1.800E-04	2.022E-04	2.059E-04	2.208E-04	2.841E-04
Np-237	2.826E-04	3.032E-04	3.278E-04	3.038E-04	3.474E-04	3.482E-04	3.639E-04	3.953E-04
Am-241	1.624E-04	1.521E-01	1.377E-01	1.144E-01	2.022E-01	2.078E-01	1.712E-01	1.981E-01
Am-242m	3.155E-04	3.539E-04	3.719E-04	2.747E-04	4.672E-04	4.849E-04	4.209E-04	4.233E-04
Am-243	1.606E-02	1.690E-02	1.649E-02	1.500E-02	2.669E-02	2.771E-02	2.563E-02	3.504E-02
Cm-242 ^c	6.995E-06	2.159E-05	1.873E-05	1.772E-05	1.170E-05	1.123E-05	2.713E-05	1.635E-05
Cm-243	5.606E-05	5.970E-05	6.547E-05	5.157E-05	9.457E-05	1.002E-04	9.728E-05	1.168E-04
Cm-244	2.460E-03	2.713E-03	3.016E-03	2.494E-03	4.897E-03	5.158E-03	4.976E-03	7.177E-03
Cm-245	1.070E-04	1.164E-04	1.564E-04	1.116E-04	2.566E-04	2.715E-04	2.628E-04	3.757E-04
Nd-143	6.958E-04	7.049E-04	7.175E-04	7.454E-04	7.594E-04	7.638E-04	7.745E-04	8.336E-04
Nd-145	5.174E-04	5.247E-04	5.283E-04	5.626E-04	5.693E-04	5.719E-04	5.809E-04	6.420E-04
Nd-146	4.732E-04	4.806E-04	4.927E-04	5.213E-04	5.356E-04	5.392E-04	5.491E-04	6.149E-04
Nd-148	2.601E-04	2.638E-04	2.698E-04	2.860E-04	2.921E-04	2.939E-04	3.003E-04	3.345E-04
Nd-150	1.174E-04	1.183E-04	1.227E-04	1.294E-04	1.330E-04	1.339E-04	1.375E-04	1.533E-04
Cs-134	1.653E-05	2.084E-05	2.285E-05	2.353E-05	2.125E-05	2.125E-05	2.713E-05	2.579E-05
Cs-137	8.375E-04	8.495E-04	8.598E-04	9.104E-04	9.457E-04	9.361E-04	9.634E-04	1.093E-03
Sm-147	1.746E-04	1.699E-04	1.677E-04	1.791E-04	1.863E-04	1.881E-04	1.815E-04	2.056E-04
Sm-149	3.972E-06	4.055E-06	4.430E-06	4.051E-06	4.139E-06	4.156E-06	4.415E-06	4.074E-06
Sm-150	1.934E-04	1.981E-04	2.033E-04	2.157E-04	2.228E-04	2.256E-04	2.310E-04	2.598E-04
Sm-151	1.268E-05	1.295E-05	1.480E-05	1.275E-05	1.414E-05	1.413E-05	1.431E-05	1.374E-05
Sm-152	7.953E-05	8.091E-05	7.877E-05	8.654E-05	8.605E-05	8.677E-05	8.924E-05	9.999E-05
Eu-151	4.206E-07	4.027E-07	4.580E-07	3.891E-07	4.672E-07	4.699E-07	4.312E-07	4.430E-07
Eu-153	6.695E-05	6.918E-05	7.203E-05	7.548E-05	8.062E-05	8.097E-05	8.231E-05	9.438E-05
Gd-155	1.972E-06	1.905E-06	2.182E-06	2.307E-06	2.528E-06	2.509E-06	2.638E-06	2.888E-06

^aCooling time for TMI-1 samples O1S1, O1S3, O12S4, and O12S6 is 1298 days (Ref. 46, p.12).

^bCooling time for TMI-1 samples O1S2, O12S5, O13S7, and O13S8 is 1529 days (Ref. 46, p.12).

^cAverage of the two values measured by TIMS and γ -spectrometry.

7.8 GÖSGEN REACTOR: ARIANE PROGRAM

Gösgen is a PWR in Switzerland with a net generating capacity of 1020 MWe, which was designed by German Kraftwerk Union AG (KWU). First power was achieved in February 1979 with an initial core consisting of RBU 15 × 15 assemblies.⁵⁷

ARIANE, an international program designed to improve the database of isotopic measurements for spent fuel source term and isotopic inventory validation, was coordinated by Belgonucleaire and completed in March 2001.⁴⁸ This collaborative project involved participants from laboratories and utilities from seven countries: Belgium, Germany, Japan, Netherlands, Switzerland, the United Kingdom, and the United States.

A key feature of the ARIANE program was that two cross-checking laboratories participated in radiochemical assay measurements to reduce the experimental uncertainties and improve confidence in the measured data: Studiecentrum voor Kernenergie–Centre d'Étude de l'Énergie Nucléaire (SCK-CEN) in Belgium and Institute for Transuranium Elements (ITU) in Germany. Measurements were carried out on both uranium dioxide (UO₂) and mixed oxide (MOX) fuels between 1996 and 1999. Only the UO₂ samples are analyzed in this report.

The three UO₂ samples considered were selected from fuel rods irradiated in the Gösgen reactor operated in Switzerland. One of these samples was obtained from an assembly with an initial enrichment of 3.5 wt % ²³⁵U that was irradiated for four consecutive cycles. The other two samples, irradiated for three cycles, were taken from a rebuilt assembly with initial fuel enrichment of 4.1 wt % ²³⁵U. The main characteristics of the three samples analyzed are summarized in Table 40.

Three UO₂ samples, identified as GU1, GU3, and GU4, were measured in the ARIANE program. Duplicate measurements for sample GU3 were carried out at two different facilities, SCK-CEN in Belgium and ITU in Germany, and the results of these two measurements were combined. Measurements for sample GU1 were performed at SCK-CEN, and measurements for sample GU4 were carried out at ITU only.

Table 40. Summary of Gösgen (ARIANE) fuel samples

Assembly	Sample No.	Measurement laboratory	Fuel Sample ID	Enrichment (wt % ²³⁵ U)	Axial location (cm) ^a	Burnup (GWd/t) ^b
12-40	1	SCK-CEN	GU1	3.5	97.7	59.7
16-01, 17-01	2	SCK-CEN, ITU	GU3	4.1	127.42	52.5
16-01, 17-01	3	ITU	GU4	4.1	7.42	29.1

^aWith respect to the bottom of the active fuel region.

The following main experimental techniques have been applied for measurements performed at SCK-CEN:

- Thermal ionization mass spectrometry (TIMS)
 - major (U, Pu) and minor (Am and ^{245,246}Cm) actinides
 - lanthanides: Nd, Sm, ¹⁴⁴Ce, ¹⁵⁵Gd, ¹⁵¹Eu, ¹⁵³Eu
 - cesium nuclides: ^{133–135}Cs
- Inductively coupled plasma mass spectrometry (ICP-MS) with external calibration
- Metallics: ⁹⁵Mo, ⁹⁹Tc, ¹⁰¹Ru, ¹⁰³Rh, ¹⁰⁹Ag

- ^{237}Np
- γ -spectrometry
 - ^{106}Ru , ^{137}Cs , ^{144}Ce , ^{154}Eu , ^{155}Eu , ^{243}Cm , ^{125}Sb
- α -spectrometry
 - ^{242}Cm , ^{244}Cm
- β -spectrometry
 - ^{90}Sr

The following two main experimental techniques have been used for measurements performed at ITU:

- TIMS
 - major actinides (uranium, plutonium)
- ICP-MS with IDA (isotope dilution analysis)
- all other measured nuclides

Because of the variety of the analysis techniques, the varying properties of the nuclides being analyzed, and their differing concentrations, uncertainties in the measured concentrations can vary considerably. Table 41 lists the measurement method used and the experimental uncertainty, expressed both as the reported⁴⁸ uncertainty at 95% confidence level and as relative standard deviation, which was calculated as half of the 95% confidence level uncertainty reported. Only the maximum uncertainty corresponding to the measurements at each laboratory is shown in Table 41.

The nuclide concentrations in mg/g U initial in the measured samples are provided in Table 42. For metallic fission products, the values represent a combination of the separate measurements done on the main solution and undissolved residue. For samples GU1 and GU4, the data shown in the table correspond to measurement dates shown in Table 43, except for ^{106}Ru , ^{125}Sb , and ^{147}Pm , for which they correspond to discharge. For sample GU3, most of the isotopes considered by the program were measured at both SCK-CEN and ITU. For the isotopes with two independent measurements, the recommended values were established by consensus of experts participating in the program, based on a detailed cross-check analysis of the measurements. The cross-check was based on a comparison of the 95% confidence intervals associated to the measured values. If there was an intersection zone between the two 95% confidence intervals, the concentration results were combined in a weighted average. If the two concentration values were outside this intersection zone, either only one of the two values was recommended based on a detailed analysis of the measurement process or both values were maintained without recommendation. The isotope concentration values shown in Table 42 for sample GU3 correspond to the discharge date for the following isotopes: ^{241}Pu , $^{242\text{m}}\text{Am}$, $^{242,243,244}\text{Cm}$, ^{90}Sr , ^{106}Ru , ^{125}Sb , $^{134,137}\text{Cs}$, ^{144}Ce , ^{147}Pm , ^{151}Sm , $^{154,155}\text{Eu}$; for the other considered isotopes, the data correspond to the measurement dates at which measurements were performed at the two laboratories presented in Table 43. There were four nuclides ($^{244,245}\text{Cm}$, ^{133}Cs , and ^{155}Gd) measured in sample GU3 for which no recommended values were provided because of disagreement between the measurement values reported by SCK-CEN and ITU. For these four nuclides, the data shown in Table 42 were calculated as weighted averages of the two results provided by the program as given in Eq. (15):

$$c_{avg} = \left(\frac{c_1}{\sigma_1^2} + \frac{c_2}{\sigma_2^2} \right) / \left(\frac{1}{\sigma_1^2} + \frac{1}{\sigma_2^2} \right), \quad (15)$$

where c_1 and c_2 are the reported concentration values and σ_1 and σ_2 the corresponding relative experimental errors. Note that the two reported concentrations for these four nuclides differed by about 6% for ^{133}Cs , 14% for ^{155}Gd , and 20% for $^{244,245}\text{Cm}$.

Table 41. Experimental techniques and uncertainties for ARIANE Program Gösgen samples

Nuclide ID	Method ^a	Measurements at SCK/CEN		Measurements at ITU		
		Uncertainty ^b		Uncertainty ^b		
		95% confidence (%)	RSD ^c (%)	95% confidence (%)	RSD ^c (%)	
U-234	TIMS	5.02	2.51	TIMS	0.02	0.01
U-235	TIMS	2.05	1.03	TIMS	2.40	1.20
U-236	TIMS	0.67	0.34	TIMS	1.57	0.79
U-238	TIMS	0.45	0.23	TIMS	0.02	0.01
Pu-238	TIMS	3.05	1.53	TIMS	2.15	1.08
Pu-239	TIMS	0.57	0.29	TIMS	0.51	0.26
Pu-240	TIMS	0.57	0.29	TIMS	0.51	0.26
Pu-241	TIMS	0.57	0.29	TIMS	3.40	1.70
Pu-242	TIMS	0.59	0.29	TIMS	0.55	0.28
Np-237	ICP-MS	20.60	10.30	ICP-MS	9.61	4.81
Am-241	TIMS	3.56	1.78	ICP-MS	11.87	5.94
Am-242m	TIMS	10.60	5.30			
Am-243	TIMS	3.56	1.78	ICP-MS	13.29	6.65
Cm-242	α -spec	7.22	3.61			
Cm-243	γ -spec	73.49	36.75			
Cm-244	α -spec	3.24	1.62	ICP-MS	12.85	6.43
Cm-245	TIMS	5.89	2.95	ICP-MS	20.29	10.15
Cm-246	TIMS	20.24	10.12			
Cs-133	TIMS	4.91	2.46	ICP-MS	3.27	1.64
Cs-134	TIMS	4.94	2.46	ICP-MS	8.20	4.10
Cs-135	TIMS	4.91	2.46	ICP-MS	3.29	1.65
Cs-137	γ -spec	4.90	2.45	ICP-MS	3.00	1.50
Ce-144	γ -spec	7.84	3.92	ICP-MS	7.49	3.75
Nd-142	TIMS	10.01	5.01	ICP-MS	10.18	5.09
Nd-143	TIMS	0.57	0.29	ICP-MS	12.32	6.16
Nd-144	TIMS	0.57	0.29	ICP-MS	11.89	5.95
Nd-145	TIMS	0.57	0.29	ICP-MS	11.78	5.89
Nd-146	TIMS	0.57	0.29	ICP-MS	14.73	7.37
Nd-148	TIMS	0.59	0.30	ICP-MS	13.4	6.70
Nd-150	TIMS	0.59	0.30	ICP-MS	13.55	6.78
Pm-147	β -spec	18.01	9.00	ICP-MS	13.51	6.76
Sm-147	TIMS	0.64	0.32	ICP-MS	21.14	10.57
Sm-148	TIMS	0.64	0.32	ICP-MS	8.01	4.01
Sm-149	TIMS	2.09	1.05	ICP-MS	42.83	21.42
Sm-150	TIMS	0.64	0.32	ICP-MS	6.87	3.44
Sm-151	TIMS	0.79	0.40	ICP-MS	67.63	33.82
Sm-152	TIMS	0.64	0.32	ICP-MS	6.41	3.21
Sm-154	TIMS	0.66	0.33	ICP-MS	11.3	5.65
Eu-151	TIMS	2.10	1.05			
Eu-153	TIMS	0.67	0.34	ICP-MS	10.97	5.49
Eu-154	γ -spec	5.29	2.65	ICP-MS	23.73	11.87
Eu-155	γ -spec	9.83	4.92	ICP-MS	32.13	16.07
Gd-155	TIMS	5.00	2.50	ICP-MS	13.72	6.86
Sr-90	β -spec	16.01	8.01	ICP-MS	0.77	0.39
Mo-95	ICP-MS	9.14	4.57	ICP-MS	2.20	1.10
Tc-99	ICP-MS	17.7	8.85	ICP-MS	1.78	0.89
Ru-101	ICP-MS	24.42	12.21	ICP-MS	1.88	0.94
Ru-106	γ -spec	28.41	14.21	ICP-MS	8.18	4.09
Rh-103	ICP-MS	9.77	4.89	ICP-MS	6.53	3.27
Ag-109	ICP-MS	18.12	9.06			
Sb-125	γ -spec	18.85	9.43			

^aMain technique is mentioned; some nuclides required multiple techniques to eliminate interferences.

^bThe maximum of the values for the two UO₂ samples measured at this facility is shown.

^cRelative standard deviation.

Table 42. Experimental results for ARIANE Program Gösgen samples

Sample ID	GU1		GU3		GU4	
Burnup ^a	59.7		52.5		29.1	
Enrichment (wt % ²³⁵ U)	3.5		4.1		4.1	
Measuring laboratory	SCK/CEN		SCK/CEN & ITU		ITU	
Nuclide ID	g/g U _{initial}	RSD ^b (%)	g/g U _{initial}	RSD (%)	g/g U _{initial}	RSD (%)
U-234	1.20E-04	2.51	1.43E-04	0.01	1.95E-04	0.01
U-235	2.11E-03	1.03	6.05E-03	0.32	1.45E-02	0.45
U-236	4.83E-03	0.34	5.65E-03	0.31	4.59E-03	0.45
U-238	9.20E-01	0.23	9.27E-01	0.01	9.44E-01	0.01
Pu-238	4.54E-04	1.53	3.72E-04	0.28	1.11E-04	1.08
Pu-239	4.89E-03	0.29	5.81E-03	0.19	5.16E-03	0.24
Pu-240	3.18E-03	0.29	2.84E-03	0.15	1.84E-03	0.26
Pu-241	1.44E-03	0.29	<i>1.82E-03</i> ^c	0.28	9.87E-04	1.70
Pu-242	1.55E-03	0.29	1.02E-03	0.02	3.10E-04	0.28
Np-237			8.11E-04	3.00	5.25E-04	2.41
Am-241	2.48E-04	1.78	2.28E-04	0.79	1.47E-04	5.94
Am-242m	6.85E-07	5.30	<i>9.30E-07</i>	5.29		
Am-243	4.03E-04	1.78	2.38E-04	1.74	4.38E-05	6.65
Cm-242	3.09E-07	3.61	<i>2.76E-05</i>	2.02		
Cm-243	3.38E-07	36.75	<i>6.24E-07</i>	9.61		
Cm-244	2.44E-04	1.51	<i>1.41E-04</i>	1.57	1.24E-05	1.57
Cm-245	1.75E-05	2.95	1.10E-05	1.43	5.74E-07	10.15
Cm-246	5.29E-06	10.12	1.44E-06	5.26		
Cs-133	1.72E-03	2.46	1.63E-03	0.94	1.08E-03	1.64
Cs-134	1.08E-04	2.47	<i>2.51E-04</i>	1.44	4.14E-05	1.27
Cs-135	5.16E-04	2.46	4.69E-04	1.12	3.73E-04	1.21
Cs-137	2.03E-03	2.45	<i>1.87E-03</i>	0.52	9.95E-04	1.50
Ce-144	3.37E-05	3.92	<i>4.41E-04</i>	1.01	3.63E-05	2.75
Nd-142	6.77E-05	5.01	4.23E-05	5.01	1.20E-05	5.09
Nd-143	9.33E-04	0.29	1.07E-03	0.28	8.62E-04	6.16
Nd-144	2.63E-03	0.29	2.14E-03	0.28	1.23E-03	5.95
Nd-145	1.04E-03	0.29	9.89E-04	0.28	6.76E-04	6.89
Nd-146	1.33E-03	0.29	1.15E-03	0.28	6.50E-04	7.37
Nd-148	6.66E-04	0.30	5.87E-04	0.29	3.47E-04	6.70
Nd-150	3.39E-04	0.30	2.86E-04	0.29	1.58E-04	6.78
Pm-147	<i>1.37E-04</i>	5.13	<i>1.93E-04</i>	9.01	<i>2.02E-04</i>	
Sm-147	2.22E-04	0.32	1.96E-04	0.32	1.61E-04	10.57
Sm-148	3.24E-04	0.32	2.54E-04	0.32	1.11E-04	4.01
Sm-149	3.28E-06	1.05	3.36E-06	1.05	3.02E-06	5.88
Sm-150	5.08E-04	0.32	4.46E-04	0.32	2.43E-04	3.44
Sm-151	1.30E-05	0.40	<i>1.47E-05</i>	0.41	1.13E-05	2.21
Sm-152	1.66E-04	0.32	1.34E-04	0.32	9.46E-05	3.21
Sm-154	8.04E-05	0.33	5.73E-05	0.33	2.64E-05	5.65
Eu-151	7.18E-07	1.05	4.20E-07	1.05		
Eu-153	2.10E-04	0.34	1.84E-04	0.33	9.39E-05	5.49
Eu-154	3.22E-05	1.95	<i>4.30E-05</i>	0.77	1.38E-05	11.87
Eu-155	1.13E-05	2.64	<i>1.53E-05</i>	4.72	4.40E-06	4.64
Gd-155	5.63E-06	2.50	3.93E-06	1.00	2.64E-06	6.81
Sr-90	9.72E-04	7.50	<i>7.75E-04</i>	0.32	5.05E-04	
Mo-95	1.23E-03	3.87	1.18E-03	1.47	7.58E-04	1.56
Tc-99	1.25E-03	6.30	1.12E-03	1.94	5.99E-04	1.18
Ru-101	1.29E-03	4.58	1.21E-03	1.75	7.49E-04	2.00
Ru-106	<i>2.56E-04</i>	2.82	<i>2.90E-04</i>	14.21	<i>1.29E-04</i>	2.69
Rh-103	6.13E-04	4.49	5.40E-04	2.44	4.54E-04	2.36
Ag-109	7.51E-05	5.18	1.19E-04	9.06		
Sb-125	<i>9.29E-06</i>	5.07	<i>7.50E-06</i>	9.43		

^aIn MWd/MTU; as reported in Ref. 48.

^bRelative standard deviation.

^cValues shown in italics are reported at the time of discharge; all other values correspond to the time of measurement listed in Table 43.

Table 43. Decay time at the time of measurement for ARIANE Program Gösgen samples

Sample ID	GU1		GU3		GU4	
Experimental facility	SCK/CEN		SCK/CEN & ITU		ITU	
Nuclides	Measurement date ^a (month/day/year)	Decay time ^b (days)	Measurement date ^a (month/day/year)	Decay time ^b (days)	Measurement date ^a (month/day/year)	Decay time ^b (days)
Uranium	4/9/97	1040	10/12/99	857	5/20/99	712
Plutonium	4/22/97	1053	10/11/99	856	8/17/99	801
Neptunium			12/22/99	928	6/16/99	739
Americium	4/9/97	1040	12/21/99	927	6/16/99	739
Curium	6/4/97	1096	7/1/99	754	6/16/99	739
Neodymium	4/9/97	1040	11/24/99	900	9/30/99	845
Cesium	5/30/97	1091	7/1/99	754	10/6/99	851
Cerium	2/28/97	1000	7/1/99	754	9/30/99	845
Samarium	4/23/97	1054	12/13/99	919	10/1/99	846
Europium	4/23/97	1054	7/1/99	754	10/4/99	849
Gadolinium			12/1/99	907	10/4/99	849
Strontium	6/24/97	1116	5/16/00	1074	11/15/99	891
⁹⁵ Mo, ⁹⁹ Tc, ¹⁰¹ Ru	4/10/00	2137	4/10/00	1038	11/15/99	891
¹⁰³ Rh, ¹⁰⁹ Ag	4/10/00	2137	4/10/00	1038	11/15/99	891
¹⁰⁶ Ru, ¹²⁵ Sb	2/28/97	1000	10/7/99	852	11/15/99	891

^aMeasurement dates from DTN: MO0808ARIANEIP.000, *Tables 3.2-CEN results.xls* and *Tables 3.2-ITU results.xls*

^bDecay time calculated based on cycle end dates of 6/4/1994 for sample GU1 (DTN: MO0808ARIANEIP.000, *ARIANE Final Report.pdf*, p. 106) and 6/7/1997 for samples GU3 and GU4 (DTN: MO0808ARIANEIP.000, *ARIANE Final Report.pdf*, p. 134).

A material balance for the ARIANE Gösigen samples was performed⁴⁸ using two independent measures to verify the consistency of the experimental data. The material balance ratio was calculated as

$$MB = \frac{1.1345 \times (W_U + W_{Pu} + W_{MA} + \Delta W)}{W_{sample}^{total}}, \quad (16)$$

where W_U , W_{Pu} , and W_{MA} are the weights of the uranium, plutonium, and minor actinides (americium and curium) measured in the dissolved solution, ΔW is the loss on the initial uranium mass due to fission, and W_{sample}^{total} is the actual mass of the fuel sample as measured on the mass balance. The coefficient 1.1345 represents the approximate ratio of the fuel weight to uranium weight. The loss due to fission, ΔW , was determined using the measured concentrations of the burnup indicator fission product ^{148}Nd . The fuel mass ratio obtained for samples GU3 and GU4 (all laboratories) was 1.00; however, the ratio obtained for sample GU1 was 1.12, indicating that the mass derived from the sum of measured actinides was about 12% greater than the actual measured fuel sample mass. The experimental data was therefore adjusted to the initial fuel mass as derived from the heavy metal isotopic measurements. The only plausible source of such significant error in the isotopic data would be the absolute measured mass of uranium in the solution.

7.9 GKN UNIT II

The REBUS (Reactivity Tests for a Direct Evaluation of the Burnup Credit on Selected Irradiated LWR Fuel Bundles) International Program⁴⁹ coordinated by Belgonucleaire was dedicated to the validation of computer codes for criticality calculations that take into account the reduction of reactivity of spent fuel as a result of burnup credit. Participants in REBUS included institutes from Belgium, France, Germany, Japan, and the United States. ORNL was a participant in the early stages of the program under support from the U.S. Nuclear Regulatory Commission (NRC) and negotiated access to the data from this program. The REBUS program was completed in December 2005.

REBUS involved critical measurements in the VENUS critical facility at SCK-CEN in Belgium using spent fuel rod segments. One of the segments was assayed to experimentally determine the isotopic content of the fuel. The results for this sample, measured by the SCK-CEN radiochemical laboratory, were reported. The sample was obtained from a fuel rod of an 18×18 PWR assembly operated in the German reactor Gemeinschaftskernkraftwerk Unit II (GKN II) in Neckarwestheim/Neckar. GKN is a PWR in Germany with a net generating capacity of 1400 MWe, which was designed by German Kraftwerk Union AG (KWU). First power was achieved in January 1989 with an initial core consisting of KWU 18×18 assemblies.⁵⁷ Although this reactor currently operates with a MOX core, the assembly was obtained from the reactor during a period when it operated with only UO_2 fuel. The measured sample had an initial enrichment of 3.8 wt % ^{235}U . The sample consisted of about three fuel pellets cut from the fuel rod identified as M11. The reported sample burnup was about 54 GWd/MTHM.

The selected sample was subjected to a two-step dissolution process followed by sample preparation for the various analytical techniques employed. The radiochemical analysis techniques included α - and γ -spectrometry, ICP-MS, and TIMS. For the actinides, the analysis was performed for isotopes of uranium, neptunium, plutonium, americium, and curium. The fission products analyzed were of two types: burnup indicators, consisting of neodymium isotopes as well as ^{137}Cs and ^{144}Ce ; and absorbing fission products, consisting of metallic species (^{95}Mo , ^{99}Tc , ^{101}Ru , ^{103}Rh , ^{105}Pd , ^{108}Pd , and ^{109}Ag), ^{133}Cs , and isotopes of Sm, Eu, and Gd. The metallic species were difficult to dissolve completely, and as a result, the dissolution residue had to be analyzed separately.

Because of the variety of the analysis techniques, the varying properties of the nuclides being analyzed, and their differing concentrations, uncertainties in the measured concentrations vary greatly. Table 44 lists the measurement method and, for each of the measured nuclides, the reported experimental uncertainty at 95% confidence level, corresponding to the experimental results reported in mg/g ^{238}U (Ref. 50). Also shown in Table 44 is the relative standard deviation calculated as half of the reported 95% confidence level uncertainty.

Nuclide concentrations were reported both in mg/g fuel and mg/g ^{238}U in the sample at the measurement date.⁵¹ For the purpose of comparison to measured data from other programs, the experimental data for the GKN II sample are presented in g/g $\text{U}_{\text{initial}}$ units in Table 45. The unit conversion was done using Eq. (9) (see Sect. 6.5).

The measurement date and the time duration from discharge to the measurement date for each of the analyzed nuclides is provided in Table 46 (Ref. 50).

7.10 GÖSGEN REACTOR: MALIBU PROGRAM

A description of radiochemical analysis data produced by the MALIBU program and used in this validation study is available in DTN: MO1003MALIBUIP.001.

Table 44. Experimental techniques and uncertainties for REBUS Program GKN II sample

Nuclide ID	Method ^a	Uncertainty ^b at 95% confidence level (%)	RSD ^c (%)
U-234	TIMS	5.0	2.5
U-235	TIMS	0.73	0.37
U-236	TIMS	0.73	0.37
U-238	TIMS	0.57	0.29
Total U		0.53	0.22
Np-237	ICP-MS	20.0	10.0
Pu-238	TIMS, α -spec	3.1	1.6
Pu-239	TIMS	0.59	0.30
Pu-240	TIMS	0.59	0.30
Pu-241	TIMS	0.59	0.30
Pu-242	TIMS	0.61	0.31
Am-241	TIMS	3.5	1.8
Am-242m	TIMS	11.0	5.5
Am-243	TIMS	3.5	1.8
Cm-242	α -spec	32.0	16.0
Cm-243	γ -spec	20.0	10.0
Cm-244	α -spec	2.5	1.3
Cm-245	TIMS	5.6	2.8
Mo-95	ICP-MS	9.9	5.0
Tc-99	ICP-MS	10.0	5.0
Ru-101	ICP-MS	9.9	5.0
Rh-103	ICP-MS	10.0	5.0
Pd-105	ICP-MS	9.8	4.9
Pd-108	ICP-MS	9.8	4.9
Ag-109	ICP-MS	10.0	5.0
Cs-133	TIMS	2.6	1.3
Cs-135	γ -spec	2.6	1.3
Cs-137	γ -spec	2.6	1.3
Nd-142	TIMS	0.78	0.39
Nd-143	TIMS	0.64	0.32
Nd-144	TIMS	0.64	0.32
Nd-145	TIMS	0.64	0.32
Nd-146	TIMS	0.64	0.32
Nd-148	TIMS	0.65	0.32
Nd-150	TIMS	0.65	0.33
Ce-144	γ -spec	10.0	5.0
Sm-147	TIMS	0.75	0.38
Sm-148 ^d	TIMS	0.75	0.38
Sm-149	TIMS	2.13	1.07
Sm-150	TIMS	0.75	0.38
Sm-151	TIMS	0.88	0.44
Sm-152	TIMS	0.75	0.38
Sm-154 ^d	TIMS	0.76	0.38
Eu-153	TIMS	0.9	0.5
Eu-154	γ -spec	3.4	1.7
Eu-155	γ -spec	6.0	3.0
Gd-155	TIMS	5.0	2.5

^aMain technique is listed; some nuclides may require multiple techniques to eliminate interferences.

^bAs reported for the measured data expressed in mg/g ²³⁸U in Ref. 50.

^cRelative standard deviation.

^dThe use of TIMS for these Sm isotopes was inferred from Ref. 50. The reference does not include these isotopes in the list of isotopes analyzed by TIMS. However, the reference indicates that TIMS was used to determine isotopic compositions and concentrations of elemental Sm.

Table 45. Experimental results for GKN II (REBUS) sample

Nuclide	Concentration^a (g/g U_{initial})	RSD^b (%)	Nuclide	Concentration^a (g/g U_{initial})	RSD^b (%)
U-234	1.49E-04	2.52	Ag-109	1.07E-04	5.01
U-235	5.12E-03	0.46	Cs-133	1.60E-03	1.33
U-236	5.35E-03	0.46	Cs-135	5.76E-04	1.33
U-238	9.21E-01	2.52	Cs-137	1.68E-03	1.33
Np-237	6.08E-04	10.0	Ce-144	4.88E-07	5.01
Pu-238	4.28E-04	1.58	Nd-142	5.22E-05	0.48
Pu-239	5.77E-03	0.41	Nd-143	1.07E-03	0.43
Pu-240	3.22E-03	0.41	Nd-144	2.26E-03	0.43
Pu-241	1.30E-03	0.41	Nd-145	9.96E-04	0.43
Pu-242	1.17E-03	0.42	Nd-146	1.18E-03	0.43
Am-241	5.25E-04	1.77	Nd-148	5.96E-04	0.43
Am-242m	1.57E-06	5.51	Nd-150	2.95E-04	0.43
Am-243	2.49E-04	1.77	Sm-147	2.99E-04	0.47
Cm-242	4.33E-09	16.00	Sm-148	2.88E-04	0.47
Cm-243	7.75E-07	10.00	Sm-149	2.39E-06	1.10
Cm-244	1.33E-04	1.28	Sm-150	4.77E-04	0.47
Cm-245	1.33E-05	2.81	Sm-151	1.43E-05	0.52
Mo-95	1.04E-03	5.01	Sm-152	1.47E-04	0.47
Tc-99	1.25E-03	5.01	Sm-154	6.70E-05	0.48
Ru-101	9.68E-04	5.01	Eu-153	1.92E-04	0.53
Rh-103	5.81E-04	5.01	Eu-154	2.30E-05	1.72
Pd-105	4.52E-04	5.01	Eu-155	6.17E-06	3.01
Pd-108	1.77E-04	5.01	Gd-155	1.01E-05	2.52

^aCalculated using Eq. (10) and the isotopic concentration values, in mg/g ²³⁸U, reported in Ref. 50 (see DVD/xls/Experimental_data.xls).

^bAccounts for reported error in measured ²³⁸U.

Table 46. Decay time data for GKN II (REBUS) sample

Measurement date (month/day/year)	Decay time (days)	Measured nuclides
9/28/2004	2600	^{144}Ce , ^{154}Eu , ^{155}Eu , ^{137}Cs
9/29/2004	2601	^{242}Cm , ^{244}Cm
11/02/2004	2635	^{238}Pu , ^{239}Pu , ^{240}Pu , ^{241}Pu , ^{242}Pu
11/15/2004	2648	^{133}Cs , ^{135}Cs
12/09/2004	2672	^{234}U , ^{235}U , ^{236}U , ^{238}U
2/10/2005	2735	^{147}Sm , ^{148}Sm , ^{149}Sm , ^{150}Sm , ^{151}Sm , ^{152}Sm , ^{154}Sm , ^{153}Eu , ^{155}Gd
2/28/2005	2753	^{142}Nd , ^{143}Nd , ^{144}Nd , ^{145}Nd , ^{146}Nd , ^{148}Nd , ^{150}Nd
3/07/2005	2760	^{243}Cm , ^{241}Am , $^{242\text{m}}\text{Am}$, ^{243}Am
4/29/2005	2813	^{237}Np , ^{95}Mo , ^{99}Tc , ^{101}Ru , ^{103}Rh , ^{105}Pd , ^{108}Pd , ^{109}Ag
6/01/2005	2846	^{245}Cm

Source: Ref. 50.

8 ASSEMBLY DESIGN AND IRRADIATION HISTORY DATA

This section describes assembly design and irradiation history data that are relevant to 2-D transport and depletion calculations for the evaluated spent fuel samples.

8.1 TRINO VERCELLESE

The Trino Vercellese Nuclear Power Plant was an 825-MW PWR located in Italy. The power plant has been permanently shut down and is being decommissioned. The steam generation plant and fuel were designed by Westinghouse Electric Corp. The reactor core was composed of square and cruciform assemblies. Details related to the geometry, material composition, and irradiation history were obtained from Refs. 12, 13, and 14. The assembly locations in the reactor core are illustrated in Fig. 2. During the first cycle, the reactor core was composed of 120 square fuel assemblies, which were organized into three radial zones of initial enrichments of 2.719, 3.13, and 3.897 wt % ^{235}U , and 52 cruciform assemblies of initial enrichment of 2.72 wt % ^{235}U . Of the 52 cruciform assemblies, 24 were permanently inserted in the core and 28 were connected to 28 cruciform control rods as “fuel bearing followers” so that if a cruciform control rod were removed, a cruciform fuel assembly would raise into the fuel. Ten cruciform control rods acted as a control group during power operation, and the remaining 18 cruciform rods acted as shut-down rods. The cruciform control rods were composed of 32 absorber rods containing Ag, In, and Cd in the ratio 80:15:5. A cross section showing the locations of the cruciform assemblies in the S-E quarter of the core during cycle 1 is presented in Fig. 3(a) and a cross section of the reactor core showing the locations of the cruciform assemblies during cycle 2, as provided in Ref. 84, Fig. 3.1, is shown in Fig. 3(b).

All square assemblies contain fuel and are based on a 15×15 lattice of fuel pins, with 16 of the outer pins excluded to accommodate cruciform assemblies or control rods, as illustrated in Fig. 4 (Ref. 14). The assemblies are surrounded by a 0.6-mm-thick stainless steel channel tube (see Fig. 4). The center position in each assembly was used for instrumentation and was represented as vacant for the depletion calculations in the current report. The cruciform fuel pins are always 2.72 wt % ^{235}U , even though the fuel assembly in which they are placed may have a higher enrichment. For the 28 lattice positions of the cruciform assembly, there are only 26 fuel pins (Ref. 12). Reactor core characteristics and design data for square fuel assemblies and cruciform fuel and absorber rods are based on the values reported in Refs. 12 and 13 and are given in Table 47. The numbers in parentheses are for the second cycle, which are mainly taken from Ref. 12. The data in both references are consistent, with the exception of the core equivalent diameter, which was listed as 240 cm in Ref. 13. Operational parameters for cycles 1 and 2 and for subcycle periods I, II, and III of cycle 1 are given in Table 48. During cycle 1, two downtime intervals occurred prior to the end of the cycle, and cycle 2 was completed with no downtime. The control rods have been inserted 30% during the first part of the first cycle in the core locations identified in Fig. 3 (Ref. 12), and they were completely withdrawn during cycle 2 (Ref. 24).

At the end of the first cycle, the 40 assemblies of the inner core (enrichment 2.719 wt % ^{235}U) and some assemblies of the intermediate and outer regions (enrichments 3.13 and 3.897 wt % ^{235}U) were unloaded from the reactor for reprocessing. The reactor core for cycle 2 was reduced by replacing eight fuel assemblies with eight dummy assemblies.¹⁴ Radiochemical assay data exist for four square fuel assemblies. Three of the assemblies, referred to as 509-032, 509-049, and 509-104, were irradiated in the core during the first cycle only. The remaining assembly, identified as 509-069, was irradiated during both first and second fuel cycles. This validation study considers 31 different Trino Vercellese fuel samples that were cut from fuel rods E11 and H9 in assembly 509-032; fuel rods J8 and L5 in assembly 509-049; fuel rods E5, E11, J9, L5, and L11 in assembly 509-069; and fuel rod M11 in assembly 509-104, with the pin locations illustrated in Fig. 5. All the mentioned fuel rods were assembly inner rods.

Note that the spent fuel samples obtained from assembly peripheral fuel rods were not selected for evaluation in this validation report because the enrichment and burnup of the adjoining square assembly were not provided in the reference documents and the use of a simplified 2-D assembly model that neglects the characteristics of the adjoining assemblies may increase the uncertainty in the calculated isotopic compositions. The measured spent fuel samples were obtained from a variety of axial locations along the fuel rods. The sample heights were not explicitly provided in Refs. 12 and 13. Rather, the sample pellet locations were identified by level number, 1 to 9, and were illustrated in relation to the positions of the assembly grids (Ref. 12, Fig. 3). Sample axial positions were determined in Ref. 14 based on the gamma-activity plots shown in Figs. 19 through 26 in Ref. 12 and Figs. 21 through 27 in Ref. 13. The sample identification and general characteristics are presented in Table 6 (see Sect. 7.1). Note that some of the gamma-activity plots show small variations (± 2 cm) from the values provided in Ref. 14. The variation occurs because the sampled fuel rods had slightly different lengths; however, neglecting those variations should have insignificant effects on the values of the calculated moderator temperature and density based on Eq. (1) (see Sect. 5.2). Note that all the considered sampled rods occupied inner assembly positions that were separated from control rods by at least four rods. In addition, samples taken from elevations 4 through 9 were clearly positioned below the control rods. Therefore, it was determined that the control rod influence is negligible on the results of the isotopic calculations.

Data for a series of input parameters were not available in the published reports. The input parameters, which include initial fuel compositions, moderator temperatures and densities, fuel and clad temperatures, operating power histories, and soluble boron content in cycle 2 for the Trino Vercellese assemblies, were determined using the methods described in Sect. 5 and additional assumptions as described below.

The calculated fuel initial isotopic compositions and mass densities are listed in Table 49. The isotopic composition values were calculated using the empirical relation described in Table 2 and the fuel initial enrichments provided in Refs. 12 and 13.

Moderator temperatures and densities at sample axial locations are listed in Table 50. The moderator temperatures were calculated using Eq. (1) and sample axial locations listed in Table 6 and the inlet and outlet temperatures listed in Table 48. The moderator densities were determined by interpolating density data for the coolant pressure of 140 kg/cm^2 , as described in Sect. 5.2.

Assembly-specific burnup values for the irradiation periods and cycles were supplied for assembly 509-069 only (see Table 48). Power histories and effective fuel temperatures for each sample are listed in Table 51. The specific power for each individual sample in a given assembly was determined from the final sample burnup (see Table 6), the specified uptimes (see Table 48), and the burnup distribution for assembly 509-069 (see Table 48) assuming that the relative burnup per depletion step is the same for assembly 509-069 and the sample. The effective fuel temperatures were computed from resonance-effective temperatures given in operating data for the similarly designed Yankee Rowe PWR (Ref. 85, Table C-1). To evaluate the magnitude of the uncertainty in the calculated isotopic concentrations due to the uncertainty associated with the effective fuel temperature values used, sensitivity calculations were performed for two Trino Vercellese samples in which the applicable Yankee Rowe effective fuel temperature values were increased by 10%. The relative percent differences between the isotopic concentrations obtained with the Yankee Rowe temperature values and the isotopic concentrations obtained with the perturbed temperature values were less than 1.2% for all isotopes of interest (see Sect. 10.2.3, Table 109). Therefore, although the uncertainty in the effective fuel temperature cannot be evaluated, the effect of the fuel temperature uncertainty on the calculated isotopic concentrations is expected to be significantly small.

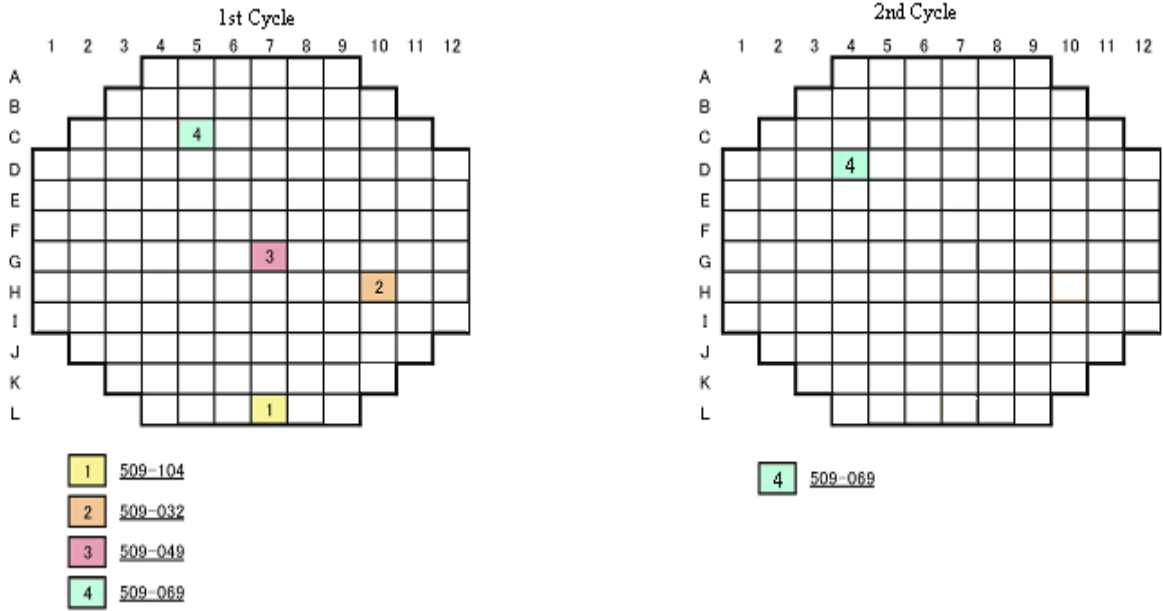
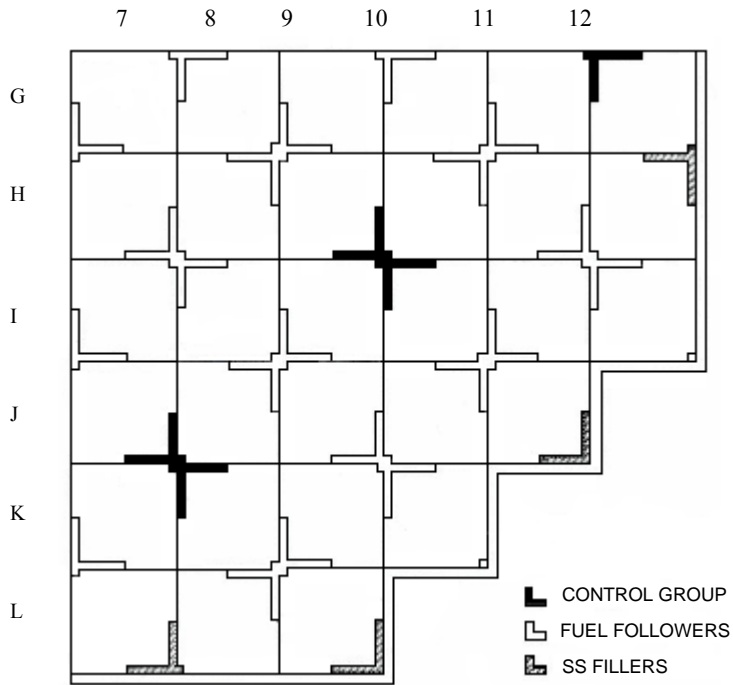
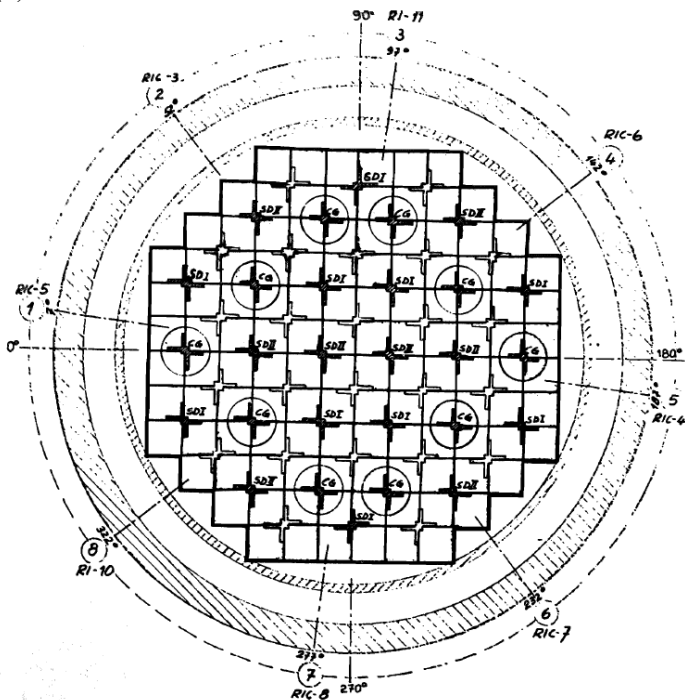


Fig. 2. Schematic core map for the Trino Vercellese reactor showing the locations of the measured assemblies during cycle 1 and cycle 2. (Source: Ref. 14, Fig. I.8.)



(Source: Ref. 12, Fig. 1.)

(a)



Note: CG = control group; SDI = shut down group 1; SDII = shut down group 2

(b)

Fig. 3. (a) S-E quarter showing locations of cruciform assemblies containing control rods, fuel rods, and stainless steel fillers during cycle 1; (b) control group locations during cycle 2. (Source: Ref. 84, Fig. 3.1.)

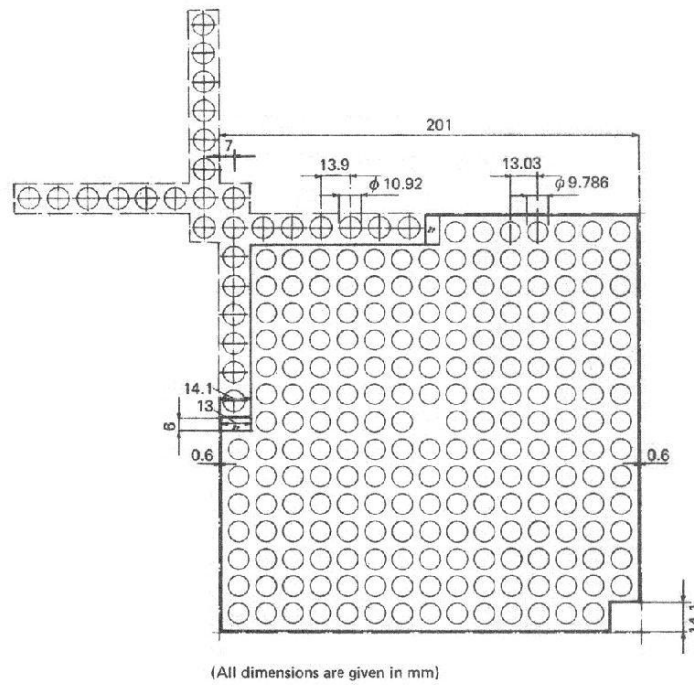


Fig. 4. Horizontal cross section of the Trino Vercellese square fuel assembly. (Source: Ref. 14, Fig. I.10.)

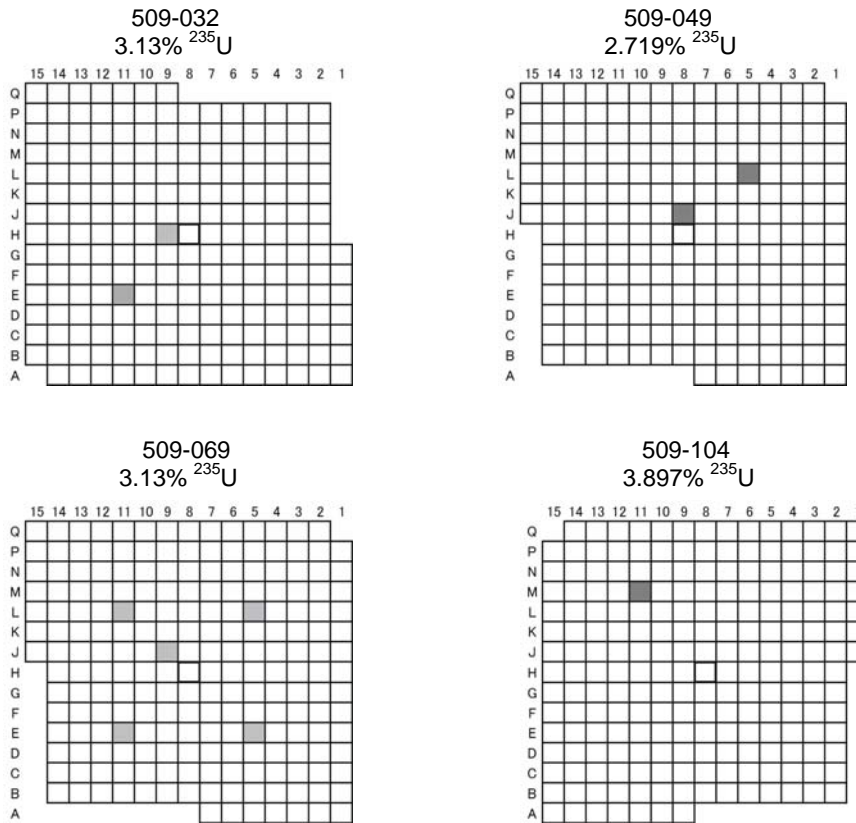


Fig. 5. Location of Trino Vercellese measured fuel rods. (Source: Ref. 13, Table 5, and Ref. 14, Fig. I.9.)

Table 47. Assembly design and operating data for Trino Vercellese

Parameter	Data
Core mechanical characteristics	
Design	Westinghouse, PWR
Number of square fuel assemblies, cycle 1 (cycle 2)	120 (112)
Number of cruciform fuel assemblies	52
Number of control rods	28
Number of enrichment regions in the core	3
Initial enrichments (square assemblies)	2.719–3.13–3.897%
Initial enrichment (cruciform assemblies)	2.719%
UO ₂ in square fuel assemblies, cycle 1 (cycle 2), kg	42,321 (39,626)
UO ₂ in cruciform fuel assemblies, kg	2,313
Total U weight, cycle 1 (cycle 2), kg	39,873 (36,968)
Assembly layout	See Fig. 4
Core thermohydraulic characteristics	
Power output, MW(th)	825
Coolant pressure, kg/cm ²	140
Coolant inlet temperature, cycle 1, °C	266.5
Coolant average temperature, cycle 1 (cycle 2), °C	282 (269)
Coolant outlet temperature, cycle 1, °C	297.5
Max. rod surface temperature, °C	340
Core average power density, cycle 1 (cycle 2), kW/l	64.4 (69.9)
Max. design linear power density, cycle 1 (cycle 2), kW/ft	12.4 (11.4)
Locations of cruciform assemblies containing control rods, fuel rods, and stainless steel fillers	See Fig. 3
General operations of cycles 1 and 2	
	See Table 48
Square fuel assembly	
Rod array	15 × 15
Number of fuel rods	208
Side of square cross section, cm	20
Total length, cm	320.88
UO ₂ weight, kg	353.81
Initial weight of one rod in Assembly No. 509-069, ^a g U	1,511.3
Pellet stack density (% TD), ^b g/cm ³	96.5% of TD
Pellet diameter, cm	0.89
Pellet length, cm	1.53
Pellet dishing depth, mm	0.33
Number of pellets per rod (approx.)	173
Length of pellet stack in fuel rod, cm	264.1
Clad-pellet clearance, mm	0.114
Clad inside diameter, cm	0.902
Clad wall thickness, mm	0.383
Clad material	SS 304 ^c
Cruciform fuel assembly	
Number of fuel rods	26
Fuel length, cm	240.3
Rod outer diameter, cm	1.092
UO ₂ weight, kg	44
Pellet diameter (assumes same clad thickness as control rod and no gap)	1.0056

Table 47. Assembly design and operating data for Trino Vercellese (continued)

Parameter	Data
Control rod	
Absorbing material, wt %	5% Cd–15% In–80% Ag
Cladding material	Type 304 stainless steel ^c
Number of absorber rods	32
Absorber length, cm	269.2
Absorber rod diameter, cm	1.001
Clad outer diameter, cm	1.095
Clad thickness, mm	0.432
Measured sample data	
Basic parameters of the measured spent fuel	See Table 6
Position of measured assemblies in the reactor core	See Fig. 2
Position of measured rod in assembly	See Fig. 5
Initial fuel compositions	See Table 49
Water temperature and density at sample locations	See Table 50
Sample burnup, specific power, and temperature	See Table 51
Description of measurement methods	See Table 7
Measurement accuracies estimated by laboratory	See Table 7
Date of measurements	See footnote on Table 9
Experimental spent fuel compositions	See Table 9

^aThe initial weight of one rod in assembly 509-069 was used to determine the fuel density for 509-069 spent fuel samples (see Table 49) since it was available in Ref. 13, Table 3. The fuel density for the other measured fuel rods was determined based on UO₂ mass in a square assembly (see Table 49).

^bTD = theoretical density; UO₂ theoretical density is 10.96 g/cm³ (Ref. 86).

^cSCALE standard composition for stainless steel 304 (Ref. 86) was assumed in the calculations.

Source: Refs. 12, 13, and 14, unless otherwise noted.

Table 48. Summary of general operation data for cycles 1 and 2

Parameter	Cycle/period data			
	1	1	1	2
Cycle	I	II	III	All of cycle
Starting date	10/23/64	8/31/65	7/11/66	5/20/70
Uptime, d	226	263	292	416
Downtime, d	86	51	1117	0
Coolant inlet temperature, ^b °C	266.5	255.3	255.3	255.3
Coolant outlet temperature, ^b °C	297.5	288.7	288.7	288.7
Control rod insertion, %	30	4	4	0 ^d
Boron concentrations, ppm ^c	1300 to 1050	1150 to 650	650 to 0	1300 to 0 ^e
Assembly 509-069 burnup, ^f GWd/MTU	2.726	4.927	6.327	7.720

^aAt the end of period I, power was increased from 615 to 825 MW(h).

^bCoolant inlet and outlet temperatures for cycle 1, Periods II and III, and cycle 2 were taken from Ref. 56.

^cAverage boron concentrations for the operation periods were used in the calculations.

^dNot given. This value was assumed because the analyzed measured fuel rods were unaffected. This assumption was also used in previous validation studies.²⁴

^eNot given, assumed similar to cycle 1 boron concentration range, consistently with previous validation studies.²⁴

^fApplied to the cycle 1 burnup for Assemblies 509-032, 509-049, and 509-104 to obtain the values shown in Table 51.

Source: Ref. 12, Tables 1 and 3, and Ref. 13, Table 4, unless otherwise noted.

Table 49. Initial isotopic composition of Trino Vercellese fuel

Assembly ID	Isotopic composition (wt %) ^a				UO ₂ density ^{a, c} (g/cm ³)
	²³⁵ U ^b	²³⁴ U	²³⁶ U	²³⁸ U	
509-049	2.719	0.024	0.013	97.244	10.3530 ^d
Cruciform	2.719	0.024	0.013	97.244	8.8672
509-032	3.13	0.028	0.014	96.828	10.3530 ^d
509-069	3.13	0.028	0.014	96.828	10.4354 ^e
509-104	3.897	0.035	0.018	96.050	10.3530 ^d

^aCalculations performed in *DVD/xls/input_data.xls*, worksheet *trino*.

^bRef. 13, Section 2, for Assembly 509-069 and Ref. 12, Table 4, for the other assemblies.

^cFuel mass was homogenized within the volume delimited by the active fuel height and fuel radius for the square assemblies and within the volume delimited by the active fuel height and clad inner radius for the cruciform assembly. In the calculations, it was assumed that the clad thicknesses for the fuel rods and control rods in the cruciform assembly were identical (0.432 mm) since the two types of rods had approximately the same outer diameter.

^dThis fuel density was obtained by averaging 10.3529 g/cm³, which is the fuel density based on the UO₂ mass in a square assembly (353.81 kg) in Ref. 12, Table 2, and 10.3531 g/cm³, which is the fuel density based on the UO₂ mass in all 112 square assemblies for Cycle 2 (39,626 kg) in Ref. 13, Table 2. Note that the fuel density based on the total UO₂ mass (42,321 kg) in 120 square fuel assemblies for Cycle 1 provided in Ref. 12, Table 2, is 10.3198 g/cm³. Sensitivity calculations performed using a fuel mass density of 10.3198 g/cm³ for a few samples irradiated during cycle 1 (see Sect.10.2.2) showed a difference in the calculated isotopic concentrations of maximum 0.5% (i.e., negligible) as compared with the results obtained using a fuel mass density of 10.3530 g/cm³.

^eThis value is based on the initial weight of one rod in assembly 509-069 (Ref. 13, Table 3).

Table 50. Moderator temperature and density at sample locations for Trino Vercellese samples

Sample axial level	Cycle 1, period I		Cycle 1, periods II and III, and cycle 2		
	Temperature ^a (K)	Density ^a (g/cm ³)	Temperature ^a (K)	Density ^a (g/cm ³)	Fraction of density in cycle 1, period I
1	570.3	0.7297	561.5	0.7471	1.024
2	568.7	0.7331	559.7	0.7505	1.024
4	561.2	0.7477	551.6	0.7650	1.023
5	556.1	0.7571	546.2	0.7744	1.023
7	546.4	0.7741	535.7	0.7911	1.022
8	542.9	0.7798	531.9	0.7971	1.022
9	540.6	0.7834	529.4	0.8009	1.022

^aCalculations performed in *DVD/xls/input_data.xls*, worksheet *trino*.

Table 51. Fuel burnup, operating power histories, and temperature for Trino Vercellese pellet samples

Assembly	Rod	Level	Burnup (GWd/MTU)	Cycle 1			Cycle 2	Cycle 1			Cycle 2
				I	II	III		I	II	III	
				Power (MW/MTU) ^a				Fuel temperature (K) ^b			
509-032	E11	1	7.243	6.249	9.706	11.226		703	740	757	
		4	15.377	13.267	20.606	23.833		779	859	894	
		7	15.898	13.717	21.304	24.641		784	867	903	
		9	11.529	9.947	15.449	17.869		743	803	829	
	H9	4	16.556	14.285	22.186	25.660		790	876	914	
		7	17.450	15.056	23.384	27.046		799	889	929	
		9	12.366	10.669	16.571	19.166		751	815	843	
509-049	L5	1	7.822	6.749	10.482	12.123		708	749	767	
		4	14.323	12.358	19.193	22.199		769	844	876	
		9	10.187	8.789	13.651	15.789		730	783	807	
	J8	1	8.713	7.518	11.676	13.504		717	762	782	
		4	14.770	12.744	19.792	22.892		774	850	884	
		7	15.193	13.109	20.359	23.548		778	856	891	
		9	11.127	9.600	14.911	17.246		739	797	823	
509-104	M11	7	12.042	10.390	16.137	18.664		748	810	838	
509-069	E5	4	23.867	13.266	20.605	23.832	20.411	779	859	894	857
		7	24.548	13.645	21.193	24.512	20.993	783	866	902	863
		9	19.208	10.677	16.582	19.180	16.427	751	815	844	814
	E11	1	12.859	7.148	11.101	12.840	10.997	713	756	775	755
		2	20.602	11.452	17.786	20.571	17.619	759	828	859	827
		4	23.718	13.184	20.476	23.683	20.283	778	858	893	856
		5	24.518	13.628	21.167	24.482	20.968	783	865	901	863
		7	24.304	13.509	20.982	24.268	20.785	782	863	899	861
		8	23.406	13.010	20.207	23.371	20.017	776	855	889	853
		9	19.250	10.700	16.619	19.221	16.462	751	816	844	814
	L5	4	24.330	13.524	21.004	24.294	20.807	782	863	899	861
		7	24.313	13.514	20.990	24.277	20.792	782	863	899	861
	L11	4	23.928	13.300	20.657	23.893	20.463	780	860	895	858
7		24.362	13.542	21.032	24.326	20.834	782	864	900	862	
J9	4	24.849	13.812	21.452	24.812	21.251	785	868	905	866	
	7	25.258	14.040	21.805	25.221	21.600	788	872	909	870	

^aSpecific powers determined from the above burnups and the specified uptimes and burnup distributions for assembly 509-069 in Table 48 (see *DVD/xls/input_data.xls*, worksheet *trino*).

^bEffective fuel temperatures computed from resonance-effective temperatures given in operating data for the similar-design Yankee Rowe PWR (Ref. 85, Table C-1) (see *DVD/xls/input_data.xls*, worksheet *trino*). The clad temperature used in calculations is 570 K based on the clad temperature data for a Yankee Rowe PWR assembly with a specific power of approximately 20 MW/MTU. Note that the calculated moderator temperature for sample axial level 1 was higher than the clad temperature by 0.3 K (see Table 50); this temperature difference is considered negligible and does not affect the accuracy of the results.

8.2 OBRIGHEIM

KWO was the first PWR in Germany built by Siemens-Schuekertwerke as a demonstration plant as part of the German Atomic Program. The reactor operated from 1968 to 2005.

This validation study considers 22 different Obrigheim rod spent fuel samples¹⁵ and five different whole spent fuel assembly compositions from assemblies BE168, BE170, BE171, BE172, and BE176 (Ref. 16) for which experimental data exists (see Sect. 7.2). The rod spent fuel samples were cut from fuel rods D1, E3, G7, and M14 of assembly BE124, and from fuel rods G14 and K14 of assembly BE210. Assembly design and operating data for the Obrigheim spent fuel samples with measured isotopic compositions are summarized in Table 52. The layout of the Obrigheim fuel assemblies showing dimensions and location of the guide tubes is illustrated in Fig. 6. The core locations for assemblies BE124 and BE210 in each irradiation cycle and the position of control rod clusters provided in Ref. 15 and Ref. 18, respectively, are shown in Fig. 7. The locations of the measured rods from assemblies BE124 and BE210 and the axial locations of the measured spent fuel samples from those assemblies are shown in Fig. 8. The samples were cut from five positions and were identified as P1, P2, P3, P4, and P5 from the bottom to the top of the rod for the assembly BE124. The sample cutting positions were identified as P1, P3(1), P4(1), P5(1), and P5(2) for the assembly BE210. In Fig. 8, the cutting positions for BE124 are shown on the left, and for BE210 are shown on the right.

Note that 13 of the evaluated Obrigheim rod samples were obtained from assembly peripheral rods and five of the evaluated rod samples were obtained from a rod adjacent to a guide tube. However, the technical information required to accurately simulate the perturbed irradiation environment of those samples was not available. Therefore, although evaluated in this report, these samples may be inadequate for use in isotopic composition bias determination due to the significant uncertainty associated with the following parameters:

1. Fuel type, initial enrichment, and burnup for the assemblies adjacent to assemblies BE124 and BE210 during irradiation cycles 2 through 5. The KWO first charge core consisted of UO₂ fuel assemblies of 2.5, 2.8, and 3.1 wt % ²³⁵U initial enrichments and the KWO core contained mixed oxide (MOX) fuel assemblies starting with the third core refueling.¹⁸ One MOX assembly and eight MOX fuel assemblies were loaded into the core during the 1972 and 1973 September refueling processes, respectively. This study assumes that the characteristics of adjacent assemblies do not differ from those of the measured assembly. Hence, assembly reflective boundary conditions were used in calculations. This assumption may impact the calculation results for rods D1 and M14 of assembly BE124 and for rods G14 and K14 of assembly BE210, which were located in the assembly periphery.
2. Exposure to control rods. This study assumes that control rods were not inserted at the core locations used for assemblies BE124 and BE210. This assumption is based on a table note provided in Ref. 15, Table II, which describes fuel rod E3 of assembly BE124 as being near a water hole and its neutron spectrum as being intermediate. Note that this assumption may impact the results for the spent fuel samples from the top of rod E3 of assembly BE124, which was adjacent to a control rod location.

Table 52. Assembly design and operating data for Obrigheim measured spent fuel

Parameter	Data
Assembly and core data	
Design	Siemens, 14 × 14 PWR
Number of fuel assemblies	121
Number of control rod clusters	32
First charge enrichment, wt % ²³⁵ U	2.5–2.8–3.1
Number of guide tubes	16
Assembly pitch, ^a cm	20.03
Total UO ₂ weight, kg	39,930
Assembly layout	See Fig. 6
Fuel rod data	
Rod pitch, cm	1.43
Active fuel length, ^b cm	275
Fuel pellet diameter (cold), ^c cm	0.913
Fuel pellet linear density, g/cm	
Fuel assembly BE124	6.68
Fuel assembly BE210	6.52
Fuel pellet density for assemblies BE168, BE170, BE171, BE172, and BE176 (cold, with dishing), ^e g/cm ³	10.05
Clad inner diameter, cm	0.9318
Clad outer diameter, cm	1.074
Clad material	Zircaloy-4
Clad temperature, ^f °C	332
Guide tube	
Inner diameter, ^d cm	1.292
Outer diameter, ^d cm	1.372
Control Rod	
Absorbing material	Ag 15–In 5–Cd
Canning material	Stainless steel
Moderator data	
Nominal pressure, ^g atm	148
Inlet temperature, ^g °C	283
Outlet temperature, ^g °C	312.4
Average moderator temperature, ^h K	571
Average moderator density, ⁱ g/cm ³	0.7299
Soluble boron in moderator—average value, ppm	450

Table 52. Assembly design and operating data for Obrigheim measured spent fuel (continued)

Parameter	Data
Measured sample data	
Basic parameters of the measured spent fuel	See Table 11 and Table 13
Position of measured assemblies in the reactor core	See Fig. 7
Position of measured rod in assembly	See Fig. 8
Initial fuel compositions used	See Table 53
Water temperature and density at sample locations	See Table 56
Sample burnup, specific power, and temperature	See Table 56
Description of measurement methods	See Table 14
Measurement accuracies estimated by laboratory	See Table 10 and Table 14
Date of measurements	Fuel discharge
Experimental spent fuel compositions	See Table 12 and Table 16

^aAssembly pitch value assumed in this validation study. The values for assembly pitch provided in Refs. 18 and 19 are 20 and 20.03 cm, respectively.

^bThe active fuel length of 295.6 cm provided in Ref. 15 seems to be incorrect. Refs. 18 and 19 show fuel pin length and the active fuel length as being 295.6 cm and 275 cm respectively.

^cValue obtained from Ref. 16. The pellet diameter provided in Ref. 15 is 0.904.

^dRef. 20.

^eFuel density with a dishing volume of 1.5% provided in Ref. 16. The density provided in Ref. 16 for cold fuel without dishing is 10.2 g/cm³. Note that this value is equivalent to the pellet linear density for assembly BE124 (6.68 g/cm) given in Ref. 15.

^fRef. 17, p. 66.

^gRef. 18.

^hDerived from moderator inlet and outlet temperatures.

ⁱModerator density corresponding to the moderator average temperature (Ref. 58).

Source: Refs. 15 and 16, unless otherwise noted.

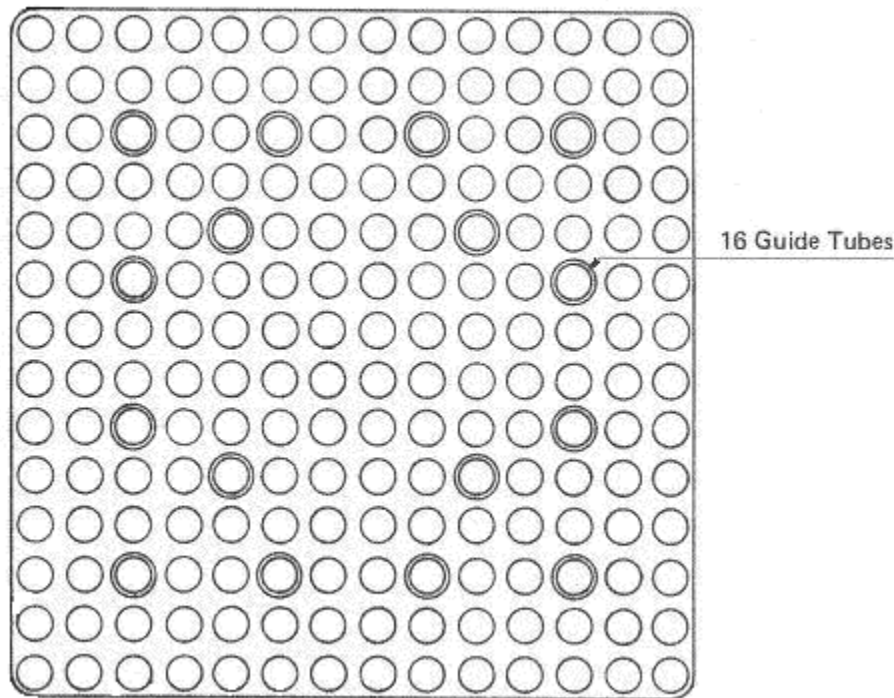
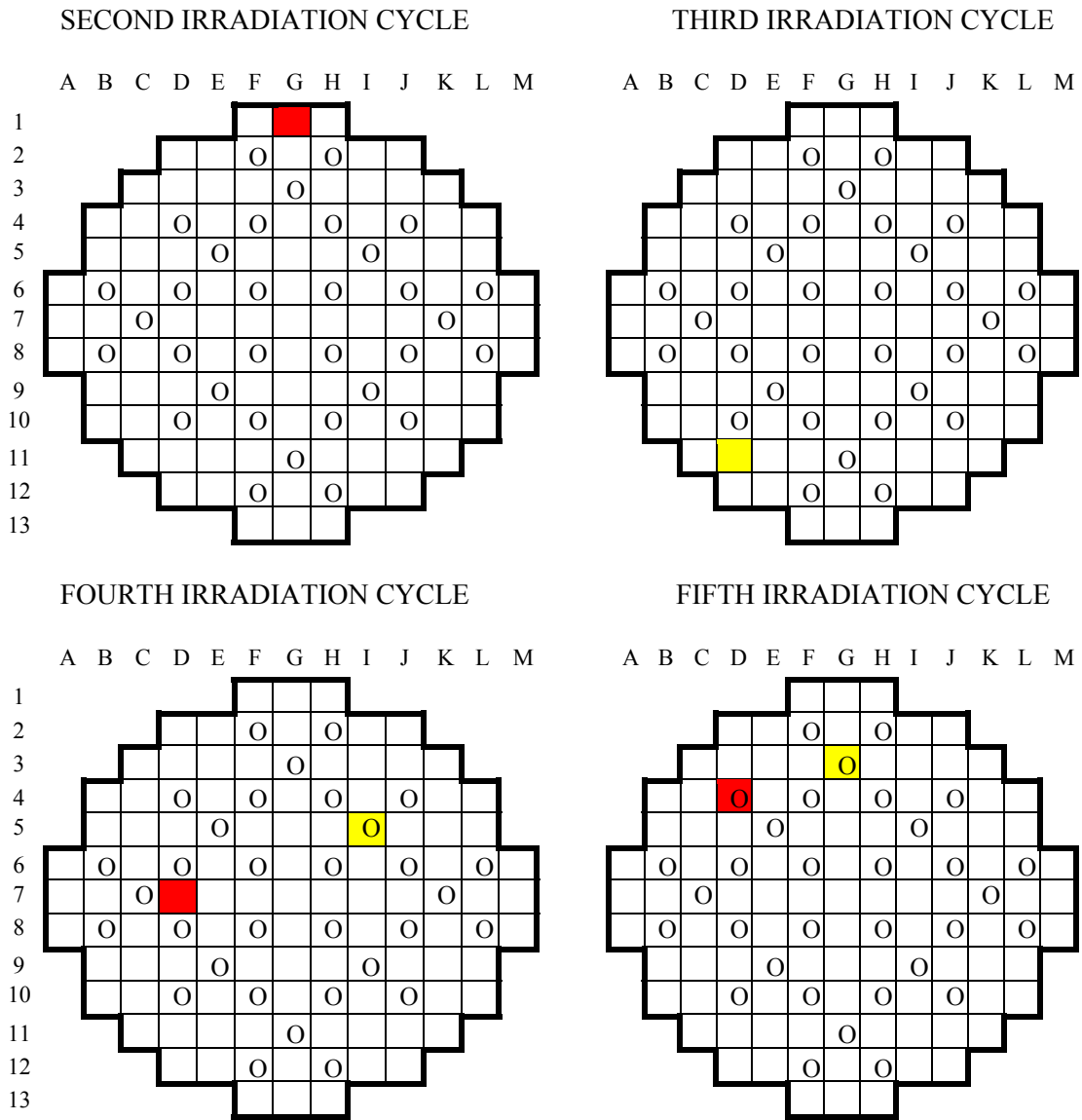


Fig. 6. Layout of the KWO fuel assemblies showing the location of the guide tubes. (Source: Ref. 18.)



- FUEL ASSEMBLY BE124 POSITIONS G1, D7, D4
- FUEL ASSEMBLY BE210 POSITIONS D11, J5,
- CONTROL ROD

Fig. 7. Core maps of the Obrigheim reactor during different irradiation cycles, showing the locations of control rods. (Note: Assembly locations during different irradiation cycles were provided in Ref. 15, whereas control rod bank locations were provided in Ref. 18.)

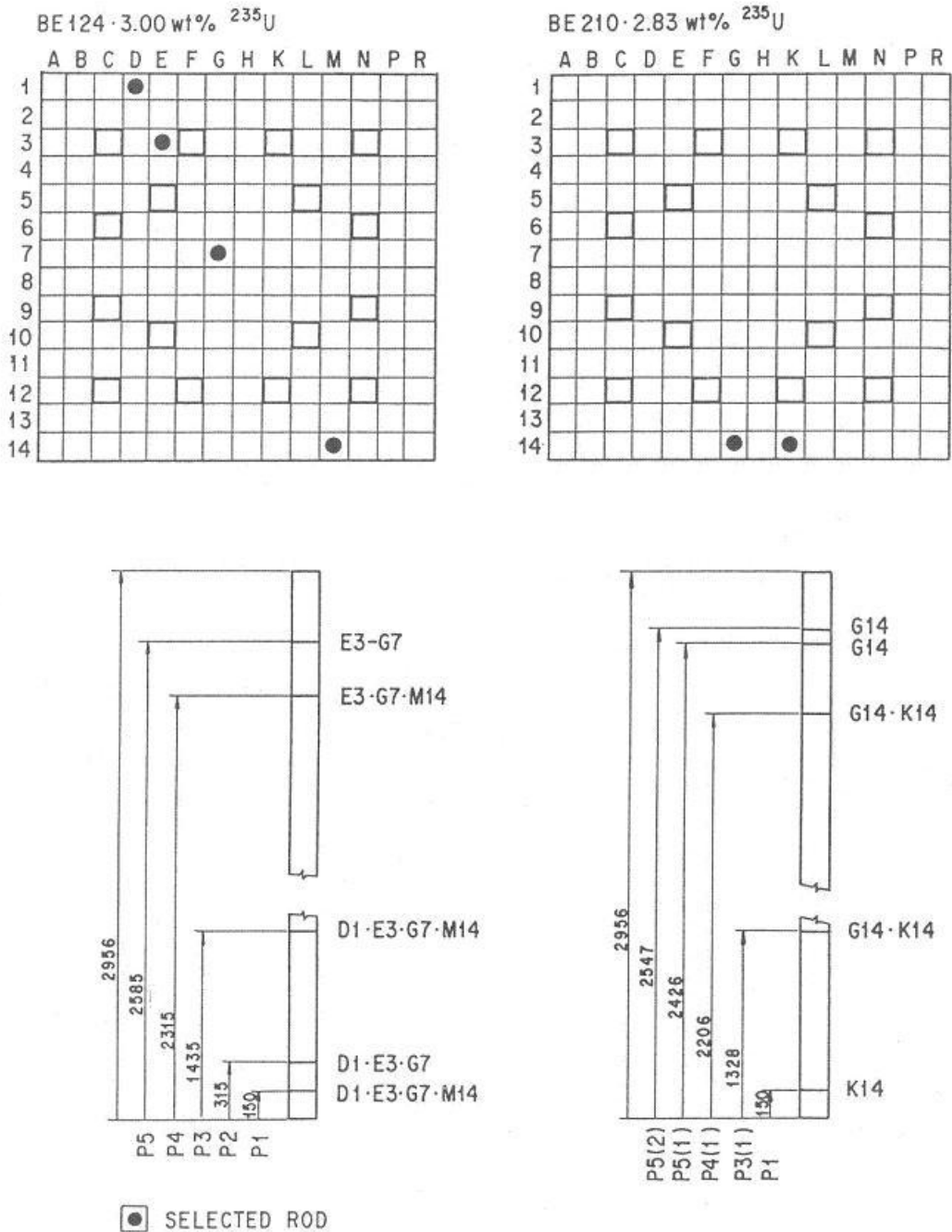


Fig. 8. Location of measured fuel rods in Obrigheim assemblies BE124 and BE210.

The irradiation histories for assemblies BE124 and BE210 are given in Table 54 (Ref. 15), and the assembly specific power and burnup according to operator data for assemblies BE168, BE170, BE171, BE172, and BE176 are given in Table 55 (Ref. 16). The derived cycle specific power values for the KWO samples are given in Table 56.

Table 53. Initial isotopic composition of KWO fuel

Assembly ID	Isotopic composition (wt %) ^a				UO ₂ density ^b (g/cm ³)
	²³⁵ U	²³⁴ U	²³⁶ U	²³⁸ U	
BE210	2.83	0.025	0.013	97.132	9.8096 ^c
BE124	3.00	0.027	0.014	96.960	10.0504 ^c
BE168, BE170, BE171, BE172, BE176	3.13	0.028 ^d	0.014	96.828	10.05

^aCalculated in spreadsheet *input_data.xls*, sheet *KWO* using the equations provided in Table 2.

^bDensity for cold fuel with dishing.

^cBased on linear density values shown in Table 52. ^dGiven as 0.03 in Ref. 16.

Table 54. Irradiation history of Obrigheim assemblies BE124 and BE210

Cycle of operation	Periods (mm/dd/yr)	Days ^a	Burnup (MWd/MTU)		
			Position in core	BE124	Position in core
Second	09.30.70 08.12.71	258	G-1	6,600	
Shut-down	08.13.71 09.29.71	48			
Third	09.30.71 09.07.72	295			D-11
Shut-down	09.08.72 10.04.72	27			
Fourth	10.05.72 09.01.73	283	D-7	18,600	J-5
Shut-down	09.02.73 09.24.73	23			
Fifth	09.25.73 08.16.74	229	D-4	29,000	G-3

^aFull power days (FPD) only.

Source: Ref. 15. Cycle assembly burnup values were used to determine the sample specific power values for each cycle shown in Table 56 (see *DVD/xls/input_data.xls*, worksheet *KWO*).

Table 55. Specific power and final burnup data for KWO assemblies BE168, BE170, BE171, BE172, and BE176

Cycle of operation	FPD	BE168	BE170	BE171	BE172	BE176
		(30.018 GWd/MTU)	(27.764 GWd/MTU)	(30.052 GWd/MTU)	(26.980 GWd/MTU)	(29.647 GWd/MTU)
Assembly specific power ^a (MW/MTU)						
Third	288	29.95	22.41	30.14	35.41	32.26
Shut-down	81					
Fourth	309	40.17	40.12	40.31	25.45	36.96
Shut-down	19					
Fifth ^b	377	0	0	0	0	0
Sixth	248	36.20	35.94	35.96	35.96	36.03

^aThe values in this table were used to determine cycle specific power values for the evaluated samples (see Table 56) based on measured sample burnup provided in Table 13 (see *DVD/xls/input_data.xls*, worksheet *KWO*).

^bThe assemblies were unloaded in the 5th cycle. The full power day (FPD) value for cycle 5 includes the shut-down period.
Source: Ref. 16.

Table 56. Operating parameter values for KWO samples

Sample ID	Sample specific power ^a (MW/MTU)					Sample temperature ^b (K)					Moderator ^c	
	Cycle					Cycle						
	2	3	4	5	6	2	3	4	5	6	Temperature (K)	Density (g/cm ³)
BE124.D1P1	18.674		30.954	33.153		720		833	855		556	0.7585
BE124.D1P3	29.771		49.348	52.853		822		1030	1072		572	0.7279
BE124.E3P1	17.801		29.507	31.602		713		819	840		556	0.7585
BE124.E3P2	25.890		42.915	45.963		785		957	991		557	0.7567
BE124.E3P3	31.986		53.018	56.784		843		1074	1122		572	0.7279
BE124.E3P4	27.275		45.210	48.422		798		982	1019		584	0.7015
BE124.E3P5	20.165		33.425	35.799		733		858	882		585	0.6991
BE124.G7P1	15.111		25.047	26.826		689		777	794		556	0.7585
BE124.G7P2	22.785		37.768	40.451		757		902	930		557	0.7567
BE124.G7P3	27.628		45.795	49.048		801		989	1027		572	0.7279
BE124.G7P4	24.443		40.517	43.395		772		931	962		584	0.7015
BE124.G7P5	22.767		37.739	40.419		757		902	930		585	0.6991
BE124.M14P1	13.761		22.810	24.430		678		757	772		556	0.7585
BE124.M14P3	25.899			45.979		785		957	991		572	0.7279
BE124.M14P4	21.965			38.994		749		888	915		584	0.7015
BE210.G14P31		41.799		47.863			934	1026	1000		570	0.7299
BE210.G14P41		39.736		45.501			913	998	974		583	0.7039
BE210.G14P51		33.626		38.505			852	919	900		584	0.7015
BE210.G14P52		27.004	34.876	30.921			790	840	826		585	0.6991
BE210.K14P1		25.532	30.058	29.236			776	823	810		556	0.7585
BE210.K14P31		40.884	47.001	46.816			924	1013	988		570	0.7299
BE210.K14P41		38.610	46.345	42.003			882	958	936		583	0.7039
BE168		29.284	39.276		35.404		817	918		878	571	0.7299
BE170		21.797	39.023		34.957		748	915		873	571	0.7299
BE171		28.739	38.436		34.279		812	909		866	571	0.7299
BE172		36.606	26.309		37.174		890	789		896	571	0.7299
BE176		31.289	35.848		34.946		837	882		873	571	0.7299

^aSpecific power values were determined from the sample burnups (Table 16) and the specified uptimes and burnup distributions for assemblies shown in Table 54 and Table 55 (see DVD/xls/input_data.xls, worksheet KWO).

^bEffective fuel temperature was calculated using an equation based on the coordinates of datapoints from the graph showing UO₂ temperature as a function of rod power in W/cm provided in Fig. 2 of Ref. 16 (see DVD/xls/input_data.xls, worksheet KWO).

^cModerator temperature and density were calculated using Eq. (1) and tabulated steam data (see Sect. 5.2).

8.3 TURKEY POINT UNIT 3

The Turkey Point Unit 3 PWR, operated by Florida Power and Light Co., was designed by Westinghouse Electric Corp. The fuel assembly design is based on a 15×15 square lattice, with 21 positions containing control rod and instrumentation guide tubes. Fuel design and operating parameters were taken from Refs. 21 and 22 and are given in Table 57. It should be noted that some of the input data for 2-D depletion calculations were not available in the aforementioned primary references, including control rod insertion data for the measured assemblies, soluble boron content, and sample specific powers. Therefore, assumptions were made consistently with the isotopic evaluations previously published.^{23,24}

The current study considers five different Turkey Point Unit 3 fuel samples, with burnups ranging from 30.51 to 31.56 GWd/MTU, that were taken from fuel rods G9, G10, and H9 in assembly D01, and from rods G9 and G10 in assembly D04. Radiochemical isotopic analyses of the five samples were analyzed by Battelle Columbus Laboratories for the Climax Spent Fuel Test and the results of the analyses are documented in Ref. 21. Assemblies D01 and D04 were irradiated in the reactor during cycles of operation 2, 3, and 4. Fig. 9 shows the configuration of the Westinghouse 15×15 assembly design and illustrates the position of each of the measured fuel rods within the assembly. Basic parameters for the measured samples, such as assembly and rod identification and burnup and axial location for each sample, are provided in Table 17 (see Sect. 7.3). A single sample was taken from each of the five different rods; the samples were taken from a location of either 167.0 or 167.6 cm above bottom of the fuel. It should be noted that fuel rod H9 was adjacent to the instrument tube and none of the measured fuel rods occupied an assembly location adjacent to a guide tube. As previously mentioned, information concerning control rod insertions for assemblies D01 and D04 is not available. Therefore, it is assumed that the guide tubes in assemblies D01 and D04 were vacant during cycles of operation 2, 3, and 4. This modeling assumption is based on engineering judgment and is considered to have either no effect or a small effect on the results of the calculations since the measured fuel rods were not adjacent to guide tubes and the samples were cut from the bottom half of the fuel rods. The sample cooling times between discharge and measurement date were not reported in Ref. 21.

Initial ^{235}U enrichment was given in Ref. 21; initial ^{234}U , ^{236}U , and ^{238}U concentrations were estimated using empirical relationships (see Sect. 5.1, Table 2) and are given in Table 58.

Burnup values for the Turkey Point fuel samples were determined based on measured ^{148}Nd concentrations.²¹ No data were available to indicate the operating power for the assemblies or core on a cycle-by-cycle basis. However, for other fuel assemblies for which power histories were available during cycles 2 through 4, the assembly power varied by less than 10% from the average power. As an example, the group of assemblies from Region 4 of the reactor, with an average burnup of 28.430 GWd/MTU, includes assemblies D01, D04, and D15 (Ref. 25). The burnup values for assembly D15 for cycles 2 through 4, which were obtained from reactor analyses and provided by Florida Power and Light Co., were 9.480, 9.752, and 8.920 GWd/MTU, respectively (Ref. 64). Hence, it was assumed that the reactor was operated at a constant power over all three cycles; average specific power was then computed for each sample based on the total length of the three cycles and the final burnup of the sample. These average specific power values are given in Table 60.

Table 57. Assembly design and operating data for Turkey Point Unit 3

Parameters	Data
Assembly general data	
Design	Westinghouse
Lattice	15 × 15
Assembly pitch, cm (in.)	21.5036 (8.466)
Number of fuel rods	204
Number of guide tubes	20
Number of instrument tubes	1
Fuel rod data	
Type fuel pellet	UO ₂
Enrichment, wt % ²³⁵ U	2.556
Stack density with gap, dish smeared in, % TD	89.72 ^a
Rod pitch, cm (in.)	1.4300 (0.563)
Clad outer diameter, cm (in.)	1.0719 (0.422)
Clad inner diameter, cm (in.)	0.9484 (0.3734)
Pellet outer diameter, cm (in.)	0.9294 (0.3659)
Clad material	Zircaloy-4
Clad temperature, K	595 ^b
Active fuel length, cm (in.)	365.76 (144)
Guide and instrument tube data	
Inner radius, cm (inner diameter as in.)	0.6502 (0.512)
Outer radius, cm (outer diameter as in.)	0.6934 (0.546)
Tube material	Zircaloy-4
General operation data for cycles 2, 3, and 4	
	See Table 59
Measured sample data	
Basic parameters of the measured spent fuel	See Table 17
Position of measured rod in assembly	See Fig. 9
Initial fuel compositions	See Table 58
Irradiation data	See Table 59
Sample specific power and effective fuel temperature	See Table 60
Water temperature at sample axial location, K	579 ^c
Water density at sample axial location, g/cm ³	0.7246 ^d
Description of measurement methods	See Sect. 7.3
Measurement accuracies estimated by laboratory	See Table 19
Date of measurements	927 days (see Sect. 7.3)
Experimental spent fuel compositions	See Table 18

^aBased on Ref. 22. The density of stack with gap is 0.8972×10.96 (theoretical density) = 9.8333 g/cm³. Fuel density is 10.235 g/cm³ for fuel mass homogenized within the volume delimited by the active fuel height and fuel radius (see *DVD/xls/input_data.xls*).

^bRef. 23.

^cModerator temperature is the average of the values determined using Eq. (1) (see Sect. 5.2), the inlet and outlet temperatures in Table 59, and sample axial locations in Table 17 (see *DVD/xls/input_data.xls*). Note that use of a single value for the three cycles is justified since all calculated cycle moderator temperatures are within ± 3 K.

^dBased on steam tables in Ref. 58.

Source: Ref. 21, Table A-1, and Ref. 22, Fig. 14, unless otherwise noted.

Table 58. Initial composition of Turkey Point fuel assemblies

Uranium isotope	Assembly D01	Assembly D04
wt % ^{235}U ^a	2.556	2.556
wt % ^{234}U ^b	0.023	0.023
wt % ^{236}U ^b	0.012	0.012
wt % ^{238}U ^b	97.409	97.409

^aRef. 22.^bValues determined using the equations provided in Table 2 (see Sect. 5.1).**Table 59. Turkey Point Unit 3 operating data**

Cycle	Cycle start ^a	Cycle end	Uptime (days) ^a	Downtime (days) ^a	System pressure (psia)	Inlet water temperature (°F)	Outlet water temperature (°C)	Soluble boron average concentration (ppm) ^e
2	12/16/74	10/26/75	314	58	1900	538.6	-	450
3	12/23/75	11/15/76	327	62	2100	539.0	-	450
4	1/16/77	11/24/77	312	927 ^b	2250 ^c	546.2 ^c	338 ^d	450

^aRef. 24 (based on personal communication with E. R. Knuckles – Florida Power and Light Co.). Residence time in reactor is 1073 days, consistent with the value for this parameter provided in Ref. 25. Note that total irradiation time in reactor, in effective full power days (EFPD), provided in Ref. 21 is 851 EFPD.^bCooling time from shutdown to date of radiochemical analyses.^cConsistent with operation parameters in Ref. 56.^dRef. 56.^eRefs. 23 and 24.

Source: Ref. 21, unless otherwise noted.

Table 60. Turkey Point sample specific powers and temperatures

Sample No.	Assembly	Rod ID	Burnup (GWd/MTU)	Specific power ^a (MW/MTU)	Effective fuel temperature ^b (K)	Clad temperature ^b (K)
1	D01	G9	30.720	32.235	922	595
2	D01	G10	30.510	32.015	922	
3	D01	H9	31.560	33.116	922	
4	D04	G9	31.260	32.802	922	
5	D04	G10	31.310	32.854	922	

^aBased on burnup values reported in Ref. 21 and sum of uptime values listed in Table 59.^bRefs. 23 and 24.

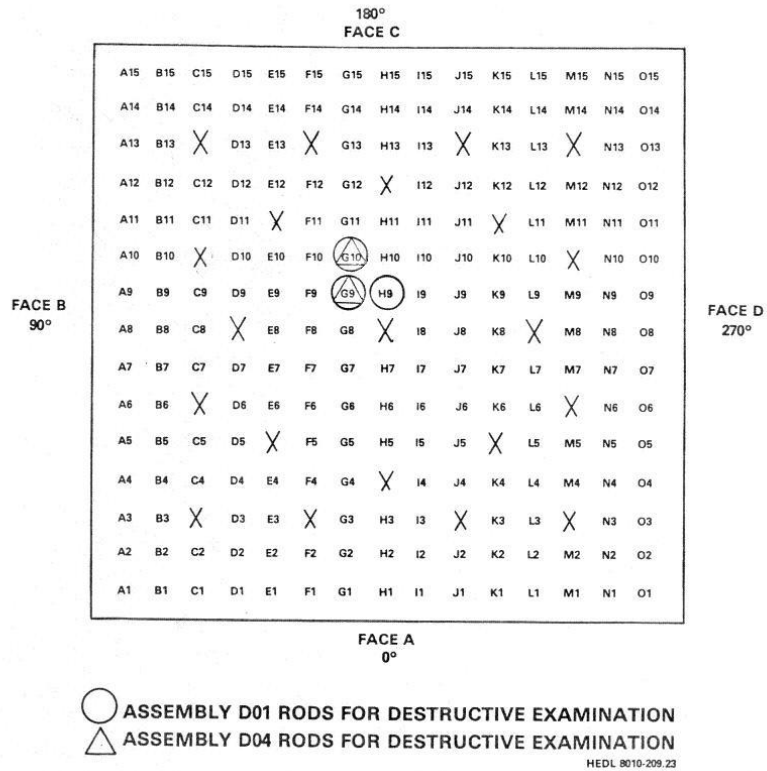


Fig. 9. Position of 21 guide tubes (×) and locations of measured fuel rods G9, G10, and H9 from Turkey Point assemblies D01 and D04. (Source: Ref. 21.)

8.4 H. B. ROBINSON UNIT 2

ATM-101 consisted of 27 fuel rod segments from nine fuel rods H. B. Robinson in assembly BO-5.²⁶ Four samples, denoted as N-9B-S, N-9B-N, N-9C-J, and N-9C-D from fuel rod N-9 of Assembly BO-5, are evaluated in the current study. Assembly BO-5 was irradiated during cycles 1 and 2 for a total of 799 effective full power days (EFPD), and then removed from the reactor on May 6, 1974. The post-irradiation examinations of the four samples were carried out in April 1984 (N-9C-D and N-9C-J) and February 1985 (N-9B-S and N-9B-N). Table 20 (see Sect. 7.4) summarizes sample general characteristics. Table 21 (see Sect. 7.4) presents the experimental results, in mg/g U_{initial} , at the cooling time shown in Table 20 for the four samples considered.

The H. B. Robinson Unit 2 PWR uses Westinghouse fuel assemblies with a 15×15 pin lattice. A standard Westinghouse burnable poison fixture was inserted into assembly BO-5 for the first cycle.²⁷ Descriptions of the design characteristics of assembly BO-5 and the burnable poison rod (BPR) present in the assembly during cycle 1 are presented in Table 61. Note that Refs. 26 (ATM-101) and 27 provide different initial fuel enrichment values and assembly descriptions for assembly BO-5. The depletion calculations in the current report use design data from Ref. 27, consistent with the input data used in previously published evaluations and calculations.^{87,38} The location within the BO-5 lattice of rod N-9 is shown in Fig. 11.

Power histories are based on axial flux measurement data available in Ref. 28 for the assembly BO-5 at approximately beginning-of-life, 25%, 50%, 75%, and end-of-life (100%) exposures and on the sample total burnups. Fig. 12 shows the axial factors for 57 equal-length rod segments along with the corresponding assembly average burnups (see figure legend). Samples N-9B-S, N-9B-N, N-9C-J, and N-9C-D correspond to segments 2, 4, 31, and 35, respectively. The sample average power and effective fuel temperature values are given in the Table 63. Reference 29 describes outage and refueling durations in terms of approximate time. Outage durations for various repair work were approximately 2 months (starting in March of 1971), 2.5 months (starting in June of 1971), 1 month (starting in May of 1972), and 12 days in November of 1973. The first refueling outage was started in mid-March and lasted for approximately 2 months. The differences between the estimated and detailed power histories should not cause a significant change in the isotopic compositions calculated at the cooling times (~10 years) of the radiochemical analyses. Moderator temperature and density values are listed in Table 64. The moderator temperatures were calculated using Eq. (1) and the inlet and outlet temperatures of 546.5°F and 600.6°F, respectively.²⁹ The moderator densities were determined by interpolating data on a temperature-pressure-density table at a pressure of 2250 psia (Ref. 29). Average soluble boron concentration for each irradiation interval was determined assuming the boron adjustment factors of 1.45 and 0.55 applied to the cycle average soluble concentration, as shown in the boron letdown example for SAS2H calculations (Ref. 67). The effective fuel temperatures were determined from the fuel temperature versus rod linear power curve in Ref. 16, Fig. 2. Although the curve was developed for the Obrigheim PWR, the rod dimensions, rod lattice pitch, and operating conditions of the H. B. Robinson and Obrigheim fuel assemblies are similar.

Table 61. Assembly design and operating data for H. B. Robinson

Parameters	Data
Reactor core	
Design	Westinghouse, PWR 15 × 15
Lattice pitch, cm (in.)	21.50364 (8.466)
Initial enrichment, ²³⁵ U wt %	1.85/2.56/3.10 ^a
Inlet coolant temperature, °F	546.5 ^a
Outlet coolant temperature, °F	600.6 ^a
Reactivity control	Soluble boron, burnable poison rods, and control rods
Average boron concentration	450 ppm ^b
Operating pressure, psia	2250
Fuel assembly	
Lattice	15 × 15 (see Fig. 11)
Number of fuel rods	204
Uranium weight, kg	443.7
Number of guide tubes	20
Number of instrument tubes	1
Fuel rod	
Type fuel pellet	UO ₂
Pellet stack density (% TD), g/cm ³	9.944 (90.73) ^c
Initial fuel composition, ^d wt % in U total	
²³⁵ U	2.561
²³⁴ U	0.023
²³⁶ U	0.012
²³⁸ U	97.404
Rod pitch, cm (in.)	1.4300 (0.563)
Rod outer diameter, cm (in.)	1.0719 (0.422)
Rod inner diameter, cm (in.)	0.9484 (0.3734)
Pellet diameter, cm (in.)	0.9294 (0.3659)
Active fuel length, cm (in.)	365.76 (144)
Clad material	Zircaloy-4
Clad temperature, K	595
Guide tube	
Material	Zircaloy-4
Inner radius, cm (in.)	0.6502 (0.256)
Outer radius, cm (in.)	0.6934 (0.273)
BPR insertions ^e	12 during cycle 1 0 during cycle 2 (see Fig. 11)
Number of guide tubes with water	8 during cycle 1 20 during cycle 2 (see Fig. 11)
Instrument tube	
Material	Zircaloy-4
Inner radius, cm (in.)	0.6502 (0.256)
Outer radius, cm (in.)	0.6934 (0.273)

Table 61. Assembly design and operating data for H. B. Robinson (continued)

Parameters	Data
Burnable poison rod	
Air outer diameter, cm (in.)	0.5677 (0.2235)
SS304 outer diameter, ^f cm (in.)	0.6007 (0.2365)
Air outer diameter, cm (in.)	0.6172 (0.2430)
Pyrex glass outer diameter, cm (in.)	1.0058 (0.3960)
Air outer diameter, cm (in.)	1.0173 (0.4005)
SS304 outer diameter, cm (in.)	1.1151 (0.4390)
B ₂ O ₃ , wt %	12.5
Borated glass chemical composition and density	see Table 62
Measured sample data	
Basic parameters of the measured spent fuel	See Table 20
Position of measured assembly in the reactor core	See Fig. 10
Position of measured rod in assembly	See Fig. 11
Water temperature and density at sample locations	See Table 64
Sample burnup, specific power, and temperature	See Table 63
Description of measurement methods	See Sect. 7.4
Measurement accuracies estimated by laboratory	See Table 22
Date of measurements	See Table 20
Experimental spent fuel compositions	See Table 21

^aRef. 29. Fuel initial enrichment for Region 2 is consistent with the design data provided in Refs. 27 and 88. Note that ATM-101 (Ref. 26) provides a value of 2.55 wt % ²³⁵U for the parameter.

^bAssumption in Ref. 27.

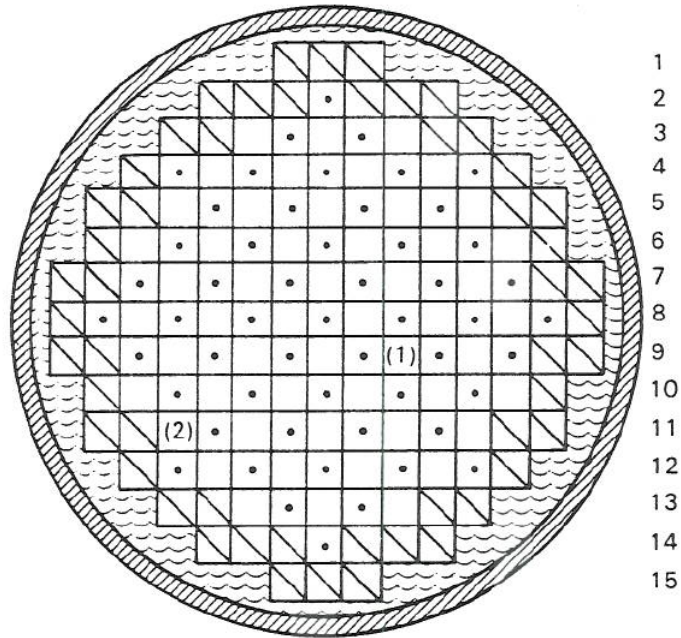
^cMass density based on homogenized UO₂ within the fuel rod volume.

^dFuel enrichment for sampled rod was taken from Ref. 29. Initial uranium composition was calculated using the empirical relationship equations provided in Table 2, Sect. 5.1.

^eThe burnable poison was removed when the average assembly burnup had reached 18,000 MWd/MTU (Ref. 27). The burnup of assembly BO-5 at the end of cycle 1 was 18,613 MWd/MTU (Ref. 28).

^fSCALE standard composition for SS304 was used in the calculations.⁸⁶

Source: Ref. 27, unless otherwise noted.



R P N M L K J H G F E D C B A

Core Arrangement - H.B. Robinson Reactor

Showing Location of Assembly BO-5
During First (1) and Second (2) Cycles

- ◻• Region 1 (Enrichment 1.85%) 53 Assemblies
- ◻ Region 2 (Enrichment 2.55%) 52 Assemblies
- ◻ Region 3 (Enrichment 3.10%) 52 Assemblies

Fig. 10. Core arrangement for H. B. Robinson Unit 2 reactor core. (Source: Ref. 26, Fig. 4.1.)

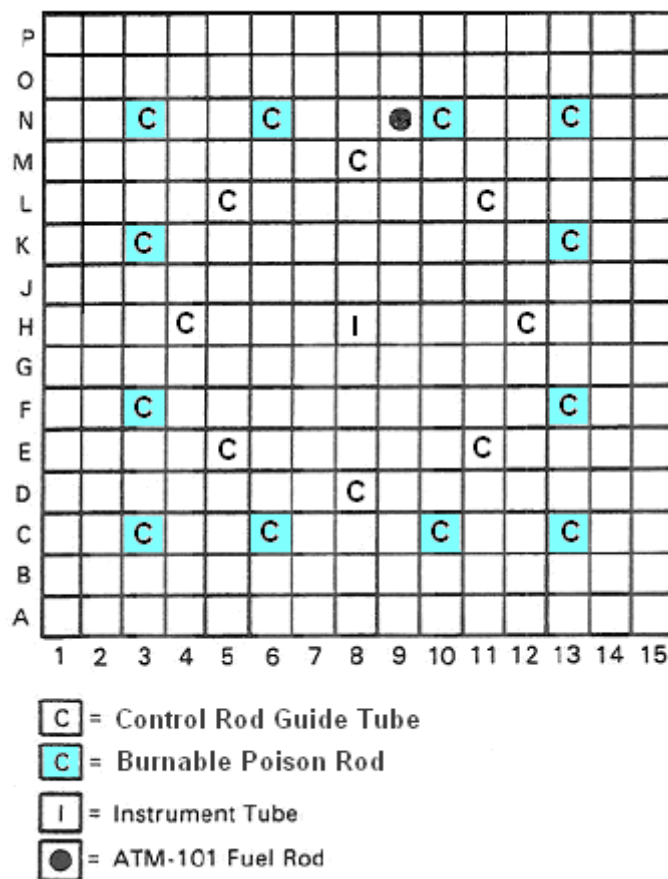


Fig. 11. Locations of fuel rod N-9, instrument tube, and guide tubes in assembly BO-5. (Source: Ref. 26, Fig. 4.2, and Ref. 27, Fig. 3.2.3-8.) Note: During cycle 1 of irradiation, 12 guide tubes contained BPR insertions, as shown in this figure. No BPR insertion was present during cycle 2 of irradiation.)

Table 62. Atom densities for borosilicate glass

Compound	Weight fraction	Element/isotope	Weight percent ^b	Atom density (atoms/cm ³ ·barn) ^c
SiO ₂	0.875	Si	40.9067	1.9560E-02
B ₂ O ₃	0.125 ^a	O	55.2092	4.6341E-02
		¹⁰ B	0.6976	9.3562E-04
		¹¹ B	3.1866	3.8871E-03

^aRef. 27.

^bRef. 89.

^cCalculated in *DVD/xls/input_data.xls* using element/isotope weight fractions, the borosilicate glass density of 2.23 g/cm³ (Ref. 86), and relative atomic masses from Ref. 63.

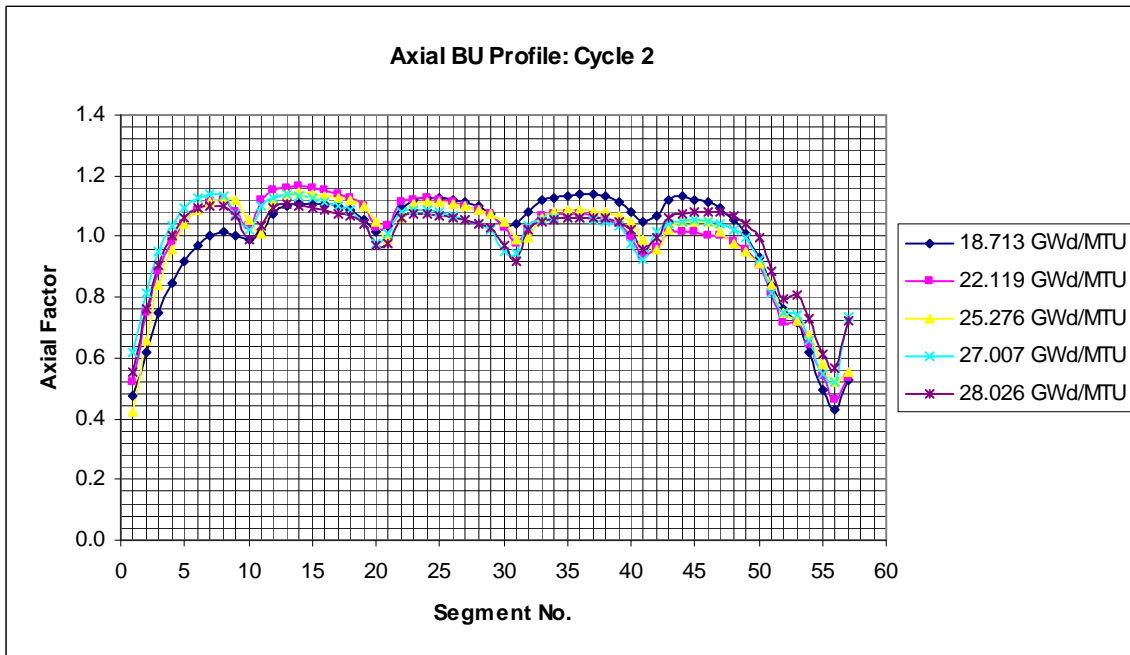
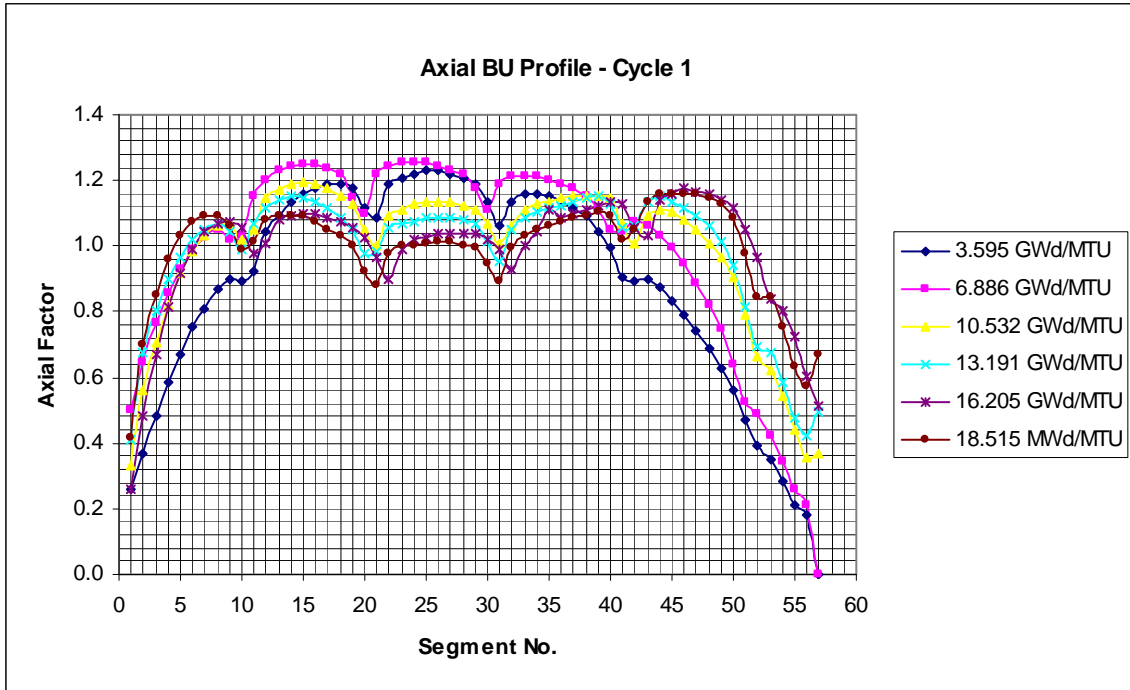


Fig. 12. Axial burnup profiles for assembly exposures during cycles 1 and 2. (Note: Samples N-9B-S, N-9B-N, N-9C-J, and N-9C-D correspond to segments 2, 4, 31, and 35, respectively. A grid plate was adjacent to sample N-9C-J.)

Table 63. Operating and fuel temperature data for H. B. Robinson spent fuel samples

Irradiation time (days)	Downtime following interval ^a (days)	N-9B-S	N-9B-N	N-9C-D	N-9C-J	N-9B-S	N-9B-N	N-9C-D	N-9C-J
		Power (MW/MTU) ^b				Effective fuel temperature (K) ^c			
Cycle 1									
92.35	0	13.47	22.73	46.56	42.38	676.65	758.00	954.91	1002.28
83.06	0	24.52	34.31	49.87	48.73	774.48	869.43	1027.74	1041.27
92.57	30	20.23	31.10	44.70	39.08	735.37	837.28	919.06	980.95
70.58	0	23.32	32.82	42.26	35.67	763.40	854.41	883.33	953.61
83.51	0	15.91	28.56	39.05	35.43	697.38	812.61	880.84	918.80
65.09	61	22.46	32.48	36.96	32.88	755.48	850.93	854.98	896.69
Cycle 2									
6.38	0	19.44	28.15	39.19	35.58	728.40	808.66	882.40	920.21
109.91	0	21.37	29.60	33.72	30.19	745.65	822.64	828.41	863.40
52.33	12	18.59	28.48	33.53	30.17	720.83	811.78	828.20	861.53
52.33	0	18.59	28.48	33.53	30.17	720.83	811.78	828.20	861.53
57.12	0	22.71	30.75	32.67	28.58	757.85	833.82	812.76	852.86
33.68	See Table 20	21.22	29.57	32.61	27.86	744.28	822.29	805.86	852.25

^aRef. 29 describes outage and refueling durations in terms of approximate time. The impact on the fuel concentrations and neutron spectrum should be negligible due to the relatively short down times allowing short lived fission products to decay and due to the fact that the reactor operated for a significant time after shutdown.

^bValues calculated in *DVD/xls/input_data.xls* using sample total burnup, the sample axial burnup profile (see Fig. 12), and the assembly average burnup of 28.03 GWd/MTU given in Ref. 26.

^cEstimated from the curve of effective fuel temperature as function of linear power for reactor rod data (Ref. 16) of similar dimensions and pitch (*DVD/xls/input_data.xls*).

Table 64. Moderator conditions for H. B. Robinson spent fuel samples

Sample ID	Axial location (cm)	Total burnup (GWd/MTU)	Moderator temperature ^a (K)	Moderator density ^b (g/cm ³)
N-9B-S	11	16.02	559	0.7540
N-9B-N	26	23.81	559	0.7535
N-9C-J	199	28.47	576	0.7206
N-9C-D	226	31.66	579	0.7135

^aDerived using the method described in Sect. 5.2 and 546.5 °F and 600.6 °F for inlet and outlet temperatures, respectively (Ref. 29).

^bDetermined from the moderator temperature and the nominal pressure of 2250 psia (Ref. 29).

Source: Ref. 26, unless otherwise noted.

8.5 CALVERT CLIFFS UNIT 1

The isotopic measurements in the ATM-103 program³⁰ were carried out on three samples from the fuel rod MLA098 belonging to fuel assembly D101, which was irradiated for three consecutive cycles, from cycle 2 to cycle 4. The samples are identified as MLA098-JJ, MLA098-BB, and MLA098-C. The measurements in the ATM-104 program³⁰ were performed on three samples from the fuel rod MKP109 belonging to assembly D047, irradiated for four cycles, from cycle 2 to 5. The samples are identified in this report as MKP109-LL, MKP109-CC, and MKP109-P. The measurements in the ATM-106 program³² were performed on three samples from the fuel rod NBD107 belonging to assembly BT03. The samples are identified as NBD107-MM, NBD107-GG, and NBD107-Q. The NBD107 rod was irradiated for four consecutive cycles, from cycle 1 to cycle 4.

Each of the assemblies D101, D047, and BT03 had a CE 14 × 14 design and contained 176 rods and 5 guide tubes. There were no burnable absorber rods or gadolinia-bearing rods in the assembly during

any of the irradiation cycles for assemblies D101 and D047. The layout of the assembly and the location of the rod from which the samples were selected are illustrated in Fig. 13 for assemblies D101 and D047. In the case of assembly BT03, there were 12 burnable absorber rods during cycle 1, and 4 test (non-fuel) rods during all irradiation time, as illustrated in Fig. 14.

The geometry data are presented in Table 65 and the sample location data in Table 66. The temperature of the moderator at the sample axial location was calculated using Eq. (1) (see Sect. 5.2). Based on the temperature values, the corresponding moderator densities (see Table 67) were calculated by using temperature vs. pressure tabulated data⁵⁸ corresponding to the operating system pressure.

The concentration of the soluble boron in moderator was available³⁵ for cycles 2 to 5, as listed in Table 68. The soluble boron concentration at the beginning of cycle shown in Table 68 was not provided and was obtained by extrapolation of the available data. As no data was available for cycle 1, an average concentration of 330 ppm as calculated for cycle 2 was used in the computational model. The effective fuel temperatures were available³⁵ only for samples in fuel rod MKP109 that was irradiated during cycles 2 to 5. Lacking more detailed fuel temperature information, the data available for this fuel rod were applied to the other two measured fuel rods too, as listed in Table 69.

Data was available^{30,31,32} for the sample burnups determined based on the measured content of ¹⁴⁸Nd, as listed in Table 70. Linear heat generation rates (LHGRs) data at the axial locations of samples, listed in Table 71, were available in detail^{34,38} for the three samples from rod MKP109 in assembly D047. At each axial location, the linear burnups of time intervals, calculated³⁸ as the product of interval size and LHGR, were summed for each cycle. The calculated linear burnups per cycle were then normalized to the total burnups of the three D047 samples to produce the sample burnups presented in Table 70. The fuel rod burnup data for rods MLA098 and NBD107 were determined based on the available linear heat generation data for these two fuel rods, which are presented in Table 72 and Table 73 for fuel rods MLA098 and NBD107, respectively. For these two rods, no detailed LHGR data were available at the sample axial location, but only as rod-averaged data. In this case, the cumulative burnup at the end of cycle k for a sample s from fuel rod r , $B_{s,r}^k$, was calculated based on the available sample total burnup $B_{s,r}^{tot}$, the fuel rod cumulative burnup at the end of each cycle B_r^k , and the fuel rod total burnup B_r^{tot} , as shown in Eq. (17). The data obtained for the sample cumulative burnup at the end of each cycle are listed in Table 74. The average cycle power for each sample can easily be obtained by dividing the sample burnup accumulated in a cycle by the time duration of that cycle provided in Table 74. The cooling time for each of the samples is shown in Table 75.

$$B_{s,r}^k = B_{s,r}^{tot} \frac{B_r^k}{B_r^{tot}} . \quad (17)$$

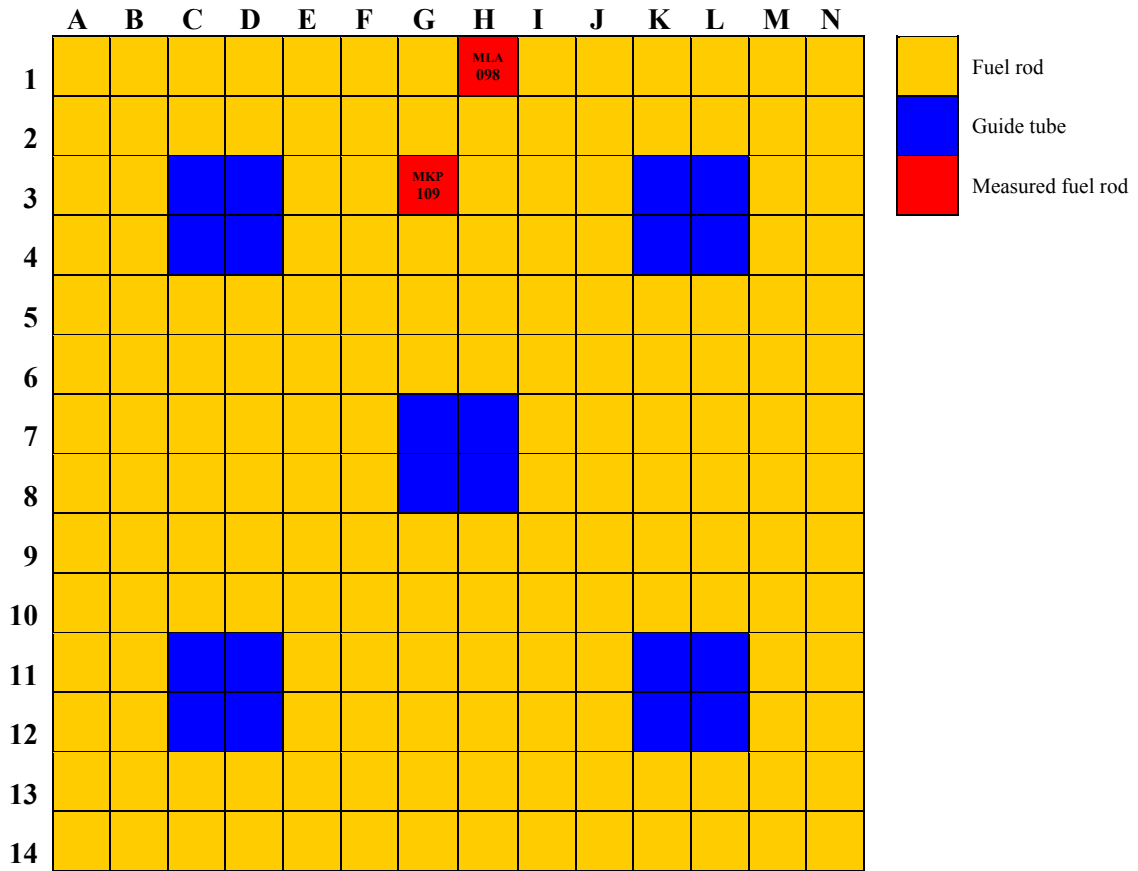


Fig. 13. Assembly layout for Calvert Cliffs samples from assemblies D047 and D101. (Source: Ref. 30, Fig. 4.3; Ref. 31, Fig. 3.3.)

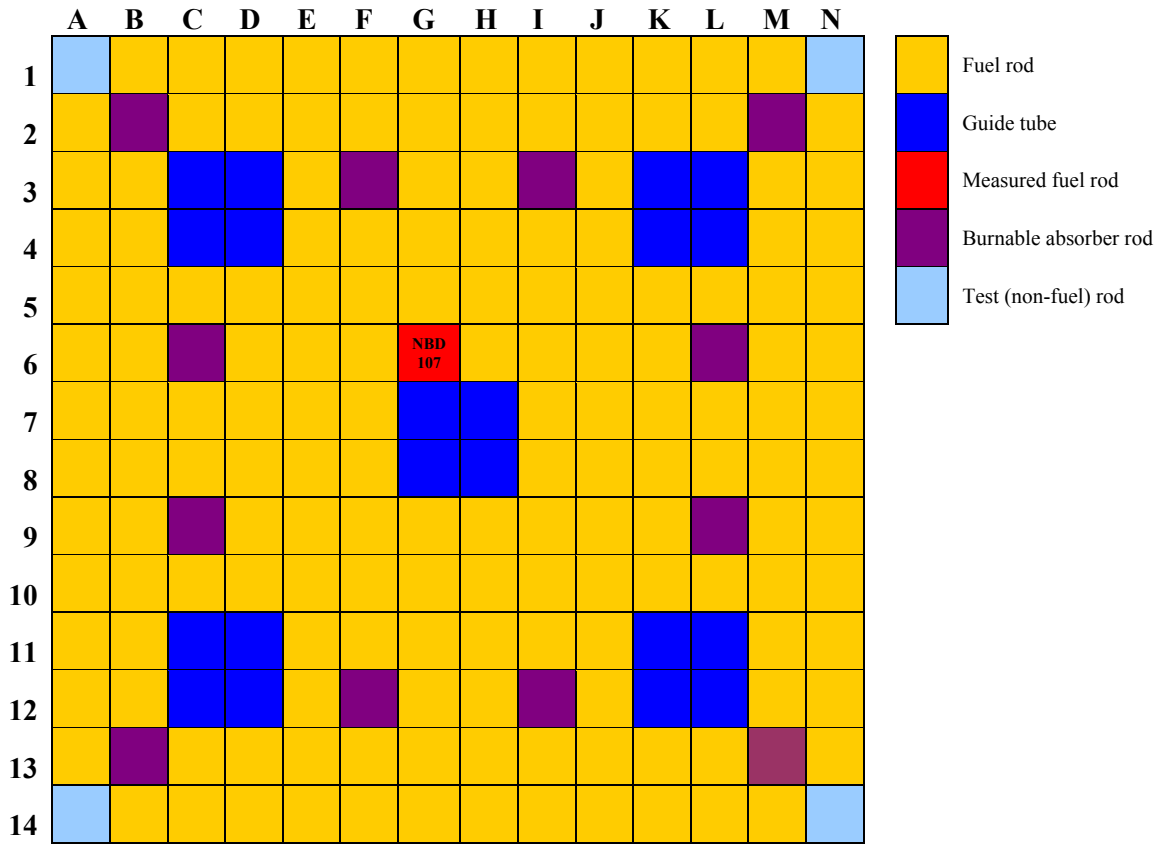


Fig. 14. Assembly layout for Calvert Cliffs samples from assembly BT03. (Source: Ref. 32, Fig. 4.3.)

Table 65. Assembly design and operating data for Calvert Cliffs measured spent fuel

Parameter	Assembly D047	Assembly D101	Assembly BT03
ASSEMBLY AND REACTOR DATA			
Reactor	Calvert Cliffs 1	Calvert Cliffs 1	Calvert Cliffs 1
Operating pressure, Pa	155 x 10 ⁵	155 x 10 ⁵	155 x 10 ⁵
Core coolant inlet temperature, ^a K	557.15	557.15	557.15
Core coolant outlet temperature, ^a K	585.15	585.15	585.15
Lattice geometry	14 × 14	14 × 14	14 × 14
Assembly design	CE	CE	CE
Rod pitch, cm	1.4732	1.4732	1.4732
Number of fuel rods ^b	176	176	160
Number of water rods	5	5	5
Number of burnable absorber rods ^b	0	0	12
Number of test (non-fuel) rods ^b	0	0	4
Assembly pitch, cm	20.78	20.78	20.78
Total fuel rod length, ^c cm	373.38	373.38	373.38
Active fuel rod length, ^c cm	347.22	347.22	347.22
Sample location	see Table 66	see Table 66	see Table 66
Fuel rod data			
Fuel material type	UO ₂	UO ₂	UO ₂
Pellet stack density, g/cm ³	10.045	10.045	10.036
Fuel pellet diameter, cm	0.9563	0.9563	0.9639
Clad material	Zircaloy-4	Zircaloy-4	Zircaloy-4
Fuel temperature, K	see Table 69	see Table 69	see Table 69
Clad inner diameter, cm	0.9855	0.9855	0.9855
Clad outer diameter, cm	1.1176	1.1176	1.1176
Average clad temperature, ^d K	620	620	620
U isotopic composition, ^e wt %			
²³⁴ U	0.027	0.024	0.022
²³⁵ U	3.038	2.72	2.453
²³⁶ U	0.014	0.013	0.011
²³⁸ U	96.921	97.243	97.514
Burnable absorber rod data ^f			
Pellet material			Al ₂ O ₃ -B ₄ C
Pellet outer diameter, cm			0.9550
Clad inner diameter, cm			0.9855
Clad outer diameter, cm			1.1176
Clad material			Zircaloy-4
Al ₂ O ₃ -B ₄ C composition, at/b-cm			
Al			0.039
O			0.058
¹⁰ B			0.000859
¹¹ B			0.00344
C			0.00107
Test (non-fuel) rod data ^f			
Central region material			void - gas
Stainless steel tube inner diameter, cm			0.660
Stainless steel tube outer diameter, cm			0.945
Clad inner diameter, cm			0.9855
Clad outer diameter, cm			1.1176
Clad material			Zircaloy-4
Moderator data			
Moderator density, g/cm ³	see Table 67	see Table 67	see Table 67
Moderator temperature, K	see Table 67	see Table 67	see Table 67
Soluble boron content, ppm	see Table 68	see Table 68	see Table 68
Guide tube data ^f			
Guide tube material	Zircaloy-4	Zircaloy-4	Zircaloy-4
Inner radius, cm	1.314	1.314	1.314
Outer radius, cm	1.416	1.416	1.416

^aProvided in Ref. 36.

^bAs provided in Ref. 39.

^cAs provided in Refs. 30, 31, 32.

^dAverage clad temperature was not available. The maximum clad temperature provided in Ref. 56 was used as average clad temperature in the calculations.

^eInitial values (fresh fuel)

^fAs provided in Ref. 40.

Source: Ref. 38 unless otherwise noted.

Table 66. Sample location data for Calvert Cliffs samples

Assembly ID	Sample ID	Distance from top of fuel rod ^a (cm)	Average distance from top of fuel rod ^b (cm)	Distance from bottom of active fuel region (cm)
D047	MKP109-P	208.656 - 209.926	209.291	164.09
	MKP109-CC	345.331 - 346.619	345.975	27.41
	MKP109-LL	360.032 - 361.320	360.676	12.70
D101	MLA098-JJ	361.013 - 362.379	361.696	11.68
	MLA098-BB	345.603 - 346.969	346.286	27.09
	MLA098-P	208.204 - 209.499	208.852	164.53
BT03	NBD107-Q	208.768 - 210.022	209.495	163.89
	NBD107-GG	350.050 - 351.320	350.685	22.70
	NBD107-MM	358.686 - 359.956	359.321	14.06

^aAs provided in Refs. 30, 31, and 32 for samples in assembly D047, D101, and BT03, respectively.

^bThe middle of the region from which the sample was cut.

Table 67. Moderator temperature and density data for Calvert Cliffs samples

Assembly ID	Sample ID	Temperature ^a (K)	Density ^b (g/cm ³)
D047	MKP109-P	569.9	0.7307
	MKP109-CC	557.6	0.7569
	MKP109-LL	557.2	0.7575
D101	MLA098-JJ	557.2	0.7576
	MLA098-BB	557.6	0.7570
	MLA098-P	570.0	0.7305
BT03	NBD107-Q	569.9	0.7308
	NBD107-GG	557.4	0.7572
	NBD107-MM	557.3	0.7575

^aThe temperature of the moderator at the sample axial location was calculated using Eq. (1) (see Sect. 5.2).

^bBased on the temperature values, the corresponding moderator densities were calculated by using temperature vs. pressure tabulated data⁵⁸ corresponding to the operating system pressure given in Table 65.

Table 68. Concentration of soluble boron in moderator for Calvert Cliffs samples

Cycle 2		Cycle 3		Cycle 4		Cycle 5	
Time interval (days)	Soluble boron ^a (ppm)	Time interval (days)	Soluble boron ^a (ppm)	Time interval (days)	Soluble boron ^a (ppm)	Time interval (days)	Soluble boron ^a (ppm)
0.0 ^b	663	0.0 ^b	910	0.0 ^b	1033	0.0 ^b	1045
7.0	654	7.9	883	46.1	960	65.0	919
30.8	614	14.4	862	24.0	889	5.5	911
16.3	563	19.7	837	22.6	827	6.6	896
11.4	533	16.8	808	25.7	759	28.6	854
12.5	507	16.3	775	30.2	706	31.2	784
23.7	468	15.4	741	41.2	788	27.0	715
22.8	418	39.1	684	50.3	720	22.7	655
23.2	368	31.2	611	11.0	673	27.1	603
8.1	333	31.8	545	32.8	527	55.2	521
31.4	290	31.8	478	23.5	460	20.9	434
34.3	218	44.3	368	29.4	370	41.9	356
16.4	162	25	291	28.1	301	21.6	281
19.2	122	59.1	224	65.4	191	27.6	226
12.8	86	28.9	120	35.7	73	19.0	173
34.2	36	81	83	85.0	31	61.2	79
1.9	0						
71.0	0						

^aThe value given for each time interval is the arithmetic mean of the boron concentration at the beginning and end of the time interval (Ref. 35).

^bValue at beginning of cycle (0.0 days) obtained by extrapolation of the available data.

Source: Ref. 35, Table II, unless otherwise noted.

Table 69. Effective fuel temperature data for Calvert Cliffs samples

Assembly ID	Sample ID	Temperature cycle 1 (K)	Temperature cycle 2 (K)	Temperature cycle 3 (K)	Temperature cycle 4 (K)	Temperature cycle 5 (K)
D047 ^a	MKP109-LL		829	850	775	709
	MKP109-CC		940	927	793	712
	MKP109-P		997	958	794	747
D101 ^b	MLA098-JJ		829	850	775	
	MLA098-BB		940	927	793	
	MLA098-P		997	958	794	
BT03 ^b	NBD107-MM	829	829	850	775	
	NBD107-GG	940	940	927	793	
	NBD107-Q	997	997	958	794	

^aEffective fuel temperatures available from Ref. 35.

^bAssumed temperature values based on available data for assembly D047.

Table 70. Burnup values for Calvert Cliffs spent fuel samples

Assembly ID	Sample ID	Burnup^a (GWd/MTU)
D047	MKP109- LL	27.35
	MKP109-CC	37.12
	MKP109- P	44.34
D101	MLA098-JJ	18.68
	MLA098-BB	26.62
	MLA098-P	33.17
BT03	NBD107- MM	31.40
	NBD107-GG	37.27
	NBD107- Q	46.46

^aAs reported in Refs. 30, 31, and 32 for samples in assembly D101, D047, and BT03, respectively.

Table 71. Linear heat generation data for fuel rod MKP109

Interval (days)	Cycle #2			Interval (days)	Cycle #3			Interval (days)	Cycle #4			Interval (days)	Cycle #5		
	LGHR ^a (kW/ft)				LGHR (kW/ft)				LGHR (kW/ft)				LGHR (kW/ft)		
	13.2 cm ^b	27.70 cm	165.22 cm		13.2 cm	27.70 cm	165.22 cm		13.2 cm	27.70 cm	165.22 cm		13.2 cm	27.70 cm	165.22 cm
7.0	2.00	3.04	5.42	7.9	2.63	3.85	7.47	46.1	2.79	3.97	6.59	65.0	1.98	2.67	4.55
30.8	2.73	4.08	6.64	14.4	2.71	3.95	7.20	24.0	2.91	4.11	6.54	5.5	2.15	2.91	4.80
16.3	2.80	4.18	6.60	19.7	2.14	3.11	5.04	22.6	3.07	4.29	6.43	6.6	2.20	2.98	4.80
11.4	2.86	4.26	6.60	16.8	3.18	4.58	7.79	25.7	3.29	4.56	6.33	28.6	2.36	3.15	4.79
12.5	2.94	4.34	6.56	16.3	3.35	4.81	7.78	30.2	1.57	2.17	3.05	31.2	2.54	3.36	4.72
23.7	3.01	4.43	6.41	15.4	3.74	5.33	8.16	41.2	1.79	2.46	3.18	27.0	2.66	3.52	4.73
22.8	3.16	4.61	6.44	39.1	3.71	5.23	7.45	50.3	1.72	2.35	3.00	22.7	2.77	3.63	4.71
23.2	3.27	4.73	6.37	31.2	3.95	5.50	7.37	11.0	3.18	4.33	5.23	27.1	2.46	3.22	4.05
8.1	3.30	4.75	6.34	31.8	4.08	5.64	7.20	32.8	3.93	5.31	6.17	55.2	2.81	3.64	4.34
31.4	3.48	4.95	6.34	31.8	4.20	5.75	7.02	23.5	4.07	5.42	6.12	20.9	3.17	4.08	4.75
34.3	3.59	5.05	6.53	44.3	4.38	5.93	6.93	29.4	4.05	5.35	5.95	41.9	3.32	4.24	4.79
16.4	3.75	5.25	6.38	25.0	0.00	0.00	0.00	28.1	4.25	5.56	6.07	21.6	3.38	4.30	4.80
19.2	3.75	5.21	6.26	59.1	4.67	6.20	6.89	65.4	4.42	5.67	5.98	27.6	3.21	4.04	4.49
12.8	3.81	5.28	6.30	28.9	4.95	6.52	7.12	35.7	4.62	5.87	6.02	19.0	3.57	4.49	4.87
34.2	3.63	4.98	5.95									61.2	3.05	3.79	4.00
1.9	3.64	4.98	5.96												

^aLinear heat generation rate.

^bAxial location of each of the three samples.

Source: Ref. 31, Table II.

Table 72. Linear heat generation data for fuel rod MLA098

Cycle 2		Cycle 3		Cycle 4	
Interval (days)	LHGR ^a (kW/ft)	Interval (days)	LHGR (kW/ft)	Interval (days)	LHGR (kW/ft)
7.1	19.1	6.8	19.1	47.0	17.4
30.8	23.5	14.3	18.6	24.1	17.2
16.4	23.5	19.5	13.1	22.5	17.3
11.4	23.5	16.5	20.7	25.5	17.3
12.5	23.5	16.1	21.2	30.7	8.4
23.4	23.5	15.1	22.4	41.0	8.6
22.8	23.4	38.8	21.2	50.1	8.6
22.9	23.3	31.0	21.3	10.9	14.9
8.5	23.3	31.6	21.2	10.7	17.7
31.4	23.5	31.6	20.9	45.1	17.9
34.2	23.3	43.9	20.9	29.3	17.6
16.6	23.7	61.7	21.2	28.0	18.1
19.1	23.3	30.2	22.0	65.1	18.0
12.8	23.5			35.7	18.2
34.3	22.2				
1.9	22.2				

^aLinear heat generation rate.

Source: Ref. 30, Table A.1

Table 73. Linear heat generation data for fuel rod NBD107

Cycle 1		Cycle 2		Cycle 3		Cycle 4	
Interval (days)	LHGR (kW/ft)	Interval (days)	LHGR (kW/ft)	Interval (days)	LHGR (kW/ft)	Interval (days)	LHGR (kW/ft)
24.2	19.2	7.2	13.3	10.9	12.6	45.0	13.8
19.6	24.1	31.0	17.1	14.1	12.4	24.1	13.8
39.7	24.1	16.4	19.0	25.3	6.7	22.4	13.9
39.7	23.9	11.4	18.9	12.2	14.0	25.2	14.1
39.4	23.7	12.6	18.9	16.3	14.2	31.0	6.7
39.3	23.6	23.2	18.9	15.1	15.2	44.8	6.3
39.1	23.5	22.7	18.9	38.1	14.3	48.1	7.0
38.9	23.6	23.0	18.9	30.9	14.6	10.9	12.4
39.0	23.6	8.2	18.8	31.4	14.6	10.6	14.9
39.1	23.5	31.0	19.3	31.5	14.6	45.3	15.2
39.1	23.3	33.8	19.4	43.2	14.8	28.7	15.1
39.4	23.1	16.5	19.8	60.0	14.9	27.9	15.6
39.3	22.9	19.1	19.6	28.0	16.1	65.9	15.5
39.3	22.6	12.8	19.8			36.1	15.7
39.3	22.4	35.2	18.4				
39.3	22.2	1.9	18.3				
19.6	22.0						
20.4	21.1						
30.8	14.9						
32.8	12.3						

Source: Ref. 32, Table A.1.

Table 74. Sample burnup at the end of each cycle for Calvert Cliffs samples

Cycle #	Duration (days)	Downtime (days)	Sample cumulative burnup (GWd/MTU)									
			MKP109-LL	MKP109-CC	MKP109-P	MLA098-JJ	MLA098-BB	MLA098-P	NBD107-MM	NBD107-GG	NBD107-Q	
1	730	81								14.59	17.32	21.59
2	306	71	6.33	8.59	10.26	6.16	8.77	10.93	20.31	24.10	30.05	
3	382	81	14.20	19.27	23.01	12.36	17.61	21.94	25.29	30.02	37.42	
4	466	85	21.13	28.68	34.26	18.68	26.62	33.17	31.40	37.27	46.46	
5	461		27.35	37.12	44.34							

Table 75. Decay time data for Calvert Cliffs samples

Assembly ID	Sample ID	Decay time (days)	
D047	MKP109-LL	1870 ^a	4171 ^b
	MKP109-CC	1870 ^a	4656 ^b
	MKP109-P	1870 ^a	4656 ^b
D101	MLA098-JJ	2374	
	MLA098-BB	2374	
	MLA098-P	2374	
BT03	NBD107-MM	2447	
	NBD107-GG	2447	5658 ^c
	NBD107-Q	2447	

^aValues correspond to PNL measurement dates (Ref. 34).

^bValues for lanthanides except for neodymium isotopes correspond to KRI measurement dates (Ref. 38). See also Sect. 7.5.

^cValues for ¹⁰³Rh and lanthanides except for neodymium isotopes correspond to KRI measurement dates (Ref. 38). See also Sect. 7.5.

8.6 TAKAHAMA UNIT 3

Radiochemical analyses were performed at JAERI on 16 samples from three fuel rods identified as SF95, SF96, and SF97.⁴¹ Rods SF95 and SF97 were standard fuel rods with 4.11 wt % ²³⁵U initial enrichment; whereas SF96 was a fuel rod with gadolinia poison that had a fuel initial enrichment of 2.6 wt % ²³⁵U and a Gd₂O₃ content of 6%. Rods SF95 and SF96 were from assembly NT3G23 and rod SF97 was from assembly NT3G24. Each of these two assemblies had a 17 × 17 configuration, with 264 fuel rods (16 of these containing gadolinia)⁴² and 25 water-filled guide tubes. They resided in the reactor core for two (assembly NT3G23) or three (assembly NT3G24) consecutive cycles, starting from cycle 5. The configuration of the assembly, including the location of the measured rods, is illustrated in Fig. 15.

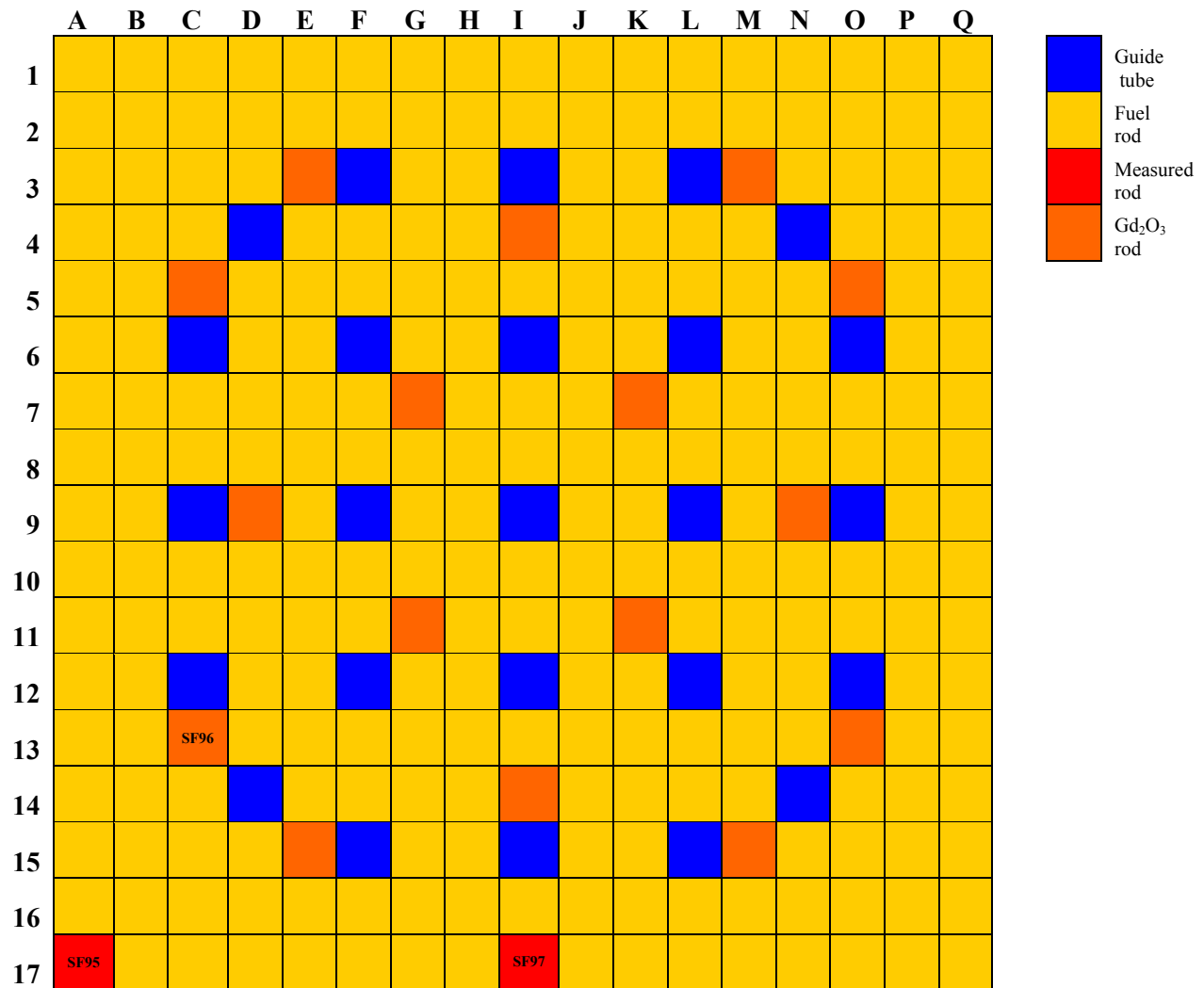


Fig. 15. Assembly layout for Takahama-3 spent fuel samples.

Assembly design data are listed in Table 76. Burnup values, sample axial location along the fuel rod, moderator density and temperature, and cycle power for each sample are shown in Table 77. Operation

history data and soluble boron concentration are presented in Table 78 and Table 79, respectively. The temperature of the moderator at the sample axial location with respect to the bottom of the active fuel region was calculated using Eq. (1) described in Section 5.2. The moderator density was determined by using temperature vs. pressure tabulated data⁵⁸ corresponding to operating pressure value⁵⁷ of 157 kg/cm². The cycle power for each sample as shown in Table 77 was obtained by averaging the power data given in Ref. 41. As the actual sample burnup was calculated to correspond to the measured ¹⁴⁸Nd content in each sample, the power used in the calculation was obtained by dividing the power data in Table 77 by the ratio of the reported burnup and actual burnup for each sample, as shown in Table 80.

Table 76. Assembly design data for Takahama-3 spent fuel samples

Parameter	Data
Assembly and reactor data	
Lattice geometry	17 × 17
Operating pressure, ^a kg/cm ²	157
Rod pitch, ^b cm	1.26
Number of fuel rods	264
Number of guide tubes	25
Assembly pitch, cm	21.4
Fuel rod data	
Fuel material type	UO ₂
Fuel pellet density (% TD)	95
Enrichment, wt % ²³⁵ U	4.11 (2.63)
Fuel pellet diameter, cm	0.805
Active fuel rod length, cm	366
Sample location, cm	See Table 77
Average fuel temperature, ^c K	900
Clad material	Zircaloy-4
Clad inner diameter, cm	0.822
Clad outer diameter, cm	0.95
Average clad temperature, ^c K	600
Number of rods with Gd ₂ O ₃	16
Gd ₂ O ₃ content, wt %	6.0
U isotopic composition, ^d wt %	
²³⁴ U	0.04 (0.02) ^e
²³⁵ U	4.11 (2.63)
²³⁸ U	95.85 (97.35)
Moderator data	
Density, g/cm ³	See Table 77
Temperature, K	See Table 77
Soluble boron, ppm	See Table 79
Inlet temperature, K	557
Outlet temperature, K	594
Guide tube data ^f	
Guide tube material	Zircaloy-4
Inner radius, cm	0.5715
Outer radius, cm	0.6121

^aRef. 57. ^bGiven as an approximate value in Ref. 43. ^cValues were assumed in Ref. 42.

^dAt beginning of life. Values in parentheses correspond to gadolinia-bearing fuel rods.

^eValues assumed in Ref. 90.

^fGuide tube data unavailable. Dimensions for a Westinghouse 17 × 17 assembly were assumed, similarly to Ref. 90.

Source: Ref. 41 unless otherwise noted.

Table 77. Burnup, power, sample location, and moderator data for Takahama-3 samples

Assembly	Rod ID	Sample ID	Burnup ^a (GWd/MTU)	Power ^b cycle 5 (MW/MTU)	Power ^b cycle 6 (MW/MTU)	Power ^b cycle 7 (MW/MTU)	Sample ^{a,c} location (cm)	Moderator ^d temperature (K)	Moderator density ^e (g/cm ³)
NT323G	SF95	SF95-1	14.30	19.21	17.17		360.6	594.13	0.6776
		SF95-2	24.35	32.72	29.25		344.6	593.84	0.6784
		SF95-3	35.42	47.59	42.54		292.6	590.60	0.6867
		SF95-4	36.69	49.30	44.06		164.6	572.74	0.7267
		SF95-5	30.40	40.85	36.51		24.6	557.56	0.7566
	SF96	SF96-1	7.79	8.01	11.72		363.1	594.14	0.6775
		SF96-2	16.44	16.90	24.71		347.1	593.91	0.6782
		SF96-3	28.20	28.99	42.40		295.1	590.83	0.6861
		SF96-4	28.91	29.71	43.46		167.1	573.13	0.7267
		SF96-5	24.19	24.87	36.37		27.1	557.65	0.7564
NT324G	SF97	SF97-1	17.69	14.76	15.74	13.97	366.4	594.15	0.6775
		SF97-2	30.73	25.65	27.36	24.28	345.7	593.87	0.6783
		SF97-3	42.16	35.19	37.53	33.31	318.0	592.60	0.6817
		SF97-4	47.03	39.26	41.87	37.16	196.8	577.84	0.7160
		SF97-5	47.25	39.44	42.06	37.33	88.1	562.19	0.7481
		SF97-6	40.79	34.05	36.31	32.23	25.1	557.58	0.7566

^aAs given in Ref. 41.

^bCycle-averaged power calculated based on data provided in Ref. 41. Cycle-averaged values were used because the time dependent specific power values were very similar.

^cDistance measured from bottom of fuel.

^dCalculated based on sample location, moderator inlet and outlet temperatures, and operating pressure, as expressed by Eq. (1) in Sect. 5.2.

^eCalculated by linear interpolation in temperature vs. pressure tabulated data. Note that use of spreadsheets for processing input parameters and unit conversions for input specifications lead to some roundoff error in last significant digit.

Table 78. Operation history data for Takahama-3 spent fuel samples

Cycle No.	Start date	End date	Duration (days)	Down (days)
5	1990/01/26	1991/02/15	385	88
6	1991/05/14	1992/06/19	402	62
7	1992/08/20	1993/09/30	406	

Source: Ref. 41.

Table 79. Soluble boron concentration in moderator for Takahama-3 spent fuel samples

Cycle No.	Cumulative time ^a (days)	Boron content (ppm)
	0	1154
5	106	894
	205	651
	306	404
	385	210
	473	1132
6	592	864
	704	613
	817	358
	875	228
	937	1154
7	996	1001
	1048	867
	1100	732
	1152	598
	1204	463
	1256	329
	1308	195
	1342	104

^aMeasured from beginning of cycle 5.

Source: Ref. 43.

Table 80. Sample burnup for Takahama-3 spent fuel samples

Sample ID	Reported ^a sample burnup (GWd/MTU)	Actual ^b sample burnup (GWd/MTU)
SF95-1	14.30	14.18
SF95-2	24.35	24.46
SF95-3	35.42	35.68
SF95-4	36.69	37.01
SF95-5	30.40	30.45
SF96-1	7.79	8.63
SF96-2	16.44	17.43
SF96-3	28.20	29.69
SF96-4	28.91	30.41
SF96-5	24.19	25.42
SF97-1	17.69	17.39
SF97-2	30.73	30.48
SF97-3	42.16	42.10
SF97-4	47.03	47.07
SF97-5	47.25	47.26
SF97-6	40.79	40.85

^aAs given in Ref. 41.

^bCalculated to correspond to the measured ¹⁴⁸Nd.

8.7 TMI UNIT 1

The samples considered were selected from two different fuel assemblies, identified as NJ05YU and NJ070G, irradiated in the TMI-1 reactor. Details related to the geometry, material composition, and irradiation history were taken from Refs. 46 and 47. Both assemblies are a 15 × 15 design, with 208 fuel rods, 16 guide tubes, and one instrument tube, as illustrated in Fig. 16 and Fig. 17.

The fuel assembly geometry and material information for the two assemblies are presented in Table 81. Assembly NJ05YU was irradiated in the reactor for two consecutive cycles, cycle 9 and cycle 10. It contained 16 burnable poison rods with Al₂O₃-B₄C absorber, which were removed at the end of cycle 9. All the fuel rods in this assembly had an initial fuel enrichment of 4.013 wt % ²³⁵U. Assembly NJ070G was present in the reactor during cycles 10 and 11. At the end of cycle 10, some of the fuel rods, were removed and replaced with stainless steel rods. However, this rod replacement is of no consequence to the analysis in this report, as the fuel rods that were measured were present in the assembly during cycle 10 only. Assembly NJ070G contained 16 BPRs during cycle 10. Four of its fuel rods had 2.0 wt % Gd₂O₃ poison, and their initial fuel enrichment was 4.19 wt % ²³⁵U. The other 204 regular fuel rods in assembly NJ070G had an initial enrichment of 4.657 wt % ²³⁵U. Guide and instrument tube data and the locations of the Gd₂O₃ poison rods in the assembly were used as given in Ref. 46.

Eleven of the 19 TMI-1 samples, those measured at ANL, were selected from a fuel rod identified as H6, located in assembly NJ05YU. The other eight TMI-1 samples, analyzed at GE-VNC, were selected from the rods identified as O1, O12, and O13, located in assembly NJ070G. The location of the measured fuel rods in the assembly is illustrated in Fig. 16 and Fig. 17. Note that all three measured fuel rods from assembly NJ070G were located at the edge of the assembly; the rod identified as O1 was located at the corner of the assembly. As noted in Section 7.7, the measured fuel rods experienced crud-induced localized corrosion.

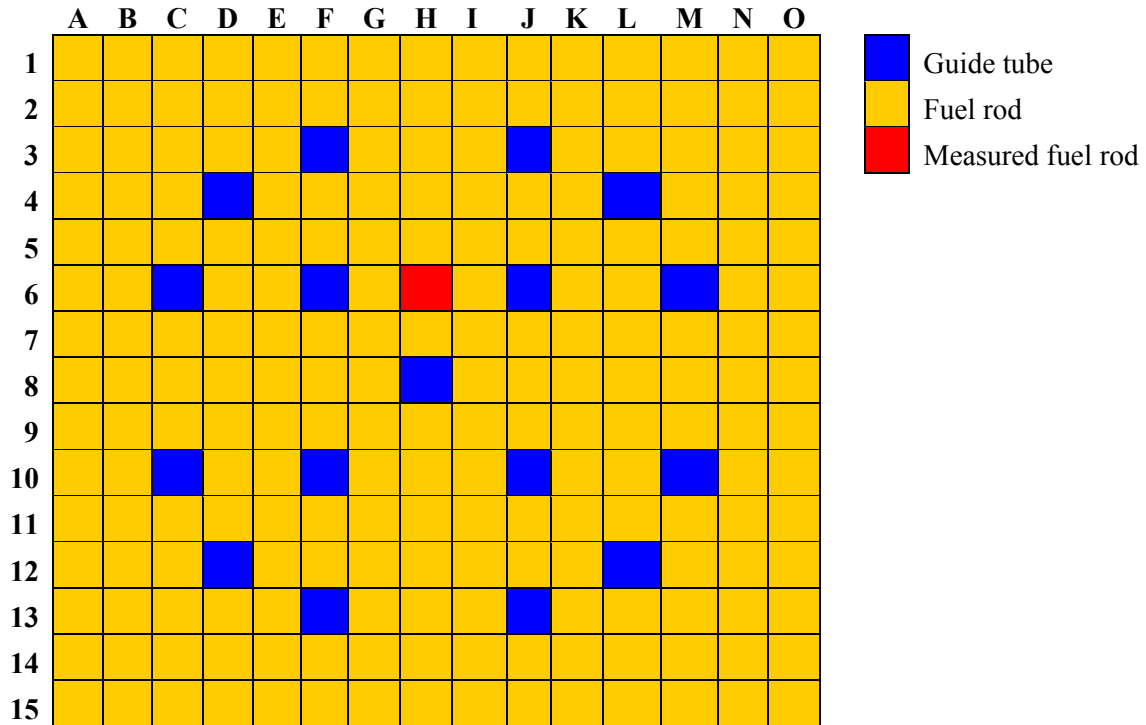


Fig. 16. Assembly layout for TMI-1 samples—NJ05YU.

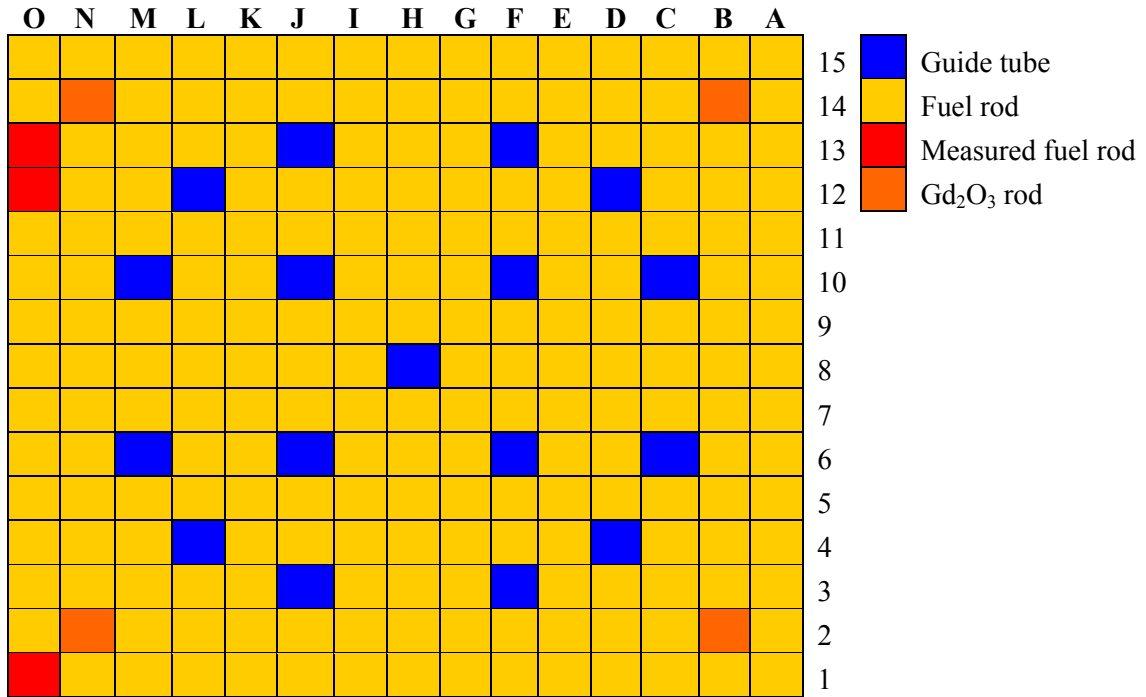


Fig. 17. Assembly layout for TMI-1 samples—NJ070G. (Note: The characteristics of the assemblies adjoining the measured fuel rods are provided in Fig. 18 and Table 89.)

Table 81. Assembly design data for TMI-1 samples

Parameter	Data for assembly NJ05YU	Data for assembly NJ070G
Assembly and reactor data		
Reactor	TMI-1	TMI-1
Design	B&W PWR	B&W PWR
Lattice geometry	15 × 15	15 × 15
Rod pitch, cm	1.44272	1.44272
Number of fuel rods	208	208
Number of guide tubes	16	16
Number of instrument tubes	1	1
Assembly pitch, cm	21.81098	21.81098
Fuel rod data		
Fuel material type	UO ₂	UO ₂
Fuel pellet density, g/cm ³	10.196	10.217
Fuel pellet diameter, cm	0.9362	0.9398
Fuel temperature, K	See Table 84	See Table 87
Enrichment, wt % ²³⁵ U	4.013	4.657
Clad material	Zircaloy-4	Zircaloy-4
Clad inner diameter, cm	0.95758	0.95758
Clad outer diameter, cm	1.0922	1.0922
Clad temperature, ^a K	619	619
Number of rods with Gd ₂ O ₃	0	4
Gd ₂ O ₃ content, wt %	NA	2.0
Initial fuel composition, wt %		
²³⁴ U	0.040	0.045 (0.0) ^b
²³⁵ U	4.013	4.657 (4.19) ^b
²³⁸ U	95.947	95.298 (95.981) ^b
Moderator data		
Moderator density at sample location, g/cm ³	See Table 82 and Table 85	See Table 82 and Table 88
Soluble boron in moderator, ppm	See Table 84	See Table 87
Burnable poison rod (BPR) data		
Absorber diameter, cm	0.8636	0.8636
Clad inner diameter, cm	0.9144	0.9144
Clad outer diameter, cm	1.0922	1.0922
Absorber material	Al ₂ O ₃ -B ₄ C	Al ₂ O ₃ -B ₄ C
Absorber material density, g/cm ³	3.7	3.7
B ₄ C content, wt %	1.7	2.1
Cladding material	Zircaloy-4	Zircaloy-4
Guide/instrument tube data ^c		
Guide/instrument tube material	Zircaloy-4	Zircaloy-4
Guide tube inner diameter, cm	1.26492	1.26492
Guide tube outer diameter, cm	1.3462	1.3462
Instrument tube inner diameter, cm	1.12014	1.12014
Instrument tube outer diameter, cm	1.25222	1.25222

Two sets of burnup values were specified in Ref. 47 for each sample: cumulative burnup based on operational data at 20 and 10 statepoints for the samples from assembly NJ05YU and for the samples from assembly NJ070G, respectively, which include the end of cycle (EOC) for cycles 9 and 10, and the total measured burnup determined from radiochemical isotopic measurements corresponding to EOC-10. The effective full power days (EFPD) for cycle 9 and 10 are 639.4 days and 660.3 days, respectively. The down time between cycles 9 and 10 was 35 days (Ref. 46). The sample EOC burnup values from reactor operational data and the reported measured sample burnup values are presented in Table 82. The sample burnup values at the various statepoints are provided in Table 83 and Table 86 for the samples from assemblies NJ05YU and for the samples from assemblies NJ070G, respectively. Sample specific average power for each irradiation interval, P_i , was determined as follows:

$$P_i = \frac{(B_i - B_{i-1})}{(t_i - t_{i-1})} \times \frac{B_{meas}}{B_{10}}, \quad i=1, \dots, 20 \text{ for NJ05YU samples and } i=1, \dots, 10 \text{ for NJ070G samples,} \quad (18)$$

where B_i and B_{i-1} are the sample burnup values for the two consecutive statepoints defining the irradiation interval i , B_{meas} and B_{10} are the sample measured burnup and the sample burnup based on operational data at EOC-10, respectively, and $t_i - t_{i-1}$ is the time interval between the two consecutive statepoints.

Moderator density values obtained at the sample axial position and at the beginning of cycle (BOC) 9 for the samples in assembly NJ05YU and at BOC 10 for the samples from assembly NJ070G are tabulated in Table 82. Moderator density variation with time for the samples from assemblies NJ05YU and NJ070G are shown in Table 85 and Table 88, respectively. The values in those two tables are multiplication factors to be applied to the moderator density values tabulated in Table 82 in order to obtain the moderator density averaged over a time interval between two consecutive statepoints.

The variations with time of the soluble boron concentration in moderator and of the fuel temperature for assemblies NJ05YU and NJ070G are shown in Table 84 and Table 87, respectively.

Data available⁴⁶ on the assemblies surrounding assembly NJ070G are illustrated in Fig. 18 and presented in Table 89. As the samples from this assembly are expected to be subjected to edge effects given their location at the periphery of the assembly, this information may be important for modeling purposes. The measured fuel rods were located at the west edge of assembly NJ070G that neighbored an assembly from batch 12A with an initial fuel enrichment of 4 wt % ²³⁵U. Assemblies in batch 12 were first irradiated in the core during cycle 10. Assemblies in batch 11 were present in the core since cycle 9.

Table 82. Burnup and starting moderator density data for TMI-1 samples

Assembly ID	Rod ID	Sample ID	Burnup ^a EOC-9 (GWd/MTU)	Burnup ^a EOC-10 (GWd/MTU)	Measured ^b burnup (GWd/MTU)	Moderator density ^c (g/cm ³)		
NJ05YU	H6	A2	28.338	51.861	50.6	0.7314		
		B2	28.444	52.089	50.1	0.7248		
		C1	28.132	51.545	50.2	0.6965		
		C3	28.230	51.696	51.3	0.7151		
		D2	26.366	48.569	44.8	0.6787		
		A1B	24.767	45.687	44.8	0.7382		
		B1B	28.230	51.696	54.5	0.7151		
		B3J	28.338	51.861	53.0	0.7314		
		C2B	28.155	51.563	52.6	0.7057		
		D1A2	28.115	51.530	55.7	0.6934		
		D1A4	28.034	50.810	50.5	0.6875		
		NJ070G	O1	O1 S1		27.498	25.8	0.7382
				O1 S2		31.377	29.9	0.7057
O12	O1 S3				30.848	26.7	0.6875	
	O12 S4				25.592	23.7	0.7382	
	O12 S5				29.271	26.5	0.7057	
	O12 S6				28.760	24.0	0.6875	
	O13 S7				25.331	22.8	0.7382	
	O13 S8				29.020	26.3	0.7057	

^aEnd of cycle (EOC) burnup values derived in Ref. 47 from the detailed fuel assembly operating history in Appendix A of Ref. 46.

^bRefs. 44 and 45.

^cModerator densities in ft³/lbm are provided in Ref. 46 at the beginning of cycle (BOC) 9 for the samples from assembly NJ05YU and at BOC 10 for the samples from assembly NJ070G. The calculations documented in Ref. 47 performed conversion to g/cm³ units.

Source: Ref. 47 unless otherwise noted.

Table 83. Burnup as a function of time for TMI-1 samples from assembly NJ05YU

Cycle No.	Sample ID Time (days)	A2	B2	C1	C3	D2	A1B	B1B	B3J	C2B	D1A2	D1A4
		Burnup (GWd/MTU)										
	0.0											
9	74.2	3.184	3.456	3.543	3.551	2.839	2.450	3.551	3.184	3.588	3.476	3.365
	141.1	6.269	6.701	6.805	6.819	5.639	4.907	6.819	6.269	6.866	6.709	6.540
	214.0	9.446	9.953	10.004	10.045	8.474	7.521	10.045	9.446	10.077	9.892	9.687
	283.9	12.660	13.178	13.142	13.213	11.359	10.245	13.213	12.660	13.218	13.030	12.813
	349.7	15.690	16.158	16.021	16.119	14.123	12.900	16.119	15.690	16.092	15.922	15.715
	425.0	19.139	19.505	19.237	19.370	17.275	16.023	19.370	19.139	19.305	19.155	18.971
	483.9	21.785	22.055	21.703	21.854	19.756	18.484	21.854	21.785	21.764	21.639	21.483
	549.2	24.662	24.819	24.376	24.550	22.490	21.227	24.550	24.662	24.433	24.331	24.208
	608.0	27.148	27.240	26.788	26.966	24.933	23.628	26.966	27.148	26.846	26.750	26.645
	639.4	28.338	28.444	28.132	28.230	26.366	24.767	28.230	28.338	28.155	28.115	28.034
	0.0											
10	68.0	30.741	31.040	30.743	30.883	28.260	26.617	30.883	30.741	30.817	30.667	29.947
	131.8	32.991	33.423	33.131	33.294	30.302	28.445	33.294	32.991	33.232	33.022	32.156
	209.0	35.730	36.253	35.944	36.121	32.841	30.742	36.121	35.730	36.053	35.820	34.852
	272.1	37.994	38.541	38.205	38.384	34.970	32.698	38.384	37.994	38.309	38.084	37.080
	347.4	40.714	41.249	40.867	41.047	37.561	35.112	41.047	40.714	40.958	40.759	39.756
	416.4	43.209	43.701	43.276	43.451	39.971	37.386	43.451	43.209	43.350	43.186	42.215
	486.4	45.728	46.153	45.689	45.856	42.435	39.740	45.856	45.728	45.744	45.621	44.706
	556.3	48.220	48.568	48.065	48.227	44.900	42.123	48.227	48.220	48.104	48.020	47.174
	626.1	50.674	50.941	50.407	50.563	47.363	44.515	50.563	50.674	50.432	50.383	49.620
	660.3	51.861	52.089	51.545	51.696	48.569	45.687	51.696	51.861	51.563	51.530	50.810

Source: Ref. 47.

Table 84. Fuel temperature and concentration of soluble boron in moderator for TMI-1 samples from assembly NJ05YU

Cycle No.	Sample ID Time (days)	A2	B2	C1	C3	D2	A1B	B1B	B3J	C2B	D1A2	D1A4	Boron (ppm)
		Temperature ^a (K)											
9	0.0												1670
	74.2	1051.15	1085.37	1105.65	1098.34	1029.01	948.65	1098.34	1051.15	1106.12	1100.73	1091.18	1481
	141.1	1040.93	1058.79	1069.12	1062.90	1025.21	957.48	1062.90	1040.39	1066.84	1068.40	1065.04	1342
	214.0	1023.32	1030.34	1034.43	1029.37	1009.34	959.34	1029.37	1023.32	1031.18	1035.79	1035.82	1175
	283.9	1002.04	1001.96	1003.15	998.18	995.65	953.48	998.18	1002.04	998.93	1006.15	1008.98	990
	349.7	982.09	976.62	976.01	971.18	982.57	947.65	971.18	982.09	971.23	980.18	985.07	772
	425.0	959.40	950.04	948.93	944.23	963.71	940.48	944.23	959.40	944.23	963.43	959.34	545
	483.9	936.51	925.90	925.46	920.59	945.73	927.57	920.59	936.51	920.98	929.87	936.23	352
	549.2	918.46	907.79	907.79	903.40	929.26	913.93	903.40	918.46	904.04	911.73	917.79	134
	608.0	888.21	884.01	900.23	889.62	924.34	886.48	889.62	888.21	895.07	904.15	909.82	13
639.4	772.90	777.37	810.43	790.98	837.01	771.65	790.98	772.90	801.65	815.26	821.01	2	
10	0.0												1800
	68.0	835.54	861.01	871.01	871.32	825.07	787.87	871.32	835.54	874.84	865.43	843.34	1649
	131.8	828.59	846.96	856.62	853.46	825.54	785.79	853.46	828.59	856.84	854.23	840.48	1521
	209.0	824.51	835.65	844.68	838.76	829.98	786.23	838.76	824.51	841.84	845.32	840.87	1322
	272.1	823.76	828.87	835.79	829.29	831.73	791.43	829.29	823.76	831.71	838.01	838.93	1140
	347.4	822.12	823.12	828.46	822.09	832.12	796.54	822.09	822.12	823.98	831.46	836.07	918
	416.4	818.71	816.71	821.65	815.18	831.46	799.84	815.18	818.71	816.96	825.09	832.48	718
	486.4	813.82	809.93	815.29	808.54	829.93	801.23	808.54	813.82	810.51	818.96	828.43	506
	556.3	807.62	802.59	808.43	801.59	827.37	800.98	801.59	807.62	803.76	812.15	823.34	298
	626.1	801.96	796.93	802.65	796.15	823.76	799.18	796.15	801.96	798.34	806.21	817.73	103
660.3	799.90	795.18	799.87	794.37	819.26	797.96	794.37	799.90	796.26	803.01	813.51	1.8	

^aFuel temperature values averaged over the time intervals between two consecutive statepoints.

Source: Ref. 46.

Table 85. Moderator density multiplication factors for TMI-1 samples from assembly NJ05YU

Cycle No.	Sample ID Time (days)	A2	B2	C1	C3	D2	A1B	B1B	B3J	C2B	D1A2	D1A4	Moderator density multiplication factor ^a
9	0.0												
	74.2	1.0000	0.9995	1.0000	1.0000	1.0000	1.0000	1.0000	1.0000	1.0000	1.0000	1.0000	1.0000
	141.1	1.0000	0.9995	1.0000	1.0000	1.0000	1.0000	1.0000	1.0000	1.0000	0.9957	1.0000	1.0000
	214.0	0.9955	0.9995	1.0000	0.9956	1.0000	1.0000	0.9956	0.9955	1.0000	0.9957	1.0000	1.0000
	283.9	0.9955	0.9995	1.0000	0.9956	1.0000	1.0000	0.9956	0.9955	1.0000	0.9957	1.0000	1.0000
	349.7	0.9955	0.9995	1.0000	0.9956	1.0000	1.0000	0.9956	0.9955	1.0000	1.0000	1.0000	1.0000
	425.0	0.9955	0.9995	1.0000	0.9956	1.0000	1.0000	0.9956	0.9955	1.0000	1.0000	1.0000	1.0000
	483.9	0.9955	0.9995	1.0000	0.9956	1.0043	1.0000	0.9956	0.9955	1.0000	1.0000	1.0000	1.0043
	549.2	0.9955	0.9995	1.0044	1.0000	1.0043	1.0000	1.0000	0.9955	1.0000	1.0000	1.0000	1.0043
	608.0	1.0046	1.0045	1.0132	1.0090	1.0172	1.0046	1.0090	1.0046	1.0134	1.0132	1.0130	1.0130
639.4	0.9910	0.9995	1.0222	1.0045	1.0351	0.9864	1.0045	0.9910	1.0134	1.0221	1.0310	1.0310	
10	0.0												
	68.0	1.0000	1.0000	1.0088	1.0045	1.0172	1.0000	1.0045	1.0000	1.0089	1.0087	1.0087	1.0087
	131.8	1.0000	1.0000	1.0132	1.0045	1.0172	1.0000	1.0045	1.0000	1.0089	1.0132	1.0087	1.0087
	209.0	1.0000	1.0000	1.0132	1.0045	1.0172	1.0000	1.0045	1.0000	1.0089	1.0132	1.0087	1.0087
	272.1	1.0000	1.0000	1.0132	1.0045	1.0172	1.0000	1.0045	1.0000	1.0089	1.0132	1.0087	1.0087
	347.4	1.0000	1.0000	1.0132	1.0045	1.0172	1.0000	1.0045	1.0000	1.0089	1.0132	1.0087	1.0087
	416.4	1.0000	1.0000	1.0132	1.0045	1.0172	1.0000	1.0045	1.0000	1.0089	1.0132	1.0130	1.0130
	486.4	1.0000	1.0000	1.0132	1.0045	1.0172	1.0000	1.0045	1.0000	1.0089	1.0132	1.0130	1.0130
	556.3	1.0000	1.0000	1.0132	1.0045	1.0126	1.0000	1.0045	1.0000	1.0089	1.0132	1.0130	1.0130
	626.1	1.0000	1.0000	1.0132	1.0045	1.0126	1.0000	1.0045	1.0000	1.0089	1.0132	1.0130	1.0130
660.3	1.0000	1.0000	1.0132	1.0045	1.0126	1.0000	1.0045	1.0000	1.0089	1.0132	1.0130	1.0130	

^aAverage values for time intervals between two consecutive statepoints. The sample average moderator density for the time interval between two consecutive statepoints is the product of sample moderator density provided in Table 82 and the sample moderator density multiplication factor for that time interval.

Source: Ref. 47.

Table 86. Burnup as a function of time for TMI-1 samples from assembly NJ070G

Cycle No.	Sample ID Time (days)	O1S1	O1S2	O1S3	O12S4	O12S5	O12S6	O13S7	O13S8
		Burnup (GWd/MTU)							
10	68.0	2.488	3.676	3.312	2.384	3.532	3.184	2.323	3.455
	131.8	4.955	7.107	6.485	4.693	6.718	6.143	4.586	6.604
	209.0	8.108	11.106	10.328	7.583	10.368	9.659	7.443	10.234
	272.1	10.769	14.205	13.397	10.004	13.201	12.462	9.849	13.053
	347.4	13.976	17.742	16.954	12.937	16.453	15.729	12.764	16.288
	416.4	16.936	20.865	20.127	15.663	19.350	18.666	15.472	19.164
	486.4	19.951	23.950	23.274	18.468	22.234	21.603	18.257	22.028
	556.3	22.982	26.970	26.355	21.311	25.081	24.499	21.079	24.856
	626.1	26.015	29.938	29.382	24.179	27.898	27.365	23.927	27.655
	660.3	27.498	31.377	30.848	25.592	29.271	28.760	25.331	29.020

Source: Ref. 47.

Table 87. Fuel temperature and concentration of soluble boron in moderator for TMI-1 samples from assembly NJ070G

Cycle No.	Sample ID Time (days)	O1S1	O1S2	O1S3	O12S4	O12S5	O12S6	O13S7	O13S8	Boron (ppm)
		Temperature (K)								
10	0.0									1800
	68.0	960.29	1119.51	1083.65	960.29	1119.51	1083.65	960.29	1119.51	1649
	131.8	960.71	1084.79	1067.32	960.71	1084.79	1067.32	960.71	1084.79	1521
	209.0	958.68	1043.23	1043.46	958.68	1043.23	1043.46	958.68	1043.23	1322
	272.1	954.18	1007.09	1016.43	954.18	1007.09	1016.43	954.18	1007.09	1140
	347.4	946.12	978.57	991.65	946.12	978.57	991.65	946.12	978.57	918
	416.4	937.15	951.57	967.21	937.15	951.57	967.21	937.15	951.57	718
	486.4	926.04	929.82	945.98	926.04	929.82	945.98	926.04	929.82	506
	556.3	914.37	912.15	928.04	914.37	912.15	928.04	914.37	912.15	298
	626.1	904.09	896.84	912.12	904.09	896.84	912.12	904.09	896.84	103
660.3	897.82	886.54	899.73	897.82	886.54	899.73	897.82	886.54	1.8	

Source: Ref. 46, Appendix A.

Table 88. Moderator density multiplication factors for TMI-1 samples from assembly NJ070G

Cycle No.	Sample ID Time (days)	O1S1	O1S2	O1S3	O12S4	O12S5	O12S6	O13S7	O13S8
		Moderator density multiplication factor ^a							
10	0.0								
	68.0	1.0000	0.9956	0.9957	1.0000	0.9956	0.9957	1.0000	0.9956
	131.8	1.0000	0.9956	0.9957	1.0000	0.9956	0.9957	1.0000	0.9956
	209.0	1.0000	0.9956	1.0000	1.0000	0.9956	1.0000	1.0000	0.9956
	272.1	1.0000	1.0000	1.0000	1.0000	1.0000	1.0000	1.0000	1.0000
	347.4	1.0000	1.0000	1.0000	1.0000	1.0000	1.0000	1.0000	1.0000
	416.4	1.0000	1.0000	1.0000	1.0000	1.0000	1.0000	1.0000	1.0000
	486.4	1.0000	1.0000	1.0000	1.0000	1.0000	1.0000	1.0000	1.0000
	556.3	1.0000	1.0000	1.0000	1.0000	1.0000	1.0000	1.0000	1.0000
	626.1	1.0000	1.0000	1.0043	1.0000	1.0000	1.0043	1.0000	1.0000
660.3	1.0000	1.0000	1.0043	1.0000	1.0000	1.0043	1.0000	1.0000	

^aAverage values for time intervals between two consecutive statepoints. The sample average moderator density for the time interval between two consecutive statepoints is the product of sample moderator density provided in Table 82 and the sample moderator density multiplication factor for that time interval.

Source: Ref. 47.

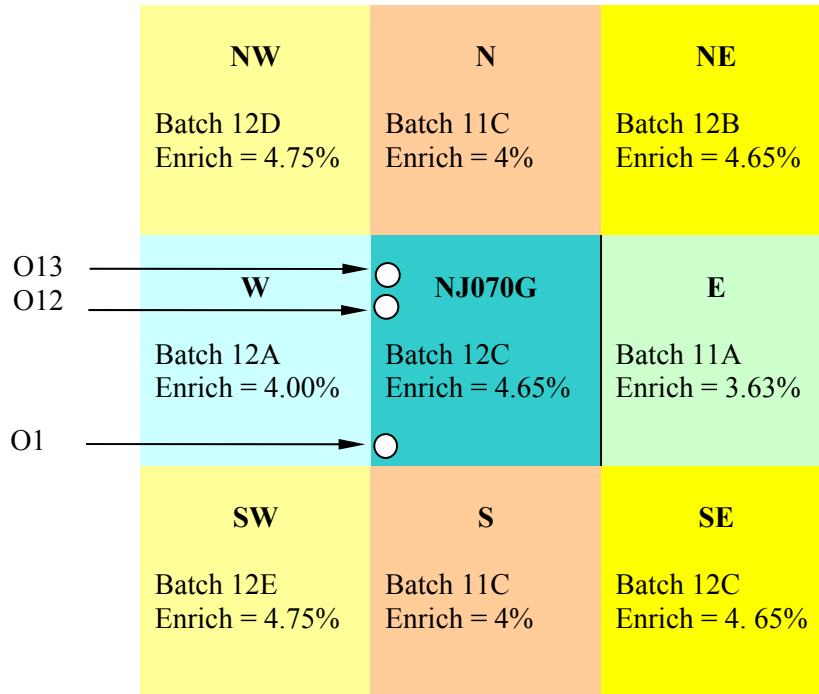


Fig. 18. Assemblies surrounding assembly NJ070G. (Source: Ref. 46, Figures 3-11, A-2, and A-4.)

Table 89. Modeling data for the assemblies adjoining the SW corner of assembly NJ070G

Cycle No.	Fresh fuel batch	wt % ²³⁵ U	Fuel pellet diameter ^a (cm)	BU ^b (GWd/MTU)	Average power ^c (MW/MTU)	Average temperature ^b (K)	BPRA ^d wt % B ₄ C
9	11C ^e	4.0	0.936244	19.352 ^f	30.266 ^f	874 ^f	0.8
				22.522 ^g	35.224 ^g	938 ^g	0.8
				22.042 ^h	34.473 ^h	936 ^h	0.8
10	12A ⁱ	4.00	0.936244	–	–	–	–
	12E ^j	4.75	0.939800	–	–	–	0.2

^aAll fuel rods have clad inner and outer diameters of 0.95758 and 1.0922 cm, respectively (Ref. 46, Table 2-2).

^bBurnup at the end of cycle 9 and cycle-averaged fuel temperature for the batch 11C assembly adjoining the south side of assembly NJ070G from Ref. 46, Table 4-82.

^cBurnup divided by 639.4 days, the length of cycle 9.

^dBurnable poison rod assembly (BPRA). The number of burnable poison rods per BPRA assembly is 16 (Ref. 46, p. 2-49).

^eRef. 46, Fig. 3-11, describes this assembly as being exposed to control rod group (CRG) #5 and containing no burnable poison rods during cycle 10. However, CRG #5 was withdrawn during cycle 10 (Ref. 46, Table 4-148).

^fValues for the assembly axial node corresponding to the axial location of sample O1S1.

^gValues for the assembly axial node corresponding to the axial location of sample O1S2.

^hValues for the assembly axial node corresponding to the axial location of sample O1S3.

ⁱRef. 46, Fig. 3-11, indicates that this assembly was exposed to CRG #1 and that CRG #1 had a safety function only. This assembly did not contain burnable poison rods in cycle 10.

^jThis fuel assembly had 4 gadolinia rods with 2.0 wt % Gd₂O₃ and 4.19 wt % ²³⁵U and contained burnable poison rods with 0.2 wt % B₄C. The assembly locations of the gadolinia rods for assemblies in batches 12C and 12E are identical (Ref. 83, Fig. 7-8).

Source: Ref. 46, Table 3-1 and Figs. 3-10 and 3-11, unless otherwise noted.

8.8 GÖSGEN: ARIANE PROGRAM

Three UO₂ samples were measured for the ARIANE program. The samples were identified as GU1, GU3, and GU4. Samples GU3 and GU4 were from the same fuel rod. The layout of the assembly, showing the location of the measured rod at the beginning of cycles 12 and 16 for samples GU1 and GU3 (GU4), respectively, is illustrated in Fig. 19. Assembly geometry and fuel data are presented in Table 90. Table 91 shows the operating history data for sample GU1 as provided:⁴⁸ irradiation cycle start and end dates, actual cycle duration and down days, effective full power days and down days, core load factor, concentration of soluble boron in the moderator, operator estimated sample burnup, and sample fuel temperature. The same type of information is presented in Table 92 for samples GU3 and GU4.

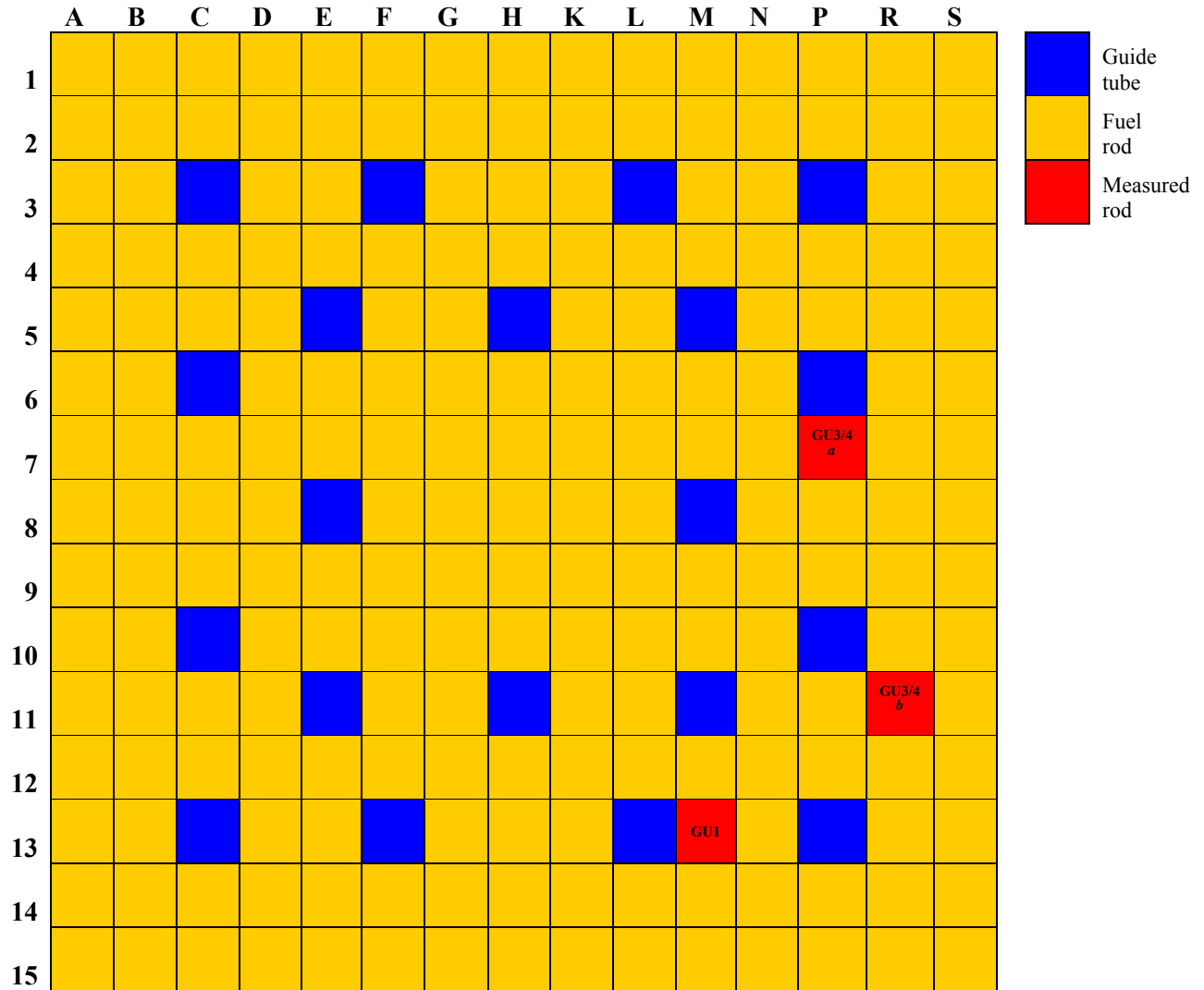
Sample GU1 was selected from a fuel rod with 3.5 wt % ²³⁵U initial enrichment of assembly 12-40, which was irradiated in the reactor for four consecutive cycles, from cycle 12 to cycle 15. The 3.3-cm sample was cut from an axial location centered at 97.7 cm from the bottom of the active region of the fuel rod. There were several changes in the fuel rod configuration of assembly 12-40 during cycles 14 and 15: in each of these cycles, three fuel rods were replaced by irradiated fuel rods from other assemblies, as specified in Ref. 48. At the start of cycle 14, three fuel rods corresponding to assembly 12-40 positions L12, M12, and N12, which were adjacent to the GU1 rod position M13 (see Fig. 19), were replaced. After cycle 14, the rods at positions N12, M14, and L14 were also replaced. The reconfiguration of the rods is potentially of consequence to the analysis because of the close proximity of the replacement rods to the measured rod, and the potential influence on the local neutronic environment of the measured sample. Further review found that the replacement rods, in general, had a burnup similar to that of the original rods for the nearest neighbors (rods located at M12 and M14) of the M13 rod. Based on diagrams provided in Ref. 48, the burnup of these above mentioned neighboring rods did not differ by more than 3–4% from the burnup of rods placed in symmetric locations, with respect to the location of the rod from which sample GU1 was cut. Because additional details were not available (e.g., location of replacement rods from the donor assemblies), reconfiguration of the rods was not simulated in the computational analysis in the current report.

Samples GU3 and GU4 were selected from different axial locations of a single fuel rod irradiated in the Gösgen reactor for three consecutive cycles: cycle 16 to cycle 18. During cycles 16 and 17, this rod belonged to assembly 16-01 with an initial fuel enrichment of 4.1 wt % ²³⁵U, whereas during last cycle 18, it was part of a different assembly identified as 17-01 with an initial fuel enrichment of 4.3 wt % ²³⁵U. The assemblies had a 15 × 15 configuration, with 205 fuel rods and 20 guide tubes. The estimated axial locations for samples GU3 and GU4 are centered at 127.42 cm and 7.42 cm, respectively, from the bottom of the active fuel region.

Four rods from assembly 16-01, including the rod from which samples were selected, were taken out of the assembly after cycle 17 and inserted into assembly 17-01. The rod from which samples GU3 and GU4 were selected at the end of cycle 18 was reconstituted in a different assembly lattice location, with respect to the layout shown in Fig. 19. The lattice location changed from P7 in assembly 16-01 to R11 in assembly 17-01. The other three replacement rods in assembly 17-01 that were transferred from assembly 16-01 into assembly 17-01 at the end of cycle 17 were located at N9, N12, and S13 in assembly 17-01. At the beginning of cycle 18, assembly 17-01 is known to have had an average burnup of about 20 GWd/MTU, whereas its burnup values at sample axial locations were 20.0 and 9.71 GWd/MTU for samples GU3 and GU4, respectively (Ref. 48, Table 3.b).

The temperature of the moderator at the sample axial location with respect to the bottom of the active fuel region was calculated using Eq. (1) provided in Sect. 5.2.

Based on the moderator temperature value for each sample, the corresponding moderator density was calculated by using tabulated temperature vs. pressure data⁵⁸ corresponding to a 154×10^5 Pa operating system pressure.



^aMeasured rod location in assembly 16-01 during cycles 16 and 17.

^bMeasured rod location in assembly 17-01 during cycle 18.

Fig. 19. Assembly layout for Gösgen (ARIANE) samples. (Source: Ref. 48, pp. 110 and 140.)

Table 90. Assembly design data for Gösgen (ARIANE) samples

Parameter	Data for GU1	Data for GU3/4
Assembly and reactor data		
Reactor	Gösgen	Gösgen
Operating pressure, Pa	150×10^5	150×10^5
Lattice geometry	15×15	15×15
Rod pitch, cm	1.43	1.43
Number of fuel rods	205	205
Number of guide tubes	20	20
Active fuel rod length, cm	340	355
Assembly pitch, cm	21.56	21.56
Fuel rod data		
Fuel material type	UO ₂	UO ₂
Fuel pellet density, g/cm ³	10.4	10.4
Fuel pellet diameter, cm	0.913	0.911
Sample axial location, ^a cm	97.7	127.42/7.42
Fuel temperature, K	See Table 91	See Table 92
U isotopic composition, wt %		
²³⁴ U	0.036	0.042
²³⁵ U	3.5	4.1
²³⁶ U ^b	0.0	0.0
²³⁸ U	96.464	95.858
Clad material	Zircaloy-4	Zircaloy-4
Clad inner diameter, cm	0.93	0.93
Clad outer diameter, cm	1.075	1.075
Average clad temperature, ^c K	619	619
Moderator data		
Inlet temperature, K	565	565
Outlet temperature, K	599	599
Moderator density, ^d g/cm ³	0.7299	0.722/0.7425
Moderator temperature, ^d K	572	575/565
Soluble boron content, ppm	See Table 91	See Table 92
Guide tube data		
Guide tube material	Zircaloy-4	Zircaloy-4
Inner diameter, cm	1.24	1.24
Outer diameter, cm	1.38	1.38

^aWith respect to the bottom of the active fuel region.

^bValue not provided; assumed value 0.

^cAssumed value; maximum clad temperature as given in Ref. 56.

^dCorresponding to sample axial location.

Source: Ref. 48.

Table 91. Operating history data for Gösgen (ARIANE) sample GU1

Cycle No.	Start date	End date	Duration (days)	Down (days)	Effective full power days	Effective ^a down days	Load factor (%)	Soluble boron in coolant (ppm)	Sample GU1	
									Nominal burnup (GWd/MTU)	Fuel temperature (K)
12	07/06/90	06/01/91	330	32	0	45	100	1511	18.649	1151.3
					6			1179		1171.5
					150			565		1136.0
					294.9			8		1078.3
					317			90.4		8
13	07/03/91	05/30/92	332	16	0	27	100	1477	33.594	919.3
					6			1145		967.7
					150			542		957.9
					292.3			7		943.1
					321.3			87.3		7
14	06/15/92	06/05/93	355	26	0	50	100	1517	47.911	888.9
					6			1178		894.4
					150			549		854.8
					290.1			5		841.4
					331.3			72.0		5
15	07/01/93	06/04/94	338	11	0	11	100	1594	59.656	806.6
					6			1243		829.8
					150			605		810.6
					301.9			5		804.0
					326.7			87.0		5

^aSum of the actual down days and the difference between the actual cycle duration and effective full-power days.
 Source: Ref. 48, p. 109.

Table 92. Operating history data for Gösgen (ARIANE) samples GU3 and GU4

Cycle No.	Start date	End date	Duration (days)	Down (days)	Effective full power days	Effective ^a down days	Load factor (%)	Soluble boron in coolant (ppm)	Sample GU3		Sample GU4	
									Nominal burnup (GWd/MTU)	Fuel temperature (K)	Nominal burnup (GWd/MTU)	Fuel Temperature (K)
16	06/29/94	06/10/95	346	25	0	34	100	1705	21.771	1203.1	11.248	731.1
					6			1347				782.0
					150			690				901.1
					320			5				1008.5
					336.8			92.0				5
17	07/05/95	06/08/96	339	22	0	32	100	1601	38.866	1052.5	21.762	744.8
					6			1247				786.9
					150			602				865.5
					299.5			9				949.8
					328.7			89.6				9
18	06/30/96	06/07/97	342	10	0	10	100	1675	52.504	944.7	29.067	687.0
					6			1300				709.1
					150			631				756.8
					301.2			17				805.6
					331.6			89.3				17

^aSum of the actual down days and the difference between the actual cycle duration and effective full-power days.

Source: Ref. 48, p. 138.

8.9 GKN II

The measured sample was selected from a fuel rod, identified as M11, in assembly 419 that was irradiated in the GKN II PWR reactor between August 1993 and August 1996. The sample was cut from an axial location on the fuel rod between 105.5 cm and 108.5 cm from the top end of the rod, which is approximately 300 cm from the bottom of the active fuel region. The estimated burnup⁵¹ based on the measured ¹³⁷Cs gamma scan data was 54.095 GWd/MTU.

The assembly had an 18 × 18 configuration, as illustrated in Fig. 20, with 300 fuel rods and 24 guide tubes. Twelve of the fuel rods contained Gd₂O₃ at 7.0 wt %. The rods with Gd₂O₃ had an initial fuel enrichment of 2.6 wt % ²³⁵U; the regular fuel rods had an enrichment of 3.8 wt % ²³⁵U. The composition of uranium in the fresh fuel was obtained from Ref. 52.

Assembly design data are listed in Table 93. The content of soluble boron in moderator as a function of the irradiation time is listed in Table 94, along with the sample cumulative burnup at the end of each cycle as reported by the utility.⁵⁰ The cycle duration and the sample cumulative burnup and average power values used in the calculations are shown in Table 95. The value for the burnup at the end of each cycle shown in Table 95 was obtained by normalizing the operator-based burnup data in Table 94 such that the sample final cumulative burnup corresponds to the reported value of 54.095 GWd/MTU based on the gamma scan (i.e., multiplying the burnup values in Table 94 by the ratio of 54.095 to 53.331, which is shown as total sample burnup in Table 94). The cycle average fuel and moderator temperatures presented in Table 96 were calculated based on a more detailed time-dependent data⁵⁰ supplied by the utility for an axial location corresponding to the measured sample. Also shown in Table 96 are the moderator density data; they were calculated based on the moderator temperature by using temperature vs. pressure tabulated data⁵⁸ corresponding to the operating system pressure of 158×10^5 Pa.

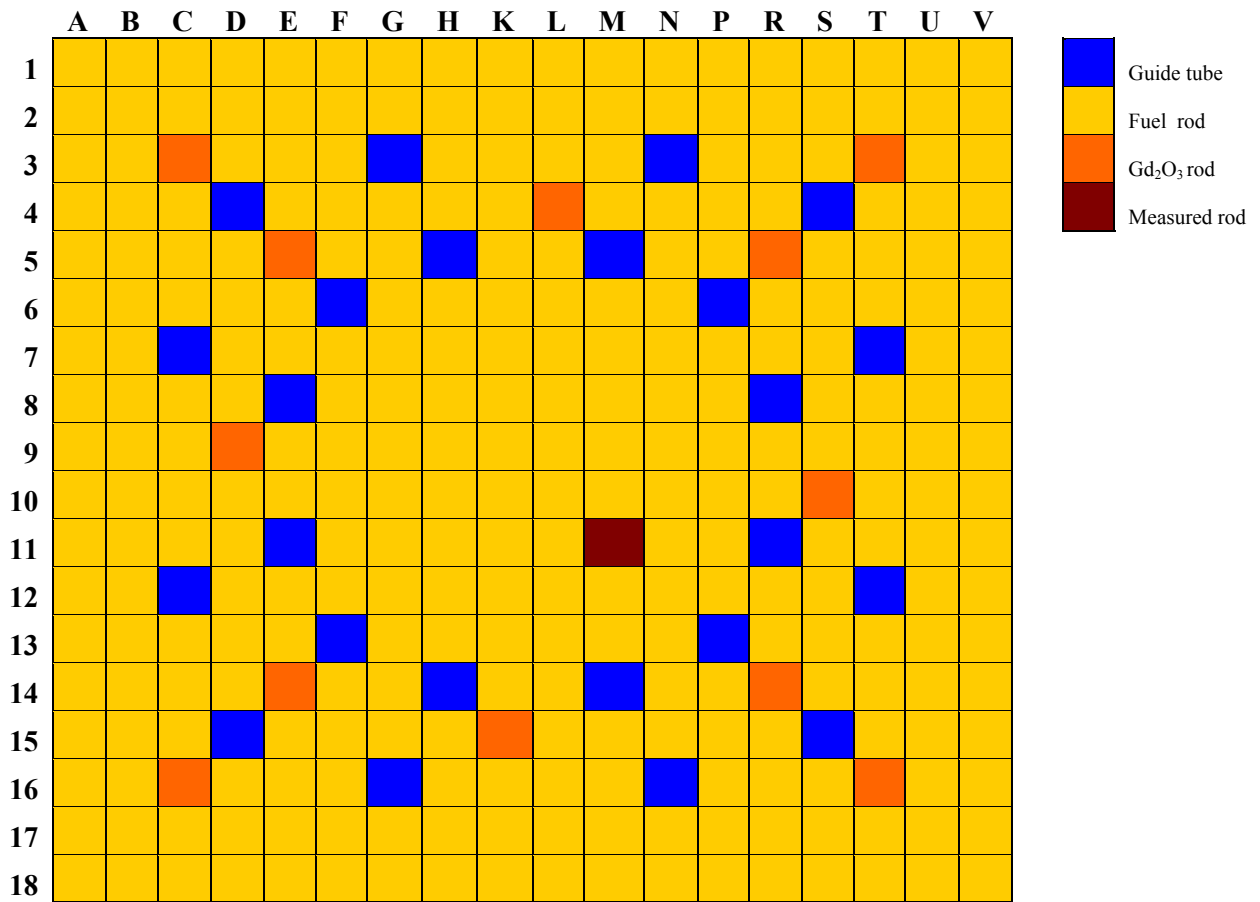


Fig. 20. Assembly layout for GKN II (REBUS) sample. (Source: Ref. 49, Sect. 1.1 and Fig. 1.1.)

Table 93. Assembly design data for GKN II (REBUS) sample

Parameter	Data
Assembly and reactor data	
Reactor	GKN II
Operating pressure, Pa	158×10^5
Lattice geometry	18×18
Rod pitch, cm	1.27
Number of fuel rods	300
Number of guide tubes	24
Active fuel rod length, ^a cm	390
Assembly pitch, cm	23.116
Fuel rod data	
Fuel material type	UO ₂
Fuel pellet density, g/cm ³	10.4
Enrichment, wt % ²³⁵ U	3.8 (2.6) ^c
Sample location, ^b cm	303
Fuel pellet diameter, cm	0.805
Fuel temperature, K	See Table 96
Clad material	Zircaloy-4
Clad inner diameter, cm	0.822
Clad outer diameter, cm	0.95
Average clad temperature, ^d K	619
Number of rods with Gd ₂ O ₃	12
Density of fuel in Gd ₂ O ₃ , g/cm ³	10.4
Gd ₂ O ₃ content, wt %	7.0
U isotopic composition, ^e wt %	
²³⁴ U	0.036 (0.0) ^c
²³⁵ U	3.798 (2.6) ^c
²³⁶ U	0.0 (0.0) ^c
²³⁸ U	96.166 (97.4) ^c
Moderator data	
Moderator temperature, K	See Table 96
Moderator density, g/cm ³	See Table 96
Soluble boron content, ppm	See Table 94
Guide tube data	
Guide tube material ^f	Zircaloy-4
Inner diameter, cm	1.110
Outer diameter, cm	1.232

^aRef. 51.^bRelative to the bottom of the active fuel region; corresponding to center of the segment (Ref. 53).^cValues in parentheses correspond to gadolinia-bearing fuel.^dMaximum clad temperature as given in Ref. 56.^eInitial (fresh fuel) values from Ref. 53.^fAssumed the same as clad material.

Source: Ref. 49 unless otherwise noted.

**Table 94. Operating history data for
GKN II (REBUS) sample**

Cycle	Cumulative ^a time (days)	Burn time (days)	Soluble ^b boron in moderator (ppm)	Cumulative ^a burnup (GWd/MTU)
	6.0	6.0	965.6	
	30.0	30.0	876.6	
	60.0	60.0	783.2	
	90.0	90.0	681.8	
	120.0	120.0	583.2	
5	150.0	150.0	489.4	
	180.0	180.0	400.9	
	210.0	210.0	308.3	
	240.0	240.0	206.9	
	270.0	270.0	99.4	
	295.4	295.4	10.0	
	310.0	310.0	10.0	17.196
Down	332.0			
	338.0	316.0	1175.9	
	362.0	340.0	1088.9	
	392.0	370.0	998.8	
	422.0	400.0	898.8	
	452.0	430.0	800.2	
	482.0	460.0	706.1	
6	512.0	490.0	617.3	
	542.0	520.0	529.3	
	572.0	580.0	432.0	
	602.0	580.0	323.7	
	632.0	610.0	212.4	
	662.0	640.0	101.8	
	687.0	665.0	10.0	
	718.7	696.7	10.0	35.356
Down	735.7			
	741.7	702.7	1016.0	
	765.7	726.7	926.5	
	795.7	786.7	833.8	
	825.7	766.7	732.3	
	855.7	816.7	632.7	
	885.7	846.7	537.4	
7	915.7	876.7	447.5	
	945.7	906.7	355.7	
	975.7	936.7	255.0	
	1005.7	966.7	148.6	
	1044.6	1005.6	7.8	
	1083.6	1044.6	7.8	49.356
Down	1098.6			
	1104.6	1050.6	1228.9	
	1128.6	1074.6	1119.9	
	1158.6	1104.6	1001.3	
	1188.6	1134.6	874.3	
	1218.6	1164.6	749.2	
	1248.6	1194.6	627.3	
8	1278.6	1224.6	509.1	
	1308.6	1254.6	395.4	
	1338.6	1284.6	282.6	
	1368.6	1314.6	169.4	
	1411.0	1357.0	11.9	
	1445.4	1391.4	11.9	53.331

^a From beginning of cycle 5 based on operating data.

^b As provided in Ref. 49.

Table 95. Cycle average power data for GKN II (REBUS) sample

Cycle #	Duration (effective power days)	Down (days)	Cumulative burnup (GWd/MTU)	Power ^a (MW/MTU)
5	310.0	22	17.442	56.265
6	386.7	17	35.862	47.634
7	347.9	15	50.063	40.820
8	346.8	–	54.095	11.626

^aDerived from cumulative burnup and effective power days.

Source: Ref. 49.

Table 96. Cycle average moderator and fuel data for GKN II (REBUS) sample

Cycle #	Moderator density ^a (g/cm ³)	Moderator temperature ^b (K)	Fuel temperature ^b (K)
5	0.646	605.01	1018.04
6	0.665	598.98	904.25
7	0.681	593.34	819.69
8	0.725	574.23	646.13

^aValues corresponding to moderator temperatures and operating system pressure

determined by interpolating steam data from Ref. 58.

^bRef. 49.

8.10 GÖSGEN: MALIBU PROGRAM

A description of the assembly design and operational data for the Gösgen spent fuel samples selected for the MALIBU program and used in this validation study is available in DTN: MO1003MALIBUIP.001.

9 SCALE TWO-DIMENSIONAL DEPLETION CALCULATION METHOD

This section describes the SCALE 2-D depletion computation method and the TRITON/NEWT models developed for the spent fuel samples evaluated in this report.

9.1 METHOD DESCRIPTION

The depletion computational method and the cross-section library being evaluated are the 2-D transport and depletion sequence TRITON/NEWT (T-DEPL) and 44GROUPNDF5 cross-section library, respectively, in the SCALE 5.1 (Ref. 1) code system. The SCALE 44GROUPNDF5 cross-section library is based on the Evaluated Nuclear Data File/B Version V (ENDF/B-V) library. The T-DEPL analysis sequence is one of the five sequences developed for the TRITON control module.² It invokes SCALE functional modules for resonance processing (BONAMI and WORKER/CENTRM/PMC or BONAMI and NITAWL); 2-D discrete ordinates transport calculations (NEWT),³ burnup-dependent cross-section preparation (COUPLE);⁹¹ and depletion calculations (ORIGEN-S).⁹² At each depletion step, the transport flux solution from NEWT is used to generate cross sections and assembly power distributions for the ORIGEN-S calculations; the isotopic composition data resulting from ORIGEN-S is employed in the subsequent transport calculation to obtain cross sections and power distributions for the next depletion step in an iterative manner throughout the irradiation history.

TRITON has the capability of simulating the depletion of multiple mixtures in a fuel assembly model. This is a very useful and powerful feature in a nuclide inventory analysis, as it allows a more appropriate representation of the local flux distribution and neutronic environment for a specific measured fuel rod in the assembly. The flux normalization in a TRITON calculation can be performed using as a basis the power in a specified mixture, the total power corresponding to multiple mixtures, or the assembly power. The first of the above-mentioned options permits specification of the burnup (power) in the measured sample, usually inferred from experimental measurements of burnup indicators (such as ¹⁴⁸Nd).

9.2 MODELING APPROACH

The input data available for modeling the measured spent fuel samples considered in this study are described in Sect. 8. This section describes the general input format and additional input parameters that are specific to the TRITON/NEWT (T-DEPL) analysis sequence, such as input options and control parameters, which were consistently used in all input files.

9.2.1 Input File Format for Depletion Calculations

The general format of an input file for the T-DEPL analysis sequence is listed below and is followed by a description of the input data for the various data blocks identified by keywords.

```
=t-depl          parm=(options)
Title or description of up to 80 characters
x-sect_lib_name
READ alias
[List of user-defined aliases (optional)]
END alias
READ composition
[List of mixture specifications (standard SCALE format)]
END composition
READ celldata
```

```

[unit cell specifications (multiple specifications allowed)]
END celldata
[optional] more data [additional cell parameters] END data
READ keyword1
[keyword 1 type data]
END keyword1
READ keyword2
[keyword 2 type data]
END keyword2
[additional keyword blocks as needed]
end

```

PARM

PARM control options: `parm=(addnux=3,nitawl)`

All the isotopes (232) for which cross sections data are available in the multigroup transport library used with NEWT were applied in updating cross sections for the ORIGEN-S fuel depletion calculation at each depletion step based on the flux solution from the transport calculation with NEWT.

BONAMI and NITAWL functional modules were invoked for cross-section processing.

Cross-section library name: `44groupndf5` (SCALE 44GROUPNDF5 cross-section library based on the ENDF/B-V library)

ALIAS

Mixture aliases were used to associate multiple mixture IDs with a single alias.

COMPOSITION

The composition block provides standard composition mixture data for fresh fuel, cladding, moderator, neutron absorber, and structural materials. SCALE standard compositions were used for cladding and structural materials (zirc4 and/or ss304). The compositions for the other mixtures are documented in Sect. 8. Note that nitrogen rather than helium was used as the filling gas in the fuel rod gap in the calculations described in this document. Both He and N have no effect on the neutron spectrum.

CELLDATA

This data block provides unit cell data description including the type of lattice cell (`latticecell squarepitch`), fuel, gap, and clad radii, fuel rod pitch, and the corresponding material mixture numbers. Input data for the unit cell data block are documented in Sect. 8.

BURNDATA

Specific power, irradiation time, and downtime/cooling time data for this block are documented in Sect. 8. The number of cross-section libraries produced per cycle was selected such that the sample burnup per library is less than 3 GWd/MTU. Burnup steps of 3 GWd/MTU are generally adequate to represent the cross section variations with burnup.⁹³

DEPLETION

This data block specifies the mixtures to be depleted and the mixture that is used to normalize the input power. The mixtures to be depleted consist of fuel mixtures and the fixed absorber mixture such as BPR or control rod mixture, if applicable. The input power was normalized to the mixture in the fuel rod from which the sample was selected.

TIMETABLE

This data block specifies time-dependent material properties such as fuel temperature, soluble boron concentration in the moderator, or moderator density. TRITON applies linear interpolation to obtain these parameters within the time intervals.

OPUS

This data block provides a partial set of OPUS commands that can be used to control post-processing of ORIGEN-S output binary files as part of the sequence of calculations. The input files requested OPUS tables providing nuclide concentrations in grams per MTU for the measured isotopes in the rod containing the measured sample.

MODEL

The MODEL data block provides assembly description data for NEWT calculations. In the models, the fuel rod that contained the measured sample and its nearest neighbor fuel rods were represented as individual geometry units, whereas the other fuel rods in the assembly were described using a single geometry unit. The model includes other assembly components for which data was available, such as guide and instrument tubes, fixed burnable absorber, or integral burnable absorber, as applicable. Assembly models used reflective boundary conditions for the four sides of the assembly because modeling data is usually unavailable for adjacent assemblies. Reflective boundary conditions are very good approximations to use in 2-D transport calculations for measured fuel rods selected from the inner assembly locations. However, these approximations may not be adequate for modeling the assembly that provided samples from outer assembly rods, such as the KWO assemblies BE124 and BE210. Note that the TRITON/NEWT models for the measured samples in the TMI-1 assembly NJ070G included information on the assembly surroundings.

BOUNDARY

The unit boundary for the pin cells defines a 4×4 rectangular grid.

PARAMETER

Default convergence control parameters were used to control spatial, angular, and eigenvalue convergence for the iterative phases of the solution process.

9.2.2 Fuel Mixture Modeling Simplifications

Typical TRITON/NEWT models used in this validation study consist of individual depleting mixtures specified for the measured rod and its adjacent nearest-neighbor fuel rods with all other fuel rods in the assembly treated as a single depletion material with uniform composition. This modeling technique was employed to reduce the overall computer time while maintaining sufficient accuracy for the results. A sensitivity study for the Turkey Point sample D01_G9 (~30 GWd/MTU burnup) showed that the relative differences between the isotopic concentration values obtained with detailed and simplified pin models are within $\pm 0.5\%$ for all isotopes and within $\pm 0.3\%$ for the burnup credit isotopes (see *DVD/xls/input_data.xls*, worksheet *Turkey-Point*). The results are summarized in Sect. 10.2.1, Table 107. Therefore, the uncertainty associated with fuel mixture modeling simplifications is expected to be significantly small.

9.2.3 Modeling Approach for H. B. Robinson Assembly BO-5, Calvert Cliffs Assembly BT03, and TMI Assembly NJ05YU

H. B. Robinson assembly BO-5, Calvert Cliffs assembly BT03, and TMI assembly NJ05YU were exposed to burnable poison rods during their first cycle of irradiation. The burnable poison rods were removed at the end of those cycles and the assemblies were irradiated for one or more subsequent cycles without being exposed to burnable poison rods. For these cases, separate TRITON models were used to represent a fuel assembly during irradiation cycles with and without burnable poison exposures. Fuel mixture compositions for an assembly containing burnable poison rods throughout the first cycle of irradiation were used as the initial fuel compositions at the beginning of the subsequent cycle(s). Because the heavy metal mass in the measured rod changes slightly due to depletion and because the power in TRITON is normalized to the heavy metal mass of the measured fuel rod at the BOC of each simulation cycle, the power values for the subsequent cycle(s) shown in the tables included in Sect. 8, which were determined using as a basis the heavy metal mass in the measured fuel rod for fresh fuel before the irradiation, were adjusted to obtain the measured sample burnup. A multiplying factor was determined as the ratio between the total heavy metal mass in the sample mixture at the beginning of the first irradiation cycle and the corresponding quantity at the end of the first irradiation cycle.

9.3 TRITON/NEWT MODELING

9.3.1 Trino Vercellese

The TRITON/NEWT models for assemblies 509-032, 509-049, and 509-069, as illustrated in Fig. 21 for assembly 509-069, represent a full square assembly with half of the cruciform assembly rods adjoining the upper left quadrant of the square assembly and use reflective boundary conditions to simulate the surrounding assembly environment. Assumptions were embedded into the model to simplify the geometric representation of a measured square assembly and surrounding assemblies because insufficient description of the surrounding assemblies was available in primary reference documents, including (1) initial enrichment and burnup values for the adjacent square assemblies and (2) the two empty lattice locations in a cruciform assembly knowing that a cruciform fuel assembly has 28 rod locations and contains 26 rods (see Sect. 8.1). In the current validation study, it was assumed that the 13 lattice positions surrounding the upper left quadrant of the square assembly illustrated in Sect. 8.1, Fig. 4, contain cruciform assembly fuel rods. The simplifying assumptions are deemed to have insignificant effects on the calculated isotopic compositions because the evaluated samples were obtained from inner assembly rods that were irradiated in either an asymptotic or intermediate (near water hole) neutron spectrum.^{12,13} Note that the model illustrated in Fig. 21 was also used for fuel rods 509-032-E11 and 509-069-L5, which were located approximately halfway between a control group and the center of the

square assembly. The control group was inserted 30%, or approximately 80 cm, from the top during period 1 of cycle 1, and each cruciform control rod was connected to a fuel bearing follower so that if a cruciform control rod were removed, a cruciform fuel assembly would raise into the fuel. Therefore, a geometric model including a control rod may be justified only for sample 509-032-E11-1, which had a rod axial location of 246.7 cm. However, the 2-D assembly model illustrated in Fig. 21 adequately represents the irradiation environment for sample 509-032-E11-1 because fuel rod 509-032-E11 was located approximately halfway between the control group and the center of the square assembly where the irradiation spectrum was asymptotic.

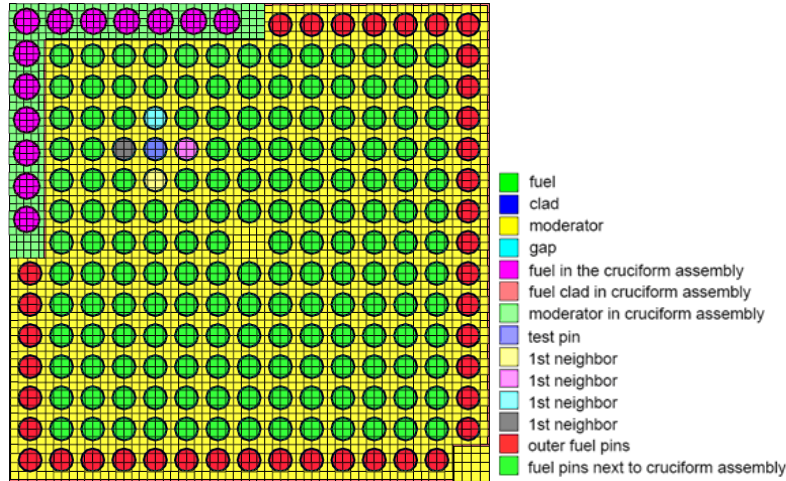


Fig. 21. TRITON/NEWT model for Trino Vercellese assembly 509-069, rod E11.

Assembly 509-104 was irradiated in a location at the core periphery, and assumptions were made for the outer core materials and their unavailable dimensions. The model for this assembly is shown in Fig. 22. A 2-cm stainless steel core liner, 10-cm borated water, and a void boundary condition were assumed for the core periphery. Reflective boundary conditions were used to represent the three adjoining assemblies. Note that neutron leakage at the core periphery has negligible effects on the measured rod since this rod was separated from the core periphery by 11 rows of rods.

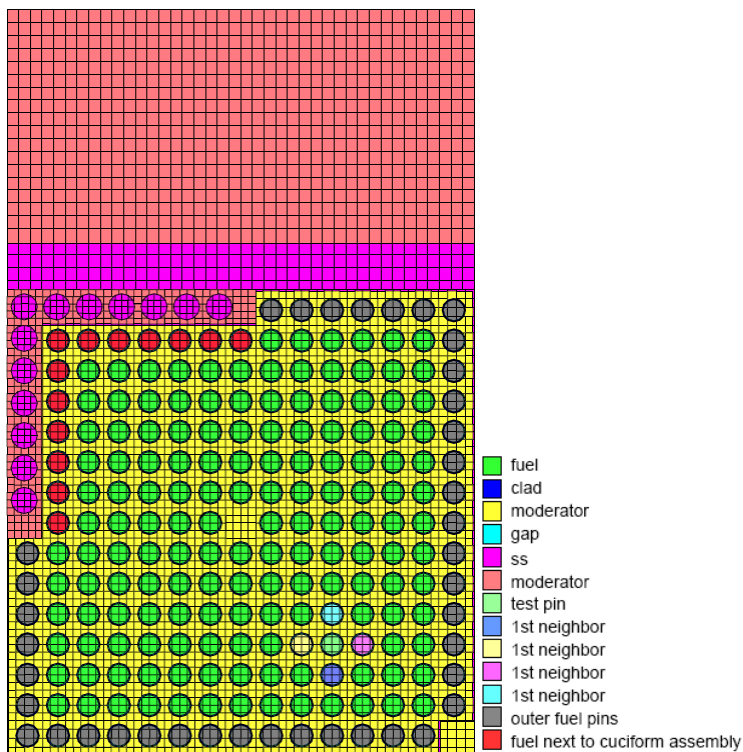


Fig. 22. TRITON/NEWT model for Trino Vercellese assembly 509-104, rod M11.

9.3.2 Obrigheim

In the TRITON/NEWT models for the KWO spent fuel samples, individual depleting mixtures were specified for the measured rod and its adjacent nearest-neighbor fuel rods. All other fuel rods were treated as a single depletion material with uniform composition. A full assembly model was developed for all KWO spent fuel samples from assemblies BE124 and BE210, as illustrated in Fig. 23 for assembly BE124, rod G7, whereas a one-quarter assembly model with a single fuel mixture was used for KWO spent fuel assemblies BE168, BE170, BE171, BE172, and BE176. Although a significant number of the evaluated Obrigheim rod samples were taken from assembly peripheral rods, reflective boundary conditions were specified in the TRITON calculations to simulate the assembly surrounding environment because the characteristics of the adjacent assemblies were not available in the primary reference documents (refer to Sect. 8.2 for a description of relevant modeling uncertainties). In addition, as illustrated in Fig. 7, assembly BE124 was irradiated at the reactor core edge during cycle 2, removed from the reactor during cycle 3, and then irradiated for two more cycles at an inner core location. Therefore, one of the measured peripheral rods in assembly BE124 could have been located near the outer core moderator during cycle 2 of irradiation. The use of reflective boundary conditions for such a rod during cycle 2 is considered to result in small uncertainties in the calculated isotopic compositions.

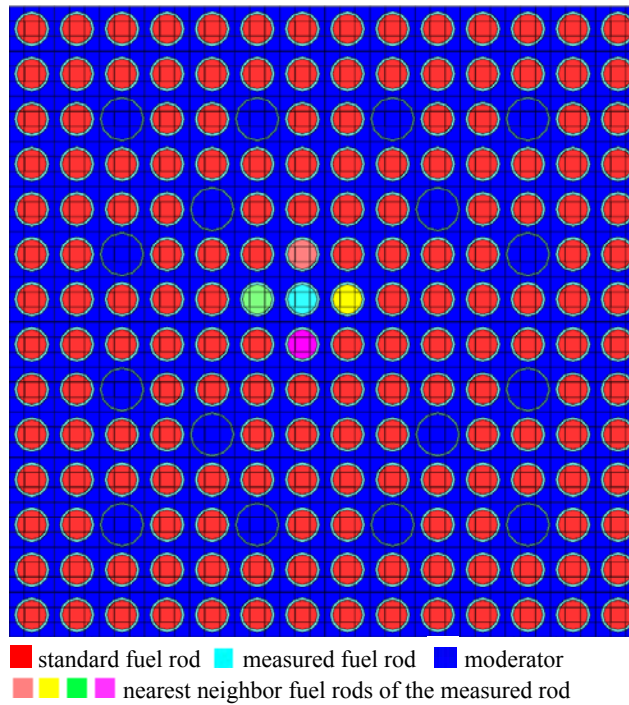


Fig. 23. TRITON/NEWT model for KWO assembly BE124, fuel rod G7.

9.3.3 Turkey Point Unit 3

The TRITON/NEWT models for the Turkey Point Unit 3 assemblies D01 and D04 consist of half of the assembly with reflective boundary conditions. The model for spent fuel samples from rod D01-G9, illustrated in Fig. 24, shows the measured rod and its nearest neighbors individually modeled and the other rods modeled as a single material mixture.

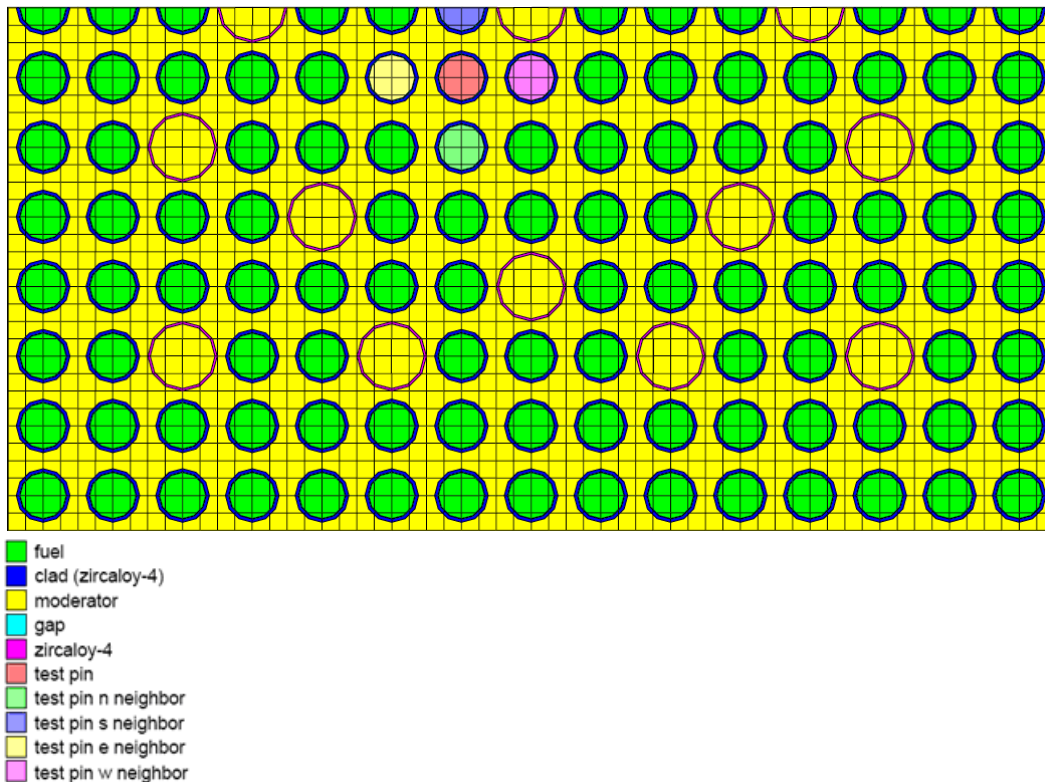


Fig. 24. TRITON/NEWT model for Turkey Point Unit 3 assembly D01, rod G9.

9.3.4 H. B. Robinson Unit 2

The TRITON/NEWT models for H. B. Robinson assembly BO-5 for cycles 1 and 2 of irradiation used the one-quarter assembly models illustrated in Fig. 25. Individual depleting mixtures were specified for the measured rod and its adjacent nearest-neighbor fuel rods, as well as for the burnable absorber material (for cycle 1 of irradiation only). All other fuel rods were treated as a single depletion material with uniform composition. It was assumed that the surrounding assemblies had the same enrichment and irradiation history as the measured assembly, so that reflective boundary conditions are applicable. This assumption has a negligible effect on the results of the calculations since the measured fuel rod had an inner assembly location.

The model shown in Fig. 25(a) provided the concentrations of nuclides in all depleted fuel mixtures at the end of cycle 1. These mixture concentrations served as input data for the second model, shown in Fig. 25(b), which was used to simulate the depletion of the assembly during cycle 2. Note that the burnable poison was removed when the average assembly burnup had reached 18,000 MWd/MTU (Ref. 27) and the burnup values of assembly BO-5 at the end of cycles 1 and 2 were 18.613 and 28.03 MWd/MTU, respectively (Ref. 28). Therefore, the assembly model illustrated in Fig. 25(a) was also used to simulate the last 613 MWd/MTU burnup in cycle 1. The impact of this modeling approximation on the accuracy of the calculation results is considered to be very small since the 613 MWd/MTU burnup represents approximately 2% of the total assembly burnup.

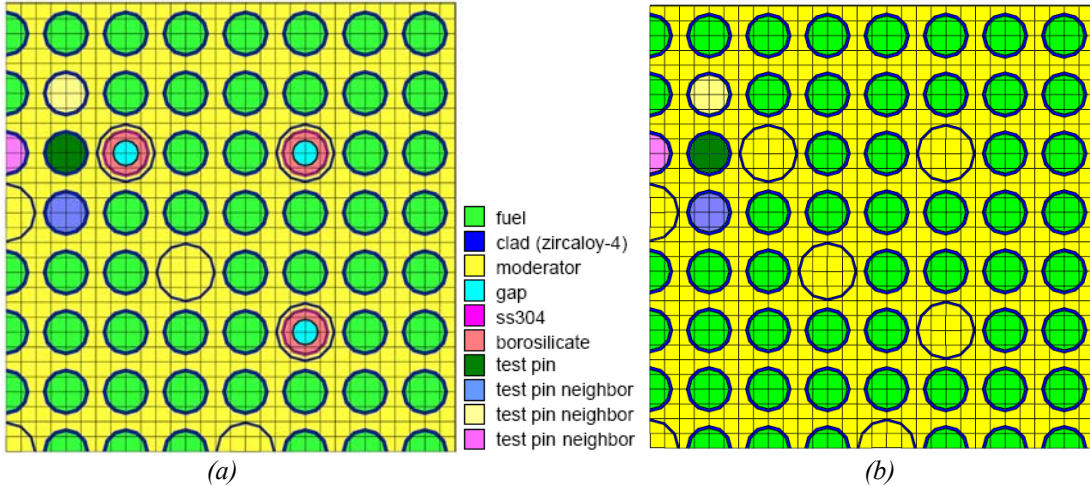


Fig. 25. TRITON/NEWT model for H. B. Robinson Unit 2 assembly BO-5:
 (a) for cycle 1 of irradiation; (b) for cycle 2 of irradiation.

9.3.5 Calvert Cliffs

Half assembly models were used for the analysis of the nine measured fuel samples, as illustrated in Fig. 26, Fig. 27, and Fig. 28 for assemblies D047, D101, and BT03, respectively. Individual depleting mixtures were specified for the measured rod and its adjacent nearest-neighbor fuel rods, as well as for the burnable absorber materials. All other fuel rods were treated as a single depletion material with uniform composition. For samples from rod NBD107 of assembly BT03, two models were used: one for cycle 1, in which the assembly included burnable absorber rods (see Fig. 28), and one for cycles 2–4, where the absorber rods were not present (see Fig. 29). The first of these two models provided the concentrations of nuclides in all depleted fuel mixtures at the end of cycle 1; these data served as input data for the second model that simulated the depletion of the assembly during cycles 2 to 4.

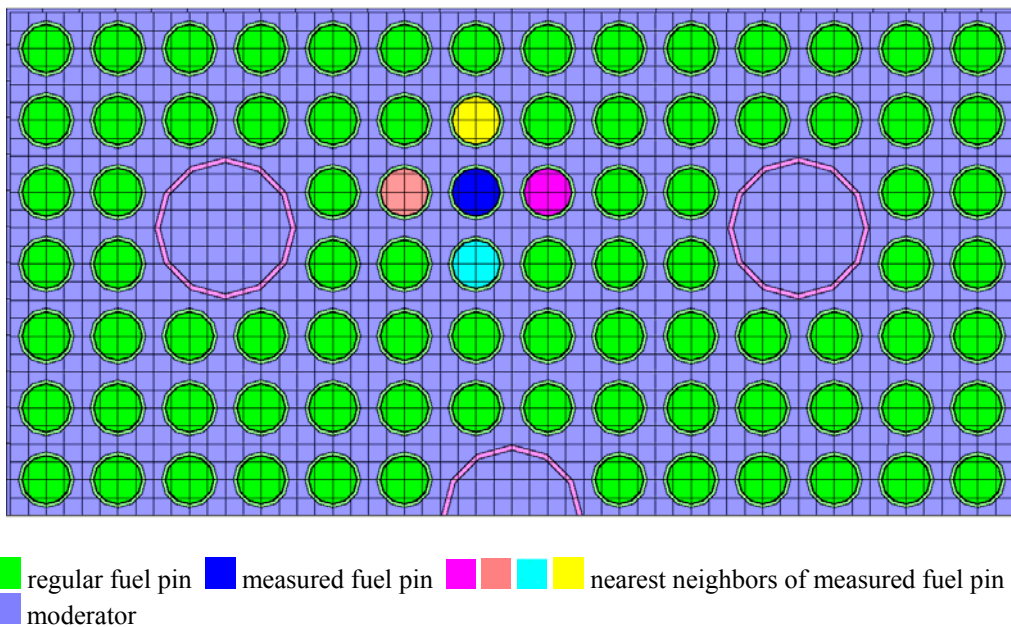
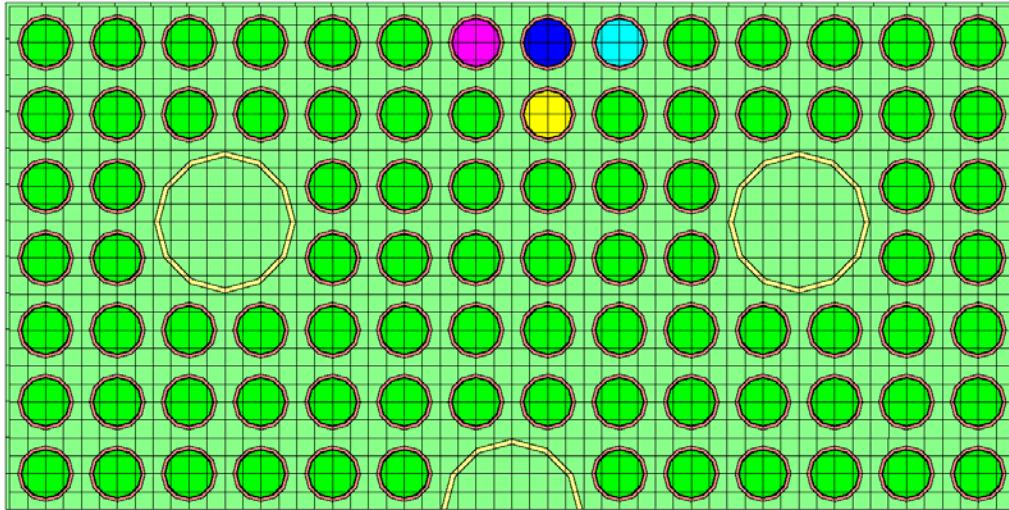
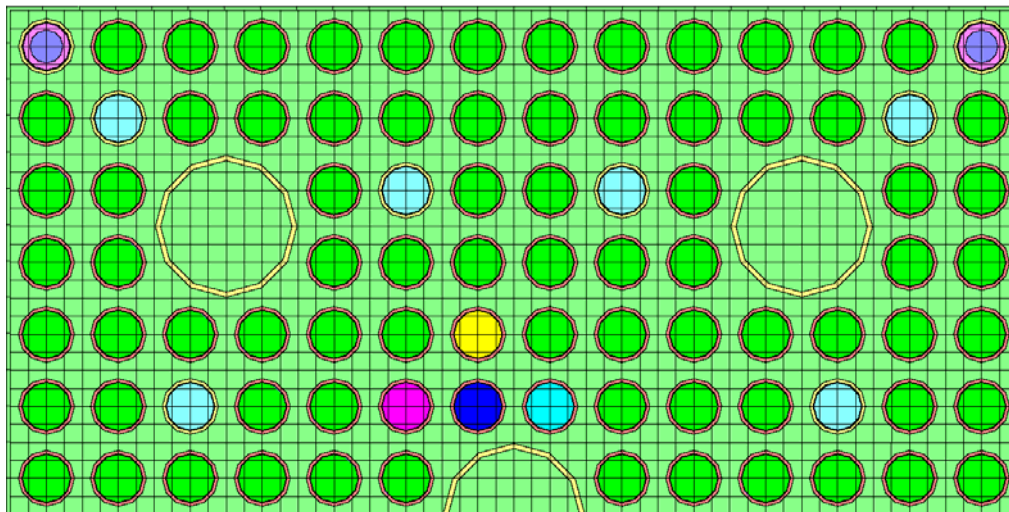


Fig. 26. TRITON/NEWT model for Calvert Cliffs samples from assembly D047.



■ regular fuel pin ■ measured fuel pin ■ ■ ■ nearest neighbors of measured fuel pin
■ guide tube ■ moderator

Fig. 27. TRITON/NEWT model for Calvert Cliffs samples from assembly D101.



■ regular fuel pin ■ measured fuel pin ■ ■ ■ nearest neighbors of measured fuel pin
■ guide tube ■ moderator ■ gap in test rod ■ test rod material SS304 ■ BPR

Fig. 28. TRITON/NEWT model for Calvert Cliffs samples from assembly BT03, cycle 1.

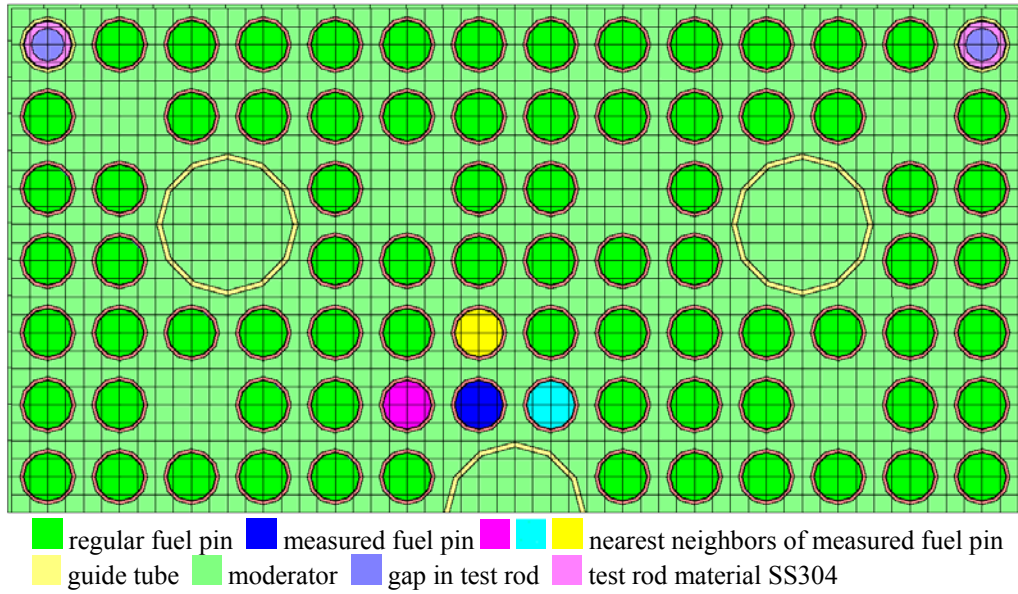


Fig. 29. TRITON/NEWT model for Calvert Cliffs samples from assembly BT03, cycles 2-4.

T-DEPL simulations were carried out for each sample. For samples from fuel rod MKP109, the available burnup and power data were slightly adjusted, in order to obtain a calculated ^{148}Nd concentration in agreement with the measured value. The calculated burnup values are 27.11, 36.90, and 44.13 GWd/MTU for sample MKP109-LL, MKP109-CC, and MKP109-P, respectively. These values are slightly different from the available burnups³⁰ of 27.35, 37.12, and 44.34 GWd/MTU, respectively (see Table 70).

9.3.6 Takahama Unit 3

Fuel rod SF97, residing in assembly NT3G24, was simulated using a one-half assembly geometry model because the rod was located on a quarter-assembly symmetry axis. The models for fuel rods SF95 and SF96 from assembly NT3G23 used a one-quarter assembly model. The three models used for each measured rod are illustrated in Fig. 30 through Fig. 32. In each model, the measured fuel rod, as well as the fuel rods adjacent to it, was individually depleted. The moderator density and temperature values are provided in Table 77. The variation of the soluble boron in the moderator given in Table 79 was simulated through the use of the TIMETABLE input block in the TRITON input. Note that fuel rods SF95 and SF97 are located on the edge of the assembly and therefore possibly subjected to edge effects. However, as no information was available on the surrounding assemblies, these assemblies were not included in the model.

As mentioned previously, the sample reported burnups were normalized to the measured ^{148}Nd content. In the case of the samples from rod SF96, the simulation using the sample power (and burnup) in Table 77 yielded a calculated ^{148}Nd concentration that was within 4 to 10% less than the measured value, depending on the sample. This difference is much larger than the maximum 3% error in burnup specified in the JAERI report.⁴¹ The sample burnup determination by JAERI was made using the ASTM E 321–79 standard method that estimates the burnup (in GWd/MTU units) by multiplying the value of the burnup rate (% FIMA = fission per initial metal atom in percent value that is based on the measured ^{148}Nd content) by a factor of 9.6 ± 0.3 (Ref. 74). However, derivation of this factor is based on a recoverable energy per fission (MeV/fission) value obtained for a system that is near critical. While this assumption is

valid for a large-scale reactor system, it may not apply on a local level. For the case of a gadolinia-bearing rod or other poison rod the absorption rate may significantly exceed the fission rate. The capture reactions in gadolinium contribute prompt capture gamma-ray energy to the system that is not accounted for in the ASTM method, but may be accounted for in modern depletion computer codes (such as ORIGEN-S). The applicability of simplified methods for burnup determination needs to be carefully considered, particularly when applied to nonstandard type fuel.

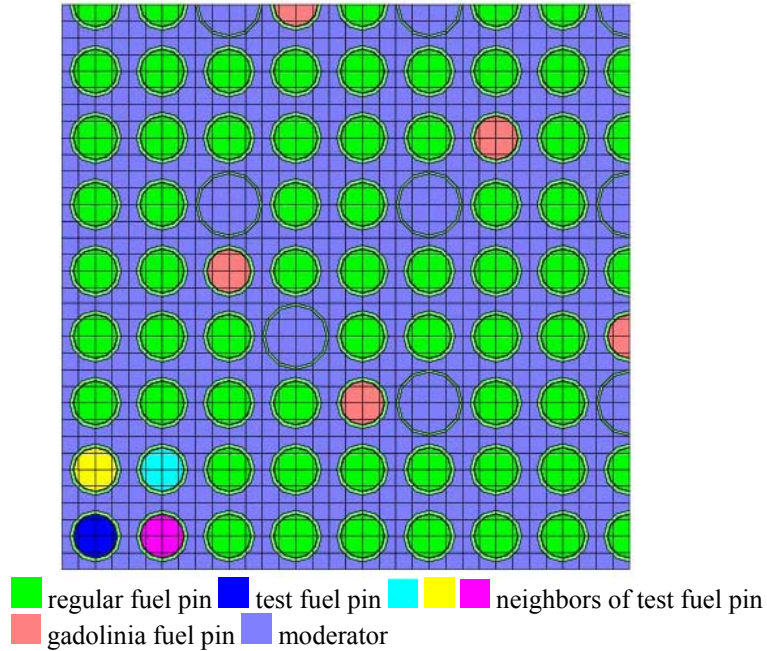


Fig. 30. TRITON/NEWT model for Takahama-3 SF95 spent fuel samples.

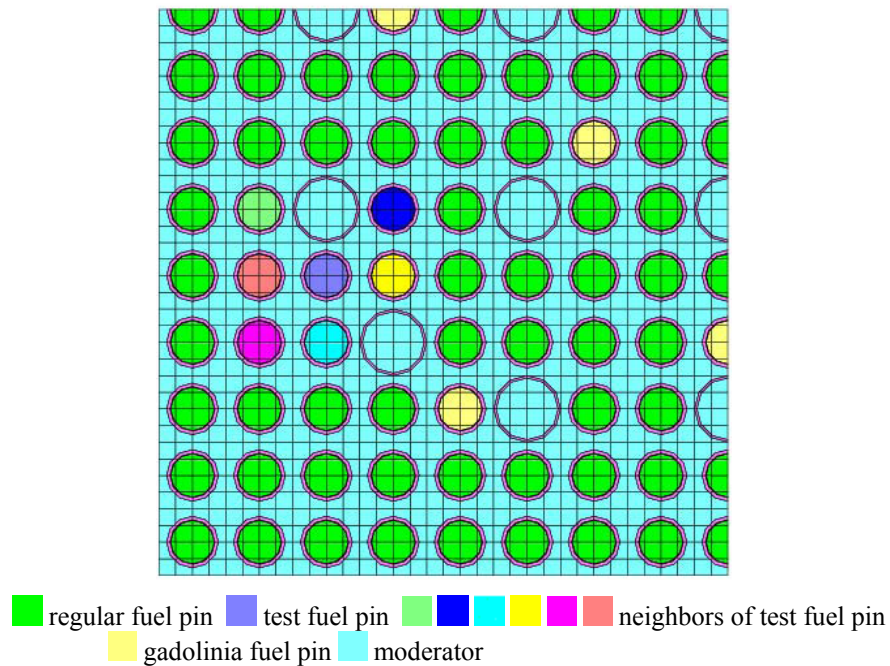


Fig. 31. TRITON/NEWT model for Takahama-3 SF96 spent fuel samples.

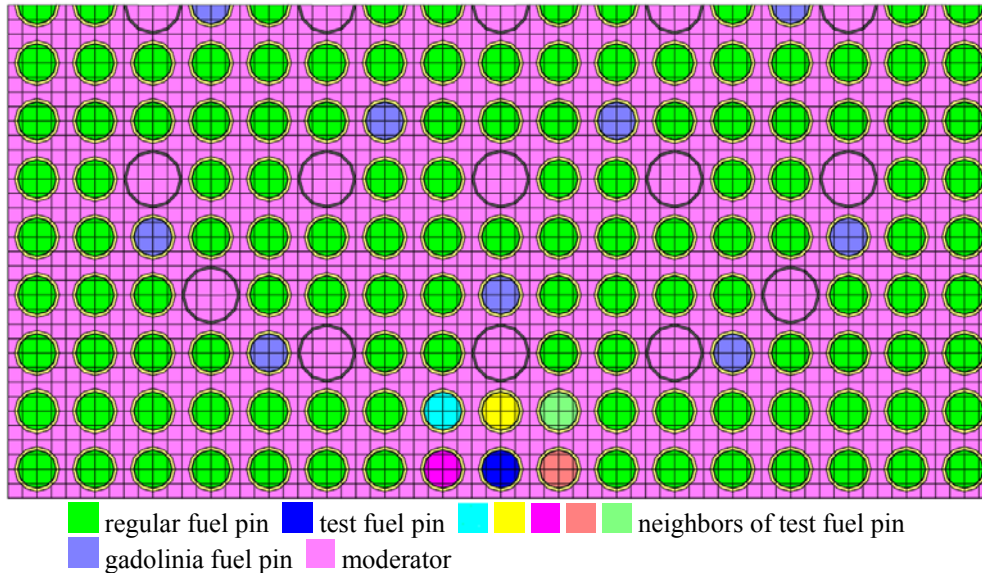
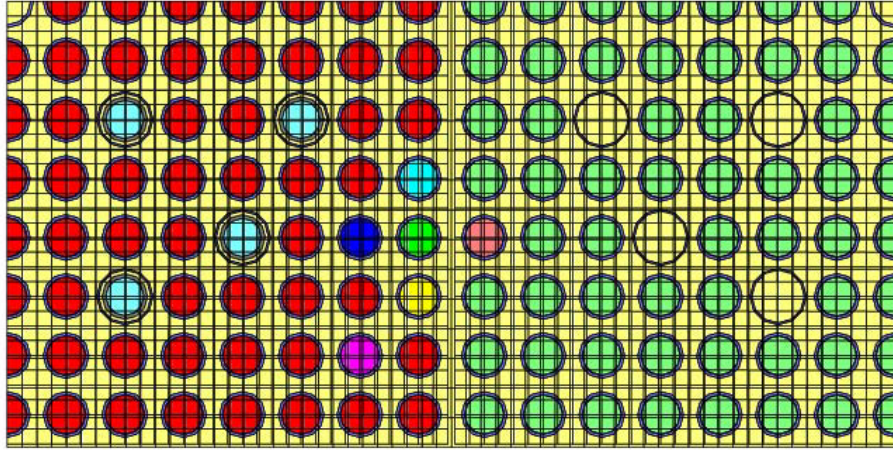


Fig. 32. TRITON/NEWT model for Takahama-3 SF97 spent fuel samples.

9.3.7 TMI Unit 1

Assembly NJ05YU that hosted the fuel rod H6 (see Fig. 16), from which 11 samples were selected, was irradiated in two consecutive cycles, cycle 9 and cycle 10. The BPRs present during cycle 9 were removed in cycle 10. Separate TRITON models were developed to accurately represent this change in the assembly geometry, as illustrated in Fig. 33. Given the symmetry and the location of rod H6 in assembly NJ05YU, the models for the analysis of samples selected from this rod represent only half of the assembly geometry, with a reflective boundary condition on the left side of the configuration and white boundary conditions on the other three bounding surfaces. The geometry and material data were used as given in Table 81, and the power data as provided in Table 82. Six fuel mixtures were specified: one corresponding to the measured rod, four to the nearest neighbor fuel rods, and one to the rest of the fuel rods in the assembly. At the end of the depletion simulation for cycle 9, the isotopic composition for each of these six fuel mixtures was extracted and used as input data in the model corresponding to cycle 10 (with no BPR present). A total of 232 nuclides present in the SCALE multigroup transport library, representing the main light elements, actinides, and fission products, were included to represent the fuel composition at the start of cycle 10. The variation of the soluble boron content in the coolant and of the temperature in fuel during irradiation, as given in Table 84 and Table 87, for samples from assemblies NJ05YU and NJ070G, respectively, was modeled through the use of the TIMETABLE input block in TRITON; ten burnup steps per cycle were used for depletion.

All three rods in assembly NJ070G, from which samples were selected for measurement, were edge rods located along one side of the assembly, with one of these rods placed at the corner of the assembly. The computational models used for the analysis of these samples include information on the assembly surroundings. The models for rods O12 and O13 are similar and include a quarter of assembly NJ070G and a quarter of the assembly surrounding it on the side on which the samples are located, as illustrated for rod O12 in Fig. 34. As observed in this figure, in order to better approximate the local environment, given the close proximity of the measured rod to the assembly boundary, the nearest neighboring rods were represented by using different mixtures; one of these neighboring rods is located in a different assembly. In the case of the corner rod O1, the TRITON model included a quarter of assembly NJ070G and a quarter of each of the three surrounding assemblies that share the same corner point with assembly



- measured fuel pin O12
- regular fuel pins in assembly NJ070G
- fuel pins in neighboring assembly
- nearest neighbors of measured pin
- gadolinia fuel pin
- moderator
- BPR absorber

Fig. 34. TRITON/NEWT model for TMI-1 samples in rod O12 of assembly NJ070G.

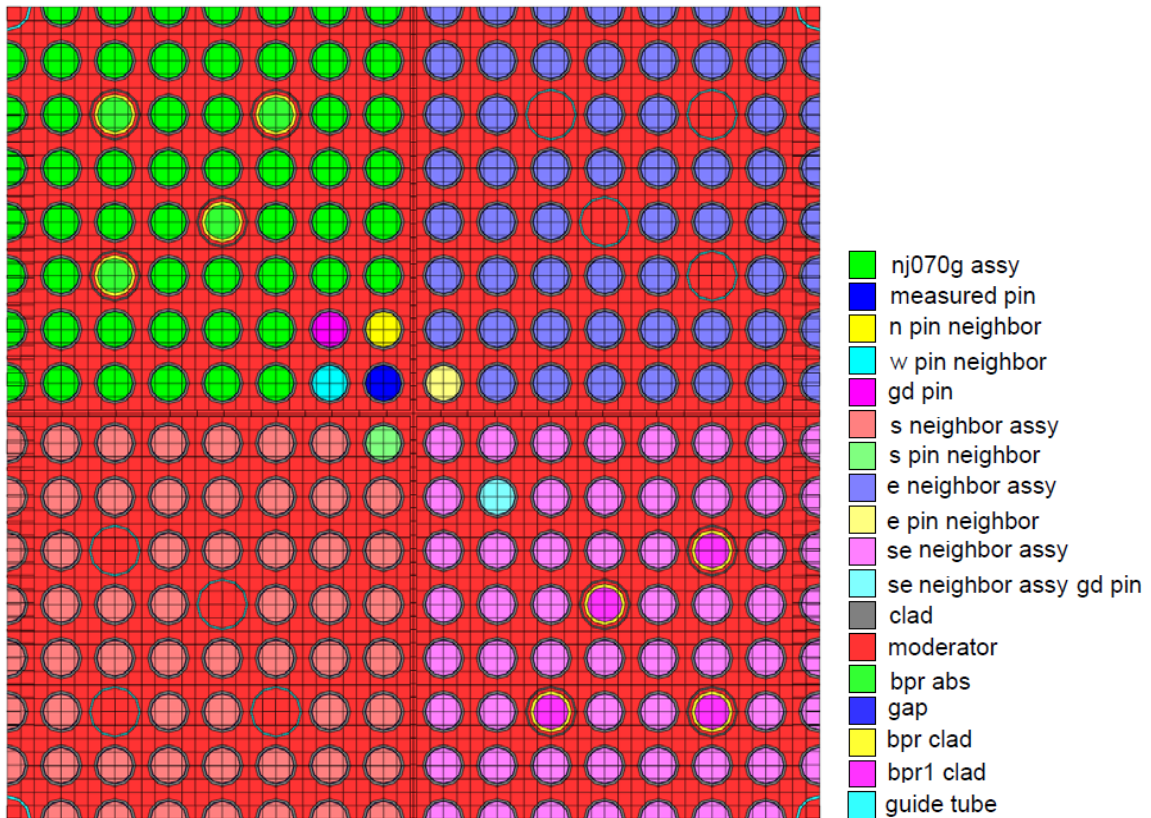


Fig. 35. TRITON/NEWT model for TMI-1 samples in rod O1 of assembly NJ070G.

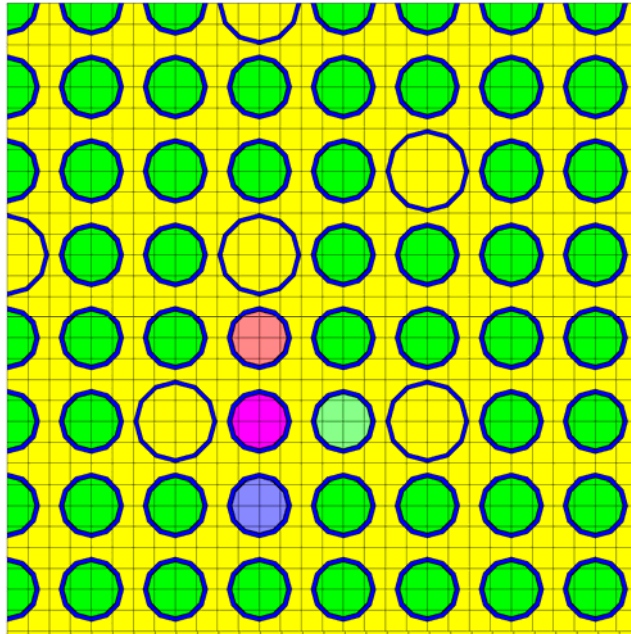
9.3.8 Gösgen: ARIANE Program

The analysis of sample GU1 was carried out by using a quarter assembly model of assembly 12-40, as shown in Fig. 36. The geometry, material, and burnup data used in the TRITON model were as given in Table 90 to Table 92. Replacement of some of the fuel rods during cycles 14 and 15 was not modeled because insufficient information on the configurations was available. However, the replacement rods were indicated to have burnup similar to that of the original rods, and not modeling the fuel rods reconfiguration was deemed to be of minor importance.

The depletion history of the fuel rod from which samples GU3 and GU4 were selected, including the reconstitution of the fuel assembly, was explicitly simulated with TRITON. One TRITON model, as illustrated in Fig. 37, was used to model the depletion of assembly 16-01 during cycles 16 and 17; individual depleting mixtures were used for the measured rod and its nearest neighbor fuel rods, whereas all other fuel rods in the assembly were treated as a single depletion material with uniform composition. The nuclide compositions for the measured rod and the average composition for the regular fuel rods in assembly 16-01 were saved at the end of the simulation for cycle 17 and used in the input file for simulating assembly 17-01 during cycle 18. The average composition for the regular fuel rods from assembly 16-01 was used as composition data for the three replacement rods that were, in addition to the measured rod, inserted in the rebuilt assembly 1701 at the beginning of cycle (BOC) 18.

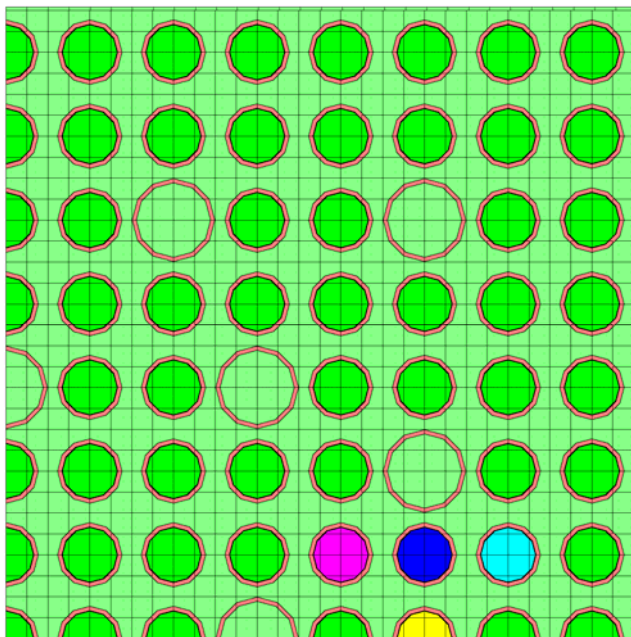
The TRITON model for assembly 17-01 is illustrated in Fig. 38. As mentioned in Section 8.8, it is known that the average burnup of assembly 17-01 at BOC-18 was about 20 GWd/MTU. To determine the composition of the spent fuel for the 201 fuel rods in this assembly from the total of 205 rods, once the composition for the four replacement rods was calculated, an additional TRITON model was used to simulate the depletion of assembly 17-01 prior to the reconstitution. This model is similar to that illustrated in Fig. 37 but considered a single depletion mixture for all the fuel rods in the assembly; this mixture was depleted to a burnup of 20 GWd/MTU for sample GU3 and to a burnup of 9.71 GWd/MTU for sample GU4 (Ref. 48, Table 3.b), and the composition of the depletion mixture was saved to be used in the depletion model of assembly 17-01 during cycle 18.

The sample burnups used in the code simulations were normalized to the measured ^{148}Nd concentration. The sample burnup values based on measured ^{148}Nd for samples GU1, GU3, and GU4 were 60.7, 53.2, and 31.1 GWd/MTU, respectively. These burnups based on experimental data are in good agreement with the burnup values 59.7, 52.5, and 29.1 GWd/MTU from operator data. The burnup history data presented in Table 91 and Table 92 were adjusted by a constant factor to correspond to the measurement-based burnup.



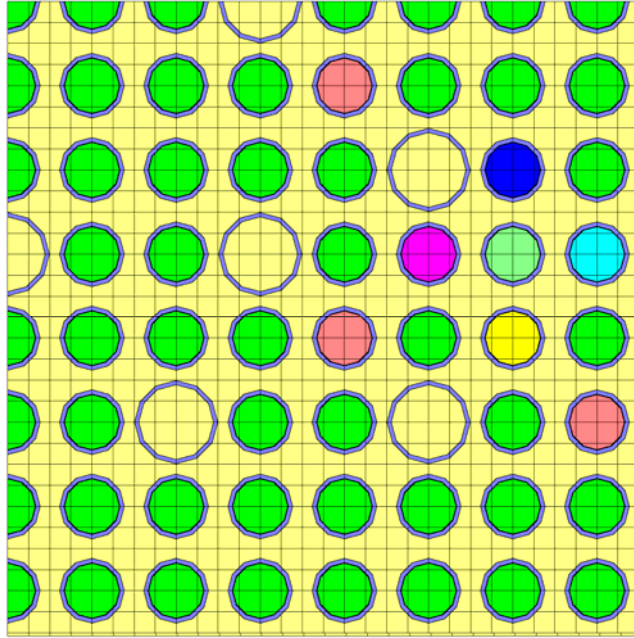
■ standard fuel rod
 ■ measured fuel rod
 ■ moderator
 ■ ■ ■ nearest neighbors of measured fuel rod

Fig. 36. TRITON/NEWT assembly model for Gösgen (ARIANE) – sample GU1.



■ standard fuel rod
 ■ measured fuel rod
 ■ ■ ■ nearest neighbors of measured fuel rod
 ■ moderator

Fig. 37. TRITON/NEWT assembly model for Gösgen (ARIANE) – sample GU3/4, cycles 16–17.

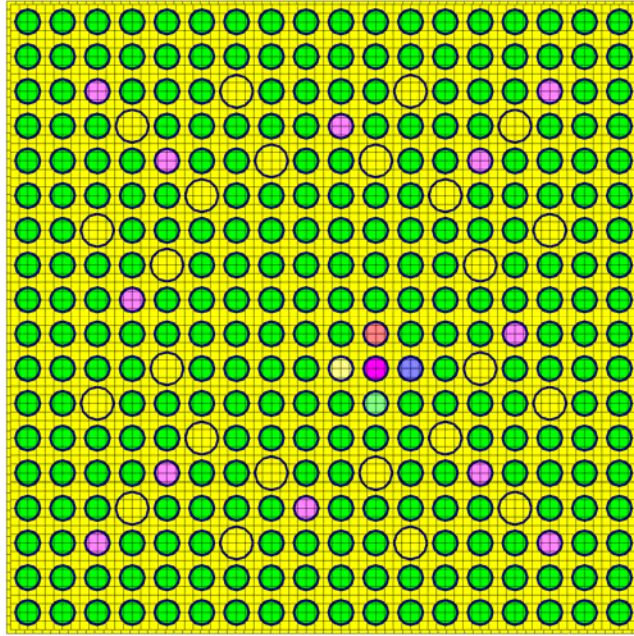


■ standard fuel rod
 ■ measured fuel rod
 ■ ■ ■ ■ nearest neighbors of measured fuel rod
■ moderator
 ■ replacement rods from assembly 1601

Fig. 38. TRITON/NEWT assembly model for Gösgen (ARIANE) – sample GU3/4, cycle 18.

9.3.9 GKN II

The geometry of the 18×18 GKN II assembly 419 was modeled in full detail, as illustrated in Fig. 39. White boundary conditions were used for the assembly bounding surfaces. As observed, there is a slight asymmetry in the assembly with respect to the placement of the gadolinia-bearing rods. The average power used in the simulations for each of the four irradiation cycles was taken from Table 94. The time-dependent variation of the boron concentration in the moderator, as well as of the moderator density and fuel and moderator temperatures, as given in Table 94 and Table 96, were simulated through the TIMETABLE input block in the TRITON input. The use of the provided sample burnup based on the gamma scan, 54.095 GWd/MTU, yielded a calculated ^{148}Nd content consistent with the measured value.



■ standard fuel rod
 ■ measured fuel rod
 ■ moderator
 ■ gadolinia fuel rod
 ■ nearest neighbors of measured rod

Fig. 39. TRITON/NEWT assembly model for GKN II (REBUS) spent fuel sample.

10 CALCULATION RESULTS

The current SCALE validation study evaluated 118 spent fuel samples from 37 fuel rods irradiated in nine PWR reactors, with sample initial enrichment varying from 2.453 to 4.657 wt % ^{235}U and burnup varying from 7.2 to 70.4 GWd/MTU (refer to Table 4 for the evaluated samples). The calculation results, which are listed in the tables included in Section 10.1, are reported as the ratio of the experimental-to-calculated (E/C) isotopic concentrations. This ratio is suitable for use in the isotopic composition validation methodology because (1) it shows the significance of deviations between calculated and measured isotopic concentrations and (2) it can be applied directly as a multiplicative correction factor to spent fuel compositions used in criticality calculations employing burnup credit to determine the impact of isotopic composition bias and bias uncertainty on k_{eff} . Graphical representations of the calculation results for the burnup-credit nuclides are presented in Appendix A.

10.1 RESULTS OF THE T-DEPL CALCULATIONS

The E/C ratios for Trino Vercellese, Obrigheim, Turkey Point, H. B. Robinson, Calvert Cliffs, Takahama, TMI, Gösgen (ARIANE), GKN, and Gösgen (MALIBU) spent fuel samples are listed in Table 97–Table 106, respectively. The tables also present the percentage deviations of the E/C values from unity, $E/C-1$ (%), to clearly indicate the significance of deviations between calculation and measurement isotopic concentrations.

Table 97. SCALE calculation results for Trino Vercellese spent fuel samples

Sample ID	509-032-E11-1		509-032-E11-4		509-032-E11-7		509-032-E11-9		509-032-H9-4		509-032-H9-7		509-032-H9-9		509-049-J8-1	
Enrichment (%)	3.13		3.13		3.13		3.13		3.13		3.13		3.13		2.719	
Burnup (GWd/MTU)	7.243		15.377		15.898		11.529		16.556		17.450		12.366		8.713	
Nuclide ID	E/C ^a	E/C-1 (%)	E/C	E/C-1 (%)	E/C	E/C-1 (%)	E/C	E/C-1 (%)	E/C	E/C-1 (%)	E/C	E/C-1 (%)	E/C	E/C-1 (%)	E/C	E/C-1 (%)
U-234	0.851	-14.92	1.071	7.09	0.657	-34.29	—	—	—	—	0.716	-28.45	0.731	-26.92	0.665	-33.48
U-235	0.973	-2.69	0.971	-2.88	0.956	-4.42	0.990	-1.04	0.995	-0.53	1.009	0.91	0.965	-3.55	0.984	-1.57
U-236	0.939	-6.14	1.003	0.27	0.946	-5.42	1.070	7.02	1.009	0.87	0.991	-0.90	0.978	-2.22	0.956	-4.38
U-238	1.000	0.00	1.000	0.01	1.000	0.03	1.000	0.02	1.000	-0.04	1.000	-0.01	0.988	-1.24	1.000	0.01
Pu-238	—	—	—	—	—	—	—	—	—	—	—	—	—	—	—	—
Pu-239	0.957	-4.30	1.006	0.58	1.002	0.23	1.010	0.97	1.012	1.19	1.005	0.53	1.032	3.24	0.981	-1.89
Pu-240	0.930	-6.99	1.008	0.79	0.996	-0.38	1.025	2.52	1.014	1.37	0.996	-0.43	1.027	2.69	0.949	-5.11
Pu-241	0.848	-15.22	1.035	3.53	1.015	1.50	1.067	6.72	1.075	7.54	1.038	3.79	1.114	11.42	0.993	-0.68
Pu-242	0.775	-22.55	1.012	1.18	1.034	3.37	1.039	3.93	1.056	5.55	0.966	-3.37	—	—	0.933	-6.74
Am-242m	—	—	—	—	—	—	—	—	—	—	—	—	—	—	—	—
Am-243	—	—	—	—	—	—	—	—	—	—	—	—	—	—	—	—
Cm-242	—	—	—	—	—	—	—	—	—	—	—	—	—	—	—	—
Cm-244	—	—	—	—	—	—	—	—	—	—	—	—	—	—	—	—
Ru-106	1.118	11.82	0.959	-4.12	0.985	-1.48	1.091	9.05	—	—	0.929	-7.14	1.086	8.57	1.068	6.76
Cs-134	1.378	37.84	1.224	22.40	1.230	22.97	1.273	27.29	—	—	1.180	17.99	1.249	24.91	1.194	19.39
Cs-137	1.025	2.46	0.996	-0.42	0.975	-2.48	0.974	-2.57	—	—	0.980	-1.98	0.975	-2.52	0.955	-4.52
Ce-144	1.231	23.06	1.010	1.01	0.957	-4.30	1.021	2.07	—	—	0.957	-4.32	1.063	6.26	1.084	8.42
Nd-148	0.998	-0.19	0.998	-0.20	0.998	-0.20	0.998	-0.21	0.998	-0.20	0.997	-0.27	0.985	-1.47	1.000	0.03
Eu-154	—	—	—	—	—	—	—	—	—	—	—	—	—	—	—	—

^aRatio of experimental-to-calculated isotopic concentrations. The experimental values are provided in Table 9. The SCALE input and output files for the evaluated samples are provided on the accompanying DVD (see Appendix B).

Table 97. SCALE calculation results for Trino Vercellese spent fuel samples (continued)

Sample ID	509-049-J8-4		509-049-J8-7		509-049-J8-9		509-049-L5-1		509-049-L5-4		509-049-L5-9		509-104-M11-7		509-069-E11-1	
Enrichment (%)	2.719		2.719		2.719		2.719		2.719		2.719		3.897		3.130	
Burnup (GWd/MTU)	14.770		15.193		11.127		7.822		14.323		10.187		12.042		12.859	
Nuclide ID	E/C ^a	E/C-1 (%)	E/C	E/C-1 (%)	E/C	E/C-1 (%)	E/C	E/C-1 (%)	E/C	E/C-1 (%)	E/C	E/C-1 (%)	E/C	E/C-1 (%)	E/C	E/C-1 (%)
U-234	0.712	-28.83	—	—	—	—	0.620	-37.98	0.775	-22.45	0.772	-22.80	—	—	—	—
U-235	0.951	-4.92	0.971	-2.87	0.983	-1.72	1.004	0.43	0.995	-0.51	0.983	-1.67	0.988	-1.22	0.998	-0.25
U-236	0.969	-3.11	0.978	-2.20	0.986	-1.40	0.935	-6.52	0.958	-4.15	1.018	1.75	1.034	3.36	1.050	4.95
U-238	1.000	0.01	0.999	-0.07	1.000	0.00	1.000	0.00	1.000	-0.01	1.000	-0.01	1.000	-0.05	1.001	0.12
Pu-238	—	—	—	—	—	—	—	—	—	—	—	—	—	—	1.055	5.50
Pu-239	0.983	-1.69	1.018	1.82	1.005	0.45	1.004	0.35	0.993	-0.70	0.999	-0.09	1.026	2.65	0.949	-5.06
Pu-240	1.013	1.27	1.024	2.44	1.016	1.57	0.995	-0.54	1.005	0.49	1.023	2.34	1.057	5.73	0.943	-5.66
Pu-241	1.066	6.61	1.085	8.54	1.084	8.41	1.035	3.51	1.040	4.04	1.090	8.96	1.116	11.61	0.949	-5.11
Pu-242	1.095	9.46	1.080	7.97	1.063	6.30	1.010	0.98	1.000	-0.05	1.063	6.29	1.119	11.93	0.931	-6.87
Am-242m	—	—	—	—	—	—	—	—	—	—	—	—	—	—	0.809	-19.06
Am-243	—	—	—	—	—	—	—	—	—	—	—	—	—	—	—	—
Cm-242	—	—	—	—	—	—	—	—	—	—	—	—	—	—	1.399	39.88
Cm-244	—	—	—	—	—	—	—	—	—	—	—	—	—	—	—	—
Ru-106	1.040	3.98	—	—	—	—	1.132	13.22	1.001	0.06	1.129	12.88	—	—	—	—
Cs-134	1.237	23.73	—	—	—	—	1.245	24.49	1.198	19.79	1.285	28.45	1.297	29.68	1.260	25.96
Cs-137	0.994	-0.60	—	—	—	—	1.000	0.00	0.990	-0.96	1.030	3.03	0.999	-0.10	1.002	0.16
Ce-144	0.997	-0.35	—	—	—	—	1.135	13.55	1.001	0.08	1.090	8.99	1.018	1.81	—	—
Nd-148	0.999	-0.10	0.998	-0.16	0.999	-0.11	—	—	1.001	0.12	0.999	-0.11	0.995	-0.50	—	—
Eu-154	—	—	—	—	—	—	—	—	—	—	—	—	—	—	1.224	22.35

^aRatio of experimental-to-calculated isotopic concentrations. The experimental values are provided in Table 9. The SCALE input and output files for the evaluated samples are provided on the accompanying DVD (see Appendix B).

Table 97. SCALE calculation results for Trino Vercellese spent fuel samples (continued)

Sample ID	509-069-E11-2		509-069-E11-4		509-069-E11-5		509-069-E11-7		509-069-E11-8		509-069-E11-9		509-069-E5-4		509-069-E5-7	
Enrichment (%)	3.130		3.130		3.130		3.130		3.130		3.130		3.130		3.130	
Burnup (GWd/MTU)	20.602		23.718		24.518		24.304		23.406		19.250		23.867		24.548	
Nuclide ID	E/C ^a	E/C-1 (%)	E/C	E/C-1 (%)	E/C	E/C-1 (%)	E/C	E/C-1 (%)	E/C	E/C-1 (%)	E/C	E/C-1 (%)	E/C	E/C-1 (%)	E/C	E/C-1 (%)
U-234	—	—	—	—	—	—	—	—	—	—	—	—	—	—	—	—
U-235	0.977	-2.29	0.958	-4.21	0.974	-2.58	0.979	-2.07	0.969	-3.08	0.983	-1.75	0.997	-0.30	0.978	-2.21
U-236	1.049	4.89	1.058	5.76	1.041	4.08	1.051	5.13	1.057	5.72	1.067	6.71	1.029	2.93	1.019	1.86
U-238	1.001	0.10	1.001	0.13	1.001	0.12	1.001	0.13	1.001	0.10	1.002	0.15	1.001	0.13	1.001	0.06
Pu-238	1.105	10.50	1.100	10.04	1.107	10.72	1.150	14.97	1.282	28.19	1.158	15.85	1.167	16.73	1.112	11.21
Pu-239	0.946	-5.39	0.925	-7.45	0.939	-6.10	0.963	-3.70	0.954	-4.55	0.986	-1.36	0.935	-6.52	0.948	-5.20
Pu-240	0.978	-2.15	0.980	-2.05	0.970	-3.01	1.005	0.51	0.987	-1.26	1.002	0.23	0.977	-2.32	0.974	-2.59
Pu-241	1.003	0.27	0.977	-2.31	0.953	-4.67	0.997	-0.28	1.023	2.26	1.019	1.92	0.990	-0.95	0.982	-1.78
Pu-242	1.003	0.34	1.018	1.80	0.932	-6.85	1.027	2.69	1.014	1.42	1.044	4.45	0.990	-1.05	0.990	-0.98
Am-242m	1.063	6.35	1.363	36.31	1.363	36.31	1.177	17.69	1.481	48.08	—	—	1.241	24.15	—	—
Am-243	0.895	-10.51	1.065	6.52	1.168	16.75	1.022	2.22	1.114	11.41	1.532	53.19	—	—	0.998	-0.20
Cm-242	1.409	40.94	1.422	42.25	1.409	40.88	1.510	51.01	1.520	52.00	1.720	72.00	1.338	33.82	1.396	39.57
Cm-244	0.994	-0.58	1.031	3.09	0.992	-0.78	1.063	6.29	0.978	-2.22	1.183	18.27	1.000	0.00	0.970	-2.95
Ru-106	—	—	—	—	—	—	—	—	—	—	—	—	—	—	—	—
Cs-134	1.224	22.37	1.179	17.94	1.154	15.45	1.166	16.63	—	—	—	—	1.178	17.77	1.170	17.04
Cs-137	1.006	0.55	0.998	-0.22	0.996	-0.45	0.988	-1.16	—	—	—	—	0.997	-0.34	1.009	0.92
Ce-144	—	—	—	—	—	—	—	—	—	—	—	—	—	—	—	—
Nd-148	1.006	0.64	1.007	0.69	1.028	2.77	1.007	0.70	1.007	0.68	1.006	0.58	1.006	0.56	1.005	0.49
Eu-154	1.224	22.41	1.183	18.34	0.984	-1.59	1.067	6.68	—	—	—	—	1.163	16.33	1.219	21.91

^aRatio of experimental-to-calculated isotopic concentrations. The experimental values are provided in Table 9. The SCALE input and output files for the evaluated samples are provided on the accompanying DVD (see Appendix B).

Table 97. SCALE calculation results for Trino Vercellese spent fuel samples (continued)

Sample ID	509-069-E5-9		509-069-J9-4		509-069-J9-7		509-069-L5-4		509-069-L5-7		509-069-L11-4		509-069-L11-7	
Enrichment (%)	3.130		3.130		3.130		3.130		3.130		3.130		3.130	
Burnup (GWd/MTU)	19.208		24.849		25.258		24.330		24.313		23.928		24.362	
Nuclide ID	E/C ^a	E/C-1 (%)	E/C	E/C-1 (%)	E/C	E/C-1 (%)	E/C	E/C-1 (%)	E/C	E/C-1 (%)	E/C	E/C-1 (%)	E/C	E/C-1 (%)
U-234	—	—	—	—	—	—	—	—	—	—	—	—	—	—
U-235	0.992	-0.76	0.978	-2.25	0.984	-1.64	1.019	1.95	0.977	-2.27	0.992	-0.77	0.974	-2.59
U-236	1.079	7.86	1.037	3.72	1.042	4.23	1.005	0.50	1.030	3.04	1.095	9.51	0.999	-0.06
U-238	1.001	0.08	1.000	0.04	1.001	0.10	1.001	0.12	0.999	-0.08	1.001	0.06	1.000	0.02
Pu-238	1.081	8.10	1.131	13.15	1.254	25.36	1.052	5.24	1.123	12.35	1.051	5.12	1.136	13.61
Pu-239	0.927	-7.35	0.937	-6.31	0.952	-4.79	0.946	-5.39	0.950	-4.95	0.951	-4.90	0.953	-4.69
Pu-240	0.949	-5.14	0.971	-2.91	0.983	-1.71	0.963	-3.67	0.986	-1.38	0.991	-0.92	0.995	-0.47
Pu-241	0.959	-4.10	0.988	-1.20	1.001	0.06	0.977	-2.34	1.000	0.01	0.987	-1.30	0.992	-0.83
Pu-242	0.965	-3.46	1.014	1.39	1.030	2.98	0.962	-3.80	0.997	-0.30	1.012	1.19	1.027	2.74
Am-242m	—	—	1.096	9.58	0.976	-2.38	—	—	—	—	1.124	12.38	—	—
Am-243	—	—	—	—	1.013	1.26	—	—	—	—	1.018	1.80	0.942	-5.80
Cm-242	1.389	38.93	1.380	37.99	1.522	52.23	1.397	39.70	1.410	40.96	1.605	60.46	1.393	39.31
Cm-244	0.839	-16.09	1.041	4.06	0.916	-8.37	0.977	-2.32	0.948	-5.25	1.010	0.98	1.038	3.77
Ru-106	—	—	—	—	—	—	—	—	—	—	—	—	—	—
Cs-134	1.225	22.49	1.171	17.08	—	—	1.135	13.55	1.172	17.23	—	—	1.185	18.53
Cs-137	1.004	0.38	1.002	0.23	—	—	0.989	-1.12	1.001	0.13	—	—	1.007	0.68
Ce-144	—	—	—	—	—	—	—	—	—	—	—	—	—	—
Nd-148	1.010	1.02	—	—	1.007	0.66	1.001	0.14	—	—	1.007	0.68	1.006	0.56
Eu-154	1.211	21.11	1.056	5.55	—	—	1.123	12.30	1.197	19.67	—	—	1.108	10.77

^aRatio of experimental-to-calculated isotopic concentrations. The experimental values are provided in Table 9. The SCALE input and output files for the evaluated samples are provided on the accompanying DVD (see Appendix B).

Table 98. SCALE calculation results for Obrigheim spent fuel samples

Sample ID	BE124.D1P1		BE124.D1P3		BE124.E3P1		BE124.E3P2		BE124.E3P3		BE124.E3P4		BE124.E3P5		BE124.G7P1	
Enrichment (%)	3.00		3.00		3.00		3.00		3.00		3.00		3.00		3.00	
Burnup (GWd/MTU)	21.17		33.75		20.18		29.35		36.26		30.92		22.86		17.13	
Nuclide ID	E/C ^a	E/C-1 (%)	E/C	E/C-1 (%)	E/C	E/C-1 (%)	E/C	E/C-1 (%)	E/C	E/C-1 (%)	E/C	E/C-1 (%)	E/C	E/C-1 (%)	E/C	E/C-1 (%)
U-235	1.116	11.63	1.012	1.18	1.017	1.66	1.065	6.52	1.080	8.03	1.002	0.20	1.047	4.70	1.032	3.16
U-236	0.947	-5.35	1.036	3.61	0.915	-8.54	1.007	0.75	1.024	2.41	1.016	1.61	1.096	9.60	1.053	5.27
U-238	1.000	-0.05	1.001	0.14	1.001	0.12	0.993	-0.68	1.001	0.09	1.001	0.06	1.000	0.01	1.000	0.04
Pu-238	0.768	-23.22	1.140	13.97	1.055	5.45	1.121	12.11	1.096	9.63	1.028	2.82	1.103	10.29	1.081	8.11
Pu-239	0.925	-7.51	0.940	-6.01	0.983	-1.66	0.972	-2.82	0.952	-4.82	0.984	-1.61	0.992	-0.75	0.968	-3.17
Pu-240	0.870	-13.01	0.984	-1.57	0.964	-3.64	0.963	-3.70	0.970	-2.98	1.009	0.89	0.974	-2.60	0.974	-2.56
Pu-241	0.816	-18.38	0.971	-2.92	0.929	-7.13	0.964	-3.57	0.954	-4.62	1.005	0.48	1.000	-0.03	0.978	-2.19
Pu-242	0.696	-30.42	0.998	-0.21	0.880	-11.99	0.928	-7.17	0.951	-4.94	1.012	1.25	0.924	-7.55	0.950	-5.02
Cm-244	0.606	-39.42	0.986	-1.45	0.801	-19.85	0.780	-22.05	0.931	-6.92	1.029	2.91	0.935	-6.50	0.810	-19.05
Cs-137	—	—	0.974	-2.61	0.956	-4.37	—	—	0.962	-3.80	0.982	-1.82	0.976	-2.35	0.979	-2.09

^aRatio of experimental-to-calculated isotopic concentrations. The experimental values are provided in Table 16. The SCALE input and output files for the evaluated samples are provided on the accompanying DVD (see Appendix B).

Table 98. SCALE calculation results for Obrigheim spent fuel samples (continued)

Sample ID	BE124.G7P2		BE124.G7P3		BE124.G7P4		BE124.G7P5		BE124.M14P1		BE124.M14P3		BE124.M14P4	
Enrichment (%)	3.00		3.00		3.00		3.00		3.00		3.00		3.00	
Burnup (GWd/MTU)	25.83		31.32		27.71		25.81		15.60		29.36		24.90	
Nuclide ID	E/C ^a	E/C-1 (%)	E/C	E/C-1 (%)	E/C	E/C-1 (%)	E/C	E/C-1 (%)	E/C	E/C-1 (%)	E/C	E/C-1 (%)	E/C	E/C-1 (%)
U-235	1.087	8.67	0.974	-2.59	1.077	7.70	0.986	-1.36	0.997	-0.30	1.035	3.54	0.974	-2.62
U-236	1.097	9.69	1.039	3.87	1.119	11.94	1.029	2.88	1.046	4.60	1.025	2.50	1.047	4.66
U-238	1.000	0.02	1.001	0.09	1.000	0.00	1.000	0.02	1.000	0.02	1.001	0.10	1.000	0.03
Pu-238	1.059	5.89	1.205	20.48	1.140	14.04	0.992	-0.77	1.097	9.71	1.050	5.02	1.043	4.28
Pu-239	0.940	-5.97	0.945	-5.53	0.960	-4.00	0.975	-2.52	0.946	-5.43	0.964	-3.57	0.969	-3.07
Pu-240	0.968	-3.22	1.010	1.01	0.998	-0.24	1.019	1.92	0.980	-1.97	0.977	-2.32	1.009	0.91
Pu-241	0.959	-4.11	0.975	-2.52	0.991	-0.87	1.013	1.29	0.953	-4.68	0.970	-3.01	1.012	1.24
Pu-242	0.919	-8.06	1.021	2.05	1.000	-0.03	1.031	3.06	0.937	-6.31	0.924	-7.60	1.049	4.87
Cm-244	0.980	-2.04	1.137	13.73	1.102	10.23	0.983	-1.67	1.323	32.28	0.973	-2.69	0.980	-1.98
Cs-137	0.952	-4.75	0.994	-0.61	0.978	-2.17	—	—	—	—	0.972	-2.82	—	—

^aRatio of experimental-to-calculated isotopic concentrations. The experimental values are provided in Table 16. The SCALE input and output files for the evaluated samples are provided on the accompanying DVD (see Appendix B).

Table 98. SCALE calculation results for Obrigheim spent fuel samples (continued)

Sample ID	BE210.G14P31		BE210.G14P41		BE210.G14P51		BE210.G14P52		BE210.K14P1		BE210.K14P31		BE210.K14P41	
Enrichment (%)	2.83		2.83		2.83		2.83		2.83		2.83		2.83	
Burnup (GWd/MTU)	37.49		35.64		30.16		24.22		22.90		36.67		32.99	
Nuclide ID	E/C ^a	E/C-1 (%)	E/C	E/C-1 (%)	E/C	E/C-1 (%)	E/C	E/C-1 (%)	E/C	E/C-1 (%)	E/C	E/C-1 (%)	E/C	E/C-1 (%)
U-235	0.980	-1.99	0.900	-9.96	0.862	-13.85	0.918	-8.21	0.997	-0.28	0.968	-3.19	0.800	-20.04
U-236	1.009	0.87	1.041	4.10	1.019	1.87	1.020	2.04	1.012	1.18	1.008	0.82	1.031	3.07
U-238	1.001	0.13	1.003	0.28	1.003	0.32	1.003	0.27	0.998	-0.20	1.002	0.19	1.002	0.19
Pu-238	0.974	-2.58	1.011	1.12	1.022	2.22	0.942	-5.81	1.149	14.89	1.048	4.79	0.946	-5.45
Pu-239	0.882	-11.82	0.838	-16.21	0.848	-15.19	0.867	-13.33	0.987	-1.25	0.913	-8.68	0.871	-12.95
Pu-240	0.951	-4.86	0.931	-6.89	0.939	-6.15	0.934	-6.59	1.025	2.51	0.958	-4.24	0.986	-1.45
Pu-241	0.935	-6.52	0.873	-12.72	0.907	-9.28	0.902	-9.84	1.072	7.23	0.946	-5.41	0.935	-6.46
Pu-242	1.046	4.59	1.007	0.68	1.040	3.99	0.993	-0.67	1.088	8.80	1.029	2.88	1.148	14.81
Cm-244	0.902	-9.77	0.960	-3.98	0.926	-7.39	0.793	-20.67	1.110	11.01	0.986	-1.43	0.911	-8.90
Cs-137	0.993	-0.68	0.983	-1.73	1.003	0.31	0.993	-0.72	0.981	-1.85	0.967	-3.32	—	—

^aRatio of experimental-to-calculated isotopic concentrations. The experimental values are provided in Table 16. The SCALE input and output files for the evaluated samples are provided on the accompanying DVD (see Appendix B).

Table 98. SCALE calculation results for Obrigheim spent fuel samples (continued)

Sample ID	BE168		BE170		BE171		BE172		BE176	
Enrichment (%)	3.13		3.13		3.13		3.13		3.13	
Burnup (GWd/MTU)	29.350		27.005		28.655		27.890		28.755	
Nuclide ID	E/C ^a	E/C-1 (%)	E/C	E/C-1 (%)	E/C	E/C-1 (%)	E/C	E/C-1 (%)	E/C	E/C-1 (%)
U-235	1.035	3.53	1.032	3.17	1.035	3.46	1.017	1.67	1.024	2.36
U-236	0.985	-1.49	0.989	-1.14	0.984	-1.63	0.980	-2.00	0.985	-1.47
U-238	1.000	0.02	1.000	0.03	1.000	0.03	1.001	0.07	1.000	0.04
Pu-238	1.149	14.94	1.042	4.24	1.045	4.53	1.008	0.76	1.075	7.53
Pu-239	0.993	-0.70	0.980	-2.01	0.981	-1.89	0.960	-4.02	0.982	-1.82
Pu-240	0.990	-1.02	0.985	-1.52	0.970	-3.02	0.963	-3.66	0.978	-2.22
Pu-241	1.053	5.25	1.049	4.89	1.036	3.56	1.019	1.87	1.048	4.79
Pu-242	1.111	11.09	1.087	8.74	1.064	6.36	1.090	8.97	1.098	9.77
Cm-244	1.124	12.42	1.178	17.79	1.141	14.06	1.155	15.54	1.182	18.20
Cs-137	—	—	—	—	—	—	—	—	—	—

^aRatio of experimental-to-calculated isotopic concentrations. The experimental values are provided in Table 12. The SCALE input and output files for the evaluated samples are provided on the accompanying DVD (see Appendix B).

Table 99. SCALE calculation results for Turkey Point Unit 3 spent fuel samples

Sample ID	D01.G9		D01.G10		D01.H9		D04.G9		D04.G10	
Enrichment (%)	2.556		2.556		2.556		2.556		2.556	
Burnup (GWd/MTU)	30.72		30.51		31.56		31.26		31.31	
Nuclide ID	E/C ^a	E/C-1 (%)	E/C	E/C-1 (%)	E/C	E/C-1 (%)	E/C	E/C-1 (%)	E/C	E/C-1 (%)
U-234	0.966	-3.37	0.961	-3.88	0.910	-8.98	0.836	-16.38	0.974	-2.56
U-235	1.038	3.76	0.989	-1.13	1.049	4.91	1.005	0.46	1.031	3.11
U-236	0.965	-3.51	0.968	-3.22	0.933	-6.73	0.930	-6.95	0.959	-4.10
U-238	1.002	0.15	1.002	0.18	1.001	0.14	1.002	0.17	1.002	0.17
Pu-238	1.019	1.93	1.036	3.56	1.025	2.54	1.004	0.35	0.992	-0.81
Pu-239	0.964	-3.64	0.966	-3.39	0.996	-0.38	0.985	-1.55	0.953	-4.73
Pu-240	0.970	-2.98	0.987	-1.27	0.966	-3.42	0.979	-2.12	0.961	-3.93
Pu-241	1.003	0.28	1.010	1.04	1.027	2.74	1.041	4.11	0.993	-0.68
Pu-242	0.937	-6.32	0.988	-1.20	0.956	-4.41	0.967	-3.31	0.934	-6.62
Nd-148	0.982	-1.76	0.982	-1.82	0.983	-1.73	0.982	-1.76	0.982	-1.82

^aRatio of experimental-to-calculated isotopic concentrations. The experimental values are provided in Table 18. The SCALE input and output files for the evaluated samples are provided on the accompanying DVD (see Appendix B).

Table 100. SCALE calculation results for H. B. Robinson Unit 2 spent fuel samples

Sample ID	N-9B-N		N-9B-S		N-9C-D		N-9C-J	
Enrichment (%)	2.561		2.561		2.561		2.561	
Burnup (GWd/MTU)	23.81		16.02		31.66		28.47	
Nuclide ID	E/C ^a	E/C-1 (%)	E/C	E/C-1 (%)	E/C	E/C-1 (%)	E/C	E/C-1 (%)
U-234	0.991	-0.92	0.992	-0.79	0.890	-10.99	0.915	-8.46
U-235	1.004	0.36	0.997	-0.34	0.980	-1.97	1.065	6.47
U-236	1.020	1.95	1.019	1.89	0.995	-0.52	0.976	-2.42
U-238	1.006	0.58	0.998	-0.18	1.001	0.07	0.994	-0.56
Pu-238	1.153	15.32	1.145	14.54	1.110	11.00	1.215	21.49
Pu-239	0.989	-1.13	0.988	-1.22	0.958	-4.21	1.064	6.43
Pu-240	0.984	-1.59	0.974	-2.60	0.961	-3.94	0.980	-2.04
Pu-241	1.060	5.98	1.056	5.65	1.017	1.72	1.113	11.32
Pu-242	1.020	1.97	0.998	-0.22	0.997	-0.35	0.982	-1.80
Np-237	1.118	11.76	1.114	11.40	0.985	-1.46	1.024	2.38
Tc-99	0.892	-10.84	0.861	-13.88	0.859	-14.10	0.844	-15.57
Cs-137	1.190	18.99	1.011	1.08	0.996	-0.42	0.981	-1.92
Nd-143	0.932	-6.79	0.950	-4.97	0.895	-10.49	0.962	-3.82
Nd-144	0.958	-4.16	0.965	-3.46	0.926	-7.38	0.949	-5.13
Nd-145	0.957	-4.34	0.962	-3.83	0.919	-8.09	0.959	-4.06
Nd-146	0.958	-4.24	0.958	-4.19	0.911	-8.91	0.956	-4.44
Nd-148	0.987	-1.33	0.976	-2.41	0.934	-6.64	0.979	-2.14
Nd-150	0.979	-2.05	0.967	-3.31	0.927	-7.33	0.978	-2.17

^aRatio of experimental-to-calculated isotopic concentrations. The experimental values are provided in Table 21. The SCALE input and output files for the evaluated samples are provided on the accompanying DVD (see Appendix B).

Table 101. SCALE calculation results for Calvert Cliffs Unit 1 spent fuel samples

Sample ID	106-NBD107-GG		106-NBD107-MM		106-NBD107-Q		104-MKP109-CC		104-MKP109-LL	
Enrichment (%)	2.453		2.453		2.453		3.038		3.038	
Burnup (GWd/MTU)	37.27		31.40		46.46		36.90 ^a		27.11 ^a	
Nuclide ID	E/C ^b	E/C-1 (%)	E/C	E/C-1 (%)	E/C	E/C-1 (%)	E/C	E/C-1 (%)	E/C	E/C-1 (%)
U-234	1.187	18.74	1.310	30.95	0.796	-20.36	1.027	2.72	1.014	1.41
U-235	1.097	9.71	1.050	5.03	1.037	3.70	1.014	1.38	1.009	0.92
U-236	1.005	0.51	0.983	-1.73	0.999	-0.14	0.976	-2.41	0.979	-2.06
U-238	1.013	1.26	1.008	0.82	1.002	0.20	1.004	0.42	1.007	0.66
Pu-238	1.116	11.58	1.118	11.82	1.130	13.00	1.078	7.84	1.103	10.25
Pu-239	1.028	2.81	1.029	2.88	0.994	-0.59	0.966	-3.42	0.973	-2.69
Pu-240	0.994	-0.60	0.992	-0.84	0.987	-1.29	0.989	-1.15	0.992	-0.85
Pu-241	1.109	10.93	1.114	11.44	1.065	6.46	1.027	2.72	1.027	2.71
Pu-242	1.052	5.19	1.055	5.52	1.068	6.79	0.999	-0.07	1.003	0.34
Np-237	0.893	-10.73	0.870	-13.05	0.857	-14.28	0.870	-13.01	0.942	-5.80
Am-241	1.233	23.31	1.098	9.83	1.671	67.14	1.113	11.30	1.049	4.85
Se-79	1.630	62.96	1.391	39.07	1.457	45.70	0.857	-14.26	0.790	-20.97
Sr-90	0.974	-2.61	0.980	-1.95	0.987	-1.35	0.993	-0.74	0.981	-1.94
Tc-99	0.678	-32.25	0.671	-32.90	0.693	-30.68	0.923	-7.67	0.939	-6.11
Rh-103	1.250	25.02	—	—	—	—	—	—	—	—
Sn-126	0.643	-35.75	0.699	-30.15	0.646	-35.40	0.782	-21.79	0.757	-24.26
Cs-133	—	—	—	—	—	—	0.981	-1.87	0.993	-0.74
Cs-135	0.954	-4.57	0.974	-2.56	1.010	0.98	0.942	-5.75	0.940	-6.01
Cs-137	0.993	-0.73	1.025	2.53	1.047	4.65	1.001	0.07	1.012	1.17
Nd-143	1.012	1.19	—	—	—	—	0.988	-1.15	0.993	-0.67
Nd-144	1.014	1.43	—	—	—	—	1.010	1.05	1.010	0.97
Nd-145	1.013	1.26	—	—	—	—	1.009	0.85	1.006	0.58
Nd-146	0.991	-0.89	—	—	—	—	0.992	-0.77	0.994	-0.65
Nd-148	1.008	0.82	—	—	—	—	1.000	-0.02	1.000	-0.05
Nd-150	—	—	—	—	—	—	0.968	-3.21	0.977	-2.29
Sm-147	1.008	0.78	—	—	—	—	0.995	-0.50	0.966	-3.40
Sm-148	1.032	3.20	—	—	—	—	1.015	1.47	1.004	0.39
Sm-149	—	—	—	—	—	—	—	—	—	—
Sm-150	0.973	-2.75	—	—	—	—	0.926	-7.41	0.940	-6.04
Sm-151	0.854	-14.56	—	—	—	—	0.780	-22.02	0.694	-30.57
Sm-152	0.812	-18.80	—	—	—	—	0.762	-23.80	0.809	-19.06
Sm-154	1.000	0.03	—	—	—	—	0.921	-7.87	1.123	12.30
Eu-153	1.047	4.66	—	—	—	—	0.966	-3.42	0.966	-3.41
Eu-154	1.045	4.47	—	—	—	—	0.985	-1.50	1.032	3.19
Eu-155	1.640	64.02	—	—	—	—	1.421	42.08	1.439	43.85
Gd-154	0.587	-41.32	—	—	—	—	0.760	-24.01	1.244	24.43
Gd-155	1.123	12.34	—	—	—	—	1.338	33.75	1.916	91.55
Gd-156	0.580	-41.96	—	—	—	—	0.731	-26.87	1.327	32.68
Gd-158	0.607	-39.29	—	—	—	—	0.708	-29.16	1.225	22.55
Gd-160	0.344	-65.59	—	—	—	—	—	—	1.927	92.67

^aBurnup based on measured ¹⁴⁸Nd.

^bRatio of experimental-to-calculated isotopic concentrations. The experimental values are provided in Table 28 and Table 29. The SCALE input and output files for the evaluated samples are provided on the accompanying DVD (see Appendix B).

Table 101. SCALE calculation results for Calvert Cliffs Unit 1 spent fuel samples (continued)

Sample ID	104-MKP109-P		103-MLA098-BB		103-MLA098-JJ		103-MLA098-P	
Enrichment (%)	3.038		2.72		2.72		2.72	
Burnup (GWd/MTU)	44.13 ^a		26.62		18.68		33.17	
Nuclide ID	E/C ^b	E/C-1 (%)	E/C	E/C-1 (%)	E/C	E/C-1 (%)	E/C	E/C-1 (%)
U-234	0.977	-2.27	0.873	-12.65	0.892	-10.77	0.958	-4.20
U-235	0.992	-0.81	1.003	0.26	0.995	-0.49	0.954	-4.55
U-236	0.982	-1.80	1.019	1.88	1.023	2.33	1.025	2.49
U-238	1.002	0.23	1.017	1.74	1.012	1.24	1.010	1.01
Pu-238	1.067	6.66	1.127	12.65	1.261	26.15	1.062	6.17
Pu-239	0.939	-6.10	0.976	-2.37	0.989	-1.15	0.919	-8.14
Pu-240	0.984	-1.61	0.981	-1.90	0.995	-0.52	0.963	-3.66
Pu-241	1.005	0.45	1.053	5.30	1.079	7.89	1.001	0.05
Pu-242	1.020	1.98	1.029	2.90	1.045	4.49	1.046	4.60
Np-237	0.942	-5.83	1.087	8.67	1.004	0.43	0.945	-5.55
Am-241	1.088	8.79	1.038	3.85	1.062	6.22	1.016	1.56
Se-79	0.790	-20.97	0.882	-11.77	0.914	-8.60	0.876	-12.40
Sr-90	0.981	-1.94	0.995	-0.47	1.004	0.37	1.006	0.62
Tc-99	0.876	-12.38	0.939	-6.12	0.975	-2.49	0.937	-6.26
Rh-103	—	—	—	—	—	—	—	—
Sn-126	0.757	-24.26	0.841	-15.85	0.823	-17.75	0.797	-20.35
Cs-133	0.970	-3.00	—	—	—	—	—	—
Cs-135	0.946	-5.36	0.936	-6.39	0.941	-5.93	0.918	-8.24
Cs-137	1.015	1.48	1.020	2.03	1.021	2.09	1.012	1.19
Nd-143	0.975	-2.51	—	—	—	—	—	—
Nd-144	1.017	1.73	—	—	—	—	—	—
Nd-145	1.008	0.85	—	—	—	—	—	—
Nd-146	0.992	-0.83	—	—	—	—	—	—
Nd-148	1.000	-0.01	—	—	—	—	—	—
Nd-150	0.960	-4.03	—	—	—	—	—	—
Sm-147	1.091	9.13	—	—	—	—	—	—
Sm-148	1.092	9.22	—	—	—	—	—	—
Sm-149	—	—	—	—	—	—	—	—
Sm-150	0.958	-4.24	—	—	—	—	—	—
Sm-151	0.783	-21.72	—	—	—	—	—	—
Sm-152	0.804	-19.60	—	—	—	—	—	—
Sm-154	1.067	6.68	—	—	—	—	—	—
Eu-153	0.965	-3.48	—	—	—	—	—	—
Eu-154	0.991	-0.91	—	—	—	—	—	—
Eu-155	1.431	43.11	—	—	—	—	—	—
Gd-154	0.759	-24.08	—	—	—	—	—	—
Gd-155	1.384	38.45	—	—	—	—	—	—
Gd-156	0.612	-38.80	—	—	—	—	—	—
Gd-158	0.662	-33.76	—	—	—	—	—	—
Gd-160	—	—	—	—	—	—	—	—

^aBurnup based on measured ¹⁴⁸Nd.

^bRatio of experimental-to-calculated isotopic concentrations. The experimental values are provided in Table 26 and Table 28. The SCALE input and output files for the evaluated samples are provided on the accompanying DVD (see Appendix B).

Table 102. SCALE calculation results for the Takahama Unit 3 spent fuel samples

Sample ID	NT3G23.SF95-1		NT3G23.SF95-2		NT3G23.SF95-3		NT3G23.SF95-4		NT3G23.SF95-5	
Enrichment (%)	4.11		4.11		4.11		4.11		4.11	
Burnup (GWd/MTU)	14.18		24.46		35.68		37.01		30.45	
Nuclide ID	E/C ^a	E/C-1 (%)	E/C	E/C-1 (%)	E/C	E/C-1 (%)	E/C	E/C-1 (%)	E/C	E/C-1 (%)
U-234	0.913	-8.73	1.015	1.50	0.794	-20.64	0.803	-19.72	1.089	8.94
U-235	0.986	-1.37	0.974	-2.55	0.973	-2.73	0.968	-3.19	0.977	-2.30
U-236	1.002	0.18	1.016	1.58	0.999	-0.07	1.000	-0.03	1.011	1.05
U-238	1.002	0.17	1.002	0.15	1.002	0.21	1.002	0.18	1.002	0.18
Pu-238	0.943	-5.69	1.035	3.54	0.945	-5.48	0.944	-5.56	0.980	-2.02
Pu-239	0.883	-11.69	0.913	-8.65	0.905	-9.52	0.910	-8.96	0.911	-8.90
Pu-240	0.944	-5.62	0.960	-4.05	0.930	-6.99	0.925	-7.54	0.932	-6.79
Pu-241	0.913	-8.70	0.991	-0.92	0.984	-1.62	0.976	-2.35	0.976	-2.43
Pu-242	0.907	-9.28	0.996	-0.42	1.002	0.21	0.989	-1.07	0.971	-2.87
Np-237	—	—	—	—	—	—	—	—	—	—
Am-241	1.088	8.80	0.808	-19.21	0.805	-19.52	0.585	-41.52	0.842	-15.80
Am-242m	0.835	-16.45	0.850	-15.02	0.851	-14.86	0.833	-16.68	0.817	-18.33
Am-243	0.769	-23.09	0.814	-18.58	0.814	-18.58	0.795	-20.52	0.808	-19.16
Cm-242	1.227	22.73	1.435	43.49	1.590	59.03	1.816	81.55	1.221	22.09
Cm-243	1.114	11.45	1.234	23.41	1.108	10.83	1.138	13.80	1.265	26.52
Cm-244	0.813	-18.66	0.999	-0.13	0.915	-8.50	0.924	-7.56	0.887	-11.29
Cm-245	0.943	-5.65	1.267	26.74	1.146	14.56	1.211	21.09	1.166	16.58
Cm-246	1.985	98.53	1.839	83.86	1.247	24.72	1.267	26.74	0.803	-19.67
Cm-247	—	—	—	—	—	—	—	—	—	—
Ru-106	0.985	-1.51	0.825	-17.48	0.766	-23.40	0.756	-24.43	0.885	-11.47
Sb-125	0.519	-48.12	0.535	-46.52	0.439	-56.10	0.359	-64.12	0.469	-53.12
Cs-134	1.117	11.69	1.156	15.61	1.132	13.20	1.129	12.92	1.146	14.56
Cs-137	1.027	2.69	1.029	2.88	1.019	1.91	1.021	2.06	1.016	1.62
Ce-144	1.031	3.10	1.017	1.72	1.046	4.60	0.952	-4.81	1.015	1.53
Nd-142	1.261	26.07	1.074	7.42	1.170	17.01	1.136	13.57	1.057	5.72
Nd-143	1.030	2.98	1.018	1.79	1.015	1.51	1.006	0.58	1.013	1.34
Nd-144	1.011	1.13	1.015	1.50	1.007	0.66	1.043	4.30	1.014	1.40
Nd-145	1.006	0.61	1.001	0.07	1.002	0.19	0.995	-0.48	0.998	-0.18
Nd-146	0.983	-1.71	0.980	-2.00	0.978	-2.17	0.978	-2.25	0.978	-2.24
Nd-148	1.001	0.08	1.000	0.04	1.001	0.06	1.000	0.04	1.001	0.05
Nd-150	1.013	1.29	0.993	-0.68	0.998	-0.18	0.995	-0.50	0.988	-1.18
Sm-147	—	—	—	—	—	—	—	—	—	—
Sm-148	—	—	—	—	—	—	—	—	—	—
Sm-149	—	—	—	—	—	—	—	—	—	—
Sm-150	—	—	—	—	—	—	—	—	—	—
Sm-151	—	—	—	—	—	—	—	—	—	—
Sm-152	—	—	—	—	—	—	—	—	—	—
Sm-154	—	—	—	—	—	—	—	—	—	—
Eu-154	0.958	-4.24	0.994	-0.60	0.951	-4.89	0.979	-2.14	0.975	-2.47

^aRatio of experimental-to-calculated isotopic concentrations. The experimental values are provided in Table 32. The SCALE input and output files for the evaluated samples are provided on the accompanying DVD (see Appendix B).

Table 102. SCALE calculation results for the Takahama Unit 3 spent fuel samples (continued)

Sample ID	NT3G23.SF96-1		NT3G23.SF96-2		NT3G23.SF96-3		NT3G23.SF96-4		NT3G23.SF96-5	
Enrichment (%)	2.63		2.63		2.63		2.63		2.63	
Burnup (GWd/MTU)	8.63		17.43		29.69		30.41		25.42	
Nuclide ID	E/C ^a	E/C-1 (%)	E/C	E/C-1 (%)	E/C	E/C-1 (%)	E/C	E/C-1 (%)	E/C	E/C-1 (%)
U-234	1.080	8.05	1.059	5.92	1.080	8.05	1.086	8.62	1.071	7.11
U-235	0.986	-1.42	0.991	-0.90	0.988	-1.22	0.980	-1.98	0.997	-0.32
U-236	1.015	1.51	1.015	1.48	1.005	0.48	1.009	0.92	1.004	0.39
U-238	1.001	0.14	1.001	0.10	1.001	0.12	1.001	0.11	1.001	0.08
Pu-238	0.850	-14.97	1.046	4.56	1.031	3.05	1.066	6.58	1.010	1.01
Pu-239	0.825	-17.51	0.964	-3.58	0.974	-2.57	0.985	-1.52	0.974	-2.65
Pu-240	0.881	-11.86	0.941	-5.92	0.935	-6.52	0.945	-5.53	0.922	-7.77
Pu-241	0.802	-19.76	0.996	-0.37	1.000	0.02	1.013	1.33	0.990	-1.00
Pu-242	0.820	-18.01	0.962	-3.81	0.974	-2.65	0.987	-1.27	0.939	-6.05
Np-237	0.742	-25.80	0.696	-30.37	0.604	-39.64	0.628	-37.20	0.658	-34.24
Am-241	0.605	-39.45	0.711	-28.88	0.795	-20.52	0.898	-10.19	0.699	-30.06
Am-242m	0.782	-21.78	0.951	-4.92	0.836	-16.36	0.956	-4.43	0.934	-6.64
Am-243	0.609	-39.09	0.810	-19.04	0.815	-18.55	0.850	-14.99	0.783	-21.68
Cm-242	1.006	0.60	1.269	26.94	1.254	25.39	1.281	28.14	1.207	20.74
Cm-243	—	—	—	—	—	—	—	—	—	—
Cm-244	0.674	-32.58	0.955	-4.47	0.948	-5.17	0.998	-0.21	0.897	-10.31
Cm-245	—	—	—	—	—	—	—	—	—	—
Cm-246	—	—	—	—	—	—	—	—	—	—
Cm-247	—	—	—	—	—	—	—	—	—	—
Ru-106	0.783	-21.69	0.658	-34.25	0.735	-26.54	0.661	-33.88	0.890	-10.98
Sb-125	0.762	-23.82	0.656	-34.39	0.457	-54.25	0.568	-43.15	0.558	-44.20
Cs-134	0.955	-4.53	1.084	8.42	1.042	4.24	1.061	6.07	1.033	3.30
Cs-137	0.962	-3.85	0.968	-3.22	0.951	-4.89	0.959	-4.07	0.938	-6.24
Ce-144	0.991	-0.86	0.948	-5.18	0.865	-13.55	0.866	-13.39	0.925	-7.46
Nd-142	—	—	—	—	—	—	—	—	—	—
Nd-143	1.033	3.35	1.024	2.45	1.020	2.02	1.016	1.57	1.031	3.11
Nd-144	1.059	5.86	1.056	5.60	1.104	10.44	1.088	8.79	1.067	6.73
Nd-145	1.001	0.12	0.994	-0.60	0.994	-0.64	0.989	-1.07	0.997	-0.27
Nd-146	1.001	0.08	0.996	-0.37	0.993	-0.67	0.993	-0.66	0.996	-0.40
Nd-148	0.992	-0.82	0.999	-0.15	1.000	-0.05	1.000	-0.03	0.999	-0.06
Nd-150	0.986	-1.44	0.993	-0.66	0.988	-1.24	0.988	-1.22	0.984	-1.62
Sm-147	—	—	—	—	—	—	—	—	—	—
Sm-148	—	—	—	—	—	—	—	—	—	—
Sm-149	—	—	—	—	—	—	—	—	—	—
Sm-150	—	—	—	—	—	—	—	—	—	—
Sm-151	—	—	—	—	—	—	—	—	—	—
Sm-152	—	—	—	—	—	—	—	—	—	—
Sm-154	—	—	—	—	—	—	—	—	—	—
Eu-154	0.966	-3.40	1.035	3.52	0.934	-6.61	0.944	-5.62	0.937	-6.31

^aRatio of experimental-to-calculated isotopic concentrations. The experimental values are provided in Table 33. The SCALE input and output files for the evaluated samples are provided on the accompanying DVD (see Appendix B).

Table 102. SCALE calculation results for the Takahama Unit 3 spent fuel samples (continued)

Sample ID	NT3G24.SF97-1		NT3G24.SF97-2		NT3G24.SF97-3	
Enrichment (%)	4.11		4.11		4.11	
Burnup (GWd/MTU)	17.39		30.48		42.10	
Nuclide ID	E/C ^a	E/C-1 (%)	E/C	E/C-1 (%)	E/C	E/C-1 (%)
U-234	0.936	-6.42	0.909	-9.15	0.935	-6.52
U-235	0.959	-4.11	0.983	-1.69	0.979	-2.09
U-236	1.002	0.19	1.007	0.73	1.004	0.39
U-238	1.003	0.27	1.001	0.09	1.001	0.08
Pu-238	0.793	-20.72	1.082	8.21	1.088	8.84
Pu-239	0.759	-24.10	0.952	-4.81	0.947	-5.33
Pu-240	0.886	-11.36	0.938	-6.16	0.925	-7.49
Pu-241	0.786	-21.41	1.033	3.26	1.022	2.25
Pu-242	0.850	-14.96	1.011	1.12	1.017	1.73
Np-237	0.822	-17.80	0.991	-0.86	0.963	-3.74
Am-241	0.587	-41.31	0.777	-22.28	0.778	-22.19
Am-242m	0.488	-51.19	0.800	-19.96	0.845	-15.51
Am-243	0.604	-39.61	0.894	-10.60	0.887	-11.25
Cm-242	0.875	-12.48	1.065	6.47	0.983	-1.67
Cm-243	0.822	-17.81	1.263	26.33	1.219	21.86
Cm-244	0.586	-41.40	1.068	6.85	1.056	5.55
Cm-245	0.621	-37.90	1.473	47.34	1.456	45.62
Cm-246	0.771	-22.87	15.748	1,474.80	1.551	55.13
Cm-247	—	—	1.581	58.13	1.513	51.33
Ru-106	1.094	9.45	1.060	5.99	1.022	2.18
Sb-125	0.776	-22.39	0.824	-17.57	0.543	-45.73
Cs-134	1.095	9.46	1.268	26.76	1.218	21.77
Cs-137	1.039	3.89	1.032	3.21	1.029	2.89
Ce-144	1.234	23.43	1.122	12.22	1.028	2.77
Nd-142	—	—	—	—	—	—
Nd-143	1.011	1.07	1.003	0.32	0.998	-0.22
Nd-144	0.987	-1.34	0.998	-0.24	1.026	2.57
Nd-145	1.012	1.17	0.994	-0.61	0.993	-0.73
Nd-146	0.994	-0.61	0.995	-0.54	0.994	-0.62
Nd-148	1.000	-0.01	1.000	-0.05	1.000	-0.04
Nd-150	0.976	-2.43	0.990	-1.00	0.986	-1.36
Sm-147	1.036	3.62	0.998	-0.21	1.017	1.74
Sm-148	0.874	-12.63	1.058	5.76	1.109	10.91
Sm-149	0.939	-6.08	1.049	4.85	0.981	-1.87
Sm-150	0.974	-2.62	0.976	-2.36	0.974	-2.58
Sm-151	0.664	-33.62	0.772	-22.77	0.749	-25.11
Sm-152	0.949	-5.05	0.820	-17.95	0.779	-22.07
Sm-154	0.986	-1.41	1.008	0.83	0.999	-0.09
Eu-154	0.857	-14.27	1.050	4.98	0.996	-0.37

^aRatio of experimental-to-calculated isotopic concentrations. The experimental values are provided in Table 34. The SCALE input and output files for the evaluated samples are provided on the accompanying DVD (see Appendix B).

Table 102. SCALE calculation results for the Takahama Unit 3 spent fuel samples (continued)

Sample ID	NT3G24.SF97-4		NT3G24.SF97-5		NT3G24.SF97-6	
Enrichment (%)	4.11		4.11		4.11	
BU (GWd/MTU)	47.07		47.26		40.85	
Nuclide ID	E/C ^a	E/C-1 (%)	E/C	E/C-1 (%)	E/C	E/C-1 (%)
U-234	0.939	-6.11	0.933	-6.71	0.924	-7.62
U-235	0.977	-2.29	0.989	-1.13	0.978	-2.16
U-236	1.005	0.48	1.004	0.38	1.007	0.72
U-238	1.001	0.07	1.000	0.04	1.001	0.12
Pu-238	1.115	11.47	1.142	14.23	1.069	6.89
Pu-239	0.954	-4.63	0.977	-2.27	0.940	-6.04
Pu-240	0.932	-6.78	0.936	-6.40	0.923	-7.70
Pu-241	1.025	2.50	1.050	5.01	1.008	0.80
Pu-242	1.024	2.42	1.029	2.90	1.004	0.39
Np-237	0.984	-1.60	1.015	1.45	1.000	0.00
Am-241	0.862	-13.85	0.900	-9.99	0.753	-24.69
Am-242m	0.933	-6.72	0.977	-2.26	0.835	-16.51
Am-243	0.901	-9.92	0.916	-8.39	0.861	-13.88
Cm-242	0.932	-6.83	0.884	-11.61	0.971	-2.87
Cm-243	1.217	21.67	1.257	25.66	1.208	20.79
Cm-244	1.074	7.39	1.103	10.34	1.003	0.26
Cm-245	1.496	49.63	1.568	56.76	1.340	33.98
Cm-246	1.625	62.47	1.691	69.06	1.490	49.01
Cm-247	1.567	56.72	1.628	62.79	1.541	54.08
Ru-106	0.919	-8.05	0.552	-44.82	1.167	16.73
Sb-125	0.585	-41.54	0.720	-28.03	0.520	-47.95
Cs-134	1.173	17.34	1.181	18.13	1.189	18.86
Cs-137	1.018	1.75	1.020	1.98	1.025	2.47
Ce-144	0.941	-5.90	0.934	-6.58	1.047	4.70
Nd-142	—	—	—	—	—	—
Nd-143	0.991	-0.87	1.001	0.05	0.995	-0.48
Nd-144	1.042	4.24	1.047	4.72	1.024	2.40
Nd-145	0.989	-1.15	0.989	-1.09	0.991	-0.89
Nd-146	0.992	-0.77	0.994	-0.63	0.988	-1.18
Nd-148	0.999	-0.06	1.000	-0.04	0.994	-0.57
Nd-150	0.986	-1.39	0.984	-1.57	0.977	-2.32
Sm-147	1.029	2.88	1.023	2.32	1.009	0.88
Sm-148	1.143	14.32	1.156	15.62	1.085	8.47
Sm-149	0.901	-9.89	0.899	-10.13	0.982	-1.79
Sm-150	0.975	-2.53	0.981	-1.87	0.957	-4.25
Sm-151	0.755	-24.52	0.786	-21.45	0.747	-25.30
Sm-152	0.769	-23.14	0.772	-22.80	0.794	-20.61
Sm-154	1.000	0.01	1.009	0.91	0.986	-1.35
Eu-154	0.987	-1.32	1.002	0.20	0.978	-2.21

^aRatio of experimental-to-calculated isotopic concentrations. The experimental values are provided in Table 34. The SCALE input and output files for the evaluated samples are provided on the accompanying DVD (see Appendix B).

Table 103. SCALE calculation results for the TMI Unit 1 spent fuel samples

Sample ID	NJ05YU.A1B		NJ05YU.A2		NJ05YU.B1B		NJ05YU.B2		NJ05YU.B3J	
Enrichment (%)	4.013		4.013		4.013		4.013		4.013	
Burnup (GWd/MTU)	44.8		50.6		54.5		50.1		53.0	
Nuclide ID	E/C ^a	E/C-1 (%)	E/C	E/C-1 (%)	E/C	E/C-1 (%)	E/C	E/C-1 (%)	E/C	E/C-1 (%)
U-234	0.955	-4.54	0.987	-1.35	0.999	-0.08	0.957	-4.31	0.956	-4.41
U-235	1.014	1.39	0.939	-6.08	1.101	10.12	0.894	-10.61	1.010	0.96
U-236	0.952	-4.79	0.990	-1.01	0.959	-4.14	0.976	-2.45	0.973	-2.70
U-238	1.002	0.16	1.002	0.15	1.002	0.17	1.002	0.22	1.001	0.14
Pu-238	1.502	50.15	1.011	1.07	1.071	7.08	0.908	-9.19	1.056	5.62
Pu-239	0.867	-13.26	0.901	-9.90	0.845	-15.52	0.882	-11.83	0.860	-13.99
Pu-240	0.836	-16.44	0.908	-9.17	0.814	-18.59	0.894	-10.56	0.841	-15.89
Pu-241	0.968	-3.17	0.918	-8.22	0.942	-5.82	0.935	-6.53	0.975	-2.49
Pu-242	0.900	-10.02	0.959	-4.06	0.868	-13.17	0.971	-2.92	1.053	5.27
Np-237	0.965	-3.53	0.968	-3.18	0.901	-9.92	0.970	-3.02	0.940	-5.96
Am-241	0.922	-7.82	1.018	1.84	0.665	-33.45	1.139	13.88	1.211	21.07
Am-242m	—	—	—	—	—	—	—	—	0.959	-4.14
Am-243	0.660	-34.03	0.954	-4.60	0.630	-37.05	0.981	-1.88	0.702	-29.83
Cm-242	—	—	—	—	—	—	—	—	—	—
Cm-243	—	—	—	—	—	—	—	—	—	—
Cm-244	—	—	—	—	—	—	—	—	—	—
Cm-245	—	—	—	—	—	—	—	—	—	—
Mo-95	1.031	3.10	1.005	0.55	0.977	-2.26	1.023	2.29	0.975	-2.53
Tc-99	1.339	33.88	0.924	-7.65	1.062	6.18	0.940	-5.98	1.026	2.56
Ru-101	1.058	5.81	0.976	-2.43	0.935	-6.50	1.025	2.51	0.947	-5.33
Rh-103	0.965	-3.51	0.918	-8.20	0.883	-11.70	0.938	-6.17	0.892	-10.80
Ag-109	0.490	-50.99	0.482	-51.76	0.321	-67.88	0.432	-56.80	0.592	-40.82
Cs-134	—	—	—	—	—	—	—	—	—	—
Cs-137	1.145	14.52	1.026	2.58	0.987	-1.31	1.027	2.66	1.000	-0.01
Nd-143	0.951	-4.89	0.870	-12.99	0.961	-3.86	0.914	-8.61	0.954	-4.62
Nd-145	0.959	-4.06	0.905	-9.49	0.965	-3.52	0.942	-5.82	0.975	-2.48
Nd-146	—	—	—	—	—	—	—	—	—	—
Nd-148	0.982	-1.85	0.985	-1.54	0.985	-1.46	0.984	-1.63	0.984	-1.56
Nd-150	—	—	—	—	—	—	—	—	—	—
Sm-147	0.900	-10.02	0.885	-11.50	0.992	-0.76	0.836	-16.35	0.965	-3.52
Sm-149	0.812	-18.79	0.984	-1.59	0.857	-14.30	0.854	-14.55	0.805	-19.52
Sm-150	0.907	-9.31	0.831	-16.90	0.959	-4.10	0.843	-15.67	0.956	-4.38
Sm-151	0.734	-26.60	0.661	-33.88	0.757	-24.26	0.701	-29.90	0.771	-22.90
Sm-152	0.736	-26.37	0.726	-27.38	0.748	-25.23	0.719	-28.14	0.752	-24.76
Eu-151	0.985	-1.50	1.885	88.45	0.760	-23.97	1.677	67.67	1.034	3.36
Eu-153	0.917	-8.33	0.919	-8.10	0.917	-8.29	0.911	-8.93	0.934	-6.57
Eu-155	2.545	154.55	2.125	112.50	2.945	194.48	2.202	120.23	2.048	104.76
Gd-155	2.047	104.69	1.496	49.57	1.876	87.60	1.899	89.92	2.030	102.97

^aRatio of experimental-to-calculated isotopic concentrations. The experimental values are provided in Table 37. The SCALE input and output files for the evaluated samples are provided on the accompanying DVD (see Appendix B).

Table 103. SCALE calculation results for the TMI Unit 1 spent fuel samples (continued)

Sample ID	NJ05YU.C1		NJ05YU.C2B		NJ05YU.C3		NJ05YU.D1A2		NJ05YU.D1A4	
Enrichment (%)	4.013		4.013		4.013		4.013		4.013	
Burnup (GWd/MTU)	50.2		52.6		51.3		55.7		50.5	
Nuclide ID	E/C ^a	E/C-1 (%)	E/C	E/C-1 (%)	E/C	E/C-1 (%)	E/C	E/C-1 (%)	E/C	E/C-1 (%)
U-234	1.017	1.72	0.938	-6.17	0.964	-3.60	1.044	4.40	0.998	-0.18
U-235	0.926	-7.39	0.979	-2.13	0.939	-6.10	1.230	23.04	1.055	5.53
U-236	0.987	-1.26	0.926	-7.37	0.957	-4.32	0.964	-3.60	0.967	-3.34
U-238	1.002	0.20	1.003	0.26	1.002	0.19	1.001	0.07	1.001	0.12
Pu-238	0.928	-7.19	1.205	20.55	0.688	-31.18	0.893	-10.71	1.045	4.54
Pu-239	0.873	-12.72	0.816	-18.41	0.910	-8.99	0.878	-12.22	0.859	-14.06
Pu-240	0.892	-10.78	0.802	-19.77	0.915	-8.49	0.820	-18.01	0.842	-15.81
Pu-241	0.932	-6.84	0.927	-7.32	0.925	-7.52	0.981	-1.94	0.999	-0.10
Pu-242	0.955	-4.48	0.904	-9.59	0.938	-6.23	0.844	-15.60	0.990	-0.98
Np-237	0.971	-2.86	0.908	-9.22	0.930	-6.99	0.879	-12.14	0.932	-6.76
Am-241	1.220	22.03	1.177	17.74	0.990	-0.97	0.750	-25.03	1.221	22.15
Am-242m	—	—	1.194	19.41	—	—	0.430	-56.99	0.586	-41.41
Am-243	0.933	-6.74	0.659	-34.14	0.888	-11.24	0.597	-40.30	0.687	-31.30
Cm-242	—	—	—	—	—	—	—	—	—	—
Cm-243	—	—	—	—	—	—	—	—	—	—
Cm-244	—	—	—	—	—	—	—	—	—	—
Cm-245	—	—	—	—	—	—	—	—	—	—
Mo-95	0.998	-0.21	0.960	-4.01	0.897	-10.34	0.929	-7.08	0.984	-1.58
Tc-99	0.932	-6.85	1.126	12.61	0.875	-12.52	0.904	-9.58	1.022	2.18
Ru-101	0.992	-0.80	0.955	-4.47	0.855	-14.47	0.872	-12.76	0.931	-6.95
Rh-103	0.918	-8.19	0.885	-11.47	0.803	-19.69	0.854	-14.58	0.890	-10.97
Ag-109	0.435	-56.48	0.499	-50.07	0.731	-26.95	0.326	-67.39	0.681	-31.91
Cs-134	—	—	—	—	—	—	—	—	—	—
Cs-137	1.062	6.19	1.025	2.50	0.975	-2.52	0.843	-15.74	1.001	0.05
Nd-143	0.888	-11.20	0.923	-7.70	0.860	-13.96	0.968	-3.25	0.974	-2.59
Nd-145	0.933	-6.72	0.946	-5.40	0.917	-8.33	0.968	-3.25	0.995	-0.55
Nd-146	—	—	—	—	—	—	—	—	—	—
Nd-148	0.983	-1.72	0.985	-1.51	0.984	-1.61	0.986	-1.40	0.982	-1.75
Nd-150	—	—	—	—	—	—	—	—	—	—
Sm-147	0.845	-15.54	0.894	-10.59	0.818	-18.20	0.982	-1.76	0.928	-7.25
Sm-149	0.812	-18.81	0.848	-15.24	0.747	-25.33	0.927	-7.32	0.878	-12.18
Sm-150	0.859	-14.10	0.892	-10.77	0.792	-20.78	0.906	-9.37	0.918	-8.22
Sm-151	0.631	-36.95	0.674	-32.58	0.643	-35.70	0.754	-24.63	0.710	-29.00
Sm-152	0.705	-29.49	0.697	-30.27	0.685	-31.48	0.731	-26.86	0.744	-25.60
Eu-151	1.399	39.92	0.941	-5.89	1.756	75.62	0.850	-14.95	0.885	-11.50
Eu-153	0.907	-9.25	0.886	-11.36	0.850	-15.01	0.910	-8.97	0.940	-6.03
Eu-155	2.387	138.71	1.991	99.12	2.063	106.34	1.810	81.03	2.666	166.62
Gd-155	1.830	83.02	1.845	84.48	1.867	86.71	1.844	84.37	2.882	188.15

^aRatio of experimental-to-calculated isotopic concentrations. The experimental values are provided in Table 37. The SCALE input and output files for the evaluated samples are provided on the accompanying DVD (see Appendix B).

Table 103. SCALE calculation results for the TMI Unit 1 spent fuel samples (continued)

Sample ID	NJ05YU.D2		NJ070G.O12S4		NJ070G.O12S5		NJ070G.O12S6		NJ070G.O13S7	
Enrichment (%)	4.013		4.657		4.657		4.657		4.657	
Burnup (GWd/MTU)	44.8		23.7		26.5		24.0		22.8	
Nuclide ID	E/C ^a	E/C-1 (%)	E/C	E/C-1 (%)	E/C	E/C-1 (%)	E/C	E/C-1 (%)	E/C	E/C-1 (%)
U-234	0.916	-8.39	1.003	0.30	0.982	-1.84	0.993	-0.67	1.019	1.91
U-235	0.823	-17.70	0.972	-2.76	0.970	-2.98	0.984	-1.59	0.954	-4.61
U-236	0.995	-0.48	1.036	3.59	1.029	2.85	1.044	4.42	1.044	4.41
U-238	1.003	0.28	1.001	0.07	1.001	0.06	0.999	-0.06	1.000	0.03
Pu-238	1.131	13.06	1.172	17.15	1.189	18.87	1.305	30.46	1.240	24.00
Pu-239	0.859	-14.08	0.973	-2.71	0.990	-1.04	1.039	3.86	0.983	-1.69
Pu-240	0.932	-6.80	1.001	0.15	1.023	2.28	1.046	4.56	1.033	3.32
Pu-241	0.946	-5.36	1.052	5.22	1.086	8.61	1.136	13.63	1.099	9.94
Pu-242	1.059	5.86	1.087	8.71	1.106	10.64	1.141	14.14	1.173	17.25
Np-237	1.041	4.08	1.073	7.27	1.018	1.76	1.088	8.79	1.056	5.55
Am-241	1.181	18.13	1.092	9.21	1.061	6.13	0.908	-9.18	1.080	7.96
Am-242m	-	-	1.084	8.45	1.057	5.69	0.948	-5.22	1.032	3.23
Am-243	0.990	-1.02	0.967	-3.34	0.998	-0.24	0.838	-16.21	1.058	5.76
Cm-242	-	-	1.635	63.48	1.441	44.13	1.270	27.05	1.403	40.33
Cm-243	-	-	1.386	38.61	1.456	45.59	1.309	30.93	1.517	51.73
Cm-244	-	-	1.165	16.46	1.216	21.57	1.088	8.84	1.303	30.28
Cm-245	-	-	1.690	68.98	1.815	81.55	1.779	77.86	1.940	94.04
Mo-95	0.916	-8.37	-	-	-	-	-	-	-	-
Tc-99	0.923	-7.68	-	-	-	-	-	-	-	-
Ru-101	0.900	-9.98	-	-	-	-	-	-	-	-
Rh-103	0.830	-17.00	-	-	-	-	-	-	-	-
Ag-109	0.441	-55.91	-	-	-	-	-	-	-	-
Cs-134	-	-	1.264	26.35	1.282	28.20	1.330	32.96	1.336	33.55
Cs-137	1.061	6.06	1.038	3.83	1.041	4.10	1.040	4.00	1.080	7.97
Nd-143	0.868	-13.16	0.974	-2.61	0.968	-3.22	0.981	-1.86	0.991	-0.89
Nd-145	0.938	-6.19	0.980	-1.96	0.973	-2.68	0.981	-1.89	1.000	0.05
Nd-146	-	-	0.988	-1.20	0.986	-1.40	0.999	-0.08	1.013	1.29
Nd-148	0.982	-1.81	0.992	-0.80	0.989	-1.06	1.002	0.24	1.017	1.68
Nd-150	-	-	0.986	-1.44	0.987	-1.28	1.004	0.43	1.019	1.87
Sm-147	0.847	-15.34	1.049	4.87	1.019	1.94	1.036	3.56	1.031	3.10
Sm-149	0.769	-23.14	0.871	-12.86	0.873	-12.71	0.948	-5.23	0.868	-13.25
Sm-150	0.882	-11.75	0.979	-2.07	0.980	-2.01	0.990	-0.98	1.001	0.12
Sm-151	0.654	-34.56	0.788	-21.21	0.799	-20.13	0.851	-14.88	0.785	-21.50
Sm-152	0.740	-26.03	0.874	-12.61	0.848	-15.23	0.848	-15.17	0.892	-10.83
Eu-151	1.466	46.59	0.839	-16.11	0.775	-22.53	0.897	-10.33	0.760	-24.03
Eu-153	0.972	-2.83	1.085	8.49	1.072	7.15	1.097	9.66	1.111	11.06
Eu-155	2.412	141.18	-	-	-	-	-	-	-	-
Gd-155	1.897	89.72	1.716	71.58	1.659	65.93	1.893	89.25	1.674	67.37

^aRatio of experimental-to-calculated isotopic concentrations. The experimental values are provided in Table 37 and Table 39. The SCALE input and output files for the evaluated samples are provided on the accompanying DVD (see Appendix B).

Table 103. SCALE calculation results for the TMI Unit 1 spent fuel samples (continued)

Sample ID	NJ070G.O13S8		NJ070G.O1S1		NJ070G.O1S2		NJ070G.O1S3	
Enrichment (%)	4.657		4.657		4.657		4.657	
Burnup (GWd/MTU)	26.3		25.8		29.917		26.7	
Nuclide ID	E/C ^a	E/C-1 (%)	E/C	E/C-1 (%)	E/C	E/C-1 (%)	E/C	E/C-1 (%)
U-234	0.998	-0.24	1.008	0.81	0.996	-0.35	0.989	-1.10
U-235	0.968	-3.21	0.973	-2.74	0.949	-5.13	0.971	-2.91
U-236	1.025	2.52	1.028	2.82	1.028	2.76	1.033	3.31
U-238	1.001	0.08	1.001	0.11	1.001	0.14	1.000	-0.01
Pu-238	1.194	19.35	1.122	12.17	1.120	12.04	1.240	23.97
Pu-239	0.970	-2.95	0.962	-3.78	0.901	-9.91	0.986	-1.43
Pu-240	1.013	1.29	0.990	-1.04	1.001	0.08	1.044	4.45
Pu-241	1.072	7.24	1.043	4.31	1.029	2.88	1.113	11.31
Pu-242	1.105	10.45	1.066	6.58	1.134	13.38	1.169	16.88
Np-237	1.024	2.38	0.966	-3.42	0.987	-1.27	1.049	4.90
Am-241	1.041	4.07	0.744	-25.57	0.881	-11.92	0.990	-0.96
Am-242m	1.026	2.64	0.762	-23.84	0.804	-19.61	0.934	-6.57
Am-243	0.983	-1.75	0.646	-35.37	0.843	-15.65	0.907	-9.27
Cm-242	1.523	52.29	1.116	11.63	1.635	63.54	1.451	45.09
Cm-243	1.404	40.40	0.922	-7.84	1.164	16.35	1.383	38.29
Cm-244	1.189	18.90	0.744	-25.61	0.994	-0.61	1.121	12.10
Cm-245	1.776	77.63	1.049	4.93	1.328	32.82	1.694	69.43
Mo-95	—	—	—	—	—	—	—	—
Tc-99	—	—	—	—	—	—	—	—
Ru-101	—	—	—	—	—	—	—	—
Rh-103	—	—	—	—	—	—	—	—
Ag-109	—	—	—	—	—	—	—	—
Cs-134	1.300	30.03	1.224	22.43	1.244	24.40	1.295	29.52
Cs-137	1.060	5.96	1.022	2.24	1.078	7.80	1.048	4.76
Nd-143	0.968	-3.22	0.965	-3.50	0.966	-3.37	0.976	-2.42
Nd-145	0.975	-2.48	0.974	-2.56	0.984	-1.62	0.982	-1.79
Nd-146	0.987	-1.27	0.981	-1.89	0.991	-0.94	0.996	-0.37
Nd-148	0.991	-0.90	0.989	-1.15	0.999	-0.07	1.003	0.34
Nd-150	0.988	-1.18	0.987	-1.32	0.995	-0.50	1.006	0.62
Sm-147	1.015	1.47	1.048	4.80	1.042	4.24	1.052	5.16
Sm-149	0.870	-13.02	0.856	-14.36	0.827	-17.33	0.918	-8.16
Sm-150	0.977	-2.32	0.966	-3.40	0.979	-2.06	0.993	-0.68
Sm-151	0.800	-20.02	0.769	-23.08	0.756	-24.44	0.805	-19.53
Sm-152	0.847	-15.32	0.860	-13.99	0.872	-12.77	0.867	-13.26
Eu-151	0.771	-22.90	0.807	-19.29	0.715	-28.55	0.830	-17.02
Eu-153	1.078	7.80	1.048	4.80	1.051	5.13	1.074	7.44
Eu-155	—	—	—	—	—	—	—	—
Gd-155	1.692	69.19	1.811	81.14	1.563	56.26	1.922	92.19

^aRatio of experimental-to-calculated isotopic concentrations. The experimental values are provided in Table 39. The SCALE input and output files for the evaluated samples are provided on the accompanying DVD (see Appendix B).

Table 104. SCALE calculation results for Gösgen (ARIANE) spent fuel samples

Sample ID	1240.GU1		1701.GU3		1701.GU4	
Enrichment (%)	3.5		4.1		4.1	
Burnup ^a (GWd/MTU)	60.7		53.2		31.1	
Nuclide ID	E/C ^b	E/C-1 (%)	E/C	E/C-1 (%)	E/C	E/C-1 (%)
U-234	0.863	-13.70	0.734	-26.62	0.708	-29.19
U-235	0.960	-4.01	1.045	4.47	0.999	-0.11
U-236	0.995	-0.52	0.999	-0.11	0.998	-0.18
U-238	1.003	0.34	1.008	0.79	1.005	0.54
Pu-238	1.024	2.44	1.028	2.82	1.026	2.62
Pu-239	0.948	-5.25	0.984	-1.56	0.955	-4.46
Pu-240	0.973	-2.69	0.952	-4.75	0.968	-3.21
Pu-241	1.002	0.20	1.038	3.80	1.027	2.69
Pu-242	1.033	3.25	0.987	-1.31	0.993	-0.73
Np-237	—	—	1.089	8.93	1.371	37.10
Am-241	0.923	-7.66	0.888	-11.18	1.032	3.18
Am-242m	0.669	-33.11	0.845	-15.50	—	—
Am-243	0.851	-14.90	0.798	-20.22	0.814	-18.60
Cm-242	1.187	18.71	1.257	25.69	—	—
Cm-243	0.330	-66.97	0.792	-20.82	—	—
Cm-244	0.981	-1.87	1.028	2.80	1.144	14.36
Cm-245	1.254	25.44	1.605	60.51	1.547	54.70
Cm-246	1.579	57.90	1.484	48.39	—	—
Mo-95	1.061	6.10	1.011	1.09	1.011	1.07
Tc-99	0.941	-5.86	0.917	-8.30	0.979	-2.10
Rh-103	0.899	-10.14	0.784	-21.55	1.003	0.33
Ru-101	0.917	-8.31	0.977	-2.33	1.014	1.38
Ru-106	0.910	-8.98	1.124	12.36	1.169	16.89
Ag-109	0.457	-54.25	0.926	-7.43	—	—
Sb-125	0.680	-32.01	0.604	-39.61	—	—
Cs-133	0.928	-7.24	0.949	-5.11	0.969	-3.11
Cs-134	1.067	6.70	1.088	8.80	1.110	11.05
Cs-135	0.984	-1.58	0.983	-1.67	0.916	-8.39
Cs-137	0.990	-0.98	0.959	-4.14	0.917	-8.32
Ce-144	1.002	0.21	0.945	-5.53	0.957	-4.31
Nd-142	0.955	-4.49	0.922	-7.77	0.844	-15.57
Nd-143	0.936	-6.45	0.971	-2.92	1.021	2.06
Nd-144	0.994	-0.59	0.980	-1.96	1.041	4.14
Nd-145	0.976	-2.44	0.982	-1.84	1.008	0.78
Nd-146	0.974	-2.58	0.984	-1.57	1.002	0.23
Nd-148	1.000	-0.04	0.998	-0.20	1.002	0.17
Nd-150	0.990	-0.96	0.986	-1.42	0.981	-1.87

^aBurnup based on measured ¹⁴⁸Nd.

^bRatio of experimental-to-calculated isotopic concentrations. The experimental values are provided in Table 42. The SCALE input and output files for the evaluated samples are provided on the accompanying DVD (see Appendix B).

Table 104. SCALE calculation results for Gösgen (ARIANE) spent fuel samples (continued)

Sample ID	1240.GU1		1701.GU3		1701.GU4	
Enrichment (%)	3.5		4.1		4.1	
Burnup ^a (GWd/MTU)	60.7		53.2		31.1	
Nuclide ID	E/C ^b	E/C-1 (%)	E/C	E/C-1 (%)	E/C	E/C-1 (%)
Pm-147	1.549	54.87	0.909	-9.14	1.099	9.94
Sm-147	1.059	5.89	0.979	-2.07	0.935	-6.49
Sm-148	1.131	13.07	1.129	12.94	1.035	3.53
Sm-149	0.984	-1.61	0.797	-20.31	0.932	-6.80
Sm-150	0.948	-5.15	0.908	-9.16	0.909	-9.12
Sm-151	0.744	-25.61	0.720	-28.00	0.738	-26.16
Sm-152	0.792	-20.77	0.712	-28.81	0.782	-21.79
Sm-154	1.023	2.27	0.922	-7.77	0.901	-9.93
Eu-151	1.745	74.46	1.218	21.80	—	—
Eu-153	0.900	-10.02	0.933	-6.73	0.967	-3.28
Eu-154	0.845	-15.52	0.985	-1.48	0.949	-5.07
Eu-155	1.416	41.60	1.541	54.08	1.490	49.03
Gd-155	1.285	28.50	1.240	23.99	2.055	105.51

^aBurnup based on measured ¹⁴⁸Nd.

^bRatio of experimental-to-calculated isotopic concentrations. The experimental values are provided in Table 42. The SCALE input and output files for the evaluated samples are provided on the accompanying DVD (see Appendix B).

Table 105. SCALE calculation results for GKN II (REBUS) spent fuel sample

Sample ID	419.M11	
Enrichment (%)	3.8	
Burnup (GWd/MTU)	54.095	
Nuclide ID	E/C ^a	E/C-1 (%)
U-234	0.837	-16.26
U-235	0.960	-4.01
U-236	1.009	0.92
U-238	1.003	0.27
Pu-238	1.085	8.45
Pu-239	0.923	-7.69
Pu-240	0.970	-2.97
Pu-241	0.993	-0.68
Pu-242	1.024	2.43
Np-237	0.789	-21.09
Am-241	0.777	-22.30
Am-242m	0.786	-21.36
Am-243	0.728	-27.17
Cm-242	0.791	-20.94
Cm-243	1.087	8.73
Cm-244	1.066	6.63
Cm-245	1.463	46.34
Mo-95	0.900	-9.99
Tc-99	1.026	2.55
Ru-101	0.769	-23.14
Rh-103	0.813	-18.66
Ag-109	0.760	-24.01
Pd-105	0.633	-36.73
Pd-108	0.626	-37.36
Cs-133	0.929	-7.12
Cs-135	0.960	-4.03
Cs-137	1.016	1.59
Ce-144	1.042	4.15
Nd-142	1.091	9.07
Nd-143	0.962	-3.77
Nd-144	1.016	1.60
Nd-145	0.993	-0.65
Nd-146	0.992	-0.80
Nd-148	1.000	-0.01
Nd-150	0.981	-1.92
Sm-147	1.053	5.31
Sm-148	1.161	16.11
Sm-149	0.953	-4.68
Sm-150	0.980	-1.96
Sm-151	0.732	-26.82
Sm-152	0.770	-22.95
Sm-154	1.018	1.80
Eu-153	0.939	-6.08
Eu-154	0.907	-9.34
Eu-155	1.735	73.45
Gd-155	1.435	43.47

^aRatio of experimental-to-calculated isotopic concentrations. The experimental values are provided in Table 45. The SCALE input and output files for the evaluated samples are provided on the accompanying DVD (see Appendix B).

Table 106. SCALE calculation results for Gösgen (MALIBU) spent fuel samples

Sample ID	1901.GGU1		1964.GGU2-1		1964.GGU2-2	
Enrichment (%)	4.3		4.3		4.3	
Burnup ^a (GWd/MTU)	70.35		50.80		46.00	
Nuclide ID	E/C ^b	E/C-1 (%)	E/C	E/C-1 (%)	E/C	E/C-1 (%)
U-234	1.005	0.51	0.996	-0.42	0.968	-3.19
U-235	1.026	2.55	1.070	7.03	0.998	-0.22
U-236	1.022	2.16	0.996	-0.39	0.989	-1.10
U-238	1.014	1.42	1.001	0.09	0.990	-1.00
Pu-238	1.047	4.66	1.113	11.31	1.116	11.61
Pu-239	0.952	-4.83	1.044	4.43	1.003	0.33
Pu-240	0.972	-2.85	0.983	-1.68	0.967	-3.31
Pu-241	1.024	2.38	1.071	7.14	1.068	6.81
Pu-242	1.048	4.81	0.993	-0.74	1.018	1.84
Np-237	0.971	-2.92	0.931	-6.91	0.909	-9.11
Am-241	1.091	9.13	1.120	12.01	0.881	-11.86
Am-242m	0.774	-22.62	1.209	20.88	0.772	-22.77
Am-243	0.971	-2.86	0.930	-7.01	0.765	-23.48
Cm-242	1.121	12.12	—	—	1.269	26.90
Cm-243	1.187	18.69	—	—	1.067	6.75
Cm-244	1.068	6.77	1.015	1.51	1.100	10.04
Cm-245	1.381	38.08	1.417	41.70	1.508	50.78
Cm-246	1.591	59.11	1.408	40.79	1.515	51.54
Mo-95	0.996	-0.44	1.096	9.59	1.007	0.75
Tc-99	0.841	-15.90	0.854	-14.55	1.026	2.59
Ru-101	0.937	-6.33	1.039	3.91	0.996	-0.45
Ru-106	0.889	-11.13	1.108	10.82	0.894	-10.61
Rh-103	0.927	-7.32	1.033	3.28	0.972	-2.85
Ag-109	0.371	-62.92	0.420	-57.97	0.997	-0.32
Sb-125	—	—	—	—	—	—
Cs-133	—	—	—	—	—	—
Cs-134	0.612	-38.82	0.865	-13.53	0.722	-27.82
Cs-135	0.961	-3.89	0.962	-3.78	0.960	-3.98
Cs-137	1.130	13.02	1.166	16.65	1.179	17.92
Ce-144	1.017	1.69	1.029	2.92	1.004	0.41
Nd-142	1.005	0.48	0.999	-0.09	1.003	0.33
Nd-143	1.067	6.73	1.089	8.87	1.088	8.75
Nd-144	0.981	-1.88	0.923	-7.74	1.152	15.22
Nd-145	0.978	-2.19	0.955	-4.47	1.137	13.68
Nd-146	0.992	-0.81	1.026	2.63	0.967	-3.25
Nd-148	1.046	4.59	1.028	2.77	0.988	-1.18
Nd-150	1.033	3.28	1.025	2.52	0.976	-2.45

^aBased on measured data for burnup indicators fission products ¹⁴⁸Nd and ¹³⁷Cs.

^bRatio of experimental-to-calculated isotopic concentrations. The SCALE input and output files for the evaluated samples are provided on the accompanying DVD (see Appendix B).

Table 106. SCALE calculation results for Gösgen (MALIBU) spent fuel samples (continued)

Sample ID	1901.GGU1		1964.GGU2-1		1964.GGU2-2	
Enrichment (%)	4.3		4.3		4.3	
Burnup ^a (GWd/MTU)	70.3		50.8		46.0	
Nuclide ID	E/C ^a	E/C-1 (%)	E/C	E/C-1 (%)	E/C	E/C-1 (%)
Pm-147	1.131	13.11	1.063	6.28	1.026	2.65
Sm-147	1.260	25.98	1.142	14.18	1.086	8.62
Sm-148	0.871	-12.88	0.920	-7.97	0.900	-9.98
Sm-149	1.041	4.08	1.000	0.04	0.957	-4.29
Sm-150	0.761	-23.89	0.831	-16.90	0.796	-20.36
Sm-151	0.797	-20.33	0.803	-19.66	0.778	-22.25
Sm-152	1.050	5.02	1.030	3.02	1.073	7.26
Sm-154	0.696	-30.44	—	—	0.894	-10.56
Eu-151	0.918	-8.21	0.960	-3.98	0.965	-3.47
Eu-153	0.897	-10.34	1.011	1.06	1.018	1.79
Eu-154	1.327	32.68	1.416	41.62	1.631	63.08
Eu-155	1.296	29.55	1.355	35.52	1.614	61.37
Gd-155	1.131	13.11	1.063	6.28	1.026	2.65

^aBased on measured data for burnup indicators fission products ¹⁴⁸Nd and ¹³⁷Cs.

^bRatio of experimental-to-calculated isotopic concentrations. The SCALE input and output files for the evaluated samples are provided on the accompanying DVD (see Appendix B).

10.2 SENSITIVITY CALCULATIONS

Sensitivity calculations were performed to evaluate the effects of a series of modeling assumptions used in this validation study on the calculated isotopic compositions. The results of the sensitivity study are tabulated in this section.

10.2.1 Assembly Model Simplifications

As described in Sect. 9.2.2, a typical TRITON/NEWT calculation model used in this validation study consists of individual depleting mixtures specified for the measured rod and its adjacent nearest-neighbor fuel rods with all other fuel rods in the assembly treated as a single depletion material with uniform composition. This simplified assembly model was used in place of a detailed assembly model that would specify individual depleting mixtures for all the pins included in the assembly model. Calculations using detailed and simplified assembly pin models for Turkey Point spent fuel sample D01-G9 were performed and the isotopic compositions in the measured sample, in g/gU_{initial}, are summarized in Table 107. As seen in the table, the isotopic compositions differ within ±0.5% for all isotopes of interest.

Table 107. Comparison between isotopic compositions obtained with detailed and simplified lattice pin model

Model characteristic	Detailed	Simplified		Model characteristic	Detailed	Simplified	
Isotope	g/g U _{initial}	g/g U _{initial}	Rel. diff. (%)	Isotope	g/g U _{initial}	g/g U _{initial}	Rel. diff. (%)
U-234	1.35E-04	1.34E-04	0.08	Nd-148	3.40E-04	3.40E-04	0.00
U-235	5.59E-03	5.58E-03	0.20	Cs-137	1.07E-03	1.07E-03	0.00
U-236	3.35E-03	3.35E-03	-0.02	Sm-147	1.51E-04	1.51E-04	0.07
U-238	9.49E-01	9.49E-01	-0.01	Sm-149	3.21E-06	3.21E-06	-0.08
Pu-238	1.34E-04	1.34E-04	-0.19	Sm-150	2.73E-04	2.73E-04	-0.04
Pu-239	5.05E-03	5.04E-03	0.12	Sm-151	1.25E-05	1.25E-05	-0.12
Pu-240	2.36E-03	2.36E-03	0.09	Sm-152	1.25E-04	1.25E-04	0.12
Pu-241	1.07E-03	1.07E-03	0.24	Eu-151	2.58E-07	2.59E-07	-0.10
Pu-242	5.47E-04	5.45E-04	0.28	Eu-153	1.11E-04	1.11E-04	0.00
Np-237	3.67E-04	3.67E-04	-0.07	Eu-155	3.60E-06	3.59E-06	0.13
Am-241	1.76E-04	1.76E-04	0.17	Gd-155	1.68E-06	1.67E-06	0.12
Am-242m	6.86E-07	6.88E-07	-0.28	Mo-95	6.92E-04	6.92E-04	0.00
Am-243	1.12E-04	1.12E-04	-0.09	Tc-99	7.45E-04	7.44E-04	0.04
Cm-242	2.53E-07	2.52E-07	0.10	Ru-101	7.34E-04	7.34E-04	0.06
Cm-244	2.83E-05	2.85E-05	-0.45	Ru-106	2.93E-05	2.92E-05	0.30
Nd-143	7.11E-04	7.11E-04	0.06	Rh-103	4.71E-04	4.70E-04	0.17
Nd-145	6.18E-04	6.17E-04	0.03	Ag-109	8.02E-05	8.00E-05	0.25

10.2.2 Trino Vercellese Fuel Density Sensitivity Calculations

The mass density value for the Trino Vercellese fuel was derived using various fuel mass data, as described in Sect. 8.1 (see Table 49). A mass density value of 10.353 g/cm³ was obtained for assemblies 509-049, 509-032, and 509-104 by averaging 10.3529 g/cm³, which is the fuel density based on the UO₂ mass in a square assembly (353.81 kg) in Ref. 12, Table 2, and 10.3531 g/cm³, which is the fuel density based on the UO₂ mass in all 112 square assemblies for Cycle 2 (39,626 kg) in Ref. 13, Table 2. The fuel density of 10.353 g/cm³ was used to obtain the E/C values presented in Sect. 10.1. The fuel density based on the total UO₂ mass (42,321 kg) in 120 square fuel assemblies for Cycle 1 provided in Ref. 12, Table 2, is 10.3198 g/cm³. Depletion calculations using a fuel mass density of 10.3198 g/cm³ were also performed, and the results of the calculations for selected samples are described in this section. A comparison between isotopic concentration, in g/g U_{initial}, obtained for the fuel density values of 10.353 and 10.3198 g/cm³ is presented in Table 108 for selected Trino Vercellese spent fuel samples. As seen in the table, the 0.32% decrease in fuel density resulted in an approximately 0.5% increase in ²⁴⁴Cm mass; 0.3% increase in ²³⁸Pu, ^{242m}Am, and ²⁴³Am mass; and 0.15% increase in ²³⁹Pu, ²⁴¹Pu, ²⁴²Pu, and ²⁴¹Am mass. The uranium isotopes were practically unaffected by the fuel density change.

Table 108. Fuel density sensitivity calculation results for Trino Vercellese spent fuel samples

Sample	509-104-M11-7			509-049-L5-1			509-032-H9-9		
	Fuel density (g/cm ³)	10.353	10.3198		10.353	10.3198		10.353	10.3198
Isotope	g/g U _{initial}	g/g U _{initial}	Rel. diff. (%)	g/g U _{initial}	g/g U _{initial}	Rel. diff. (%)	g/g U _{initial}	g/g U _{initial}	Rel. diff. (%)
U-234	2.93E-04	2.93E-04	0.00	2.08E-04	2.08E-04	-0.01	2.29E-04	2.29E-04	-0.02
U-235	2.70E-02	2.70E-02	0.00	1.96E-02	1.96E-02	0.01	1.96E-02	1.96E-02	0.01
U-236	2.46E-03	2.46E-03	0.00	1.53E-03	1.53E-03	0.02	2.26E-03	2.26E-03	0.08
U-238	9.52E-01	9.52E-01	0.00	9.66E-01	9.66E-01	0.00	9.59E-01	9.59E-01	0.00
Pu-238	1.43E-05	1.43E-05	0.26	6.69E-06	6.67E-06	0.24	1.54E-05	1.53E-05	0.24
Pu-239	4.47E-03	4.46E-03	0.09	3.60E-03	3.59E-03	0.10	4.31E-03	4.30E-03	0.13
Pu-240	6.78E-04	6.77E-04	0.03	5.18E-04	5.18E-04	0.02	8.12E-04	8.12E-04	0.03
Pu-241	3.11E-04	3.11E-04	0.13	1.97E-04	1.97E-04	0.15	3.67E-04	3.67E-04	0.16
Pu-242	2.73E-05	2.73E-05	0.15	1.52E-05	1.52E-05	0.11	4.20E-05	4.20E-05	0.08
Am-241	8.15E-06	8.13E-06	0.15	4.98E-06	4.97E-06	0.16	9.15E-06	9.14E-06	0.12
Am-242m	1.25E-07	1.25E-07	0.25	7.09E-08	7.07E-08	0.26	1.48E-07	1.48E-07	0.22
Am-243	1.96E-06	1.95E-06	0.30	8.29E-07	8.27E-07	0.30	3.22E-06	3.21E-06	0.25
Cm-242	7.03E-07	7.01E-07	0.21	3.83E-07	3.82E-07	0.21	1.03E-06	1.03E-06	0.17
Cm-244	1.62E-07	1.61E-07	0.48	5.28E-08	5.25E-08	0.48	2.90E-07	2.89E-07	0.44
Ru-106	3.97E-05	3.97E-05	0.10	2.75E-05	2.75E-05	0.06	4.65E-05	4.65E-05	0.03
Cs-134	1.63E-05	1.62E-05	0.13	8.40E-06	8.39E-06	0.11	1.83E-05	1.83E-05	0.11
Cs-137	4.49E-04	4.49E-04	0.00	2.91E-04	2.91E-04	-0.02	4.61E-04	4.61E-04	-0.02
Ce-144	1.78E-04	1.78E-04	0.00	1.17E-04	1.17E-04	-0.02	1.84E-04	1.84E-04	-0.01
Nd-148	1.36E-04	1.36E-04	0.00	8.79E-05	8.79E-05	0.00	1.39E-04	1.39E-04	-0.01
Eu-154	3.23E-06	3.23E-06	0.19	1.65E-06	1.65E-06	0.18	3.63E-06	3.63E-06	0.16

Source: TRITON/NEWT input and output files are provided in DVD/TrinoVercellese/sen-fuelden. The relative difference values were obtained in DVD/xls/input_data.xls, worksheet Trino.

10.2.3 Trino Vercellese Fuel Temperature Sensitivity Calculations

Effective fuel temperature data for the measured Trino Vercellese samples were not available in the primary experimental reports, and the effective fuel temperature data for the Yankee Rowe PWR, which had a similar assembly design, were used in the depletion calculations (see Table 51). To evaluate the magnitude of the uncertainty in the calculated isotopic concentrations due to the uncertainty associated with the effective fuel temperature values used, calculations were performed for Trino Vercellese samples 509-032-E11-4 (15.377 GWd/MTU) and 509-069-E11-5 (24.518 MTU) in which the applicable Yankee Rowe effective fuel temperature values were increased by 10%. As seen in Table 109, the relative percent differences between the isotopic concentrations obtained with the Yankee Rowe temperature values and the isotopic concentrations obtained with the perturbed temperature values were less than 1% for all isotopes of interest. The sensitivity calculation results suggest that the uncertainty in the fuel temperature data used for the Trino Vercellese samples will likely impact the calculated ²³⁹Pu, ²⁴¹Pu, ²⁴¹Am, and ^{242m}Am isotopic concentrations.

Table 109. Fuel temperature sensitivity calculation results for Trino Vercellese spent fuel samples

Sample Fuel temperature	509-032-E11-4			509-069-E11-5		
	Nominal ^a	Perturbed ^b		Nominal ^a	Perturbed ^b	
Nuclide	g/g U _{initial}	g/g U _{initial}	Rel. diff. (%)	g/g U _{initial}	g/g U _{initial}	Rel. diff. (%)
U-234	2.16E-04	2.16E-04	-0.02	1.85E-04	1.85E-04	-0.06
U-235	1.78E-02	1.78E-02	-0.15	1.26E-02	1.26E-02	-0.28
U-236	2.63E-03	2.63E-03	0.08	3.48E-03	3.47E-03	0.13
U-238	9.56E-01	9.56E-01	0.00	9.48E-01	9.48E-01	0.02
Pu-238	2.92E-05	2.92E-05	0.08	1.06E-04	1.06E-04	-0.11
Pu-239	5.24E-03	5.28E-03	-0.93	6.40E-03	6.47E-03	-1.01
Pu-240	1.11E-03	1.11E-03	-0.26	1.85E-03	1.85E-03	-0.13
Pu-241	5.93E-04	5.98E-04	-0.86	1.09E-03	1.10E-03	-0.79
Pu-242	8.33E-05	8.36E-05	-0.45	2.58E-04	2.58E-04	-0.17
Am-241	1.48E-05	1.49E-05	-0.95	8.49E-05	8.56E-05	-0.92
Am-242m	2.76E-07	2.78E-07	-0.97	2.04E-06	2.06E-06	-1.16
Am-243	8.96E-06	9.00E-06	-0.47	4.71E-05	4.72E-05	-0.28
Cm-242	2.16E-06	2.18E-06	-0.54	1.83E-05	1.84E-05	-0.44
Cm-244	1.11E-06	1.12E-06	-0.32	1.00E-05	1.00E-05	0.02
Ru-106	6.69E-05	6.72E-05	-0.33	7.44E-05	7.46E-05	-0.24
Cs-134	2.94E-05	2.94E-05	0.15	5.28E-05	5.26E-05	0.21
Cs-137	5.72E-04	5.72E-04	0.00	8.61E-04	8.61E-04	0.00
Ce-144	2.23E-04	2.22E-04	0.10	1.60E-04	1.60E-04	0.07
Nd-148	1.72E-04	1.72E-04	0.01	2.73E-04	2.73E-04	0.08
Eu-154	6.19E-06	6.19E-06	0.00	1.53E-05	1.53E-05	0.00

^aResults obtained with the effective fuel temperature values presented in Table 51.

^bThe perturbed fuel temperatures were $1.1 \times$ the effective fuel temperature values presented in Table 51.

Source: TRITON/NEWT input and output files are provided in *DVD/TrinoVercellese/sen-fueltemp*. The relative difference values were obtained in *DVD/xls/input_data.xls*, worksheet *Trino*.

10.3 GRAPHICAL REPRESENTATIONS OF E/C VALUES FOR THE BURNUP CREDIT ISOTOPES

The graphs illustrated in Figs. A-1 through A-28, Appendix A, show the ratio of the experimental-to-calculated isotopic concentrations as a function of sample burnup for the burnup-credit nuclides (refer to Sect. 6.1 for the list of burnup-credit nuclides). The error bar for each data point shown in the graphs represents one standard deviation from the E/C value and is entirely based on the reported experimental uncertainties for the burnup-credit isotopes (see Sect. 7).

11 SUMMARY

This calculation report provides an evaluation of radiochemically assayed data for 118 spent fuel samples obtained from low-, moderate-, and high-burnup spent fuel assemblies from the following nine PWRs: Trino Vercellese, Kernkraftwerk Obrigheim, Turkey Point Unit 3, H. B. Robinson Unit 2, Calvert Cliffs Unit 1, Three Mile Island Unit 1, Takahama Unit 3, Gösgen, and GKN II. The initial enrichment and burnup of the evaluated spent fuel samples vary from 2.453 to 4.657 wt % ^{235}U and from 7.2 to 70.4 GWd/MTU, respectively. Most of the measured spent fuel samples have been selected from typical UO_2 assemblies; however, spent fuel samples from assemblies containing burnable poison rods and from gadolinia rods are also included in the current evaluation. The number of the isotopes with measured concentrations varies depending on the experimental program. The earlier experimental programs provided measurement data for the uranium and plutonium isotopes mainly, whereas the more recent experimental programs provided measurement data for up to 50 isotopes, including actinide and fission product isotopes relevant to burnup credit.

The documentation of the evaluated data and calculations performed is very comprehensive in the current report. Section 6 of the report describes the measurement methods used by each experimental program, the reported measured isotopic concentrations, sample burnup values, and measurement uncertainties. The input parameters for use in 2-D depletion and decay calculations are documented in Sect. 8, whereas a series of assumptions employed in determining some of the input parameters for calculations are described in Sect. 5. The TRITON/NEWT models developed for performing calculations for the evaluated spent fuel samples are described in Sect. 9. The results of the calculations are provided as the ratio of experimental-to-calculated isotopic concentrations in the tables included in Sect. 10.1 and may directly be used in subsequent criticality safety analyses employing burnup credit. Graphical representations of the E/C values are provided in Appendix A to support qualitative evaluations of the results. All the electronic files consisting of MS Excel spreadsheet applications and SCALE 5.1 input and output files that were generated are provided on the DVD that accompanies this report; a listing of the files included on the DVD is given in Appendix B.

12 REFERENCES

1. *SCALE: A Modular Code System for Performing Standardized Computer Analyses for Licensing Evaluations*, ORNL/TM-2005/39, Version 5.1, Vols. I–III, November 2006. Available from Radiation Safety Information Computational Center at Oak Ridge National Laboratory as CCC-732.
2. M. D. DeHart, “TRITON: A Two-Dimensional Transport and Depletion Module for Characterization of Spent Nuclear Fuel,” Vol. I, Book 3, Sect. T1 in *SCALE: A Modular Code System for Performing Standardized Computer Analyses for Licensing Evaluations*, ORNL/TM-2005/39, Version 5.1, Vols. I–III, November 2006. Available from Radiation Safety Information Computational Center at Oak Ridge National Laboratory as CCC-732.
3. M. D. DeHart, “NEWT: A New Transport Algorithm for Two-Dimensional Discrete Ordinates Analysis in Non-Orthogonal Geometries,” Vol. II, Book 4, Sect. F21 in *SCALE: A Modular Code System for Performing Standardized Computer Analyses for Licensing Evaluations*, ORNL/TM-2005/39, Version 5.1, Vols. I–III, November 2006. Available from Radiation Safety Information Computational Center at Oak Ridge National Laboratory as CCC-732.
4. S. M. Bowman, M. E. Dunn, D. F. Hollenbach, and W. C. Jordan “SCALE Cross-Section Libraries,” Vol. III, Sect. M4 in *SCALE: A Modular Code System for Performing Standardized Computer Analyses for Licensing Evaluations*, ORNL/TM-2005/39, Version 5.1, Vols. I–III, November 2006. Available from Radiation Safety Information Computational Center at Oak Ridge National Laboratory as CCC-732.
5. *Test Plan for: Isotopic Validation for Postclosure Criticality of Commercial Spent Nuclear Fuel*, TP-OCRWM-LL-ORNL-02 Rev. 00, CN 01.
6. *Calculation Packages*, ORNL OCRW-19.1, Revision 03, CN 00.
7. *Scientific Investigations*, ORNL OCRW-21.0, Revision 03, CN 00.
8. *Control of the Electronic Management of Data*, ORNL-OCRW-23.0, Revision 01, CN 01.
9. *Software Control*, ORNL-OCRW-19.0, Revision 06, CN 00.
10. *SCALE-YMP Software Verification Report for Linux_2*, ORNL OCRW-SQA-011, Revision 03, CN 00.
11. “*Standard Review Plan for Dry Cask Storage Systems*,” NUREG-1536, U.S. Nuclear Regulatory Commission, Washington, DC (1997).
12. A. Bresesti, M. Bresesti, and S. Facchetti, *Post-Irradiation Analysis of Trino Vercellese Reactor Fuel Elements*, EUR-4909, Joint Nuclear Research Centre Ispra and Karlsruhe Establishments, 1972.
13. P. Barbero, G. Bidoglio, and M. Bresesti, *Post-Irradiation Examination of the Fuel Discharged from the Trino Vercellese Reactor after the 2nd Irradiation Cycle*, EUR-5605, Joint Research Centre Ispra and Karlsruhe Establishments, 1977.

14. S. Guardini and G. Guzzi, *Benchmark: Reference Data on Post-Irradiation Analyses of Light Water Reactor Fuel Samples. A Review of 12 Years' Experience: Results Obtained and Their Characterization*, EUR-7879, Commission of the European Communities, Luxembourg, 1983.
15. P. Barbero, G. Bidoglio, A. Caldiroli, F. Daniele, R. DeMeester, R. Ernstberger, S. Facchetti, A. Frigo, S. Guardini, G. Guzzi, P. Hansen, L. Lezzoli, L. Koch, W. Konrad, L. Mammarella, F. Mannone, A. Marell, A. Schurenkamper, P. R. Trincerini, and R. Wellum, *Post Irradiation Analysis of the Obrigheim PWR Spent Fuel*, EUR 6589en, Commission of the European Communities, Joint Research Center, Ispra Establishment, Italy. Also published in *European Appl. Res. Rept. –Nucl. Sci. Technol.* **2**(1), 129–177 (1980).
16. U. Hesse, *Verification of the OREST (HAMMER-ORIGEN) Depletion Program System Using Post-Irradiation Analyses of Fuel Assemblies 168, 170, 171, and 176 from the Obrigheim Reactor*, ORNL-TR-88/20, GRS-A-962, Oak Ridge National Laboratory, Oak Ridge, Tenn., 1984.
17. U. Fisher and H. W. Wiese, *Improved and Consistent Determination of the Nuclear Inventory of Spent PWR Fuel on the Basis of Cell-Burnup Methods Using KORIGEN*, ORNL-TR-5043 (translated from the German report KfK 3014, Institute for Neutron Physics and Reactor Technology, Reprocessing and Waste Treatment Project, Karlsruhe Nuclear Research Center, 1983), Oak Ridge National Laboratory, Oak Ridge, Tenn.
18. “Obrigheim,” sections in *Nuclear Power Experience, Plant Description, and Histories*, Vol. PWR-1, pp. 1–10, Aug 1974, p. 1, Dec 1983, and p. 2, Jun 1985.
19. D. Gupta et al., *Safeguarding Fissile Material Flow at Strategic Points in Power Reactors*, KfK 803, Kernforschungszentrum Karlsruhe, February 1969.
20. *Brennelement-Daten für das Project KWO*, A1C-1309011-1, private communication with J. C. Neuber, AREVA NP GmbH, Dept. NEEA-G, Germany, September 15, 2008.
21. S. D. Atkin, *Destructive Examination of 3-Cycle LWR Fuel Rods from Turkey Point Unit 3 for the Climax – Spent Fuel Test*, HEDL-TME 80-89, Hanford Engineering Development Laboratory, June 1981.
22. E. M. Green, *Spent Fuel Data for Waste Storage Programs*, HEDL-TME 79-20, Hanford Engineering Development Laboratory, September 1980.
23. J. C. Ryman et al., *Fuel Inventory and Afterheat Power Studies of Uranium-Fueled Pressurized Water Reactor Fuel Assemblies Using the SAS2 and ORIGEN-S Modules of SCALE with an ENDF/B-V Updated Cross Section Library*, NUREG/CR-2397 (ORNL/CSD-90), prepared for the U.S. Nuclear Regulatory Commission by Oak Ridge National Laboratory, September 1982.
24. M. D. DeHart and O. W. Hermann, *An Extension of the Validation of SCALE (SAS2H) Isotopic Predictions for PWR Spent Fuel*, ORNL/TM-13317, Oak Ridge National Laboratory, Oak Ridge, Tenn., September 1996.
25. F. Schmittroth, G. J. Neely, and J. C. Krogness, *A Comparison of Measured and Calculated Decay Heat for Spent Fuel Near 2.5 Years Cooling Time*, TC-1759, Hanford Engineering Development Laboratory, August 1980.

26. J. O. Barner, *Characterization of LWR Spent Fuel MCC-Approved Testing Material - ATM-101*, PNL-5109, Rev. 1, Pacific Northwest Laboratory, 1985.
27. Letter, O. Ozer of Electric Power Research Institute to W. B. Lowenstein and B. A. Zolotar, "EPRI-CELL Test Calculations of Isotopes as a Function of Burnup," April 1976.
28. P. E. MacDonald, "Transmittal of CPL Assembly BO5 Axial Flux Measurements – MacD-67-75," Aeroject Nuclear Company, Inc., Idaho, September 11, 1975.
29. "Robinson 2," Sections in *Nuclear Power Experience, Plant Description, and Histories*, Vol. PWR-1, p. 5, May 1972, and p. 1, September 1975.
30. R. J. Guenther, D. E. Blahnik, T. K. Campbell, U. P. Jenquin, J. E. Mendel, L. E. Thomas, and C. K. Thornhill, *Characterization of Spent Fuel Approved Testing Material— ATM-103*, Pacific Northwest Laboratory, PNL-5109-103 (UC-70), April 1988.
31. R. J. Guenther, D. E. Blahnik, U. P. Jenquin, J. E. Mendel, L. E. Thomas, and C. K. Thornhill, *Characterization of Spent Fuel Approved Testing Material—ATM-104*, Pacific Northwest Laboratory, PNL-5109-104 (UC-802), December 1991.
32. R. J. Guenther, D. E. Blahnik, T. K. Campbell, U. P. Jenquin, J. E. Mendel, and C. K. Thornhill, *Characterization of Spent Fuel Approved Testing Material— ATM-106*, Pacific Northwest Laboratory, PNL-5109-106 (UC-70), October 1988.
33. M. C. Brady-Raap and R. J. Talbert, *Compilation of Radiochemical Analyses of Spent Nuclear Fuel Samples*, PNL-13677, Pacific Northwest National Laboratory, Richland, WA, September 2001.
34. S. R. Bierman and R. J. Talbert, *Benchmark Data for Validating Irradiated Fuel Compositions Used in Criticality Calculations*, PNL-10045, Pacific Northwest Laboratory, October 1994.
35. S. R. Bierman, "Spent Reactor Fuel Benchmark Composition Data for Code Validation," *Proceedings of International Conference on Nuclear Criticality Safety*, Oxford, United Kingdom, September 1991.
36. SFCOMPO—Spent Fuel Isotopic Composition Database, operated by the NEA Nuclear Science Division under the supervision of the Working Party on Nuclear Criticality Safety, Nuclear Energy Agency web site: <http://www.nea.fr/html/science/wpncs/sfcompo/>.
37. A. A. Rimski-Korsakov, A. V. Stepanov, A. D. Kirikov, *Radiochemical Analysis of Spent Reactor Fuel Sample*, 1993; A. A. Rimski-Korsakov, T. P. Makarova, V. M. Alexandruk, B. N. Beljaev, V. D. Domkin, and A. V. Lovtsus, *Radiochemical Analysis of Spent Reactor Fuel Samples*, April 1995; A. V. Stepanov, L. S. Buljanitsa, P. A. Galtzev, and A. B. Bogorodizkii, *Radiochemical Analysis of Spent Reactor Fuel Sample 87-108*, March 1996; A. V. Stepanov, T. P. Makarova, V. M. Alexandruk, T. A. Demjanova, B. N. Beljaev, V. D. Domkin, and A. V. Lovtsus, *Radiochemical Analysis of Spent Reactor Fuel Samples: Report on the Results of Determination of Rare Earth Isotopic Abundances*, April 1996; reports of the European Analytical Services, Inc., representing the V. G. Khlopin Radium Institute, St. Petersburg, Russia. Information and data are reproduced in PNL-13677, September 2001.

38. O. W. Hermann, S. M. Bowman, M. C. Brady, and C. V. Parks, *Validation of the SCALE System for PWR Spent Fuel Isotopic Composition Analyses*, ORNL/TM-12667, Oak Ridge National Laboratory, Oak Ridge, Tenn., March 1995.
39. M. Rahimi, E. Fuentes, D. Lancaster, *Isotopic and Criticality Validation for PWR Actinide-only Burnup Credit*, DOE/RW-0497, Office of Civilian Radioactive Waste Management, May 1997.
40. J. W. Roddy, H. C. Claiborne, R. C. Ashline, P. J. Johnson, and B. T. Rhyne, *Physical and Decay Characteristics of Commercial LWR Spent Fuel*, ORNL/TM-9591/V1, Oak Ridge National Laboratory, Oak Ridge, Tenn., October 1985.
41. Y. Nakahara, Y. Suyama, and T. Suzaki, *Technical Development on Burnup Credit for Spent LWR Fuels*, JAERI-Tech 2000-071 (ORNL/TR-2001/01), English Translation, Oak Ridge National Laboratory, Oak Ridge, Tenn. (2002).
42. K. Suyama, H. Mochizuki, and Y. Nakahara, "Revised Burnup Code System SWAT: Description and Validation Using Postirradiation Examination Data." *Nucl. Technol.* **138**, 97–110 (2002).
43. Y. Nakahara, K. Suyama, J. Inagawa, R. Nagaishi, S. Kurosawa, N. Kohno, M. Onuki, and H. Mochizuki, "Nuclide Composition Benchmark Data Set for Verifying Burnup Codes on Spent Light Water Reactor Fuels," *Nucl. Technol.* **137**, 111–126 (2002).
44. S. F. Wolf, D. L. Bowers, and J. C. Cunnane, *Analysis of Spent Nuclear Fuel Samples from Three Mile Island and Quad Cities Reactors: Final Report*, Argonne National Laboratory, Argonne, Ill., November 2000.
45. R. D. Reager, R. B. Adamson, and K. W. Edsinger, *TRW Yucca Mountain Project Test Report, Phase I and 2*, Ref. TRW Purchase Order No. A09112CC8A, General Electric Nuclear Energy (1999).
46. *Summary Report of Commercial Reactor Criticality Data for Three Mile Island Unit 1*, TDR-UDC-NU-000004 Rev 01, Bechtel SAIC Company, Las Vegas, Nev. (2001).
47. *Three Mile Island Unit 1 Radiochemical Assay Comparisons to SAS2H Calculations*, CAL-UDC-NU-000011, Rev A, Bechtel SAIC Company, Las Vegas, Nev. (2002).
48. *ARIANE International Programme—Final Report*, ORNL/SUB/97-XSV750-1, Oak Ridge National Laboratory, Oak Ridge, Tenn., May 2003.
49. *REBUS International Program—Reactivity Tests for a Direct Evaluation of the Burnup Credit on Selected Irradiated LWR Fuel Bundles, Fuel Irradiation History Report*, SCK-CEN, Belgonucleaire, RE 2002/18, Rev. B, June 2005.
50. *REBUS International Program—Reactivity Tests for a Direct Evaluation of the Burnup Credit on Selected Irradiated LWR Fuel Bundles, Destructive Radiochemical Spent Fuel Characterization of a PWR UO₂ Fuel Sample*, SCK-CEN, Belgonucleaire, RE 2005/35, Rev. A, May 2006.
51. *REBUS International Program—Reactivity Tests for a Direct Evaluation of the Burnup Credit on Selected Irradiated LWR Fuel Bundles, Gamma Spectroscopy PIE on Irradiated GKN II Fuel Rods*, SCK-CEN, Belgonucleaire, RE 2004/29, December 2004.

52. *REBUS International Program—Reactivity Tests for a Direct Evaluation of the Burnup Credit on Selected Irradiated LWR Fuel Bundles, VENUS Fuel Characterization Report*, SCK-CEN, Belgonucleaire, RE 2001/13, Rev. C, May 2006.
53. *REBUS International Program—Reactivity Tests for a Direct Evaluation of the Burnup Credit on Selected Irradiated LWR Fuel Bundles, Final Report*, SCK-CEN, Belgonucleaire, RE 2005/37, February 2006.
54. MALIBU Program, *Radiochemical Analysis of MOX and UOX LWR Fuels Irradiated to High Burnup*, Final Report on the Basic Scope, MA 2006/11, December 2007.
55. MALIBU Program, *Radiochemical Analysis of MOX and UOX LWR Fuels Irradiated to High Burnup*, Irradiation Data Report, MA 2003/05, Rev. D, December 2007.
56. *1998 World Nuclear Industry Handbook*, Nuclear Engineering International (1998).
57. *2004 World Nuclear Industry Handbook*, edited by Nuclear Engineering International (2005).
58. L. Haar, J. S. Gallagher, and G. S. Kell, *NBS/NRC Steam Tables: Thermodynamic and Transport Properties and Computer Programs for Vapor and Liquid States of Water in SI Units*, Taylor & Francis, Levittown, PA, 1984.
59. Evaluated Nuclear Structure Data File—a computer file of evaluated experimental nuclear structure data maintained by the National Nuclear Data Center, Brookhaven National Laboratory (file as of January 2005).
60. Nuclear Data Sheets – Elsevier B.V., Amsterdam. Evaluations published by mass number for $A = 21$ to 294. See page ii of any issue for the index to A-chains. See also Energy Levels of $A = 21$ –44 Nuclei (VII), P. M. Endt, Nuclear Physics A521, 1 (1990). Supplement, *Nuclear Physics A633*, 1 (1998).
61. Nuclear Physics – North Holland Publishing Co., Amsterdam – Evaluations for $A = 3$ to 20.
62. G. Audi, A. H. Wapstra, and C. Thibault, The AME2003 atomic mass evaluation—(II) Tables, graphs and references, *Nuclear Physics A729*, 337–676 (2003).
63. J. R. Parrington, H. D. Knox, S. L. Breneman, E. M. Baum, and F. Feiner. *Nuclides and Isotopes, Chart of the Nuclides*. 15th Edition. San Jose, California: General Electric Company and KAPL, Inc, 1996.
64. O. W. Hermann, C. V. Parks, and J. P. Renier, *Technical Support for a Proposed Decay Heat Guide Using SAS2H/ORIGEN-S Data*, NUREG/CR-5625 (ORNL/TM-2005/39), prepared for the U.S. Nuclear Regulatory Commission by Oak Ridge National Laboratory, July 1994.
65. J. R. Lamarsh and A. J. Baratta, *Introduction to Nuclear Engineering* (3rd Edition).
66. W. J. M. de Kruijf and A. J. Janssen, “The Effective Fuel Temperature to be Used for Calculating Resonance Absorption in a $^{238}\text{UO}_2$ Lump with a Nonuniform Temperature Profile,” *Nucl. Sci. Eng.* **123**, 121–135 (1996).

67. I. C. Gauld and O. W. Herman "SAS2: A Coupled One-Dimensional Depletion and Shielding Analysis Module," Vol. I, Book 3, Sect. S2 in *SCALE: A Modular Code System for Performing Standardized Computer Analyses for Licensing Evaluations*, ORNL/TM-2005/39, Version 5.1, Vols. I–III, November 2006. Available from Radiation Safety Information Computational Center at Oak Ridge National Laboratory as CCC-732.
68. *Disposal Criticality Analysis Methodology Topical Report*, YMP/TR-004Q, Rev. 02, Yucca Mountain Site Characterization Project, Las Vegas, Nevada (2003).
69. *Calculation of Isotopic Bias and Uncertainty for PWR Spent Nuclear Fuel*, CAL-DSU-NU-000001 Rev A, Bechtel SAIC Company, Las Vegas, Nev. (2002).
70. O. W. Hermann, M. D. DeHart, and B. D. Murhpy, *Evaluation of Measured LWR Spent Fuel Composition Data for Use in Code Validation—End-User Manual*, Oak Ridge National Laboratory Report ORNL/M-6121, February 1998.
71. D. Boulanger, M. Lippens, L. Mertens, J. Basselier, and B. Lance, "High Burnup PWR and BWR MOX Fuel Performance: A Review of BELGONUCLEAIRE Recent Experimental Programs," ANS International Meeting on LWR Fuel Performance, Orlando, FL, USA, September 19–22, 2004.
72. P. Baeten, P. D'hondt, L. Sannen, D. Marloye, B. Lance, A. Renard and J. Basselier, "The REBUS Experimental Programme for Burn-up Credit," ICNC 2003–7th Int. Conf. on Nuclear Criticality Safety Tokai Mura, Japan, October 19–24, 2003.
73. *CSNF Loading Curve Sensitivity Analysis*, ANL-EBS-NU-000010 REV 00, Sandia National Laboratories, Las Vegas, Nev., February 2008.
74. American Society for Testing and Materials Standard Method E 321-96 (Reapproved 2005), "Standard Test Method for Atom Percent Fission in Uranium and Plutonium Fuel (Neodymium-148 Method)," (2005).
75. J. S. Kim, Y. S. Jeon, K. S. Choi, B. C. Song, S. H. Han, and W. H. Kim, "Burnup Measurement of Spent U3Si/Al Fuel by Chemical Methods Using Neodymium Isotope Monitors," *J. Korean Nucl. Soc.* **33**(4), 375–385, August 1002.
76. K. Suyama, H. Mochizuki, "Corrections to the ¹⁴⁸Nd Method of Evaluation of Burnup for the PIE Samples from Mihama-3 and Genkai-1 Reactors," *Annals of Nuclear Energy*.
77. J. Tuli, *Nuclear Wallet Cards 7th Edition*, National Nuclear Data Center, Brookhaven National Laboratory, Upton, NY (2005).
78. American Society for Testing and Materials Standard Method E 267-90(2001), "Standard Test Method for Uranium and Plutonium Concentrations and Isotopic Abundances" (withdrawn 2006).
79. Department of Energy, "Energy Information Administration," Form RW-859, Nuclear Fuel Data (2002).
80. W. B. Wilson, R. J. LaBauve, and T. R. England, "Spent LWR Fuel Inventory Benchmarks, in Applied Nuclear Data Research and Development," April 1, 1982–September 30, 1982, Los Alamos National Laboratory, LA-9647-PR, pp. 75–88, 1982.

81. American Society for Testing and Materials Standard Method E 692-00, "Standard Test Method for Determining the Content of Cesium-137 in Irradiated Nuclear Fuels by High-Resolution Gamma-Ray Spectral Analysis" (2000).
82. M. D. DeHart, M. C. Brady and C. V. Parks, *OECD/NEA Burnup Credit Computational Criticality Benchmark Phase I-B Results*, NEA/NSC/DOC(96)-06, ORNL-6901, Oak Ridge National Laboratory, Oak Ridge, Tenn., June 1996.
83. *TMI-1 Cycle 10 Fuel Rod Failures – Volume 1: Root Cause Failure Evaluations*, EPRI Report TR-108784-V1, 1998.
84. Trino Vercellese Nuclear Power Plant Research Program for the Development of Closed-Cycle Water Reactor Technology, Commission of the European Communities EUR 4827 (1973).
85. J. B. Melehan, *Yankee Core Evaluation Program Final Report*, WCAP-3017-6094, Westinghouse Electric Corp., 1971.
86. L. M. Petrie, P. B. Fox, and K. Lucius "Standard Composition Library," Vol. III, Sect. M8 in *SCALE: A Modular Code System for Performing Standardized Computer Analyses for Licensing Evaluations*, ORNL/TM-2005/39, Version 5.1, Vols. I–III, November 2006. Available from Radiation Safety Information Computational Center at Oak Ridge National Laboratory as CCC-732.
87. *Calculation of Isotopic Bias and Uncertainty for PWR Spent Nuclear Fuel*, CAL-DSU-NU-000001 REV A, Las Vegas, Nev.: Bechtel SAIC Company, 2002.
88. Department of Energy, "Energy Information Administration," Form RW-859, Nuclear Fuel Data (2002).
89. CRC Depletion Calculations for McGuire Unit 1. B00000000-01717-0210-00003 REV 00. Las Vegas, CRWMS M&O, 1998.
90. C. E. Sanders and I. C. Gauld, *Isotopic Analysis of High-Burnup PWR Spent Fuel Samples from the Takahama-3 Reactor*, NUREG/CR-6798 (ORNL/TM-2001/259), Oak Ridge National Laboratory, Oak Ridge, Tenn., January 2003.
91. I. C. Gauld and O. W. Hermann, "COUPLE: SCALE System Module to Process Problem-Dependent Cross Sections and Neutron Spectral Data for ORIGEN-S Analyses," Vol. II, Book 1, Sect. F6 in *SCALE: A Modular Code System for Performing Standardized Computer Analyses for Licensing Evaluations*, ORNL/TM-2005/39, Version 5.1, Vols. I–III, November 2006. Available from Radiation Safety Information Computational Center at Oak Ridge National Laboratory as CCC-732.
92. I. C. Gauld, O. W. Hermann, and R. M. Westfall, "ORIGEN-S: SCALE System Module to Calculate Fuel Depletion, Actinide Transmutation, Fission Product Buildup and Decay, and Associated Radiation Source Terms," Vol. II, Book 1, Sect. F7 in *SCALE: A Modular Code System for Performing Standardized Computer Analyses for Licensing Evaluations*, ORNL/TM-2005/39, Version 5.1, Vols. I–III, November 2006. Available from Radiation Safety Information Computational Center at Oak Ridge National Laboratory as CCC-732.

93. I. C. Gauld, S. M. Bowman, and J. E. Horwedel, "ORIGEN-ARP: Automatic Rapid Processing for Spent Fuel Depletion, Decay, and Source Term Analysis," Vol. I, Book 2, Sect. D1 in *SCALE: A Modular Code System for Performing Standardized Computer Analyses for Licensing Evaluations*, ORNL/TM-2005/39, Version 5.1, Vols. I-III, November 2006. Available from Radiation Safety Information Computational Center at Oak Ridge National Laboratory as CCC-732.

APPENDIX A:
GRAPHICAL REPRESENTATION OF THE RATIO OF
EXPERIMENTAL-TO-CALCULATED
ISOTOPIC CONCENTRATION
AS A FUNCTION OF BURNUP FOR ISOTOPES RELEVANT TO BURNUP CREDIT

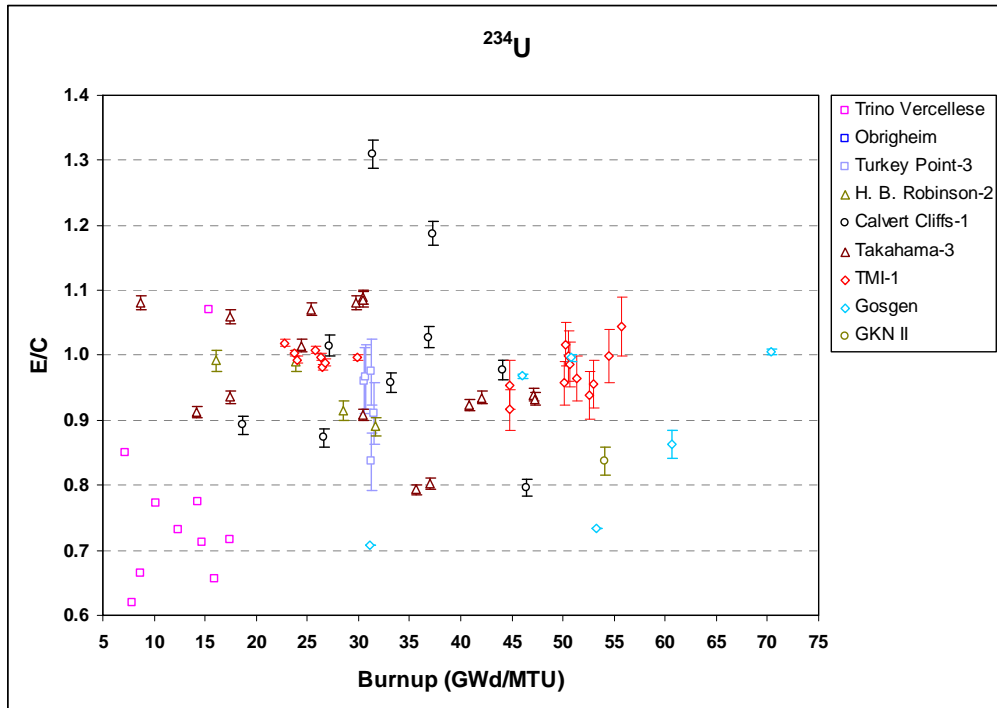


Fig. A.1. Ratio of experimental-to-calculated (E/C) ^{234}U concentration versus sample burnup. The error bars show the one-sigma measurement uncertainty.

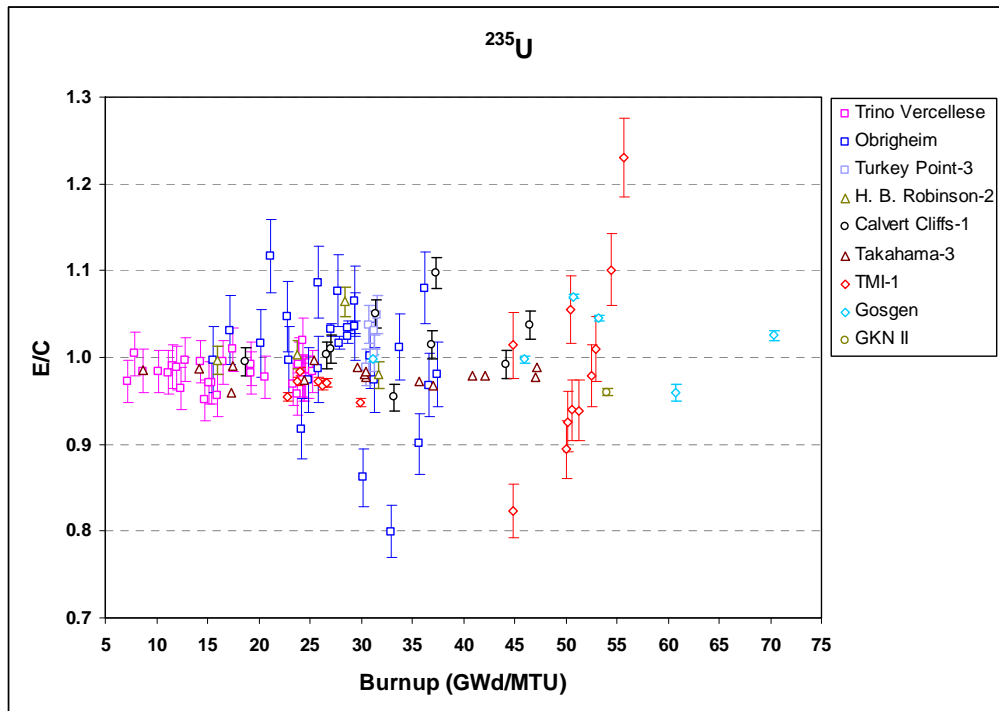


Fig. A.2. Ratio of experimental-to-calculated (E/C) ^{235}U concentration versus sample burnup. The error bars show the one-sigma measurement uncertainty.

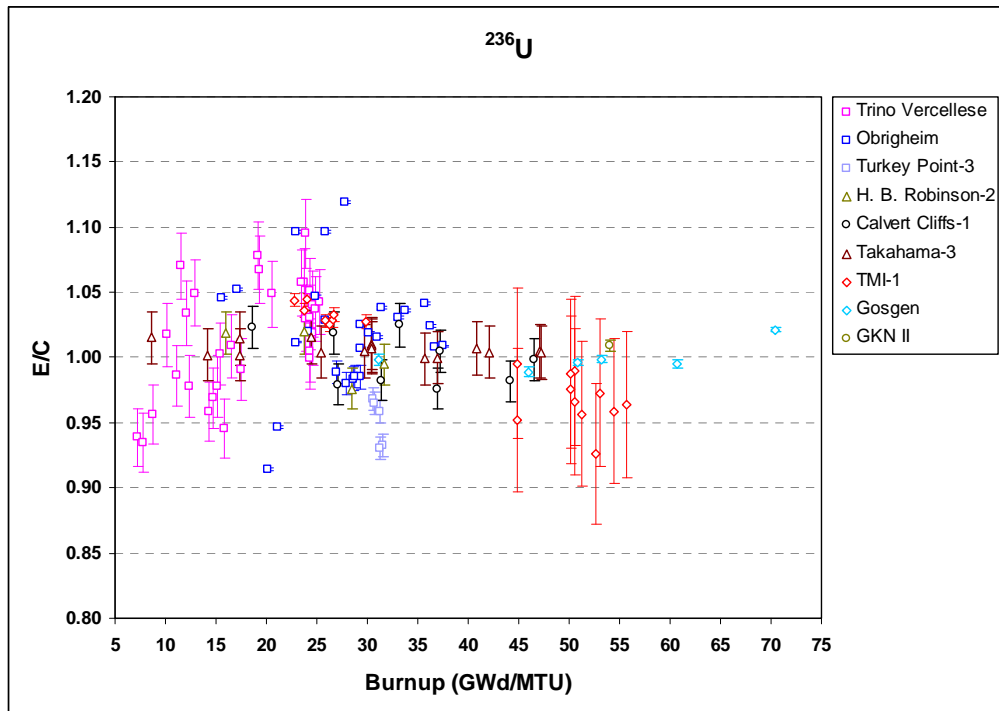


Fig. A.3. Ratio of experimental-to-calculated (E/C) ^{236}U concentration versus sample burnup. The error bars show the one-sigma measurement uncertainty.

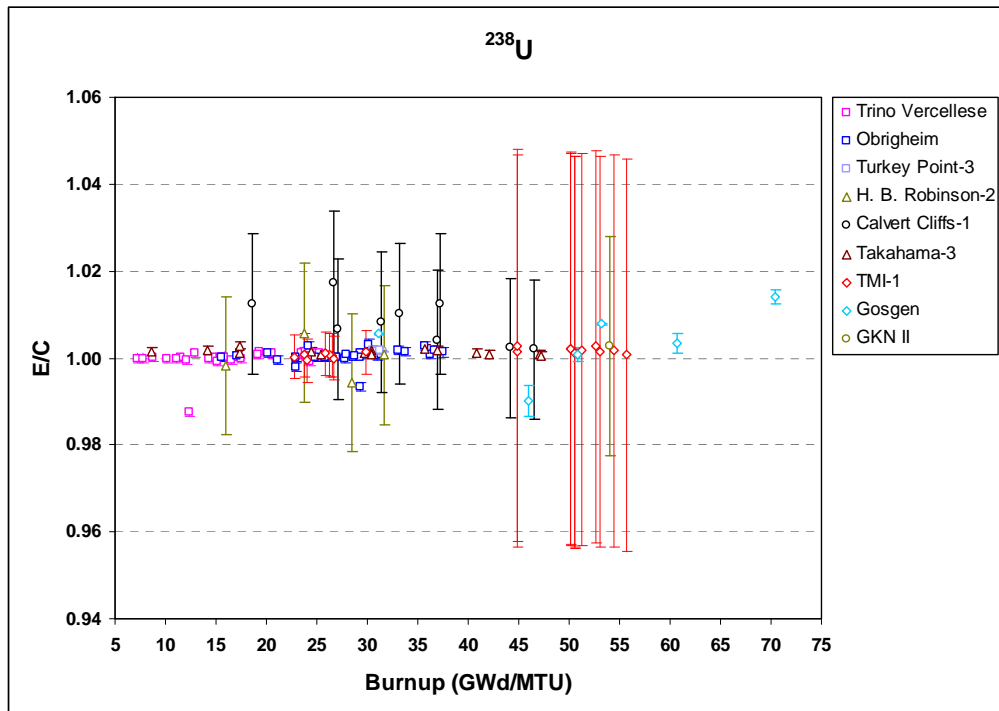


Fig. A.4. Ratio of experimental-to-calculated (E/C) ^{238}U concentration versus sample burnup. The error bars show the one-sigma measurement uncertainty.

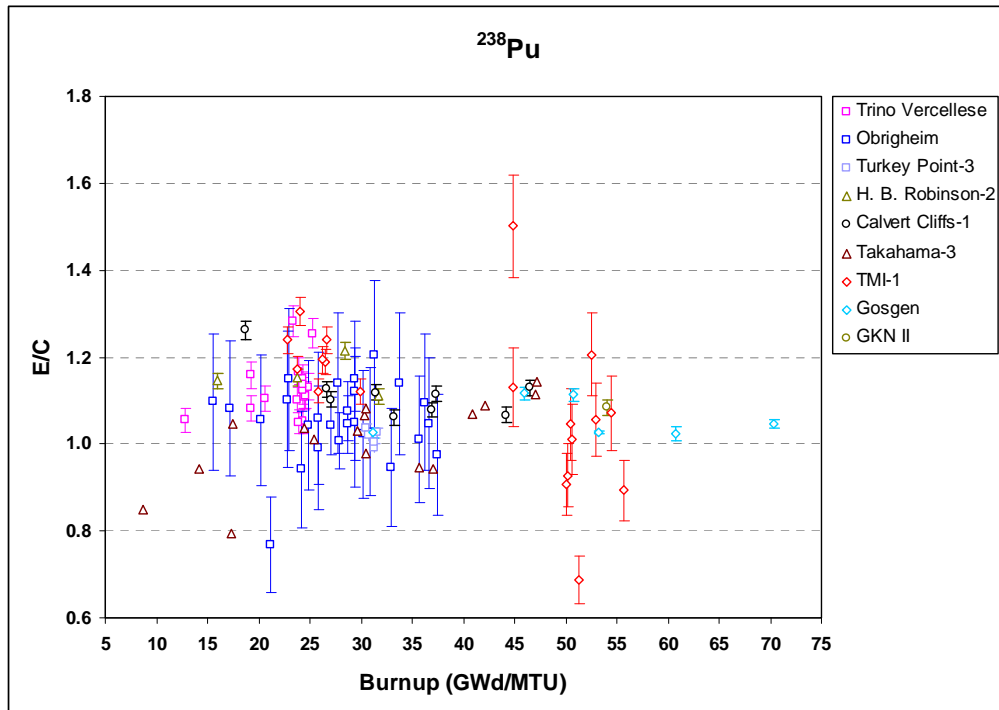


Fig. A.5. Ratio of experimental-to-calculated (E/C) ^{238}Pu concentration versus sample burnup. The error bars show the one-sigma measurement uncertainty.

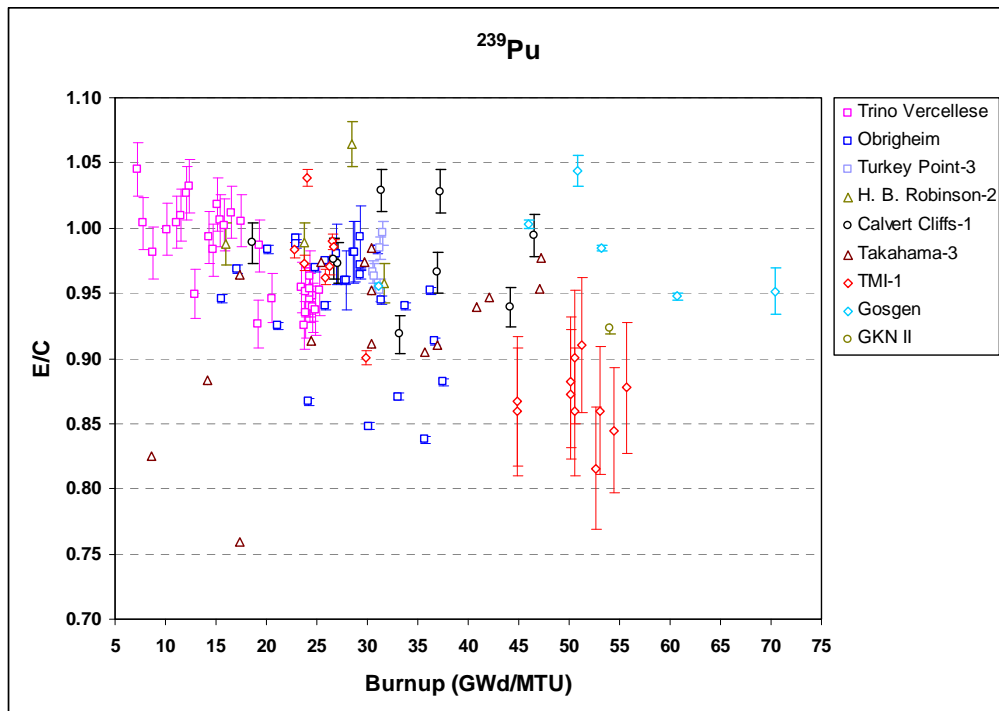


Fig. A.6. Ratio of experimental-to-calculated (E/C) ^{239}Pu concentration versus sample burnup. The error bars show the one-sigma measurement uncertainty.

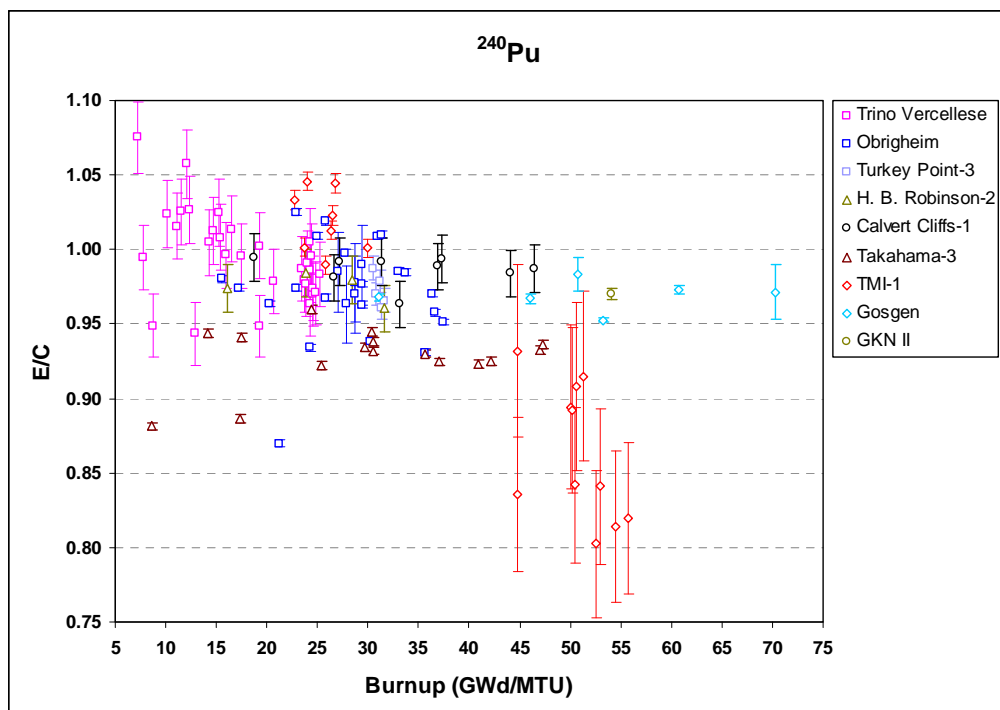


Fig. A.7. Ratio of experimental-to-calculated (E/C) ²⁴⁰Pu concentration versus sample burnup. The error bars show the one-sigma measurement uncertainty.

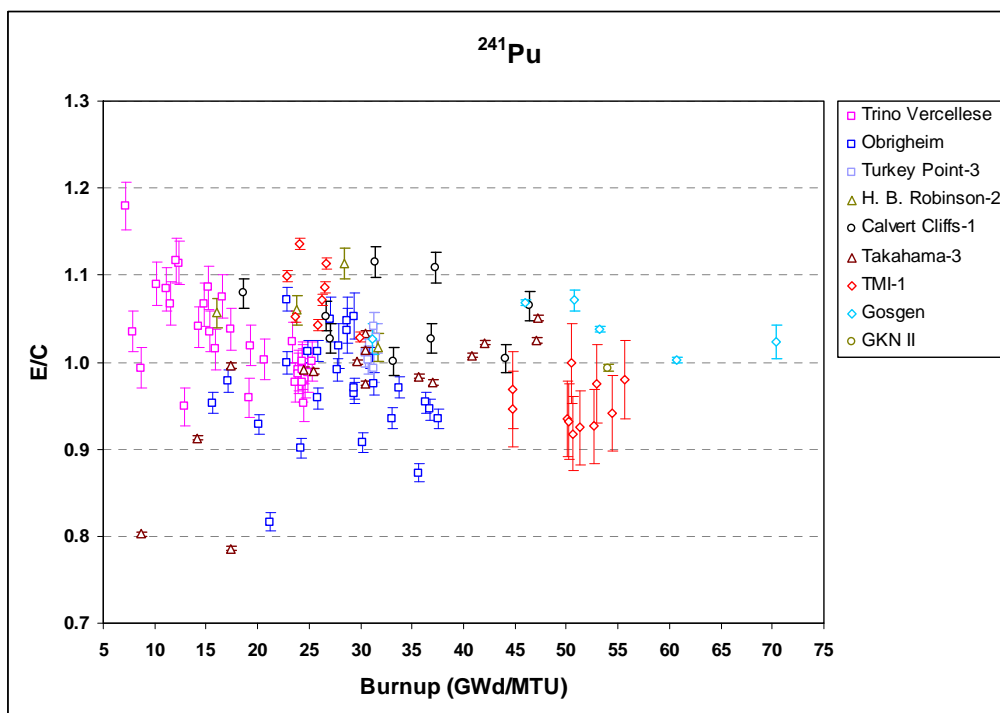


Fig. A.8. Ratio of experimental-to-calculated (E/C) ²⁴¹Pu concentration versus sample burnup. The error bars show the one-sigma measurement uncertainty.

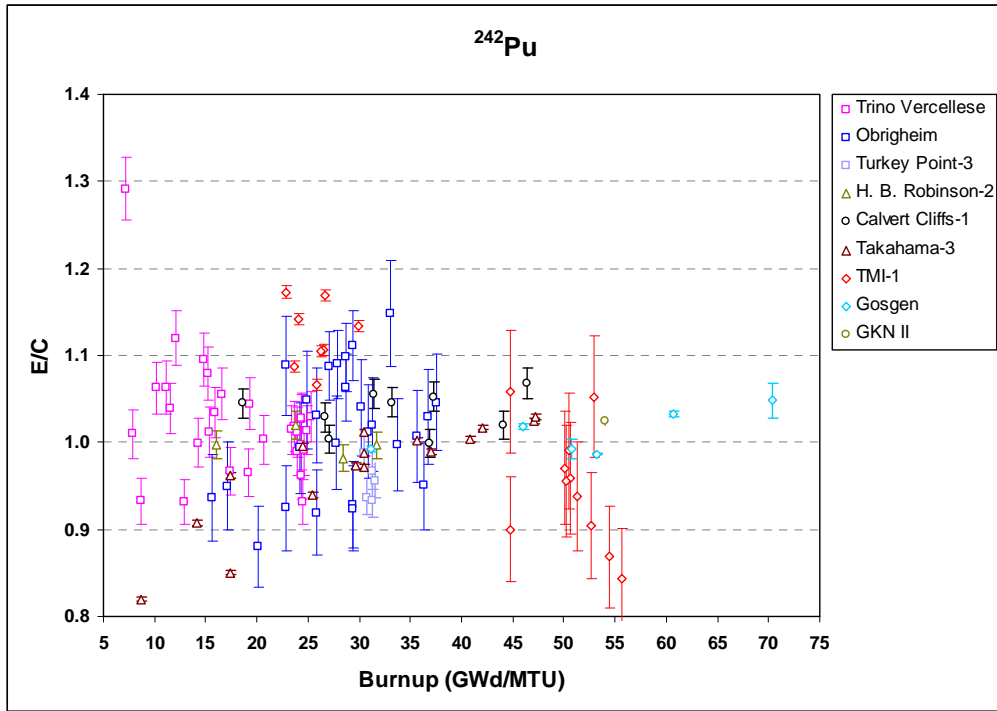


Fig. A.9. Ratio of experimental-to-calculated (E/C) ²⁴²Pu concentration versus sample burnup. The error bars show the one-sigma measurement uncertainty.

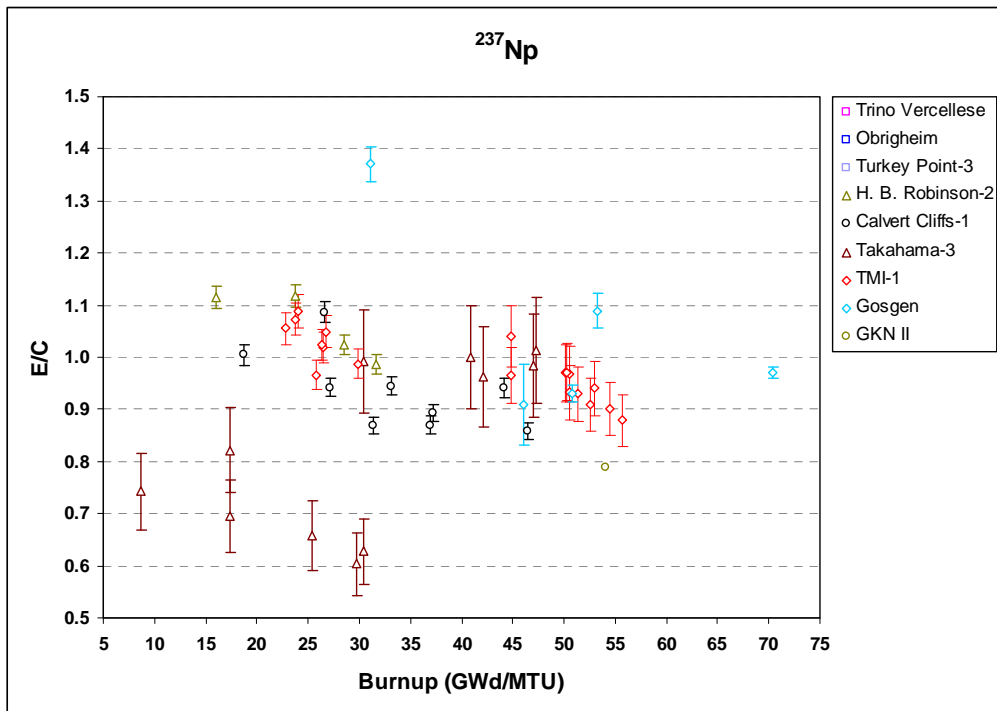


Fig. A.10. Ratio of experimental-to-calculated (E/C) ²³⁷Np concentration versus sample burnup. The error bars show the one-sigma measurement uncertainty.

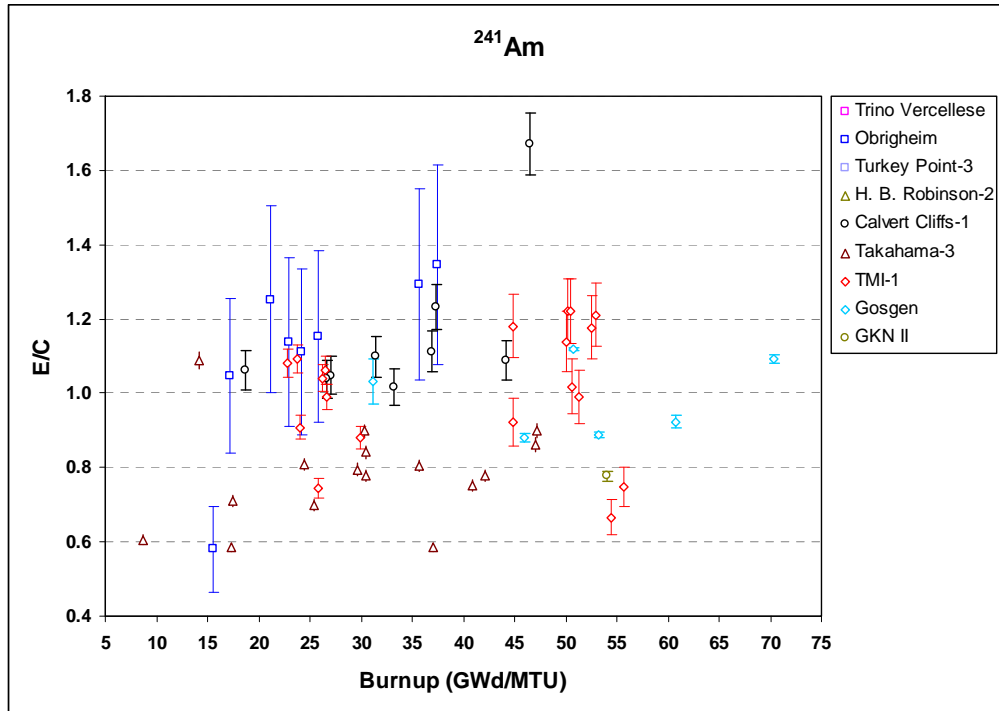


Fig. A.11. Ratio of experimental-to-calculated (E/C) ²⁴¹Am concentration versus sample burnup. The error bars show the one-sigma measurement uncertainty.

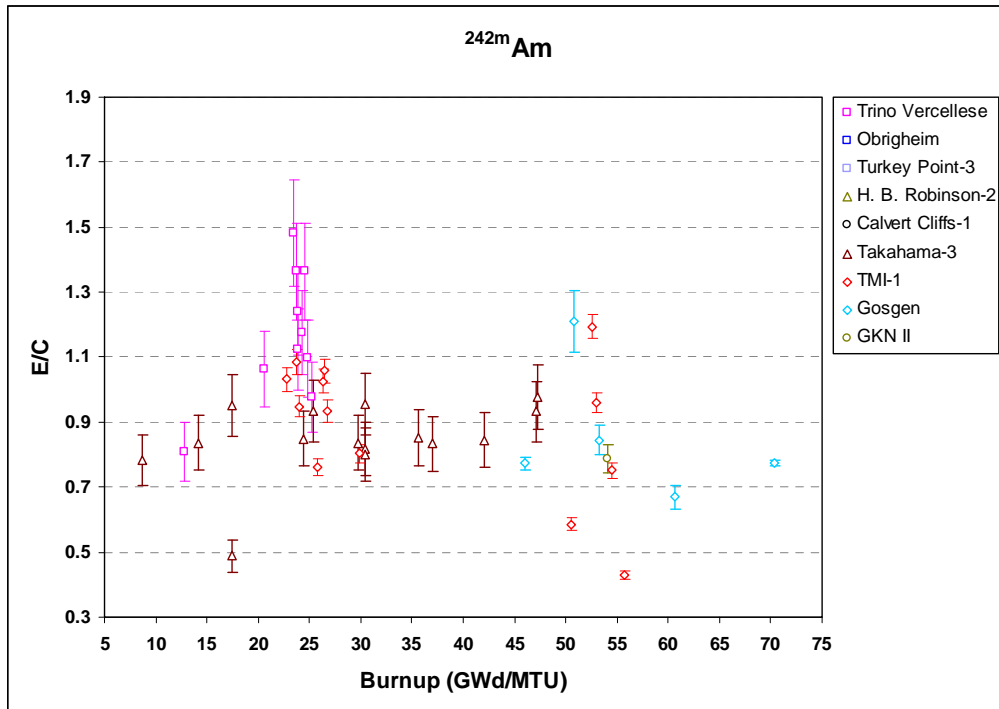


Fig. A.12. Ratio of experimental-to-calculated (E/C) ^{242m}Am concentration versus sample burnup. The error bars show the one-sigma measurement uncertainty.

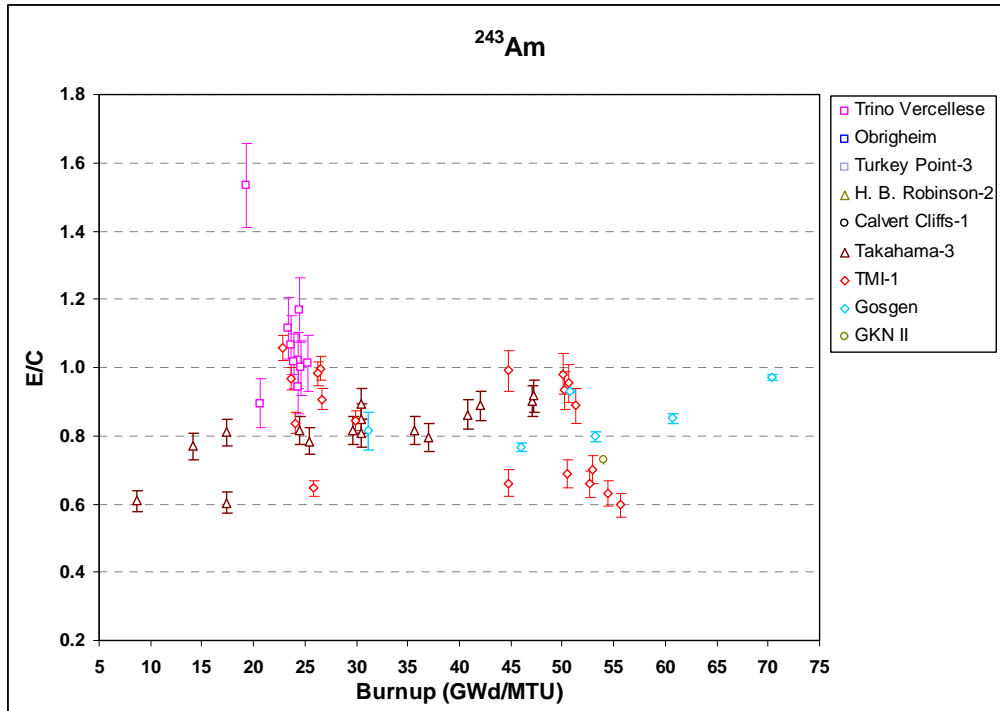


Fig. A.13. Ratio of experimental-to-calculated (E/C) ²⁴³Am concentration versus sample burnup. The error bars show the one-sigma measurement uncertainty.

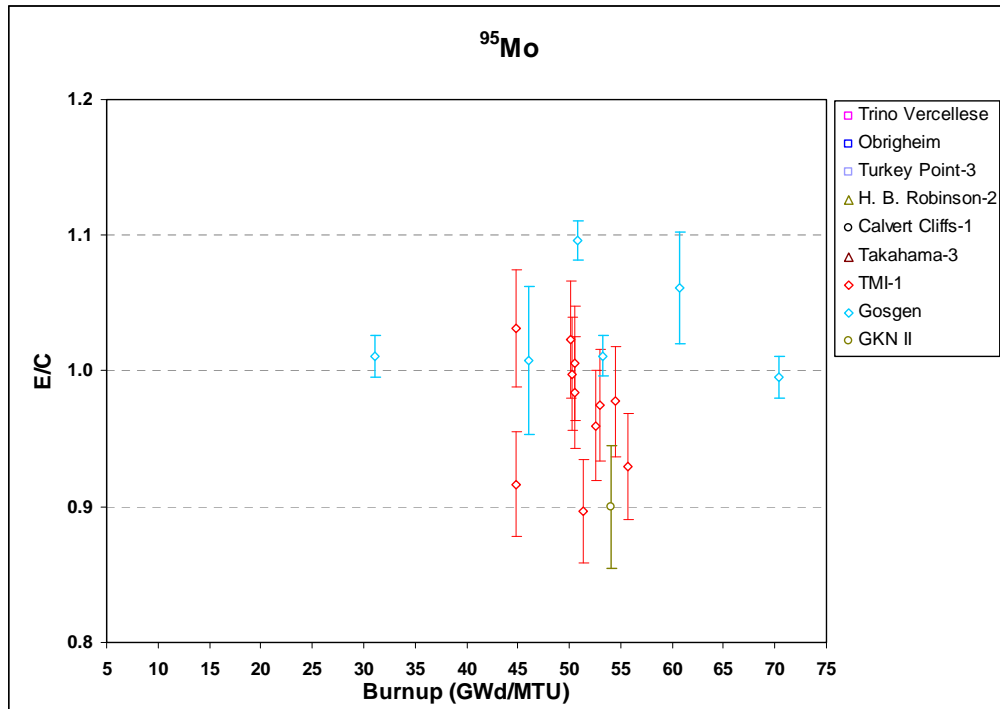


Fig. A.14. Ratio of experimental-to-calculated (E/C) ⁹⁵Mo concentration versus sample burnup. The error bars show the one-sigma measurement uncertainty.

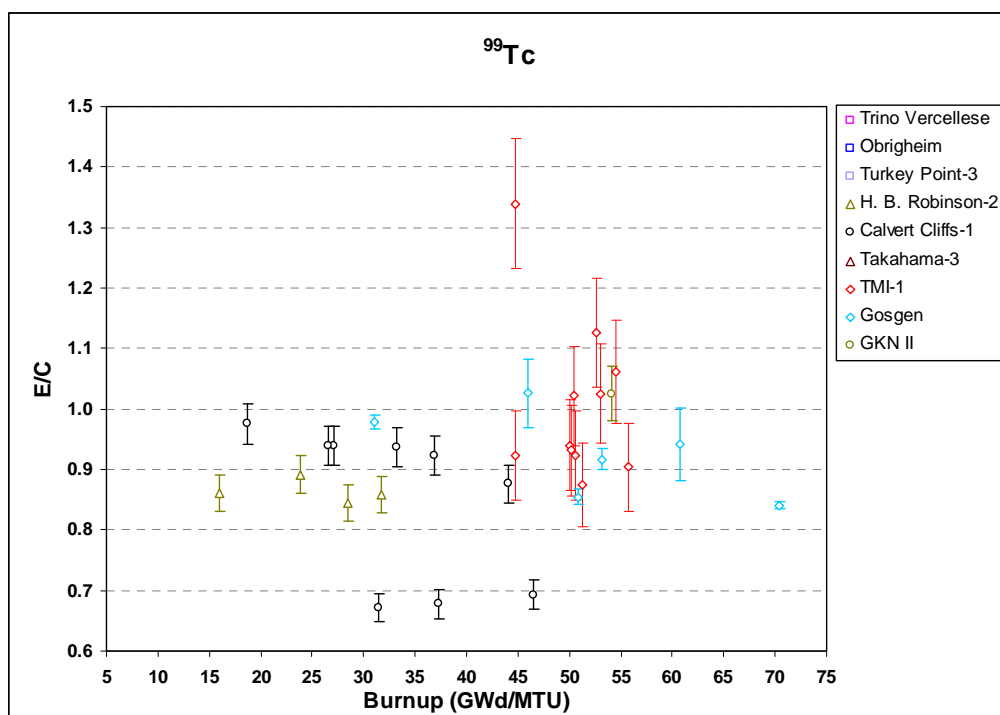


Fig. A.15. Ratio of experimental-to-calculated (E/C) ⁹⁹Tc concentration versus sample burnup. The error bars show the one-sigma measurement uncertainty.

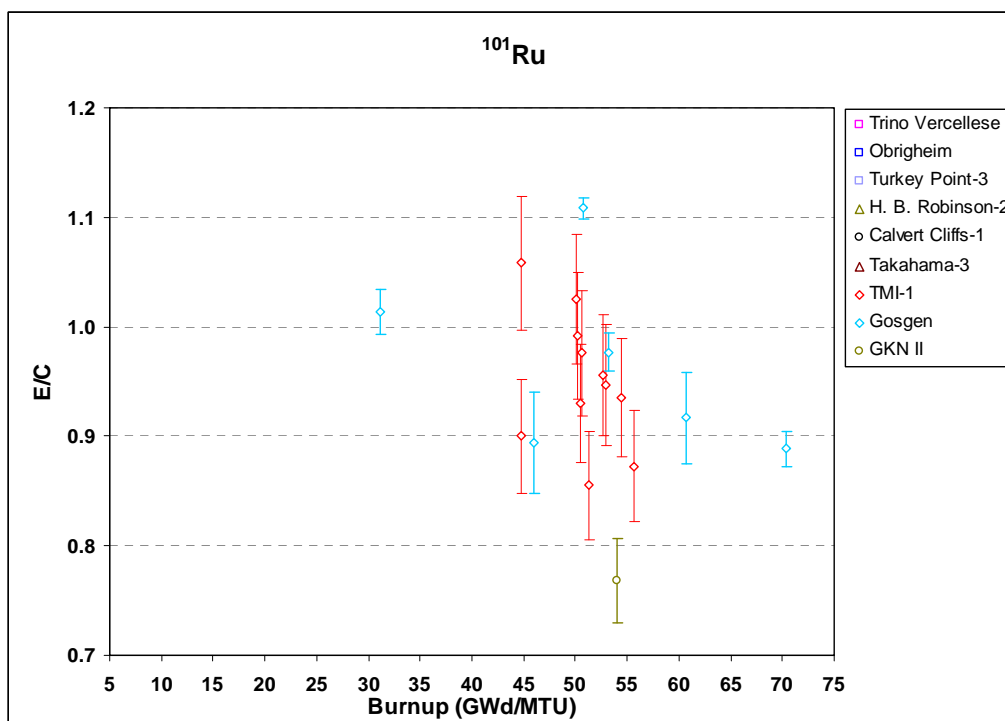


Fig. A.16. Ratio of experimental-to-calculated (E/C) ¹⁰¹Ru concentration versus sample burnup. The error bars show the one-sigma measurement uncertainty.

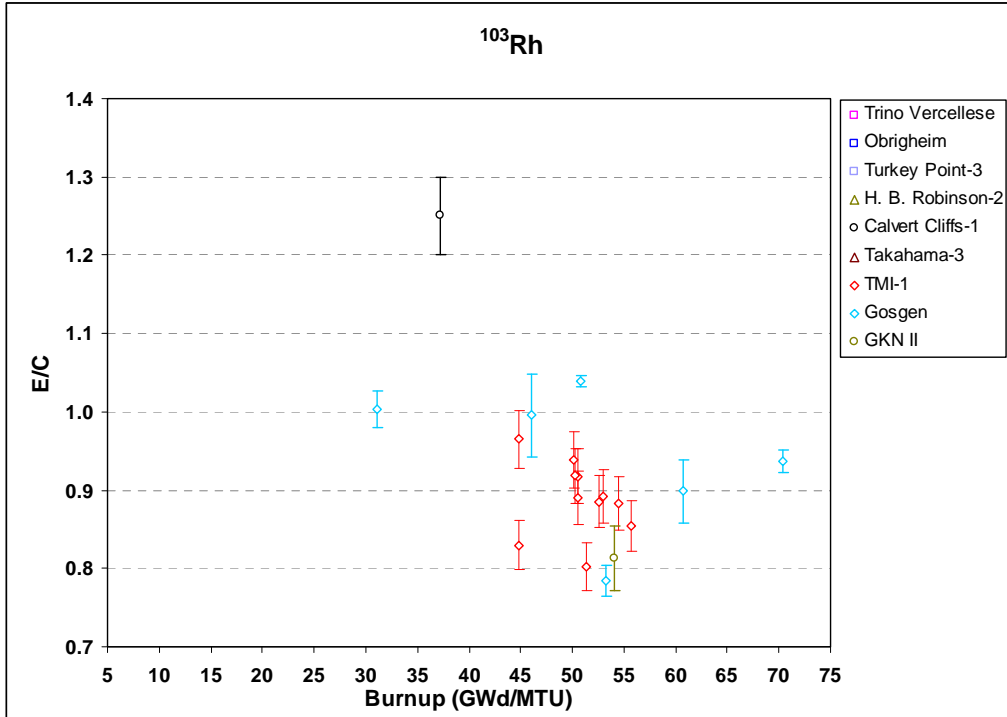


Fig. A.17. Ratio of experimental-to-calculated (E/C) ¹⁰³Rh concentration versus sample burnup. The error bars show the one-sigma measurement uncertainty.

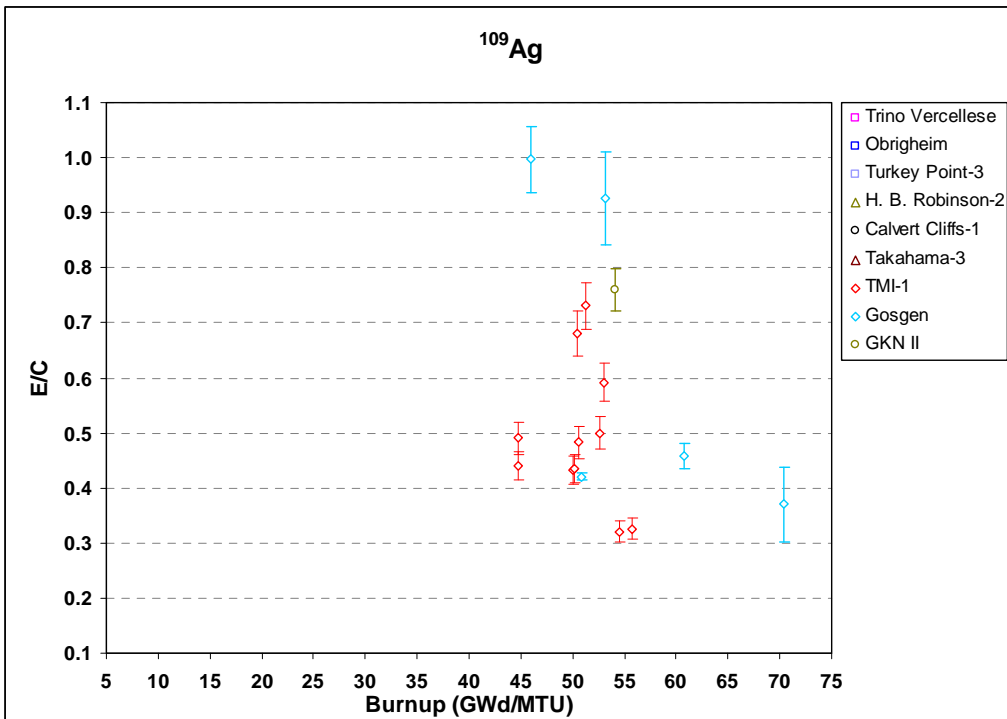


Fig. A.18. Ratio of experimental-to-calculated (E/C) ¹⁰⁹Ag concentration versus sample burnup. The error bars show the one-sigma measurement uncertainty.

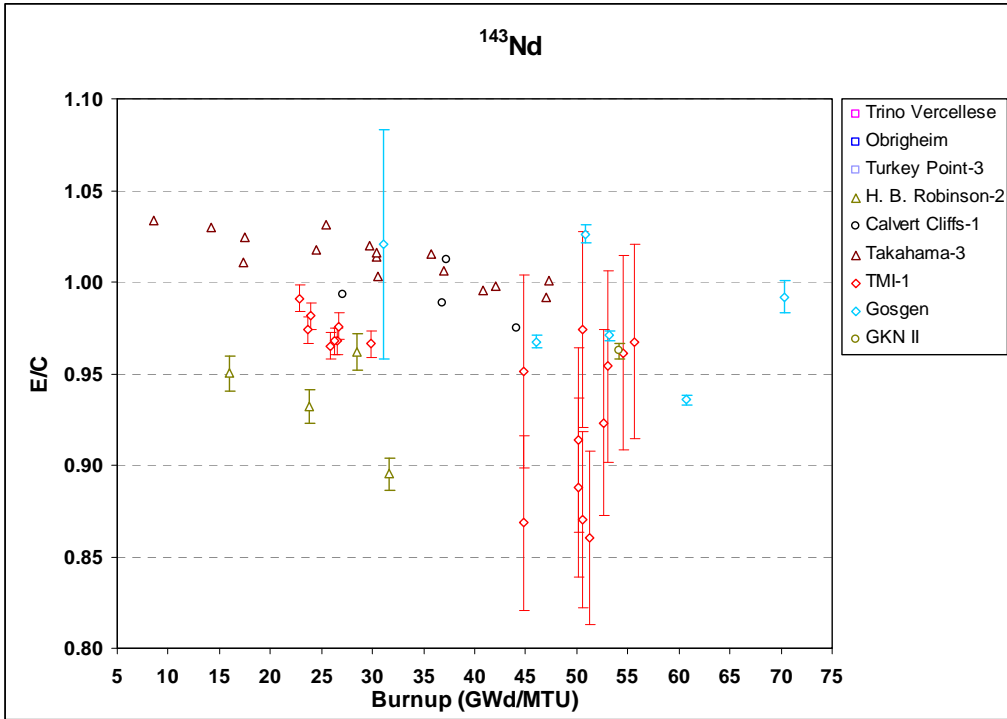


Fig. A.19. Ratio of experimental-to-calculated (E/C) ¹⁴³Nd concentration versus sample burnup. The error bars show the one-sigma measurement uncertainty.

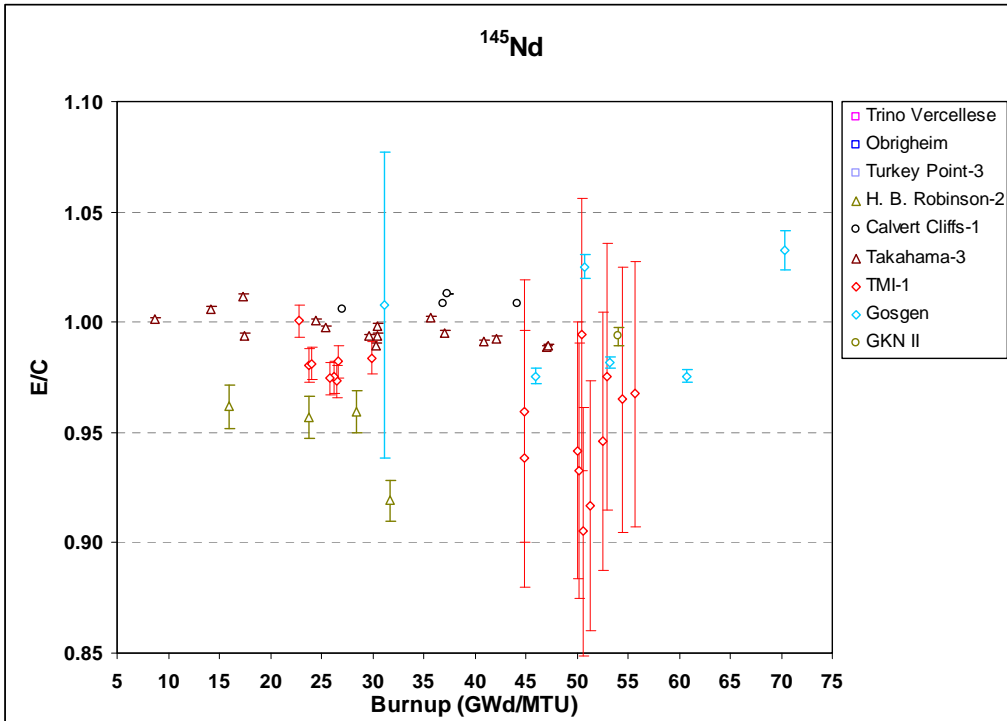


Fig. A.20. Ratio of experimental-to-calculated (E/C) ¹⁴⁵Nd concentration versus sample burnup. The error bars show the one-sigma measurement uncertainty.

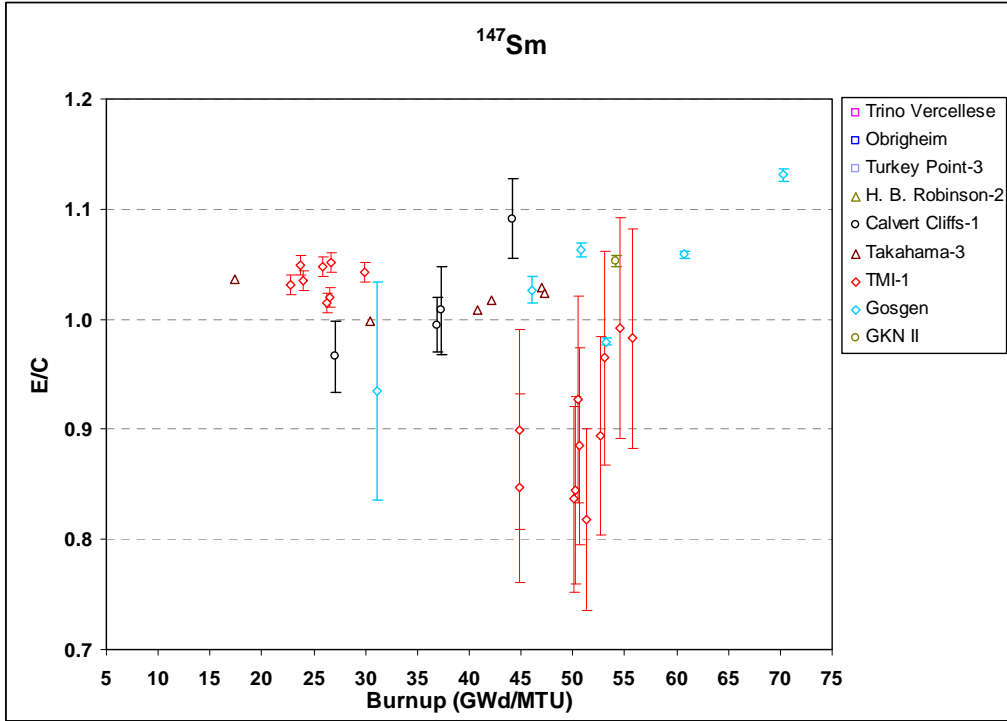


Fig. A.21. Ratio of experimental-to-calculated (E/C) ¹⁴⁷Sm concentration versus sample burnup. The error bars show the one-sigma measurement uncertainty.

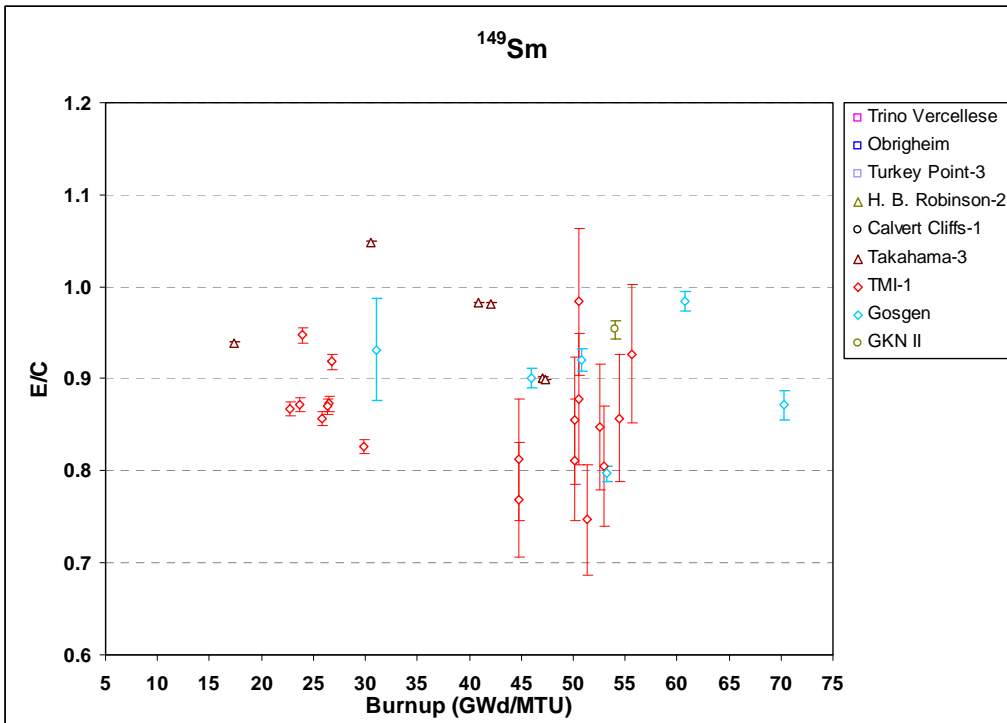


Fig. A.22. Ratio of experimental-to-calculated (E/C) ¹⁴⁹Sm concentration versus sample burnup. The error bars show the one-sigma measurement uncertainty.

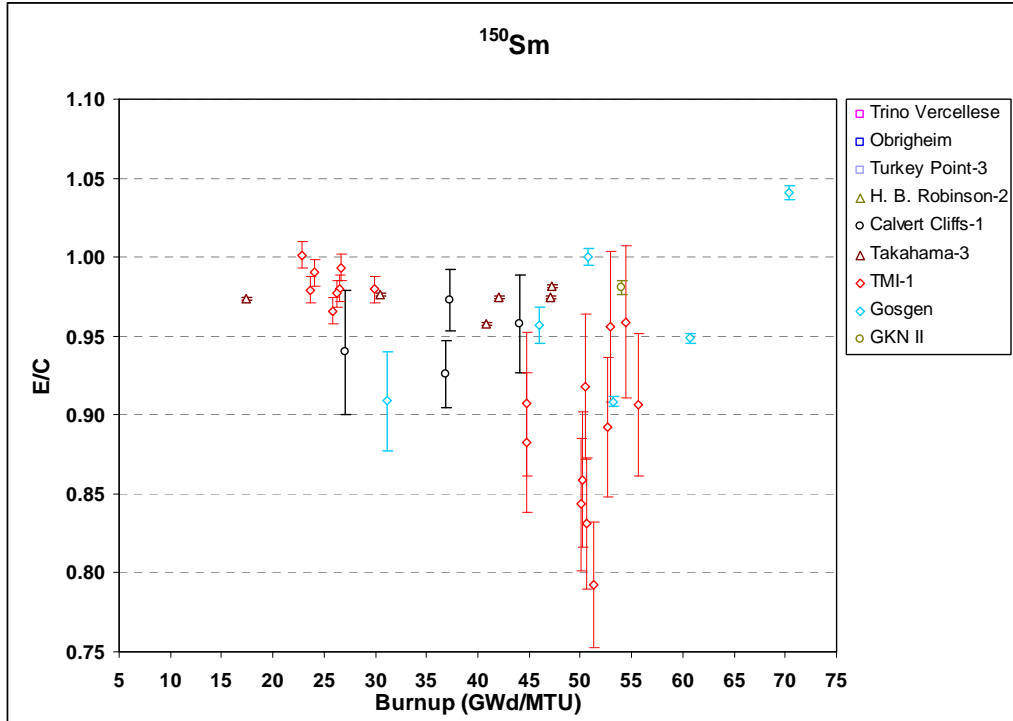


Fig. A.23. Ratio of experimental-to-calculated (E/C) ¹⁵⁰Sm concentration versus sample burnup. The error bars show the one-sigma measurement uncertainty.

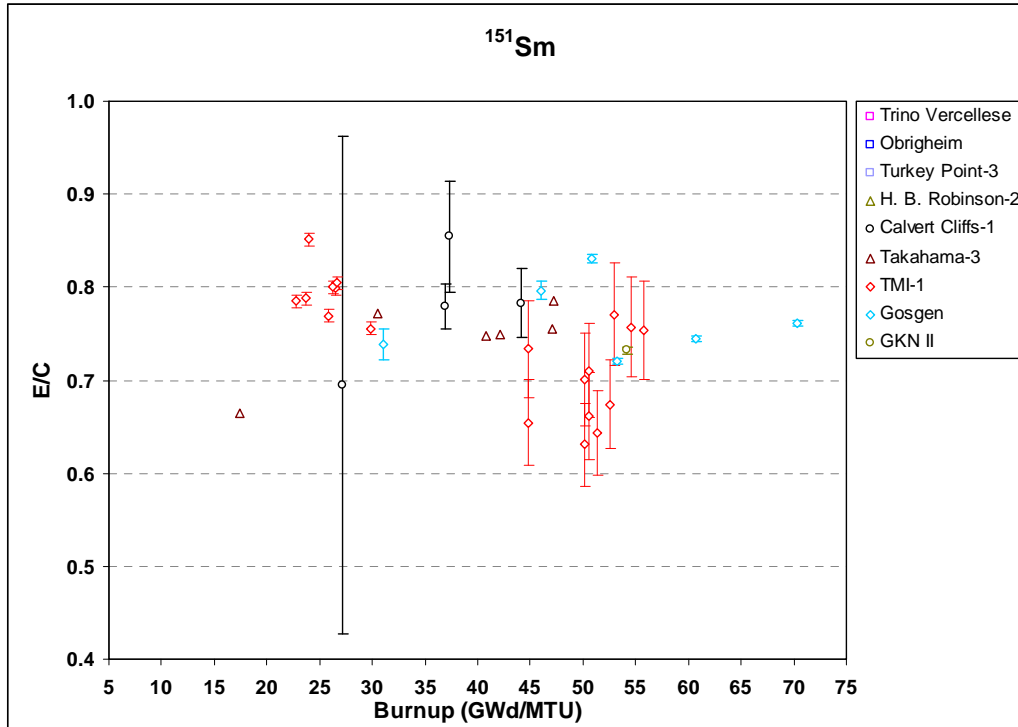


Fig. A.24. Ratio of experimental-to-calculated (E/C) ¹⁵¹Sm concentration versus sample burnup. The error bars show the one-sigma measurement uncertainty.

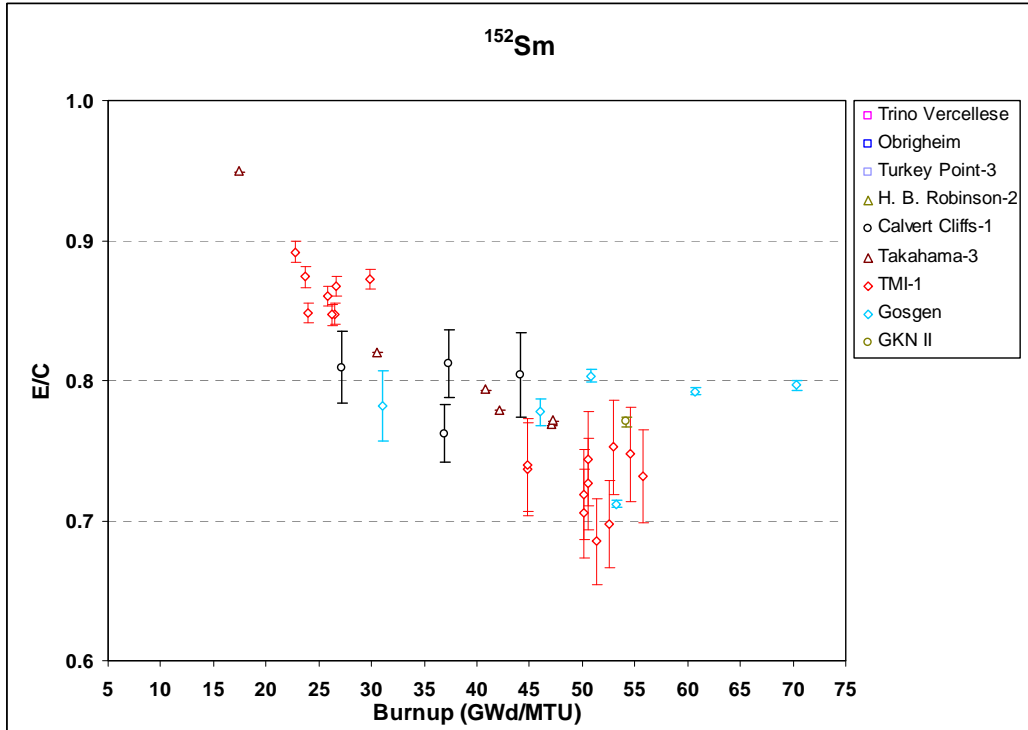


Fig. A.25. Ratio of experimental-to-calculated (E/C) ^{152}Sm concentration versus sample burnup. The error bars show the one-sigma measurement uncertainty.

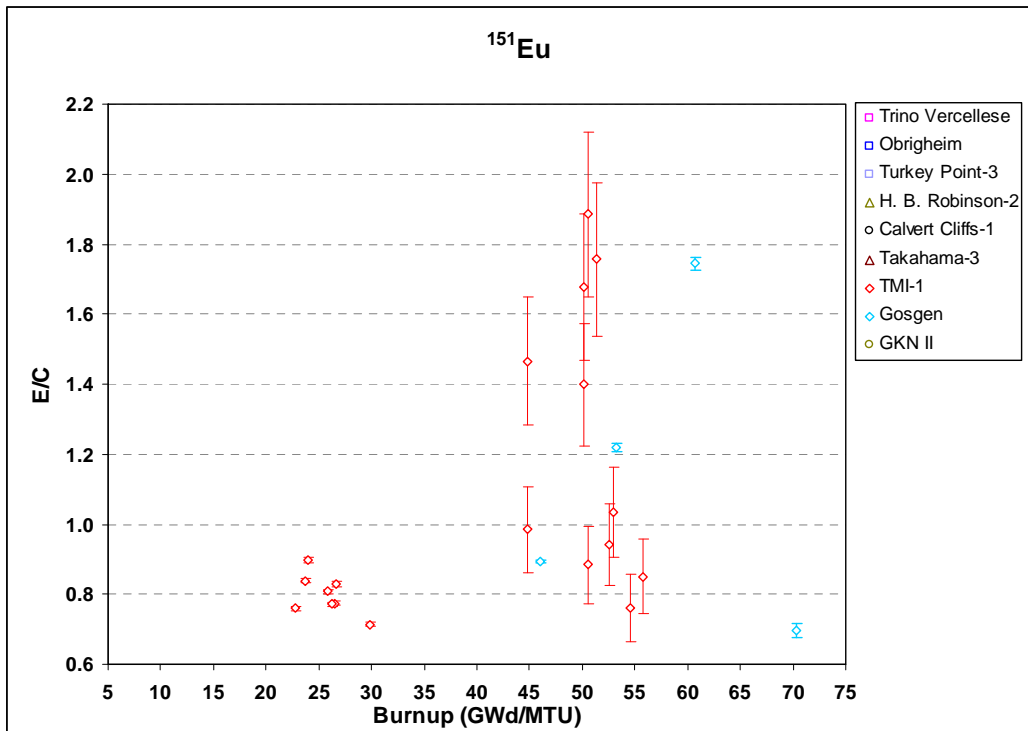


Fig. A.26. Ratio of experimental-to-calculated (E/C) ^{151}Eu concentration versus sample burnup. The error bars show the one-sigma measurement uncertainty.

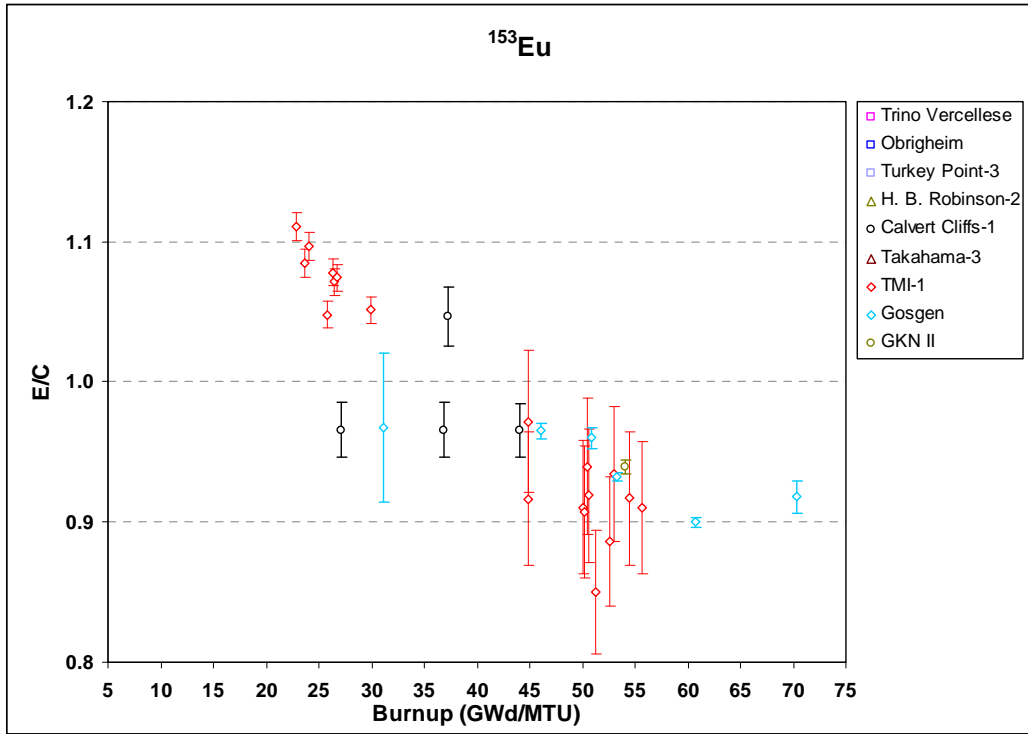


Fig. A.27. Ratio of experimental-to-calculated (E/C) ¹⁵³Eu concentration versus sample burnup. The error bars show the one-sigma measurement uncertainty.

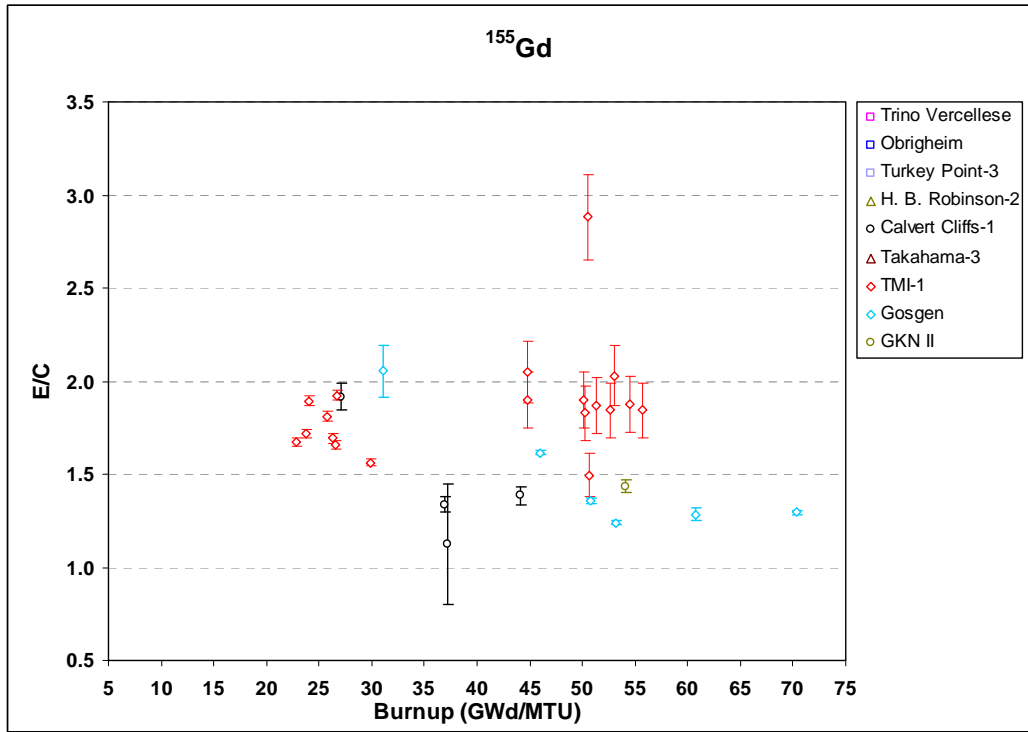


Fig. A.28. Ratio of experimental-to-calculated (E/C) ¹⁵⁵Gd concentration versus sample burnup. The error bars show the one-sigma measurement uncertainty.

APPENDIX B:
ELECTRONIC DATA SPECIFICATIONS

This appendix contains a listing and description of the files contained in the Digital Versatile/Video Discs (DVD+R format) that are attached to the calculation report *SCALE 5.1 Predictions of PWR Spent Nuclear Fuel Isotopic Compositions*. The operating system used to create the electronic data on the DVDs was Microsoft Windows XP Professional, Version 2002. The files stored on the electronic media contain zipped archives consisting of SCALE input and output files (text format) and Microsoft Excel files, which were created using standard Windows XP compress capabilities. The following process controls for storage and protection of electronic data apply.

Medium: DVD
 Conditions: Fireproof cabinet kept at ambient temperature
 Location: OCRWM QA Records, currently stored in Building 5700, Room H330
 Retention Time: Lifetime
 Security: Fireproof cabinet is locked
 Access: Project manager and records custodian only

The attributes of the electronic files are as follows:

File name	Size (bytes) (on disk)	Number of files	File date ^b	File time	Description
DVD					
xls.zip	1,929,216	19	3/29/2010	11:02:54 am	Archive containing all Microsoft Excel files used in this calculation
CalvertCliffs.zip	163,706,880	213	3/22/2010	3:41:07 pm	Archive containing SCALE depletion and decay files for the Calvert Cliffs spent fuel samples
GKN_Rebus.zip	23,313,432	30	3/22/2010	3:28:42 pm	Archive containing SCALE depletion and decay files for the GKN II spent fuel samples
Gosgen_Ariane.zip	126,485,528	209	3/25/2010	5:29:03 pm	Archive containing SCALE depletion and decay files for the Gösgen (ARIANE Program) spent fuel samples
HBRobinson.zip	57,681,920	56	3/22/2010	1:31:09 pm	Archive containing SCALE depletion and decay files for the H.B. Robinson Unit 2 spent fuel samples
Obrigheim.zip	215,351,296	127	3/22/2010	1:28:11 pm	Archive containing SCALE depletion and decay files for the Obrigheim spent fuel samples
Takahama.zip	430,202,880	208	3/22/2010	2:47:56 pm	Archive containing SCALE depletion and decay files for the Takahama Unit 3 spent fuel samples
TMI1.zip	251,276,312	394	3/22/2010	3:02:34 pm	Archive containing SCALE depletion and decay files for the TMI Unit 1 spent fuel samples
TrinoVercellese.zip	380,110,848	141	3/22/2010	9:55:23 am	Archive containing SCALE depletion and decay files for the Trino Vercellese spent fuel samples
TurkeyPoint.zip	76,744,704	27	3/22/2010	10:03:16 am	Archive containing SCALE depletion and decay files for the Turkey Point Unit 3 spent fuel samples
DVDr^a					
Gosgen_Malibu.zip	122,482,688	84	3/22/2010	3:35:03 pm	Archive containing SCALE depletion and decay files for the Gösgen (MALIBU Program) spent fuel samples

^aRestricted Contract Data (MALIBU Experimental Program).

^bAll DVDs were created on March 29, 2010, by G. Radulescu.